Technical Report

TR-02-15

Final report of the TRUE Block Scale project

3. Modelling of flow and transport

Antti Poteri, VTT Processes

Daniel Billaux, Itasca Consultants SA

William Dershowitz, Golder Associates Inc

J Jaime Gómez-Hernández, UPV

Vladimir Cvetkovic, KTH-WRE

Aimo Hautojärvi, Posiva Oy

David Holton, Serco Assurance

Agustin Medina, UPC

Anders Winberg, Conterra AB (ed)

December 2002

Svensk Kärnbränslehantering AB
Swedish Nuclear Fuel
and Waste Management Co
Box 5864
SE-102 40 Stockholm Sweden
Tel 08-459 84 00
+46 8 459 84 00
Fax 08-661 57 19
+46 8 661 57 19

Final report of the TRUE Block Scale project

3. Modelling of flow and transport

Antti Poteri, VTT Processes

Daniel Billaux, Itasca Consultants SA

William Dershowitz, Golder Associates Inc

J Jaime Gómez-Hernández, UPV

Vladimir Cvetkovic, KTH-WRE

Aimo Hautojärvi, Posiva Oy

David Holton, Serco Assurance

Agustin Medina, UPC

Anders Winberg, Conterra AB (ed)

December 2002

Keywords: advection, block scale, diffusion, heterogeneity, modelling, processes, retention, sorption, tracer tests, Äspö HRL.

Foreword

This report constitutes the third in a series of four final reports of the TRUE Block Scale Project, the latter run within the framework of the Tracer Retention Understanding Experiments at the SKB Äspö Hard Rock Laboratory, Sweden.

Funding organisations of the project are:

ANDRA (France)

ENRESA (Spain)

JNC (Japan)

Nirex (United Kingdom)

Posiva (Finland)

SKB (Sweden)

The work done could not have been accomplished without the active participation and efforts made by the analysis teams from the organisations involved:

ANDRA-Itasca: Benoit Paris and Xavier Rachez

ENRESA-UPV/UPC: Jesús Carrera, Harrie-Jan Hendricks Franssen, Amaranta Marcuello and Daniel Sendrós

JNC-Golder: Aaron Fox, Kate Klise, Thomas Doe, Shinji Takeuchi and Masahiro Uchida

SKB-GEOSIGMA: Peter Andersson, Johan Byegård and Rune Nordqvist

SKB-KTH/WRE: Hua Cheng

Their important contributions to realising the work presented in this report are hereby gratefully acknowledged.

Abstract

A series of tracer experiments were performed as part of the TRUE Block Scale experiment over length scales ranging from 10 to 100 m. The *in situ* experimentation was preceded by a comprehensive iterative characterisation campaign – the results from one borehole was used to update descriptive models and provide the basis for continued characterisation. Apart from core drilling, various types of laboratory investigations, core logging, borehole TV imaging and various types of hydraulic tests (single hole and cross-hole) were performed. Based on the characterisation data a hydrostructural model of the investigated rock volume was constructed including deterministic structures and a stochastic background fracture population, and their material properties. In addition, a generic microstructure conceptual model of the investigated structures was developed. Tracer tests with radioactive sorbing tracers performed in three flow paths were preceded by various pre-tests including tracer dilution tests, which were used to select suitable configurations of tracer injection and pumping in the established borehole array. The *in situ* experimentation was preceded by formulation of basic questions and associated hypotheses to be addressed by the tracer tests and the subsequent evaluation. The hypotheses included address of the validity of the hydrostructural model, the effects of heterogeneity and block scale retention. Model predictions and subsequent evaluation modelling was performed using a wide variety of model concepts. These included stochastic continuum, discrete feature network and channel network models formulated in 3D, which also solved the flow problem. In addition, two "single channel" approaches (Posiva Streamtube and LaSAR extended to the block scale) were employed. A common basis for transport was formulated. The difference between the approaches was found in how heterogeneity is accounted for, both in terms of number of different types of immobile zones included, and if and how heterogeneity in retention parameters was accounted for. The integration of the modelling performed emphasised assessment the relative roles of advection, diffusion and sorption. The evaluation results showed similar retention characteristics for the three tested flow paths, which in turn were found to be similar to those seen in the flow paths tested by the TRUE-1 experiment. The evaluation modelling showed that the most consistent interpretation of the performed tests is obtained when diffusional mass transfer and sorption in immobile zones is included. It was also noted that no additional phenomena/processes (apart from surface sorption) were required to explain the observed *in situ* retention. It was further found not possible to fully discriminate the relative importance of potentially available immobile zones along the flow paths using available data. It was finally observed that heterogeneity in retention properties calls for additional analysis of "effective" retention parameters in order to improve understanding and interpretation of *in situ* retention parameters.

Sammanfattning

En serie spårförsök genomfördes inom ramen för TRUE Block Scale projektet över avstånd mellan 10 till 100 m. Transportförsöken föregicks av en omfattande karakterisering som genomfördes iterativt – resultatet från ett karakteriseringsborrhål utnyttjades för att uppdatera beskrivande modeller och för att ge underlag för fortsatt karakterisering. Förutom kärnborrning genomfördes kärnloggning, olika typer av laboratorieundersökningar på geologiskt material, borrhåls-TV och olika typer av hydrauliska tester (enhåls- och mellanhålstester). Med hjälp av tillgängliga karakteriseringsdata byggdes en beskrivande modell av den undersökta bergvolymen som innehöll deterministiskt beskrivna strukturer och en stokastisk beskrivning av bakgrundssprickor, och dessas materialegenskaper. Vidare konstruerades en generisk mikrostrukturell konceptuell modell av undersökta strukturer. Spårförsök med radioaktiva sorberande spårämnen genomfördes i tre flödesvägar, föregångna av olika typer av förförsök, bl a utspädningsmätningar vars resultat utnyttjades för att välja lämpliga konfigurationer för injicering och provtagning av spårämnen i befintliga borrhål. *In situ* experimenten föregicks av formulering av viktiga frågeställningar och hypoteser baserade på dessa, att belysas av efterföljande experiment och utvärdering. Hypoteserna behandlade giltigheten hos den upprättade beskrivande modellen, effekter av heterogenitet samt retention i blockskala. Modellprediktioner och utvärdering genomfördes med ett stort utval av modellkoncept. Dessa inkluderade modeller baserade på stokastiskt kontinuum, diskreta nätverk och kanalnätverk som samtliga även löser flödesproblemet. Dessutom utnyttjades två koncept som ansluter mer till en kanalbeskrivning (Posiva Streamtube och LaSAR utvidgat till blockskala. En gemensam plattform för formulering av transportproblemet utvecklades. Det noterades att den huvudsakliga skillnaden mellan koncepten vad gäller transport ligger i hur heterogenitet behandlas, dels i termer av antalet immobila zoner som inkluderas i analysen, samt om och hur heterogenitet i retentionsparametrar inkluderas. Den integrering av olika modellresultat som genomförts underströk belysning av de relativa rollerna som advektion, diffusion och sorption har. Resultatet av utvärderingen visade likvärdiga retentionsegenskaper för de tre undersökta flödesvägarna, som vidare visade likvärdiga egenskaper som de flödesvägar som undersöktes i TRUE-1. Modelleringen påvisade att den mest konsistenta tolkningen av de utförda försöken erhålls när diffusiv masstransport parad med sorption i immobila zoner inkluderades. De påvisades att inga ytterligare processer (utöver ytsorption) behövdes för att förklara den observerade retentionen *in situ*. Det visade sig vara svårt att fullt ut diskriminera den relativa betydelsen av möjliga immobila zoner längs flödesvägen med hjälp av tillgängliga data. Slutligen noterades att heterogenitet i retentionsparametrar påvisat behovet av ytterligare analys av ”effektiva” retentionsparametrar för att förbättra förståelsen och tolkningen av *in situ* retention och dess parametrisering.

Executive Summary

Background and overview of project

The main objective of the TRUE Block Scale Project is to improve the understanding of radionuclide transport and retention in a network of conductive structures in crystalline rock. The length scales studied range from about 10 to 100 metres.
The initial stages of the project involved an iterative characterisation that included successive development of the borehole piezometer array and parallel development of descriptive hydrostructural models. The hydraulic characterisation used relatively simple techniques to establish the location of conductive structures and their connectivity between boreholes. Hydraulic conductors were associated with geological features established from borehole TV imaging and existing corelogs. Updates of the hydrostructural models were developed following the drilling of new exploration boreholes. Potential source and sink sections in the borehole array were identified using cross-hole interference tests and tracer dilution tests. Some of the dilution tests were extended to cross-hole tracer tests that demonstrated the ability to run tracer tests over longer distances. The concluding Tracer Test Stage included a dedicated campaign of selecting source sections for radioactive sorbing tracer tests. Following a demonstration that a sufficiently high mass recovery could be obtained, a series of four injections of radioactive sorbing tracers were made in three different source-sink pairs covering distances between 15 and 100 m along structures interpreted from the hydrostructural model. The transport paths involved between 1 and up to 3 interpreted structures.
The results of the tracer tests indicated that the interpreted single structure flow path (Injection C3) was more complex than anticipated. Likewise the results from the interpreted multi-structure flow path (Injection C2) indicated that it was significantly shorter than indicated by the projected flow path along the interpreted deterministic structures. The three injections C1 through C3 were subject to numerical model prediction and evaluation using a variety of model approaches. The current report presents the results of this modelling work and conjectures and conclusions about block scale transport and retention.

Basic questions asked

Three basic questions have been posed in relation to the performed tracer test work. These are:

Q1) “What is the geometry of conductive structures of the defined target volume for tracer tests within the TRUE Block Scale rock volume? Does the most recent structural model reflect this geometry with sufficient accuracy to allow design and interpretation of the planned tracer tests?”

Q2) “What are the properties of fractures and fracture zones that control transport in fracture networks?"

Q3) “Is there a discriminating difference between breakthrough of sorbing tracers in a detailed scale single fracture, as opposed to that observed in a fracture network in the block scale?”

These questions help to define hypotheses that could be tested by the *in situ* tracer tests and the subsequent model evaluation.

Overview of modelling programme

The iterative approach to characterisation and structural modelling employed in the TRUE Block Scale Project also included use of numerical flow and transport modelling interactively as part of the characterisation process. The objective was to provide guidance and optimisation in the characterisation process relative to the defined project objectives. Initially, only one modelling concept, the discrete feature network (DFN) concept was employed. Towards the end of the characterisation process, additional approaches were included (stochastic continuum (DFN) and channel network (DFN/CN) models). For the predictions and evaluations associated with the radioactive sorbing tracer tests performed as part of Phase C, two additional approaches were introduced (the LaSAR and Posiva Streamtube concepts). To these five modelling approaches should also be added the advection-dispersion analytical model employed by the SKB-GEOSIGMA team in their basic evaluation. This model has been applied to all tracer tests performed as a part of the TRUE project. Common to all transport model approaches employed is the assumption of a parallel plate with 1D diffusion orthogonal to the fracture plane where fluid flow takes place.

Consideration of groundwater flow is not the main focus of the TRUE Block Scale Project. However, assumptions about the macro-properties of the flow field are an important aspect of the analysis of transport and retention. A basic understanding of groundwater flow therefore is a prerequisite for design and planning of a transport experiment. In this context a well-performing numerical (or analytical) model of groundwater flow can be an effective tool for design calculations and model predictions. Three of the model approaches (SC, DFN and DFN/CN) provide full a 3D description of groundwater flow. In addition, the way groundwater flow is treated has implications on the degree of dispersion introduced to solute transport, and also has direct implications for the flow-related aspects which governs retention.

Overview of modelling concepts

The concept used is in the SKB-GEOSIGMA approach is a one-dimensional advection-dispersion model where dispersivity and mean travel times are determined using an automated parameter estimation program which employs a non-linear least square regression where statistics (correlation, standard errors and correlation between parameters) also are obtained.

The ENRESA-UPV/UPC stochastic continuum (SC) approach used a stochastic approach to groundwater flow and mass transport in which the medium is conceptualised as a heterogeneous continuum. Modelling of the flow and transport processes is carried out using two different numerical tools. The flow model uses a finite-difference code that is conditioned condition to transmissivity and piezometric head data. The geometry and material property distribution of this model are used as inputs to the finite element code in which transport is solved.

The Nirex-Serco team used a Discrete Fracture Network (DFN) approach to model the tracer tests. This approach uses an accurate representation of all of the key structures characterised as part of the hydrostructural model and of the in-plane heterogeneity within the structures. The latter to reflect the observed intra- and inter-variability in transmissivity of modelled fractures. Transport was solved using a one-dimensional transport model using path lines with processes (advection, dispersion, and rock-matrix diffusion) included.

The Posiva-VTT modelling concept is based on a simplistic representation of the streamtube (i.e. a collection of streamlines) that connects the source and sink of a given tracer test. The transport model comprises two parts: the mobile part of the pore space where the advection takes place (streamtube) and the immobile part of the pore space that is adjacent to the streamtube (matrix, fault gouge, stagnant pools etc).

The SKB-KTH/WRE team employed the Lagrangian Stochastic Advection-Reaction (LaSAR) approach. This model is extended in two ways. The model is generalised to account for aperture variability, as well as for longitudinal heterogeneity in retention parameters. In addition the model was generalised from a single heterogeneous fracture to a network of heterogeneous fractures, where tracer particle trajectories extend over a series of fractures.

The JNC-Golder team used a Channel Network/Discrete Fracture Network (DFN/CN) approach that combines a direct implementation of the project 3D hydrostructural model with an ability to control definition of flow and transport pathways (channels) within the modelled structures/fractures. An option is provided to include stochastic background fractures, thereby representing the features not included explicitly in the hydrostructural model, yet known to occur within the rock block. Finally, an option is provided to include enhanced connectivity, transmissivity, or storage at fracture intersection zones (FIZ). The transport problem, including advection, dispersion, and diffusion (ADD) transport is solved for multiple interacting immobile zones.

Predictive modelling

Predictive modelling was employed during various phases of the TRUE Block Scale Project. The main prediction activity was performed on the Phase C radioactive sorbing tracer tests. The modelling groups were given access to the results of the performed cross-hole interference tests, tracer dilution tests and results of relevant non-sorbing tracer tests performed in the flow paths at relevant pump rates. The groups were also provided with a generalised description of the various immobile zones and selected parameter values. Values of diffusivity and sorption distribution coefficients based on

unaltered wall rock and altered wall rock from the TRUE-1 site were available. In addition, sorption coefficients for the fine-grained fault gouge material were estimated using available caution exchange capacities, selectivity coefficients combined with site-specific mineralogy and groundwater chemistry. The modelling groups were then asked to predict the reactive tracer breakthrough and associated mass recovery. Despite the seemingly large body of data specifying the properties, some aspects were left to the modellers for interpretation, mostly regarding assumptions about the flow field and immobile zone geometries, but also regarding material properties. Figure EX-1 shows the various breakthrough curves predicted for the Rb-86 tracer administered as part of the C1 injection (L=16 m). The produced comparative graphs provide graphical illustrations of the diversity of model predictions. Different choices of material properties explain, to a large extent, the variations in the predicted breakthrough. However, a full comparison of these results must also take into account the conceptualisation of the studied system (flow field and micro-structure model and immobile zones included). As part of the evaluation of the performed tracer tests, attempts were made to assess the relative effect of the modelled flow field on the evaluated retention.

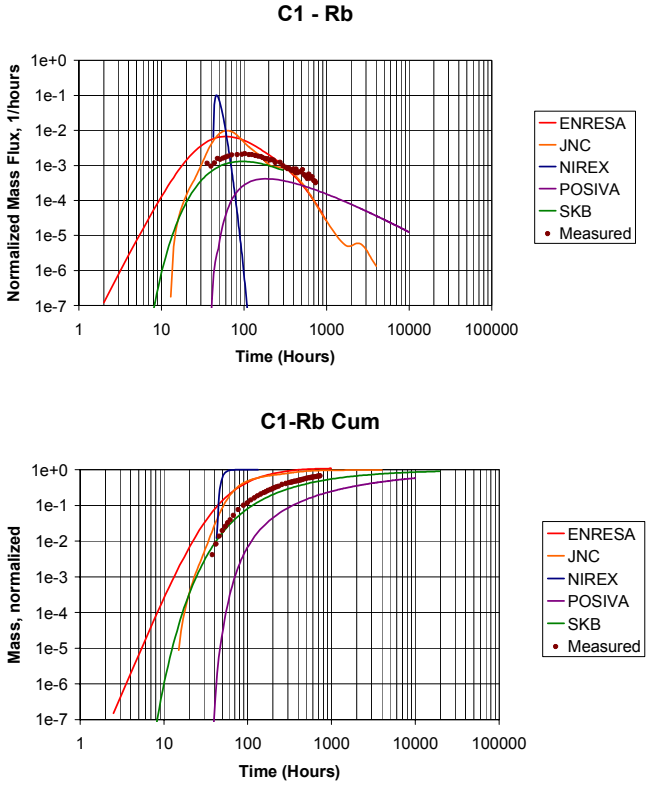

Figure EX-1. *Predicted and measured breakthrough curves for Rubidium, test C1. a) log-log, b) cumulative.*

Testing of hydrostructural model

This part of the analysis addressed whether the proposed hydrostructural model properly accounted for rock mass heterogeneity, whether it is consistent with observed connectivity patterns, and finally, whether the hydrostructural model is consistent with the results of the tracer tests. The SC model analysis indicated the need for conductive structures that could provide hydraulic connection between the northwest trending structures. The evaluation of the hydraulic interference tests showed a primary compartmentalised response pattern, i.e. an equitable normalised drawdown over orders of magnitude variation in normalised distance. This was found to be inconsistent with the basic hydrostructural model which provides extensive interconnection throughout the investigated rock mass, this even without the additional connectivity provided by the background fracture population. The apparent over-connectivity was also in general evident in the significantly lower drawdown in the DFN/CN model compared to the *in situ* results. On the contrary, the SC model required the rock mass between the deterministic structures to obtain a reasonable inversion. The overall finding from the analysis was that the hydrostructural framework could not be shown "inconsistent" with available *in situ* data (steady state and transient hydraulic responses and tracer breakthrough data).

It was further shown that background fractures did not play a significant role for explaining the observed breakthrough curves. This was true for the DFN/CN model indicating that the investigated flow paths are dominated by transport in a radially converging flow field in deterministic structures of the hydrostructural model.

Viewed as an inverse problem the developed hydrostructural model is by no means unique. On the other hand the degree of flexibility included in the hydrostructural model appears to allow implementation of numerical models which are consistent with *in situ* measurements.

Testing of effects of macroscale heterogeneity

Heterogeneity is fundamental to the understanding of flow and transport in the TRUE Block Scale rock volume. Heterogeneity is evident in a variety of geologic forms and at a variety of scales, affecting both flow and transport. Macro-scale heterogeneity is apparent in effects of background fractures (see preceding section), the variability in fracture aperture, as observed in the core/TV logs, bifurcation and multiplicity of sub-parallel fractures making up the conductive structures as well as in the distribution of fine-grained fault gouge material along the flow path. Micro-scale heterogeneity includes local variations in the fault gouge material and the alteration rims of the wall rock adjacent to conductive fractures, and associated retention parameters.

Spatial variability in hydraulic conductivity was introduced in the rock mass and the deterministic structure units of the SC model, in both cases with a correlation length of 40 m. The SC model was initially conditioned to hydraulic conductivity only. Through the use of a self-calibrating algorithm the heterogeneity in the deterministic structures as well as in the rock mass were modified to match the available steady state and transient head data. The DFN model included a correlation length of 5 m for the transmissivity

data in individual structures. Despite the relatively short correlation, multiple transport paths and channelling developed.

The evaluation of Basic Question #2, as stated above, also included analysis of whether or not the effects of fracture intersection zones (FIZ) could be detected in available breakthrough curves. Testing of this hypothesis requires that intersection effects are differentiable from other forms of heterogeneity within individual planar structures. It is noted that the constitution of FIZ's in essence could resemble those of channels developed in fracture planes. This primarily attributed to the fact that FIZ's most likely do not exhibit a clear-cut characteristic, but rather can show a combination of barrier and conductor characteristics. Modelling studies focused on assessing whether or not fracture intersection zones (FIZ) could have a significant effect on transport pathways. The simulations showed that for (synthetic) tracer tests fracture intersections may be difficult to distinguish from other forms of heterogeneity. On the other hand, a FIZ that connects a tracer pathway to a hydraulic boundary can divert tracer mass to that boundary and reduce the mass recovery at the sink. A correlation was noted between tracer mass loss and flow paths passing fracture intersection zones. However, the tests concerned are all longer paths, such that connections to other alternative secondary sinks are plausible.

Concepts of processes

The investigated crystalline rock volume is conceptualised as a dual porosity (mobile-immobile zone) system. Indivisible tracer particles (e.g. radionuclide ions) enter the flow field at the injection borehole and are transported through one or several fractures to the detection (pumping) borehole. The mobile pore space is a relatively small portion of the total pore space in the conductive fractures. Water in the remaining pore space, in the rock matrix, in non-flowing (stagnant pool) parts of the fractures, and in fracture filling material is effectively immobile. The tracer experiments were carried out through a network of structures/fractures that provides possibility to study both network effects in advective transport as well as in mass transfer processes between the mobile and immobile pore spaces.

All modelling approaches applied to the TRUE Block Scale tracer experiments consider linear retention, motivated by the fact that the tracer tests are sufficiently diluted. The common form of transport equations employed can be written as:

$$R\frac{\partial C}{\partial t}+V\frac{\partial C}{\partial x}=D_l\frac{\partial^2 C}{\partial x^2}-\sum_{i=1}^{N}\frac{\alpha^i\theta^i D_m^i}{b^i}\frac{\partial C_m^i}{\partial z}\bigg|_{z=0}, \qquad \text{(EX-1a)}$$

and

$$R_m^i\frac{\partial C_m^i}{\partial t}-\frac{\partial}{\partial z}D_m^i\frac{\partial C_m^i}{\partial z}=0 \qquad \text{(EX-1b)}$$

where notations are given in Section 6.1.

The above equations can account, in principle, for all the types of heterogeneity for which data are available, both in terms of flow and retention. Different modelling teams have used different simplifications of Equation (EX-1), employed different techniques of solution, and different strategies to account for random and deterministic distributions of flow and retention parameters.

Effects of advection on retention

Properties of the flow field are crucial for transport and have an important role in determining the retention properties that are assigned to the different transport paths. With advection we here denote transport of an ideal non-sorbing and non-diffusive tracer through the mobile pore space.

The advective flow field determines the relative importance of the different retention processes. In a steady-state flow field, flow paths of the tracer particles coincide with the streamlines of the flow field. Advective transport is governed by the properties of the streamlines.

The flow problem has been handled differently by the five modelling approaches employed in the evaluation of the Phase C tests. Three approaches model the flow problem explicitly applying comprehensive 3D numerical models, SC, DFN and DFN/CN, respectively. The remaining two approaches do not address the flow problem explicitly. The latter two models apply simple 1D connections between the sink and the source. The flow is conditioned to the measured flow in the injection section (Posiva Streamtube). Alternatively, flow-dependent transport properties are provided by independently calculated 3D particle tracking data and conservative tracer residence time distributions observed in relevant tracer pre-tests (LaSAR).

The treatment of heterogeneity (macro scale as well as microscale retention parameters) fundamentally differentiates the different modelling approaches. Some modelling approaches try to reproduce the full flow field, in which case the macro-scale heterogeneity is calibrated and conditioned against the available hydraulic data.
If the modelling approach uses a simplified flow field, such as for a one-dimensional streamtube model, the heterogeneity in flow is taken into account indirectly in the groundwater transit time distribution using the results of tracer pre-tests using non-sorbing tracers.

Under steady state and purely advective flow conditions, the tracer molecules follow the streamlines of the flow field. This means that the residence times of the ideal non-retarded tracer molecules are those of the streamlines. This residence time distribution is also referred to as the “groundwater residence time distribution”.

A comparison of the groundwater residence time distributions using an ideal non-diffusional and non-sorbing tracer breakthrough curve is meaningful only if the breakthrough curves are calculated for the Dirac’s delta function source (input) function (or a sufficiently short pulse).

A comparison of the advective fields employed by the five modelling groups that predicted and evaluated the Phase C tracer experiments show different emphasis on spreading due to the flow field relative to that imposed by retention processes, cf Figure EX-2. In order to match *in situ* results, models that produce narrow peaks in the simulated Dirac breakthrough curves should have retention models that produce more spreading than models that produce dispersed breakthrough already as a consequence of their advective field.

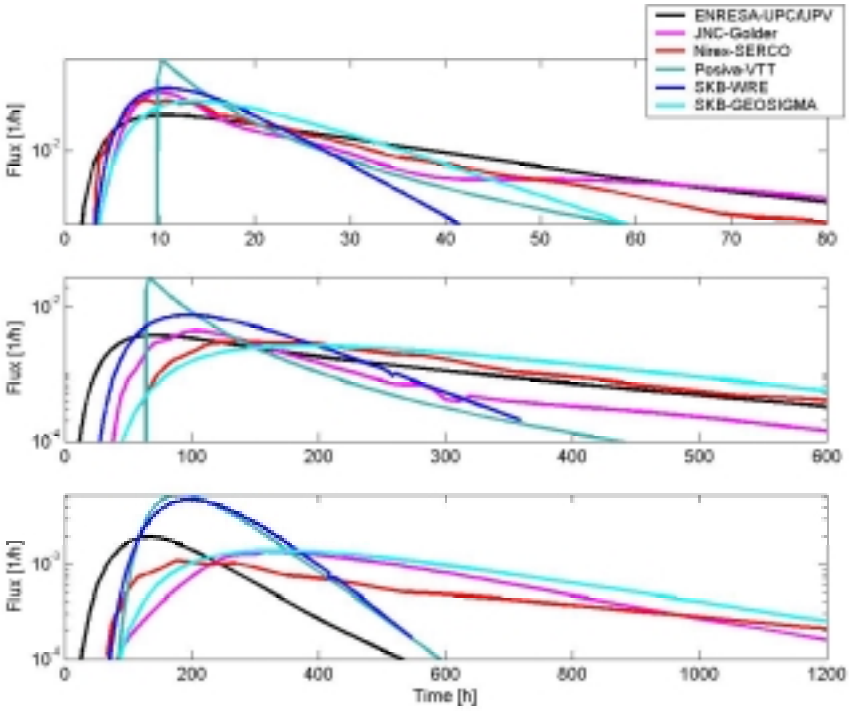

Figure EX-2. *Groundwater residence time distributions (no matrix diffusion or sorption) for the C1, C2 and C3 tracer tests as provided by the different models.*

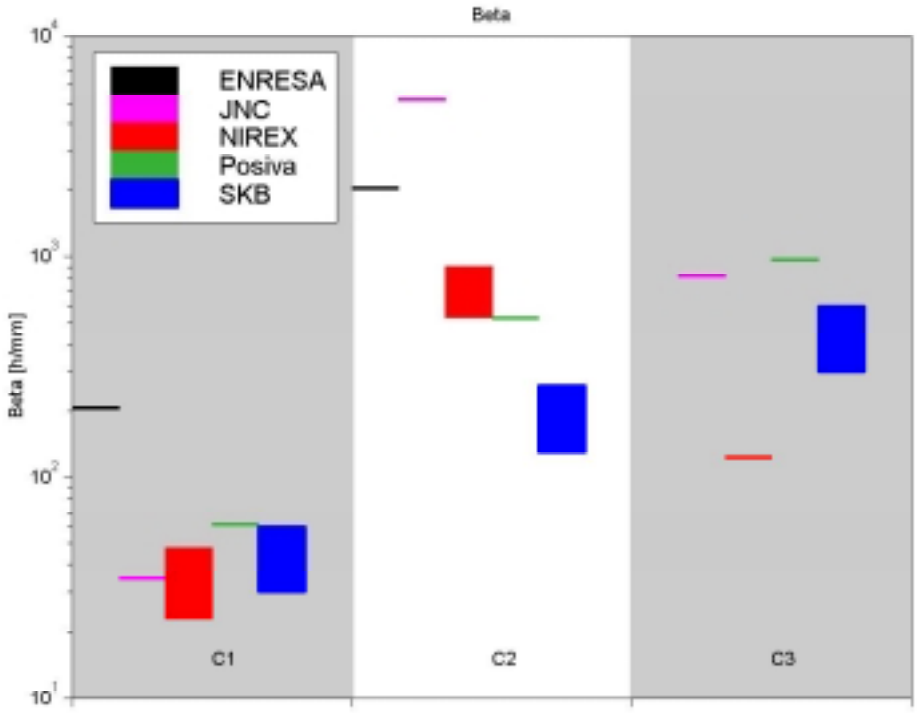

Figure EX-3. *Evaluated parameter β which describes the average flow geometry of the flow paths of the various models and flow paths (tracer tests).*

The hydrodynamic control of the retention (in terms of the parameter β (water residence time per unit half-aperture, for the parallel plate case β equates to 2WL/q) in different models can be estimated based on the information on the groundwater transit times and retention apertures. Figure EX-3 presents β values for different flow paths and different models. Flow path I (C1) shows a consistent grouping of most of the models, showing values between 20 to 60 h/mm. It is noted, that flow path I gave breakthrough for the largest number of tracers and thereby the constraining power of the breakthrough curves is highest for this flow path. The retention parameter β should increase with increasing path length which is also clearly visible in Figure EX-3 (estimated relative path length is C1<C3<C2).

Retention due to diffusion

Diffusion to the immobile pore space, sorption in the immobile pore space and surface sorption on the fracture surfaces along the transport paths are interpreted to be the main retention processes in all prediction and evaluation models applied to the TRUE Block Scale experiments. The main support for this assumption is the residence time distributions associated with the TRUE Block Scale tracer experiments (for both sorbing and non-sorbing tracers) which show tailing and spreading that may be

indicative diffusive processes. This kind of behaviour is indicated by a power-law tailing in the breakthrough curve. Diffusion to an infinite immobile zone should show a $t^{-3/2}$ tailing in the breakthrough curve.

The simulation results support the interpretation that diffusional mass transfer is important over the time scales employed in the TRUE Block Scale tracer experiments. The evaluation using different models also indicates that the measured residence time distributions can be reproduced more accurately with the diffusional mass transfer invoked.

The present conceptualisation of the transport paths includes immobile pore spaces in the rock matrix (including altered rim zone and high porosity coating), fault gouge, fault breccia and stagnant zones. These four immobile zones exhibit differences that may influence the retention properties e.g. the total volume or thickness of the available pore space. It is obvious that the rock matrix has effectively an infinite capacity for an *in situ* tracer experiment conducted over practical time scales. Unlike the rock matrix, the fault gouge is composed of small particles that have very limited capacity. It is thus possible that in the fault gouge the effects of the matrix diffusion dissipate relatively fast and the retardation can be modelled as a part of the equilibrium surface sorption.

In addition to the variable capacity of the pore spaces, the multiple and parallel appearance of the available immobile pore spaces causes superposition of similar response characteristics in the measured breakthrough curves. This means that it is not possible to unambiguously distinguish the different contributions to the aggregate breakthrough behaviour of diffusion to the different pore spaces using the breakthrough data alone.

Tracer retardation depends on the integrated (effective) retention property along the flow paths. This integrated property is composed of the porosity and pore diffusivity of the immobile zones paired with the sorption properties of the tracer and the properties of the flow field. It is not possible to evaluate the individual physical retention parameters, or at least not in a unique way without additional constraints. The interpretation of the retention properties from the breakthrough curves is also strongly linked to the underlying assumptions related to the advective flow field and equilibrium surface sorption. Both of these processes can produce similar characteristics in the breakthrough curves as the matrix diffusion.

Heterogeneity in the immobile zone properties can influence the interpretation of the retention. Site-specific measurements indicate that the porosity immediately adjacent to the fracture surface is much higher than the average porosity of the intact unaltered rock. The high porosity zone of limited extent adjacent to the fracture (including a very thin high-porosity coating) has significant impact on tracer retardation over experimental time scales. This difference may partly explain the noted differences between the retention observed in the laboratory and that observed *in situ*.

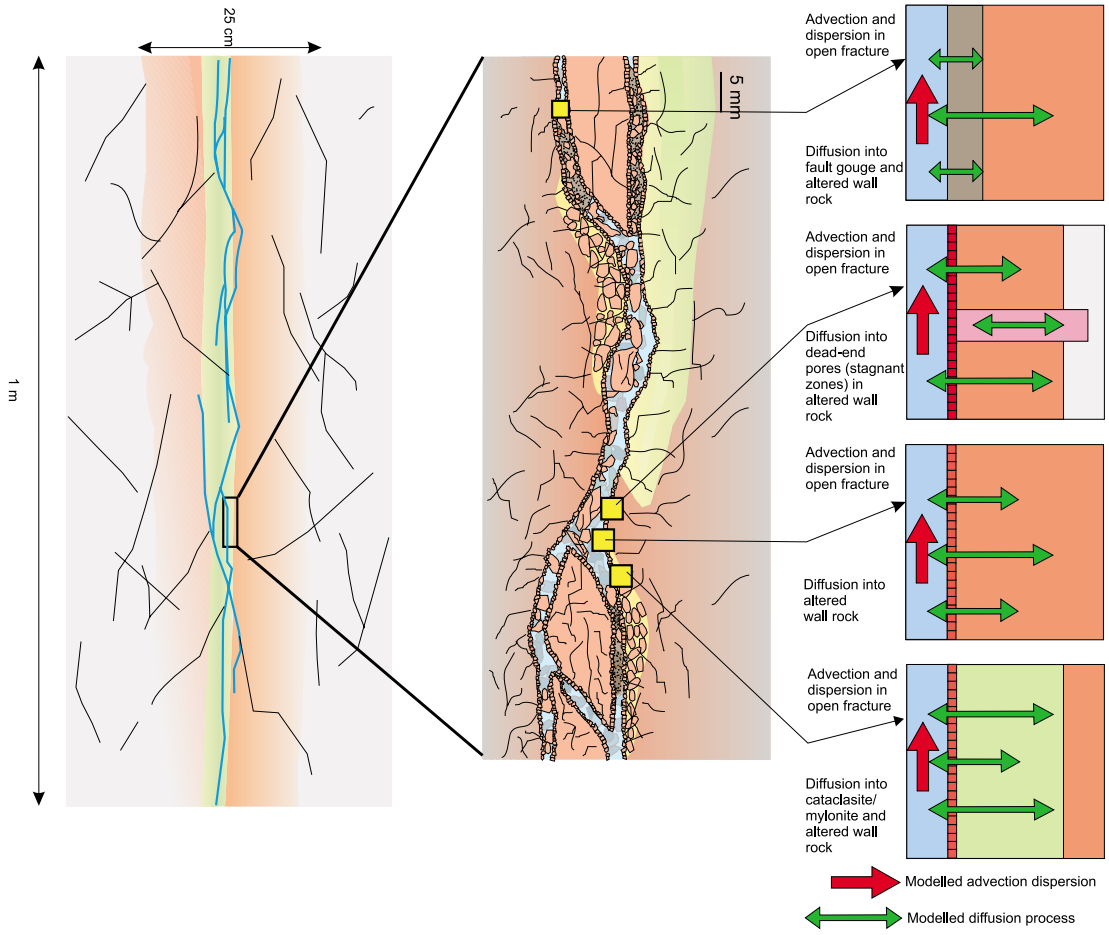

Figure EX-4. *Simplification of the pore space structure as applied in the evaluation models.*

Diffusion from the mobile part of the pore space to the immobile parts is modelled as a one-dimensional process. This leaves some freedom in the geometrical definition of the pore spaces. The conceptualisation of a typical flow path into different diffusion sub-processes is presented in Figure EX-4. In the direction normal to the fracture plane the tracer experiences (altered) rock matrix and possibly high porosity coating at the surface of the fracture. Stagnant pools, fault gouge and fault breccia may also be located in the fracture planes in the lateral direction and normal to the extension of the flow path.

The simulations of the Phase C tracer tests by all five modelling approaches include diffusion to the immobile pore space as a retention process. Most of the approaches account for a limited depth of the immobile zone. The thickness of the immobile zone varies from 0.1 mm to 1 m. One model (SKB-WRE) applies a depth-dependent porosity in the analysis.

Retention due to sorption

Transport of selected tracers and radionuclides in crystalline bedrock is reactive. This means that the tracer particles interact with the groundwater-rock system by various chemical reactions during transport along the flow paths. In transport modelling, all these reactions, such as adsorption and ion exchange, are referred to as "sorption".

Sorption may take place onto any geological material that is available along the transport path. Potential sorption sites along the flow paths investigated in the TRUE Block Scale experiments are located in the available pore spaces. These are located in the altered rim zone of the wall rock matrix, fault breccia pieces and fragments, fault gouge and on the surfaces of the fractures making up the mobile pore space of the flow paths.

The sorption models that have been applied by the modelling groups in the analysis of the TRUE Block Scale experiment are based on simplified representations of the real system. All models employ reversible and instantaneous equilibrium sorption. Fixed distribution coefficients, K_d, or K_a, are used to parameterise sorption of the different tracers. The latter two parameters depend only on the tracer used, the geological material and the groundwater composition. Depending on the modelling approach, the applied sorption values are based either on the fitting of breakthrough curves from previous *in situ* experiments at Äspö HRL and/or laboratory measurements that have been interpreted using the K_d approach.

The sorptivity of the fault gouge material collected from the borehole intercepts of the deterministic structures involved in the TRUE Block Scale Phase C experiments has not been determined experimentally. However, estimates of K_d for the fine-grained fault gouge have been calculated based on the cation exchange capacity (CEC) using the mineralogical composition of the material of a grain size smaller than 125 μm. Estimates of the K_d for the fine-grained size fraction of the fault gouge material based on CEC show resulting K_d values that are substantially higher (a factor of about 20 to 60) than those based on the investigated larger size fraction of intact unaltered bedrock from the TRUE-1 site.

Integrated retention of the immobile zones

Figure EX-5 shows the integrated immobile zone parameter $\kappa=\theta\,(D(1+K_d\,\rho/\theta))^{1/2}$ associated with individual tracers used by the modelling groups in their evaluation modelling of the Phase C tracer tests. The large spread in the applied values of immobile zone properties indicates a large uncertainty. The majority of values applied are higher than values associated with intact unaltered wall rock (the so-called MIDS data set).

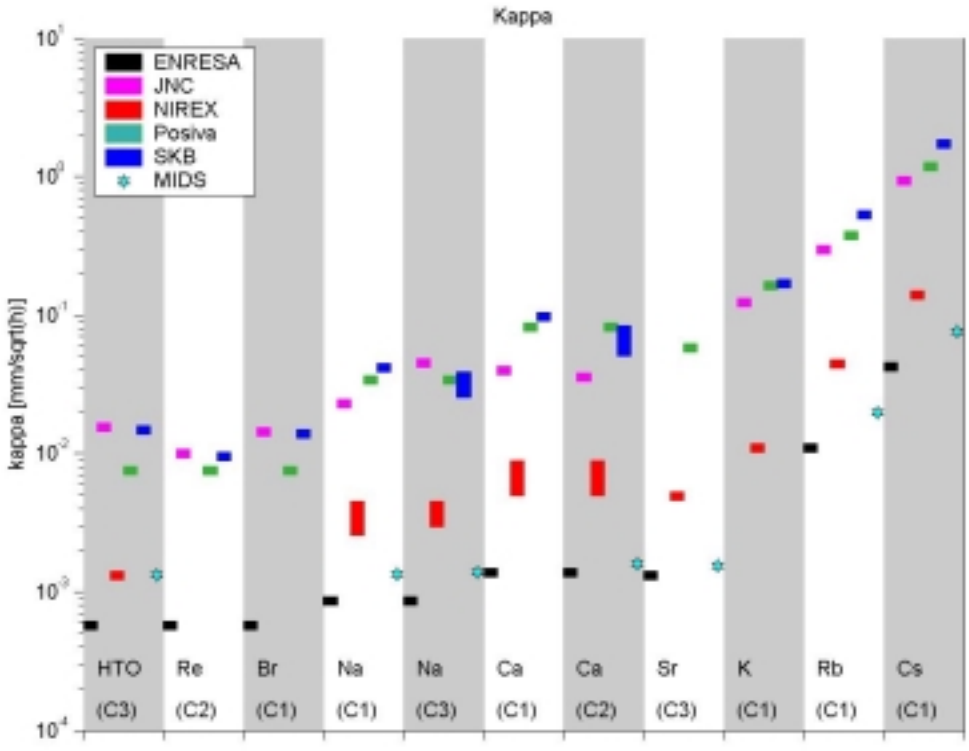

Figure EX-5. *Evaluated retention material parameter group* $\kappa=\theta\,(D(1+K_d\,\rho/\theta))^{1/2}$ *for the respective evaluation models and tests (C1, C2 and C3).*

Comparison with detailed scale retention (TRUE-1)

No new transport phenomena (processes) were required when taking the step from modelling of detailed scale (TRUE-1, L=5 m) to modelling block scale (TRUE Block Scale, L= +50 m) transport phenomena and retention. In this context it was observed that the explicit new block scale feature, the fracture intersection zone (FIZ), was not found to be crucial, neither for explaining the hydraulic responses, nor for the transport results.

The material property group κ for retention (and where applicable, also individual retention parameter values) obtained from the evaluation of the block scale tests with radioactive sorbing tracers were for the most part found to be in the same order of magnitude as those evaluated for the corresponding TRUE-1 tests. In fact, the C1 breakthrough (L=15 m) could be predicted fairly well by combining the conservative tracer results obtained in earlier phases of the TRUE Block Scale tracer tests and retention properties deduced from the TRUE-1 experiments and compilations of TRUE Block Scale characteristics related to fault breccia and fault gouge materials.

The finding of similar *in situ* retention at the TRUE-1 and TRUE Block Scale sites is potentially significant for performance assessment. The implication being that spatial scaling effects related to transport and retention in the "near field" (corresponding to the distance to the nearest major (local) fracture zone) of a deep geological repository may not be as important as previously conceptualised. It is noted that temporal scaling when taking the step from experimental to performance assessment time scales may be more complicated.

Reconsideration of basic questions and formulated hypotheses

Hypothesis 1: The modelling studies show that the developed deterministic hydrostructural model cannot be rejected using the experimental data. It is however indicated that the hydrostructural model is overconnected to the boundaries compared to what is seen in the *in situ* data. A self-calibrating technique, which integrated available transmissivity/hydraulic conductivity data and steady state and transient hydraulic head data, early on directed attention towards north-northwesterly conductors that were later identified and presently are part of the hydrostructural model. Background fractures were found to be insignificant when explaining the hydraulic responses using the DFN/CN model. On the contrary, the SC model required the rock mass between the deterministic structures to obtain a reasonable inversion. It was further found unnecessary to introduce background fractures along the tested flow paths in order to explain the *in situ* breakthrough curves using the DFN/Cn model.

Hypothesis 2: Various assignments of macro-scale heterogeneity in hydraulic conductivity and transmissivity of the rock mass and the deterministic structures have been employed. Attempts have also been made to distinguish effects of fracture intersection zones (FIZ) from the intra-planar heterogeneity. No significant effect on retention has been observed. Fracture intersection zones are however interpreted to provide connection to alternative sinks (boundaries) resulting in a reduced mass recovery for some tracer tests.

Hypothesis 3: All modelling groups include diffusion into geological material as an important retention process. The different groups put different emphasis on the immobile zones. Some attribute the main retention to the fine grained fault gouge along the flow path whereas others attribute the noted retention to the altered rim zone of the wall rock. In the latter case the added importance of heterogeneity in retention parameters along the flow path has been high-lighted as well as effects of a decreasing trend in porosity away from the fracture. No characteristic differences in the breakthrough curves of the Phase C tests can be noted, whether single structure flow path or multiple structure flow paths. Likewise, a similar retention is noted in the TRUE Block Scale and TRUE-1 flow paths.

Main conclusions regarding block scale retention

The following conclusions regarding block scale retention can be drawn from analysis of the TRUE Block Scale tracer experiments;

- The observed block scale *in situ* retention is comparable to that observed in the detailed scale TRUE-1 experiments.

- The most consistent interpretation of observed tracer breakthrough curves for all tracers of Phase C tests is obtained if coupled diffusional mass transfer and sorption in immobile zones are assumed.

- There is no need to include additional phenomena/processes in the interpretation of the TRUE Block Scale tracer tests (in networks of fractures/structures) in order to explain the observed *in situ* retention.

- It is not possible to fully discriminate the relative importance of potentially available immobile zones along the flow paths using available data.

- In view of observed heterogeneity in material retention properties, further analysis of "effective" retention parameters and their definition is required for better understanding and interpreting estimated *in situ* retention parameters.

Contents

1 Introduction

1.1 Background

Concepts for deep geological disposal of spent nuclear fuel include multi-barrier systems for isolation of nuclear waste from the biosphere. Waste forms, and concepts for encapsulation of the waste and engineered barriers may vary between countries. Most concepts, however, rely on a natural geological barrier that should provide a stable mechanical and chemical environment for the engineered barriers, and should also reduce and retard transport of radionuclides released from the engineered barriers. In case of early canister damage, the retention capacity of the host rock in relation to short-lived radionuclides such as Cs and Sr becomes important.

In planning the experiments to be performed during the Operating Phase of the Äspö Hard Rock Laboratory, the Swedish Nuclear Fuel and Waste Management Company (SKB) identified the need for a better understanding of radionuclide transport and retention processes in fractured crystalline rock. The needs of performance assessment included improved confidence in models to be used for quantifying transport of sorbing radionuclides. It was also considered important, from the performance assessment perspective, to be able to show that adequate transport data and parameters (distribution coefficients, diffusivity, parameters similar to the "flow wetted surface area", etc) could be obtained from site characterisation, or field experiments, and that laboratory results could be related to retention parameters obtained *in situ*. To address these needs, SKB in 1994 initiated a tracer test programme named the Tracer Retention Understanding Experiments (TRUE). The objectives of TRUE are given in Section 1.2.

The First Stage of TRUE (TRUE-1) /Winberg et al, 2000/ was performed in the detailed scale (0–10 m) and was focused on characterisation, experimentation and modelling of what was interpreted as a single fracture. Work performed included staged drilling of five boreholes, site characterisation, and installation of multi-packer systems to isolate interpreted hydraulically active structures. Subsequent cross-hole hydraulic tests and a comprehensive series of tracer tests were used to plan a series of three tracer tests with sorbing radioactive tracers. The *in situ* tests were supported by a comprehensive laboratory programme performed on generic as well as on site-specific material from the studied feature. In addition techniques for characterisation of the pore space of the investigated flow paths using epoxy resin have been developed and successfully tested *in situ*.

The various phases of tracer testing performed as part of TRUE-1 were subject to blind model predictions and subsequent evaluation /Elert, 1999; Elert and Svensson, 2001/. The results of the TRUE-1 experiments showed clear evidence of diffusion, by some researchers attributed to diffusion into the matrix with associated sorption on inner rock matrix surfaces. Other researchers claim that the observed retention can be attributed to diffusion/sorption in fine-grained fault gouge material. A distinction between the two

alternative interpretations can only be achieved with a full implementation and analysis of the developed resin technology.

When the TRUE Programme was set up it was identified that the understanding of radionuclide transport and retention in the Block Scale (10–100 m) also required attention in terms of a separate experimental programme. This programme was realised in the TRUE Block Scale Project.

This report presents the results of model calculations performed using various approaches/codes related to the block scale tracer tests with non-sorbing (conservative) and sorbing (reactive) tracers performed in the identified fracture network in the investigated TRUE Block Scale rock volume.

1.2 Rationale

1.2.1 Performance assessment

The block scale is important since it corresponds to the distance, "security distance" as defined by various national programs, between the geological repository and the nearest major fracture zone. It is also assumed that the bulk of the retention provided by a crystalline bedrock barrier is provided in this region.

As a consequence, the block scale is also an important modelling issue, cf Section 1.2.3. Prioritised aspects are to improve understanding of the nature of transport paths in block scale crystalline rock and the geological control on retention, and to assess the flow wetted surface, or equivalent properties, on the scale in question.

1.2.2 Site characterisation

The block scale is also important from a site characterisation perspective. Firstly, to provide the necessary data from which the geometrical, conceptual and numerical models are built, which are used to assess a given site. In addition the data collected in the block scale, whether obtained from the surface or from underground openings, are important for the detailed layout and design of a repository. This applies both to the positioning of storage tunnels and possible canister boreholes.

An experiment in the block scale hence provides a training ground for developing tools and methodologies to be employed in future site characterisation for a geological repository.

1.2.3 Modelling

Block scale (10–100 m) description of flow and transport provide opportunity for application of a variety of different modelling approaches and test relative to available experimental results. Among the 3D approaches (which can provide description of both flow and transport in low-permeable crystalline rocks) are stochastic continuum (SC), discrete feature network (DFN) modelling and channel network modelling (DFN/CN). Interesting questions arise at this particular scale. Depending on the problem at hand and the type of heterogeneity seen in the rock, can a smallest scale be identified at which the stochastic continuum approach can resolve flow and transport phenomena? Is it necessary to use discrete approaches below this threshold length scale to account for needs to incorporate and account for a higher degree of complexity/heterogeneity?

At the same time, the block scale constitutes a challenge for the more performance assessment related modelling approaches such as the LaSAR and Posiva approaches. Despite the simplification of the natural system employed in the TRUE Block Scale modelling; do the models provide adequate descriptions of flow and transport and are the model results adequate?

One of the basic ideas embedded in the TRUE Programme is that experimentation at various scales, laboratory (< 0.5 m), detailed scale (< 10 m) and block scale (10–100 m) will provide a basis for improved understanding on how to model flow and transport, and how this can be linked to transport models and transport parameters at different scales. It is expected that through this approach the uncertainties associated with extrapolation and prediction on a site scale (0.1–1 km) will be reduced. The TRUE Block Scale experiment described here constitutes the higher end member of the studied experimental scales.

1.2.4 Transport and retention

The principal difference between the TRUE-1 experiments and the TRUE Block Scale is obviously the difference in spatial scale of the experimentation. Of principal interest is whether the longer transport distances in themselves, through a higher degree of heterogeneity, will provide exposure to larger surface area, and thus more retention.

In addition, the performance of tracer tests in a network of structures implies that flow paths/transport routes will, to a variable degree, be affected by heterogeneity as exerted by variability in material properties as distributed over the fracture planes (intraplanar heterogeneity). An entity which potentially may add to the heterogeneity experienced along a flow path in a fracture network are the junctions or intersections between fracture planes. To what extent, and what conditions may these fracture intersection zones (FIZ) affect flow and transport? Is it possible to distinguish possible FIZ effects from that exerted by the intraplanar heterogeneity? Although the TRUE Block Scale does not provide an experimental array with the specific aim to investigate FIZs, the results from the performed experiments may still provide indirect evidence of the possible effects and relevance of FIZs. These because both multi-structure flow paths

and interpreted single structure flow paths have been investigated using non-sorbing (conservative) tracers.

The results from the TRUE-1 experiments /Winberg et al, 2000/ showed a consistent relative order amongst the utilised radioactive sorbing tracers (in order from lowest sorptivity); $Na^{+} < Ca^{2+} \approx Sr^{2+} << Rb^{+} \approx Ba^{2+} < Cs^{+}$. This relative order was observed both in the laboratory and *in situ*. An observation of this relative order at the larger scale would prove a conceptual verification of the retention properties and sorption processes at a larger scale.

Explicit evidence of the existence of gouge material (fault breccia and fine-grained fault gouge) have not been found in the investigated Feature A at the TRUE-1 site /Winberg et al, 2000/. Modelling performed within the Äspö Task Force has shown that assumptions of a geologic material with increased porosity/sorptivity in direct contact with the flowing groundwater, e.g. gouge material, can explain the observed increased retention in TRUE-1. In the network of structures investigated as part of TRUE Block Scale, however, there is firm evidence of fault breccia from the core logging, cf /Andersson et al, 2002a/. Laboratory analyses, taking into account uncertainties about the distribution of gouge material, are expected to provide a means for assessing the relative contribution to retention from the rock matrix and gouge material, respectively.

1.3 Previous experience of modelling block scale flow and transport

Development of modelling of flow and transport has experienced a dramatic evolution during the past 20 years. In parallel with evolution of computing power, the description of flow and transport in fractured media has equally had a dramatic evolution, where more and more realistic descriptions of fractured media have been introduced and the possibility to describe and analyse the effects of the natural variability and heterogeneity of the medium studied has been facilitated. Various ways to solve the governing partial differential equations have been introduced (DFN, FEM and BEM). In addition more powerful numerical solvers have become available.

A series of international studies which capture this evolution of conceptual and numerical models, associated solvers and the possibility to analyse various types of flow and transport problems are the INTRACOIN /SKI, 1984, 1986/, HYDROCOIN /OECD/NEA,1992/ and INTRAVAL /OECD/NEA, 1996/ studies. These series of model inter-comparison and validation studies involved benchmarking of various types of numerical and analytical models against suitable generic, laboratory and *in situ* experiments related to different geological media. These international comparative studies, all aimed at increasing confidence in modelling tools have been flanked by a number of GEOVAL symposia /e.g. OECD/NEA, 1995/ focused on increasing confidence in long-term safety assessment of geological repositories using i.a. modelling.

The above series of international studies can be regarded as a step-ladder where the issues raised, the analysis results, discussion and conclusions made, constitute a thermometer of the gradual evolution of understanding of flow and transport processes in subsurface geological formations. Although the studies performed obviously cover a wide range of geological media, attention has throughout been focused on fractured hard rock. It is therefore of interest to present the know-how gained during this 20 year period to put in context what has been achieved in the TRUE Block Scale Project. In this context it should be mentioned that one of the major accomplishments of the above studies is that they have provided discussion and policy forums for philosophical, scientific and practical relationship to the meaning and implication of words like "model verification" and "model validation". It is beyond the scope of this report to discuss this evolution but the reader is referred to /OECD/NEA, 1996/ for in depth accounts and discussion.

One of the general conclusions of the initial INTRACOIN study /SKI, 1986/ was that "*existing codes can reproduce results from field experiments*". The field experiments in this case were a) simulation of a dual tracer injection-withdrawal test in a sandy Aquifer /Pickens et al, 1981/ and b) Tracer test in a vertical fracture over a 30 m distance at a depth of about 100 m /Gustafsson and Klockars, 1981/. However, it was identified that the "*two field experiments leave too many degrees of freedom in describing different experimental conditions to allow validation in a stringent sense*". It was further identified *that* "*a crucial point in conjunction with the design of experiments aimed at validating transport modelling is the characterisation of heterogeneities and flow channels in the medium*". In conclusion, it was identified that "*there is an obvious need for better and more detailed experiments in the context of validation of models and codes for radionuclide transport. Experiments directly designed for the purpose of validation should be performed in order to reduce the degrees of freedom in interpreting the experimental situation. There is a need for closer collaboration between field experimenters, geologists, laboratory experimenters and modellers, in order to design and perform experiments which do not allow multiple interpretations*".

The HYDROCOIN study comprised analysis of the impact of different solution algorithms on groundwater flow calculations, the capability of models to describe field and laboratory experiments and assessment of the impact of the incorporation of various physical phenomena on groundwater flow calculations. The project was performed step-wise including code verification, model validation and sensitivity and uncertainty analysis of groundwater flow calculations. "*It was demonstrated that experiments for model validation purposes need to be designed and conducted over a range of conditions*". "*Experiments performed at a series of spatial and temporal scales are needed in order to demonstrate that there is an adequate understanding of scaling and averaging processes*". It was further concluded that "*several performance measures should be used in order to fully explain the system*" and "*parameter estimation results must be carefully examined for instability and insensitivity problems*". Finally, it was concluded that the "*choice of conceptual model can have a great influence on the outcome of an assessment*".

The INTRAVAL study concluded in 1996 but was continued by the INTRACOIN and HYDROCOIN studies with the overall objective of demonstrating the "fitness for purpose" of models which are intended for use in predicting natural system performance over large time and space scales. As in the case of the preceding studies, INTRAVAL

covers a wide range of geological environments. In the case of flow and transport in hard fractured rocks the following principal findings were stated /OECD/NEA, 1996/;

The test analysed test cases (Test Cases lB, 2, 4, 5, 6, and 9) involved the evaluation of alternative conceptual models for flow and transport in hard fractured rocks applied to scales of observation varying between a few centimetres up to several tens of metres. The largest experiments involving up to 0.25 Mm^3 of rock.

"*Performance assessment models of radioactive waste repositories often treat radionuclide transport through these type of rocks in a very conservative manner, often assuming channelled flow in notional single fractures or streamtubes. The INTRAVAL test cases were designed to simulate flow and transport experiments using models which accounted, to varying extent, for scale dependent dispersion, stochastic descriptions of spatial variability including fracture networks, channelled flow within fractures, mixing between channels, and diffusion of tracers from the fractures into and out of immobile pore fluids. Significantly, none of the test cases was able to define the* "*plumbing*" *system deterministically in terms of real or potential flow channels. Rock matrix diffusion can potentially provide a very important retardation mechanism. However, it is not clear whether the process will lead to significant retardation in the conditions appropriate to groundwater transport from a repository at a specific site. For one test case, there was evidence to suggest that the process was significant in the circumstances of the case, but the circumstances (short time scales) of most of the test cases were such that rock-matrix diffusion would be expected to have little effect. For conditions appropriate to a repository (longer times and sorbing species), matrix diffusion might play an increasingly important role*".

"*In general, it was found that tracer test results could be simulated with rather simple models that involve only a few parameters, if they were adequately conditioned. More complex, multi-parameter models did not perform as well as the simple models, unless they were conditioned with the large amounts of data available from a well characterised site/experiment. The main drawback to such complex models is that many of the parameters cannot be measured but must be estimated or derived. Ideal models may be those which capture salient features of geological complexity with a relatively small number of parameters*".

"*The predictive capability of typical, greatly simplified performance assessment flow and transport models was not tested in INTRAVAL, and clearly needs to be explored in site specific circumstances. Where predictions were made for repository-scale problems using different models, calibrated with laboratory experiments, equally good fits to the laboratory data could yield very different results when applied at the larger scale*".

"*Few of the test cases dealt with reactive (sorbing) tracers, focusing on advection and dispersion rather than other radionuclide transport mechanisms. In reality, many tracers interact chemically or physically with the rock to various extents*".

"*Heterogeneities and anisotropy in physical properties exert a profound influence on flow and transport on a broad range of scales. Similarly, the perturbing effect of underground excavations is such that considerable care is required to ensure that observations made in shafts and tunnels do not give a distorted and inaccurate picture of intact rock behaviour*".

It should be mentioned that the legacy of INTRACOIN, HYDROCOIN and in particular INTRAVAL has been continued within the context of the OECD/NEA GEOTRAP series of workshops focused on Radionuclide migration in geologic, heterogeneous media /OECD/NEA, 1998, 2002/.

It is of interest to assess the TRUE Block Scale Project achievements and accomplishments in relation to shedding more insight on the various issues and demands expressed as outcomes of the various international model studies described above. This discussion can be found in Section 8.7.

1.4 Main findings from modelling TRUE-1

The first stage of the Tracer Retention Understanding Experiments (TRUE-1) /Winberg et al, 2000/ was performed as a SKB funded project. The overall objectives of TRUE are to develop the understanding of radionuclide migration and retention in fractured low-permeable rock, to evaluate the realism in applied model concepts, and to assess whether the necessary input data to the models can be collected from site characterisation, cf Section 1.5. Further, to evaluate the usefulness and feasibility of different model approaches, and finally to provide *in situ* data on radionuclide migration and retention. The impetus to use multiple model approaches in prediction and post-experiment evaluation is facilitated through a close collaboration with the Äspö Task Force on Modelling of Groundwater Flow and Transport of Solutes. The TRUE programme is a staged programme which addressed various scales; from laboratory (< 0.5 m), detailed scale (< 10 m) and block scale (10–100 m). The First TRUE Stage was performed at the detailed scale with the specific objectives of providing data and conceptualising the investigated feature using conservative and sorbing tracers. Further, to improve methodologies for performing tracer tests, and to develop and test a methodology for obtaining pore volume/aperture data from epoxy resin injection, excavation and subsequent analyses.

The experimental site is located at approximately 400 m depth in the north-eastern part of the Äspö Hard Rock Laboratory. The identification of conductive fractures and the target feature has benefited from the use of BIPS borehole TV imaging combined with detailed flow logging. The assessment of the conductive geometry has been further sustained by cross-hole pressure interference data. The investigated target feature (Feature A) is a reactivated mylonite, which has later undergone brittle deformation. The feature is oriented northwest, along the principal horizontal stress orientation, and is a typical conductor for Äspö conditions. Hydraulic characterisation shows that the feature is relatively well isolated from its surroundings. The near proximity of the experimental array to the tunnel (10–15 m) implies a strong gradient (approximately 10%) in the structure, which has to be overcome and controlled during the experiments.

A methodology for characterising fracture pore space using resin injection, excavation using large diameter coring and subsequent analysis with photo-microscopic and image analysis techniques was developed and tested at a separate site. The results show that epoxy resin can be injected over several hours, and that the estimated areal spread is in

the order of square metres. The mean apertures of the two investigated samples were 239 and 266 microns, respectively. Assessment of spatial correlation shows practical ranges in the order of 3–5 millimetres.

Performed tracer tests with conservative tracers in Feature A show that the feature is connected between its interpreted intercepts in the borehole array. The parameters evaluated from the conservative tests; flow porosity, dispersivity and fracture conductivity are similar, indicating a relative homogeneity.

Previous work has identified cationic tracers, showing sorption by ion exchange, as the most suitable tracers for sorbing tracer experiments at ambient Äspö conditions. Laboratory experiments on generic Äspö material and site-specific material included batch sorption experiments on various size fractions of the geological material, and through diffusion experiments on core samples of variable length on a centimetre length scale. The sorption capacity was found to be strongly affected by the biotite content and the sorption was also found to increase with contact time. The sorption capacity was found to follow the relative order; $Na^+ < Ca^{2+} \approx Sr^{2+} << Rb^+ \approx Ba^{2+} < Cs^+$.

The field tracer tests, using essentially the same cocktail of sorbing tracers as in the laboratory, were found to show the same relative sorption capacity as seen in the laboratory. A test using radioactive $^{137}Cs^+$ showed that after termination of the test, some 60% of the injected activity remained sorbed in the rock.

1.4.1 SKB TRUE Project team analysis

The interpretation of the *in situ* tests with sorbing tracers was performed using the LaSAR approach /Cvetkovic et al, 1999/, developed as a part of the TRUE project. In this approach the studied flow path is viewed as a part of an open fracture. Key processes are spatially variable advection and mass transfer. The evaluation showed that laboratory diffusion data based on intact unaltered wall rock are not representative for *in situ* conditions. A close fit between field and modelled breakthrough is obtained only when a parameter group which includes diffusion/sorption (in terms of $k \cdot \kappa$, cf Section 6.1) is enhanced by a factor varying between 32–50 for all tracers and experiments (except for Cs) and 140 for Cs^+. The interpretation attributed the noted enhancement being mainly due to higher diffusivity/porosity and higher sorption in the part of the altered fracture rim zone of the feature which is accessible over the time scales of the *in situ* experiments, compared to data obtained from analysis of core samples of unaltered rock in the laboratory. Estimates of *in situ* values of the important transport parameters are provided under an assumption of a valid range of porosity in the accessible part of the fracture rim zone is in the order of 2–2.4%.

Unlimited diffusion/sorption in the rock matrix was interpreted as the dominant retention mechanism on the time scales of the TRUE-1 *in situ* experiments. The effects on tracer retention by equilibrium surface sorption and sorption in fine-grained fault gouge material were found to be observable, but of secondary importance. Similarly, the effect of sorption into stagnant water zones within the fracture was found to be limited.

1.4.2 Alternative interpretation

The TRUE-1 experiments have also been predicted and analysed using various other modelling concepts within the context of the Äspö Task Force on modelling of groundwater flow and solute transport. Evaluation of the modelling work is presented by /Elert, 1999/, /Elert and Svensson, 2001/ and /Marschall and Elert, in prep/.

Some of the concepts/models employed in the analysis of the TRUE Block Scale test data were also employed in the analysis of the TRUE-1 results (JNC-Golder and Posiva-VTT). Results from some of the alternative conceptual models and modelling approaches employed to the TRUE-1 data set were presented and discussed at the 4th International Äspö Seminar /SKB, 2001/ which was focused on the results and conclusions of TRUE-1 tracer tests and associated modelling.

The outcome of the discussion at the TRUE-1 seminar can be summarised in the following main bullets;

- Retardation of sorbing solutes showed the same order as in the laboratory scale experiments. The extent of retardation was greater *in situ* than what laboratory experiments on intact unaltered wall rock suggested.

- There is a general consensus that the observed retardation observed in the TRUE-1 experiments requires diffusion into immobile pore spaces to be an active process. This was supported by the –3/2 slope noted in log-log breakthrough curves. Whether this is due to diffusion (and subsequent sorption) in the altered matrix rock (fracture rim zone), or in possible fault gouge cannot be differentiated with available data.

- Some researchers claim that the observed enhanced retardation compared to laboratory data may be explained by diffusion into stagnant water pools, pure surface sorption, or may be due to an underestimation in the flow-wetted surface area /Neretnieks, 2002/. Yet another alternative explanation to the noted retention is a more complex flow path (multi-layered structure) combined with exposure to fine-grained fault gouge /Mazurek et al, 2002; Jakob et al, 2002/,

- A clear differentiation between the principal active process can only assessed by performing the planned resin injection and subsequent excavation and analysis.

- It was identified that experiments of TRUE-1 type are important for improving the understanding of retention processes. However, this type of experiment may not necessarily be part of an actual a site characterisation programme.

- It was recommended to broaden the data base from the TRUE-1 site before characterising pore space with resin techniques. This includes tracer dilution tests using sinks in other features than Feature A.

1.5 Objectives

The overall objectives of the Tracer Retention Understanding Experiments (TRUE) are to:

- develop an understanding of radionuclide migration and retention in fractured rock,
- evaluate to what extent concepts used in models are based on realistic descriptions of a rock volume and if adequate data can be collected in site characterisation,
- evaluate the usefulness and feasibility of different approaches to model radionuclide migration and retention,
- provide *in situ* data on radionuclide migration and retention.

The specific objectives of the TRUE Block Scale Project given in the developed test plan /Winberg, 1997/ were:

1. increase understanding of tracer transport in a fracture network and improve predictive capabilities,
2. assess the importance of tracer retention mechanisms (diffusion and sorption) in a fracture network,
3. assess the link between flow and transport data as a means for predicting transport phenomena.

1.6 Tested hypotheses

Before coming to the point where block scale tracer experiments could be realised a vast effort had been invested in site characterisation and development of hydrostructural models /Andersson et al, 2002a/. It was decided that the experimental work and subsequent evaluation modelling should be should be guided by a series of hypotheses. Three basic questions were therefore posed in relation to the performed tracer tests /Winberg, 2000/, their planning and evaluation. These are:

Q1) “What is the conductive geometry of the defined target volume for tracer tests within the TRUE Block Scale rock volume? Does the most recent hydrostructural model, cf Figure 1-3, reflect this geometry with sufficient accuracy to allow design and interpretation of the planned tracer tests?”

Q2) “What are the properties of fractures and fracture zones that control transport in fracture networks?”

Q3) “Is there a discriminating difference between breakthrough of sorbing tracers in a detailed scale single fracture, as opposed to that observed in a fracture network in the block scale?”

On the basis of these questions corresponding hypotheses have been formulated /Winberg, 2000/, to be addressed by the tracer tests and the subsequent evaluation;

H1) “The major conducting structures of the target volume for tracer tests in the TRUE Block Scale rock volume trend northwest and are subvertical. Being subvertical, and subparallel, they do not form a conductive network in the designated target volume. For the purpose of testing fracture network flow and transport effects in the current borehole array, second-order NNW features are required to provide the necessary connectivity between the major conducting NW structures!” For geometrical reference, cf Figures 1-1–1-4.

H2a) “Fracture intersections have distinctive properties and have a measurable influence on transport in fracture/feature networks. These distinctive properties may make the intersection a preferential conductor, a barrier, or a combination of both!”

H2b) “In-plane heterogeneity and anisotropy have a measurable influence on transport of solutes in a block scale fracture network!”

H3) “It is not possible to discriminate between breakthrough curves of sorbing tracers in a single fracture from those obtained in a network of fractures!”

1.7 Location and configuration of the experiment

1.7.1 Location of experiment

A restriction in selecting a block for the TRUE Block Scale experiment was the overall usage of the experimental level of the Äspö HRL, cf Figure 1-1. The north-eastern part of the laboratory was allocated for the REX and TRUE-1 experiments. At the time of locating the TRUE Block Scale Experiment the inner part of the tunnel spiral, south of the TBM assembly hall was used by the ZEDEX experiment, the Demonstration Repository facility and by the Long-term tests on buffer materials. The area inside the tunnel spiral and north of the TBM was not used by any experiment. However, previous analysis had shown that the inner part of the laboratory exhibits a high degree of hydraulic connectivity /Winberg et al, 1996a/. In the western part of the laboratory the Chemlab experiments was in progress in borehole KA2512A. This experiment is sensitive to changes in the chemical composition of the groundwater, but does not create any hydraulic disturbances. The final part of the TBM tunnel was allocated for the development of the Prototype Repository project.

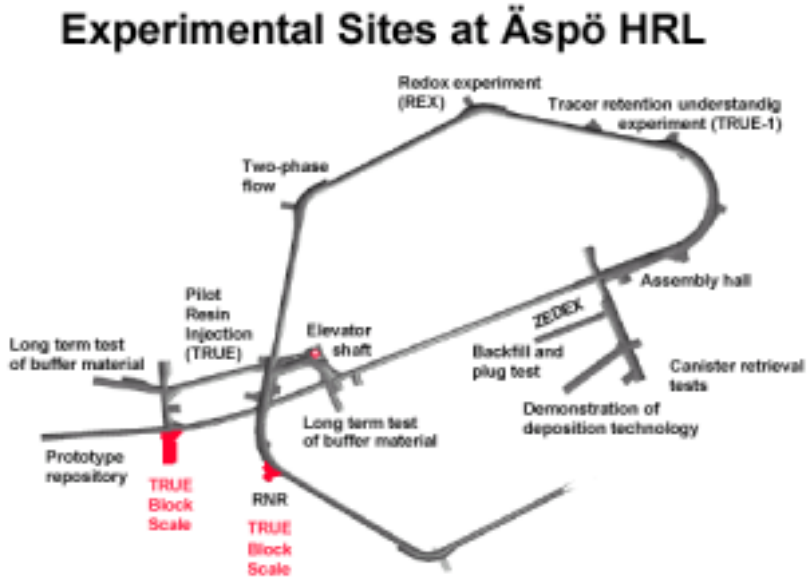

Figure 1-1. *Location of the TRUE Block Scale experiment.*

A set of desired experimental conditions were defined for positioning the TRUE Block Scale experiment /Winberg, 1997/. Of particular relevance for performance of block scale tracer tests are;

- Location of experimental site outside tunnel spiral.
- Location away from major fracture zones (i.e. EW-1 and NE-1).
- Access from multiple locations (vertically) in the laboratory.
- No adverse hydraulic interference from other activities in the laboratory.
- Transmissivity range of fractures making up the studied fracture network in the range ; $T = 5 \cdot 10^{-8} – 5 \cdot 10^{-7}$ m^2/s.
- Small hydraulic gradient ($I < 0.05$).
- Flow velocities such that diffusion can be made a measurable process.

The rationale used for selecting the particular site used for TRUE Block Scale is discussed by /Hermanson et al, 2002/, /Winberg and Hermanson, 2002/ and /Andersson et al, 2002a/ and the final location of the experimental volume is indicated in Figure 1-1. All the criteria defined above were met by the experimental site selected.

1.7.2 Definitions

The TRUE Block Scale site is located in the south-western part of the experimental level at the Äspö HRL, cf Figure 1-1. The area covered by the developed borehole array is denoted "TRUE Block Scale Rock volume" and has a lateral extent of 250x200 m, cf Figure 1-1, and extends between –500 masl to –350 masl in the vertical direction. The area containing the fracture network used in the tracer tests is about 100x100x50 m and is denoted the "TRUE Block Scale Tracer Test volume (TTV)", cf Figure 1-2.

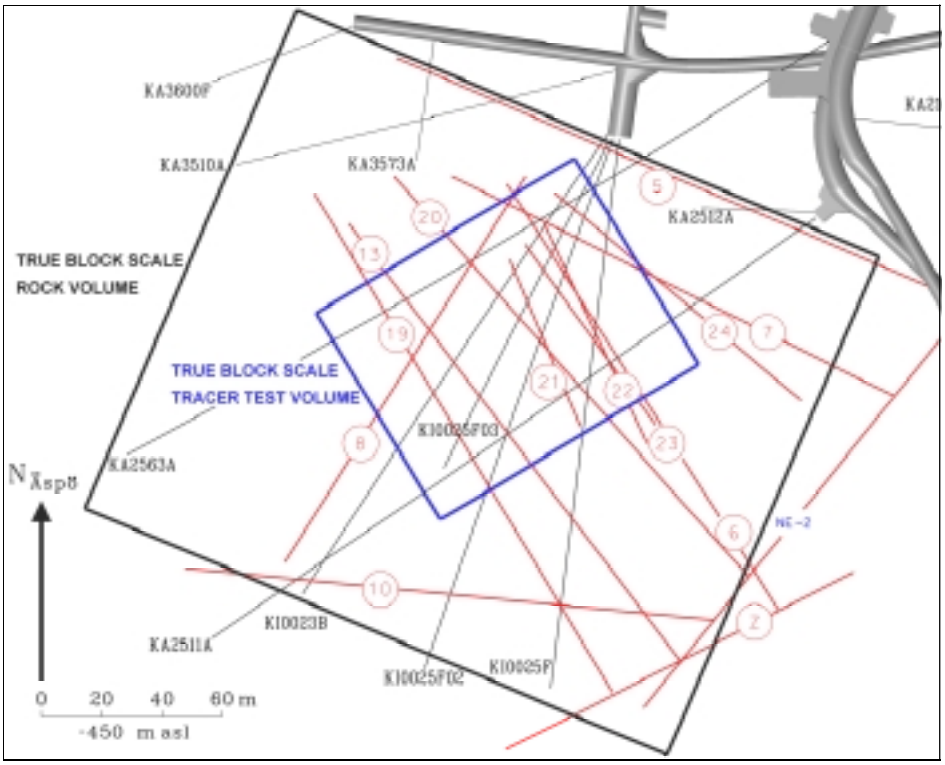

Figure 1-2. *Definition of experimental volumes related to the TRUE Block Scale experiments.*

1.8 Experimental strategy and staging

The TRUE Block Scale Project adopts a staged approach. The key element desired in the experimental strategy was expressed as "Iterative characterisation with strong interaction between modelling and experimental work to ensure flexibility". This implied that site characterisation data from each new borehole was used to update the hydro-structural model of the investigated block, whereby a successive refinement is obtained which is implemented in design, predictive modelling, performance and evaluation of block scale experiments. The performed work has been divided into five basic stages;

The "Scoping Stage" was intended to determine whether the identified experimental site fulfil the basic requirements /Andersson et al, 2002a/. Field work included drilling and characterisation of boreholes KA2563A and KA3510A. The Scoping Stage was followed by a technical review in October 1997 and a decision to proceed in accordance with the developed test plan.

The field work of the "Preliminary Characterisation Stage" included drilling and characterisation of boreholes KI0025F and KI0023B. A series of cross-hole hydraulic interference and tracer dilution tests were carried out /Andersson et al, 2001a/. One of the tracer dilution tests was prolonged and the breakthrough of the injected tracer was observed. The basic results of this stage is presented by /Winberg, 1999/.

The field work of the "Detailed Characterisation Stage" included drilling and characterisation of borehole KI0025F02. In addition a comprehensive series of cross-hole hydraulic interference and tracer dilution and tracer tests were carried out /Andersson et al, 2001b/.

The "Tracer Test Stage" included drilling and characterisation of the final borehole, KI0025F03, which was drilled to verify the March'99 hydro-structural model /Doe, 2001/ with an additional objective to furnish additional tracer injection points. The resulting hydro-structural model /Hermanson and Doe, 2000/ is presented in Figure 1-3. The work scope of this stage included, apart from drilling and characterisation of a new borehole, optimisation of existing multi-packer installations. However, the main activity was a series of three tracer test phases; Phase A which was focused on identifying the best pumping (sink) section /Andersson et al, 2000a/, Phase B which was devoted to demonstrating sufficiently high mass recovery of non-sorbing species to allow usage of radioactive sorbing tracers /Andersson et al, 2000b/, and finally Phase C /Andersson et al, 2001c/, which included performance of four injections with radioactive sorbing tracers in three sections.

The last of the five stages, the "Evaluation and Reporting Stage," include evaluation of experimental data and modelling results and reporting.

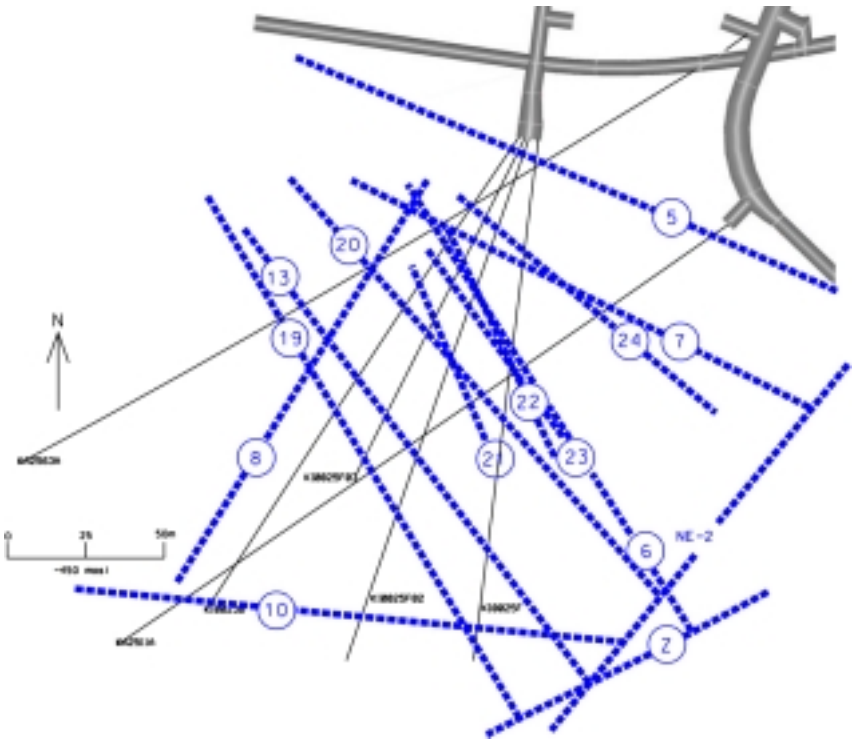

Figure 1-3. *Hydro-structural model based on characterisation data from KI0025F03 /Hermanson and Doe, 2000/.*

1.9 Boreholes and installations

1.9.1 Boreholes

The TRUE Block Scale borehole array is made up of 10 cored boreholes. Five of those have been drilled specifically within the TRUE Block Scale Project. The remainder have been drilled as part of the development of the spiral access tunnel, or as part of the characterisation for other projects, i.a. the Prototype Repository project.

The boreholes are with two exceptions of 76 mm drilled using the triple-tube technique, cf Section 3.1. The boreholes penetrating the investigated rock volume are presented in Table 1-1 and Figure 1-4.

Table 1-1. Compilation of data on boreholes penetrating the TRUE Block Scale Rock volume (detailed list of borehole coordinates, bearings and inclinations is provided by /Andersson et al, 2002a/). TT=Triple tube core barrel, Solexp.=ANDRA/Sol-experts multi-packer system.

Borehole Id	Diameter (mm)	Length (m)	Completed	Project
KA2511A	56	293.0	1993-09-05	Turn 2
KA2563A	56	263.4	1996-08-24	TRUE BS
KA3510A	76 TT	150.1	1996-09-09	Various
KI0025F	76 TT	193.8	1997-04-25	TRUE BS
KI0023B	76 TT, Solexp.	200.7	1997-11-20	TRUE BS
KI0025F02	76 TT, Solexp.	204.2	1998-08-25	TRUE BS
KI0025F03	76 TT	141.7	1999-08-13	TRUE BS
KA3548A	76 TT	30.0	1998-06-26	Prototype
KA3573A	76 TT	40.1	1997-09-11	Prototype
KA3600F	76 TT	50.1	1997-09-24	Prototype

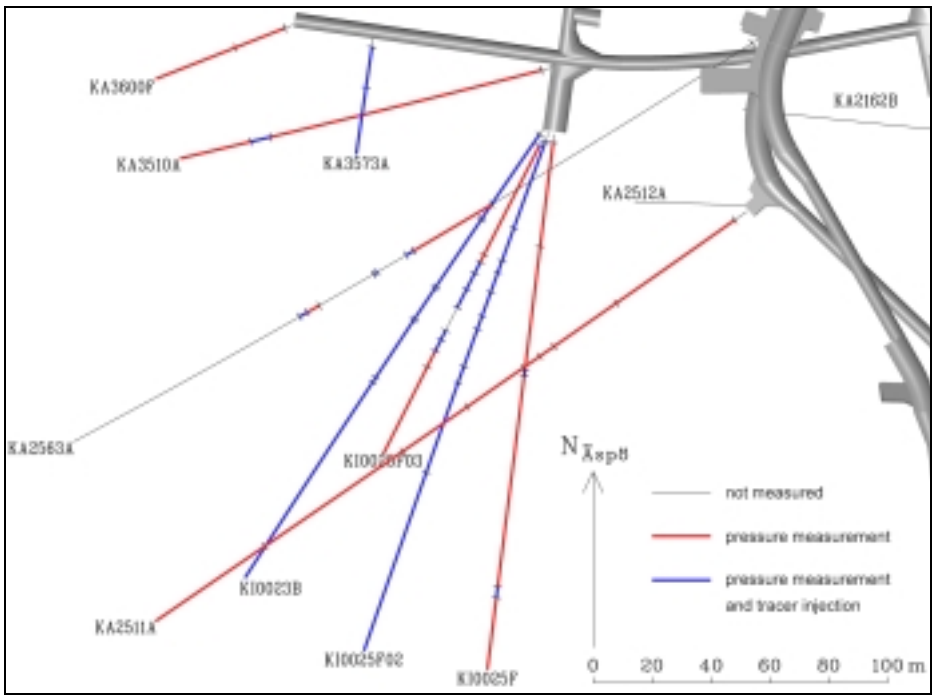

Figure 1-4. *TRUE Block Scale borehole array and disposition. The figure also indicates the locations of packed off intervals in the boreholes (per June 2000).*

1.9.2 Installations

Of the boreholes listed in Table 1-1, seven have been instrumented as part of the project. The exceptions being the boreholes drilled as part of the Prototype Repository experiment. In the boreholes instrumented by the TRUE Block Scale Project two types of packer equipment have been utilised; The so-called "SKB/GEOSIGMA system" and the "ANDRA/Solexperts system". A brief description of the two systems is provided in /Andersson et al, 2002a/.

1.10 Outline of report series

The series of final reports from the TRUE Block Scale Project include the following four volumes;

1. Characterisation and model development /Andersson et al, 2002a/.

2. Tracer tests /Andersson et al, 2002b/.

3. Modelling of flow and transport (this present report).

4. Synthesis of flow, transport and retention in the block scale /Winberg et al, 2002/.

The four volumes of the final report series are supported by a series of progress reports. In the case of volume no 3 more detailed accounts of the modelling presented therein are presented by /Paris, 2002; Rachez and Billaux, 2002; Fox and Dershowitz, 2002; Dershowitz et al, 2002a,b; Dershowitz and Klise, 2002; Poteri, 2002; Gómez-Hernández et al, 2002; Holton, 2002; Cvetkovic and Cheng, 2002/.

2 Overview of modelling programme and approaches

One of the original ideas of the TRUE Block Scale Project was to establish understanding of the investigated site in an iterative manner, and further to use modelling interactively in the characterisation process. Initially, only one modelling concept, the discrete feature network concept was employed. Towards the later parts of the characterisation, additional approaches were included (stochastic continuum and channel network models). For the final round of predictions and evaluations, associated with the radioactive sorbing tracer tests making up Phase C, two additional approaches were introduced (the LaSAR and Posiva Streamtube concepts). To these five modelling approaches should be added the SKB-GEOSIGMA advection-dispersion analytical model employed in the basic evaluation of transport parameters employed to all tracer tests performed during the TRUE Block Scale Project.

The wide range of model approaches applied to the available data constitutes a test of the ability of the site characterisation /Andersson et al, 2002a/ to satisfy the needs of the various approaches. The use of a multitude of model approaches clearly invites a comparison. It should be emphasised that model comparison is not the primary focus of the project. Rather the comparison was driven towards an overall improved understanding of flow and transport in fractured crystalline rock where the collective effort and experience enhances our understanding.

In the following sections the basic mathematics of flow and transport in fractured crystalline rock is presented in a condensed format, Sections 2.1–2.2. The latter section is finished with a common conceptual basis for transport and retention that will be discussed in more detail in Section 6.1. Subsequently, a suite of descriptions of the various approaches are presented with their respective mathematical and conceptual basis, cf Sections 2.3–2.8. Care has been taken to make the notation as internally consistent as possible.

2.1 Modelling of groundwater flow

Groundwater flow is certainly not the main focus of the TRUE Block Scale Project. However, assumptions about the macro-properties of the flow field are an important aspect of the study of transport and retention. A basic understanding of groundwater flow therefore is a prerequisite for design and planning of a transport experiment. In this context modelling is not a critical necessity, but a well-performing numerical (or analytical) model of groundwater flow can be an important element in design calculations and model predictions.

This section attempts to highlight the common "flow" basis of the various models presented in subsequent sections of this chapter, as well as important differences between the models. The "microscopic scale" properties of the flow field, i.e. the short range variations in aperture (groundwater velocity) that have a direct bearing on dispersion properties, are not discussed.

The level of detail of the flow simulations employed in the project is varied, ranging from a transient, three-dimensional, continuum representation by a large finite difference model (Stochastic Continuum approach, cf Section 2.4) to the direct use of non-sorbing tracer test results for evaluating travel times (Posiva streamtube approach, cf Section 2.6, and the LaSAR approach, cf Section 2.7).

All models which include description of groundwater flow solve some variant of the classical diffusivity equation:

$$div(K\nabla h) = S_S \frac{\partial h}{\partial t} + q, \qquad (2\text{-}1)$$

where:
K : hydraulic conductivity tensor [LT^{-1}],
h : hydraulic head [L],
S_s : specific storage [L^2],
q : source term [L^3T^{-1}].

Note that for all models but one (the Stochastic Continuum), since flow is assumed to be at steady state, Equation (2-1) reduces to:

$$div(K\nabla h) = q, \qquad (2\text{-}2)$$

with the same notations as above. Also, when flow is restricted to one-dimensional elements (JNC-Golder approach, cf Section 2.8), the diffusivity equation is further reduced to:

$$T \frac{\partial^2 h}{\partial x^2} = 0\,, \qquad (2\text{-}3)$$

where:
T is the integrated hydraulic transmissivity of each pipe [L^3T^{-1}];
x is the coordinate along the pipe [L].

The differences in the approach to modelling of groundwater flow between the various groups can be expressed in terms of "dimensionality" of the elements used to discretise the different types of heterogeneities of fractured crystalline rock, as outlined in Table 2-1.

Table 2-1. Main entities used to represent the flow domain.

Modelling group/model	Representation of flow domain
ENRESA-UPV/UPC (Stochastic Continuum)	Multiple 3-D elements
Nirex-Serco (Discrete Fracture Model)	Multiple interconnected 2-D elements
JNC-Golder (Channel Network)	Multiple interconnected 1-D elements
Posiva-VTT (Streamtube)	Non-connected 1-D paths
SKB-WRE (LaSAR)	Non-connected 1-D paths

2.2 Modelling of transport/retention

Under this heading, we consider all processes pertaining to transport and retention, including the microscopic, or "local", flow model explicitly used by some groups (see the Posiva streamtube approach, Section 2.6, for example). In the same manner as in the preceding paragraph, the basic equations that represent the phenomena simulated by the various modelling groups are reviewed. The governing equations are successively "expanded" by adding physical processes one by one, trying to emphasise "common ground" and differences between the groups, in order to provide a better perspective on the work performed and presented in subsequent sections of the report.

2.2.1 Advection

All models use, either explicitly or implicitly, the assumption that advection is one of the mechanisms for mass transfer. This can be written as:

$$\theta \frac{\partial C}{\partial t} + V_i \frac{\partial C}{\partial x_i} = 0 \qquad (2\text{-}4)$$

where:
C is the solute concentration [ML^{-3}],
t is the time [T],
V_i is the macroscopic velocity in direction i (advective, or Darcy velocity) [LT^{-1}],
θ is the porosity [–],

Indexation implies a summation over the three coordinates in 3D.

Note that deducing the macroscopic velocity in Equation (2-4) from flow computations is not always a straightforward problem. When dealing with fracture flow, a "geometrical" parameter must be inputted, that relates flow rates in the fracture with the velocities in Equation (2-4). This is often done by assuming a (transmissivity vs aperture) relationship.

For three models (JNC Channel Network, Posiva streamtube, and SKB LaSAR), advection is only one-dimensional, so the above equation reduces to a scalar one.

2.2.2 Dispersion

Still accounting for flow, but this time at the microscopic level, three models (ENRESA Stochastic Continuum, Nirex Discrete Fracture Model, and JNC Channel Network) use a lumped dispersion, thus solving for the following advection-dispersion equation:

$$\theta\frac{\partial C}{\partial t}+V_i\frac{\partial C}{\partial x_i}=\frac{\partial}{\partial x_i}\left(D_{ij}\frac{\partial C}{\partial x_j}\right), \qquad (2\text{-}5)$$

where D_{ij} is the component of the dispersion tensor [L^2T^{-1}].

More precisely, the only fully three-dimensional model (the Stochastic Continuum model described in Section 2.4) uses an anisotropic dispersion tensor (different longitudinal and transverse dispersivities), and the model with a two-dimensional flow domain (the Discrete Feature Network model described in Section 2.5) uses a longitudinal dispersion only, as does the Channel Network model (cf Section 2.8). Also, the porosity θ is equal to unity when considering that flow occurs only in the fracture (Discrete Feature Network and Channel Network models), which further simplifies the equation. For a one-dimensional model an example of the simplified equation reads:

$$\frac{\partial C}{\partial t}+V\frac{\partial C}{\partial x}=D_l\frac{\partial^2 C}{\partial x^2}, \qquad (2\text{-}6)$$

where:
V is the one-dimensional velocity [LT^{-1}];
x is the single spatial coordinate [L];
D_l is the longitudinal dispersion coefficient [L^2T^{-1}].

The main differences between the five models can already be identified, with two models that put more emphasis on the flow field, and tend to use lumped parameters for transport processes (i.e. the ENRESA Stochastic Continuum and the Nirex Discrete feature Network models), two models that essentially do not consider the macroscopic flow field (no attempt is made to predict it) but try to reproduce in somewhat more detail the local transport processes (i.e. the Posiva streamtube approach and the SKB LaSAR approach), and one model forming a midway alternative, i.e. the JNC-Golder Channel network model.

Molecular diffusion within the flow domain is taken into account explicitly by Posiva as part of the mechanism for "dispersion". It enables solute to "jump" from one streamline to the adjacent ones, therefore smoothing out the variations in transit time between various stream lines. Instead of using a longitudinal dispersion coefficient, the Posiva group therefore directly deduces the distribution of transit times from an hypothesis on the velocity profile along fractures, and the value of molecular diffusion, whereas all other groups implicitly include diffusion through use of a mechanical dispersion parameter.

2.2.3 Surface sorption

Diffusion within the flow domain is also considered as the mechanism enabling the migration of solutes to the surfaces of a fracture, and therefore permitting both sorption onto the surfaces, and further diffusion into the rock matrix. In a first step, taking into account linear equilibrium sorption on the fracture surfaces adds a retardation factor to the equation. Its form then becomes:

$$R\frac{\partial C}{\partial t}+V\frac{\partial C}{\partial x}=D_l\frac{\partial^2 C}{\partial x^2}\,. \qquad (2\text{-}7)$$

In the case of a homogeneous channel, the retardation factor R [–] can be related to the surface sorption coefficient, K_a [L], in the following manner:

By definition,

$$R = \frac{m_s + m_a}{m_s}\,, \qquad (2\text{-}8)$$

where:
m_s : mass in solution [M];
m_a : adsorbed mass [M].

We introduce the adsorbed fraction F [ML^{-2}],

$$F=K_aC=K_a\frac{m_s}{V_w}=\frac{m_a}{S}\,, \qquad (2\text{-}9)$$

where:
S is the surface available for adsorption [L^2];
V_w is the volume of water containing the solute mass [L^3];

Computing the value of m_a from these two equations, and equating them, we get:

$$K_a m_s \frac{S}{V} = m_s (R-1), \tag{2-10}$$

Therefore :

$$R = 1 + K_a \frac{S}{V_w} \tag{2-11}$$

Note that the quantity $\frac{S}{V_w}$ $[L^{-1}]$ is the Flow Wetted Surface (FWS) per unit volume of fluid.

2.2.4 Diffusion and adsorption into the rock matrix

The diffusion and adsorption of solutes into the rock matrix brings in an additional term in the equation for transport in the fracture, while a new equation governs transport within the matrix. Note that all groups consider the transport in the matrix to be only diffusive, and to be one-dimensional, therefore the new equation is of a well known type.

$$R\frac{\partial C}{\partial t} + V\frac{\partial C}{\partial x} = D_l \frac{\partial^2 C}{\partial x^2} - 2\frac{\theta D_m}{2b}\frac{\partial C_m}{\partial z}\bigg|_{z=0}, \tag{2-12a}$$

and

$$R_m \frac{\partial C_m}{\partial t} - D_m \frac{\partial^2 C_m}{\partial z^2} = 0 \tag{2-12b}$$

where:
b is the half aperture of the fracture $[L]$;
θ is the porosity of the rock matrix [–];
C_m is the concentration in the rock matrix $[ML^{-3}]$;
D_m is the pore diffusivity into the rock matrix $[L^2T^{-1}]$;
z is the distance normal to the fracture $[L]$;
R_m is the matrix sorption retardation factor [–].

Note that all quantities pertaining to the matrix are given index "m": C_m $[ML^{-3}]$, R_m [–], D_m $[L^2T^{-1}]$ are the concentration, retardation coefficient and diffusion coefficient, respectively, inside the pores of the matrix.

In the same manner as R can be related to the surface sorption coefficient K_a, R_m can be related to the volume sorption coefficient K_d [–]:

R_m is defined similarly by:

$$R_m = \frac{m_s + m_a}{m_s}, \tag{2-13}$$

where this time:
m_s [M] and m_a [M] are the mass in solution and the adsorbed mass in the matrix.

In this case the adsorbed fraction F_m [–] is defined by:

$$F_m = K_d C_m = K_d \frac{m_s}{V_\phi} = \frac{m_a}{m_{sol}}, \tag{2-14}$$

where:
V_Φ is the volume of the matrix pore space [L^3];
m_{sol} is the mass of the adsorbing material [M].

We thus have:

$$m_{sol} = \rho V_{sol} = \rho V_\phi \frac{1-\theta}{\theta}, \tag{2-15}$$

where:
ρ is the density of the solid fraction [ML^{-3}].

Computing m_a by using Equation (2-13), and on the other part by combining Equations (2-14) and (2-15), we get:

$$m_s(R_m - 1) = K_d \frac{m_s m_{sol}}{V_\phi} = K_d m_s \rho \frac{1-\theta}{\theta}, \tag{2-16}$$

which yields :

$$R_m = 1 + K_d \rho \frac{1-\theta}{\theta} \tag{2-17}$$

Not all groups are using the full form of Equations (2-12a) / (2-12b). For example, the Posiva-VTT and SKB-WRE groups do not include the dispersion term $D_l \frac{\partial^2 C}{\partial x^2}$, because it is accounted for in the distribution of transit times, while the ENRESA group did not include matrix diffusion explicitly in its full-fledge three-dimensional model, but used a simpler geometry to test its effect and add it indirectly.

2.2.5 Heterogeneity

The properties in Equations (2-12a) / (2-12b) may be spatially heterogeneous. Among the many possible types of heterogeneities, two received special attention from some modelling groups in the course of the TRUE Block Scale modelling:

- The "matrix" is constituted of several types of retention zones, with various properties: fault gouge, fault breccia, altered fracture rim zones (Posiva-VTT group).
- The pore diffusion coefficient D_m may depend on the distance from the fracture wall z (SKB-WRE group).

Accounting explicitly for these yields a slightly different set of equations,

$$R\frac{\partial C}{\partial t}+V\frac{\partial C}{\partial x}=D_l\frac{\partial^2 C}{\partial x^2}-\sum_{i=1}^{N}\frac{\alpha^i\theta^i D_m^i}{b^i}\frac{\partial C_m^i}{\partial z}\bigg|_{z=0}, \qquad \text{(2-18a)}$$

and

$$R_m^i\frac{\partial C_m^i}{\partial t}-\frac{\partial}{\partial z}D_m^i\frac{\partial C_m^i}{\partial z}=0. \qquad \text{(2-18b)}$$

where:
N is the number of retention zones;
i is the index of a retention zone, noted as superscript for all quantities concerned;
α^i is the fraction of the fracture unit area in contact with retention zone "i". ($\Sigma\alpha^i=1$)

Note that instead of 2 equations, we now have one equation "(2-18a)", plus N equations "(2-18b)".

2.3 1D Advection-Dispersion

This approach used by SKB-GEOSIGMA has been used as a basic evaluation tool for all tracer tests performed within the TRUE programme, including all TRUE-1 and TRUE Block Scale tracer tests. The approach was not used to predict the TRUE Block Scale tracer tests.

The concept used is a one-dimensional advection-dispersion model /Van Genuchten and Alves, 1982/ where dispersivity and mean travel times were determined using an automated parameter estimation program, PAREST /Nordqvist, 1994/. PAREST uses a non-linear least square regression where regression statistics (correlation, standard errors and correlation between parameters) also are obtained.

The chosen one-dimensional model assumes a constant fluid velocity and negligible transverse dispersion, according to Equation (2-6).

According to /Ogata and Banks, 1961/ and /Zuber, 1974/, the dispersion in a radially converging flow field can be calculated with good approximation by equations valid for one-dimensional flow. Although a linear flow model (constant velocity) is used for a converging flow field, it can be demonstrated that breakthrough curves and parameter estimates are similar for Peclet numbers of about 10 and higher.

/Van Genuchten and Alves, 1982/ gives a solution for step input with dispersion over the injection boundary /cf Winberg et al, 1996/. Variable injection schemes were simulated by superposition of the solution. The fit of the breakthrough curves using a three-parameter fit included velocity $V\ [LT^{-1}]$, dispersion coefficient D_l [L^2T^{-1}], and the so called F-factor [–], a proportionality factor that accounts for the dilution in the fracture system (same definition as *pf* in Section 2.3.1).

2.3.1 Retention parameters

The evaluation of the TRUE Block Scale Phase C tracer tests also included modelling using a one-dimensional advection-dispersion model with matrix diffusion and sorption. Unlike earlier modelling approaches within the TRUE project the evaluation this time also included sorption and diffusion parameters by fitting the so-called A-parameter which is a lumped parameter including both matrix diffusion and sorption. The governing equations are Equations (2-12a) and (2-12b) discussed earlier.

For zero initial concentration and a constant concentration at the inlet during the tracer injection, a solution to these equations is given by /Tang et al, 1981/. The parameters that were estimated using PAREST /Nordqvist, 1994/ were the mean travel time, t_m, Peclet number, *Pe*, the so called *pf*-factor [–], the retardation factor, R_a [–] and the so called *A*-parameter [$T^{1/2}$] where;

$$Pe = \frac{Vx}{D_l} \tag{2-19}$$

and the proportionality factor *pf* [–] is introduced in order to obtain the actual concentration in the sampling borehole, C_{bh},

$$C_{bh} = pf \cdot C(t) \tag{2-20}$$

where *pf* represents the dilution in the sampling borehole and other proportional losses.

In an ideal radially converging flow field, *pf* equals the (dimensionless) ratio of the injection flow rate to the pumping flow rate. However, under non-ideal conditions *pf* may also be used to account for e.g. incomplete mixing and incomplete recovery. In addition, since flow rates and tracer injection concentration (i.e. injected tracer mass) cannot be used with absolute certainty, *pf* may be used as an estimation parameter which also accounts for such uncertainties.

In the model, it is thus assumed that a non-time dependent surface retardation is occurring for the transport in the fracture. The classical relationship (see Equation (2-11)) is assumed between the retardation factor R and the surface sorption coefficient K_a. By making the further hypothesis that the fracture is wide compared to its aperture, the factor S/V_w (Flow Wetted Surface) in Equation (2-11) can be simplified to $1/b$, yielding:

$$R = 1 + \frac{K_a}{b} \tag{2-21}$$

Furthermore, a contact time dependent retardation process is occurring and can be described by the parameter $A\ [T^{1/2}]$, which is defined by:

$$A = \frac{bR}{\sqrt{\theta D_m(\theta + K_d \rho)}} = \frac{b + K_a}{\sqrt{\theta D_m(\theta + K_d \rho)}} \tag{2-22}$$

The modelling procedure as applied to the TRUE Block Scale *in situ* data is described and discussed in detail by /Andersson et al, 2002b/.

2.4 Stochastic continuum

2.4.1 Model description

The stochastic continuum (SC) model uses a stochastic approach to groundwater flow and mass transport in which the medium is conceptualised as a heterogeneous continuum. Modelling of the flow and transport processes is carried out using two different numerical tools. The flow model uses a finite-difference code that can be made conditional to transmissivity and piezometric head data. This model is used as input to the finite element code in which transport is solved.

The model is stochastic; therefore, alternative representations of reality are produced in a manner consistent with the data. Any such representation (or realisation) could be considered as a plausible image of reality. The analysis of all the realisations generated can be used within a Monte-Carlo framework to make a statement about the uncertainty on model predictions.

2.4.2 Strategy and hypothesis

For the flow model, the study volume is discretised into equal-sized cells, and then the geometrical descriptions of the feature zones are used to classify the cells. Those cells intersected by a feature are assigned conductivities according to the intersecting feature, and those that are not are considered as representative of the background fracturing and the rock matrix.

For the transport model, the conditional realisations of conductivity that were built with the flow model are used as input to a finite element model in which the advection-dispersion equation, including retardation, decay and matrix diffusion, is solved.

The key issue of this model is heterogeneity. We consider that both flow and transport are strongly influenced by the heterogeneity of hydraulic conductivity and transmissivity. We consider also that a non-negligible proportion of the total flow and transport occurs in the background fracturing, therefore it is needed to model this flow and transport explicitly. In fact, although the average hydraulic conductivity for structure and background fractures is several orders of magnitude different due to heterogeneity, there are some cells representing deterministic structures with a hydraulic conductivity below some of the cells representing background fractures.

2.4.3 Concepts

The modelling flow can be summarised by Figure 2-1. The hydrostructural model is used to define the geometry of both the flow and transport models. Then, the flow model takes the observational data on conductivity and piezometric head to generate calibrated heterogeneous conductivity fields and boundary conditions. (An important feature of the self-calibrating approach to flow modelling is that calibration is not limited to just conductivities but also to the boundary conditions. In studies like this one for which the boundary location is somehow arbitrarily chosen, there is significant uncertainty in the prescribed boundary conditions.) The calibrated heterogeneous conductivity fields extend over an area larger than the one that will be used by the transport model; thus, before they can be used for transport predictions there is a need to transfer the flow-model conductivities, which are defined on a constant support, onto the finite element grid, which contains both two-dimensional elements for the features, and three dimensional elements for the background, of varying supports (small elements close to boreholes, large elements away from boreholes); and, there is also a need to transfer the piezometric heads obtained in the flow to the boundaries of the finite element model. Once the transfer of information from the flow model to the transport model is completed, the observational breakthrough curves are used to calibrate porosities and dispersivities and then predictions are made. For the transport model, porosities and dispersivities are considered homogeneous over the entire study area.

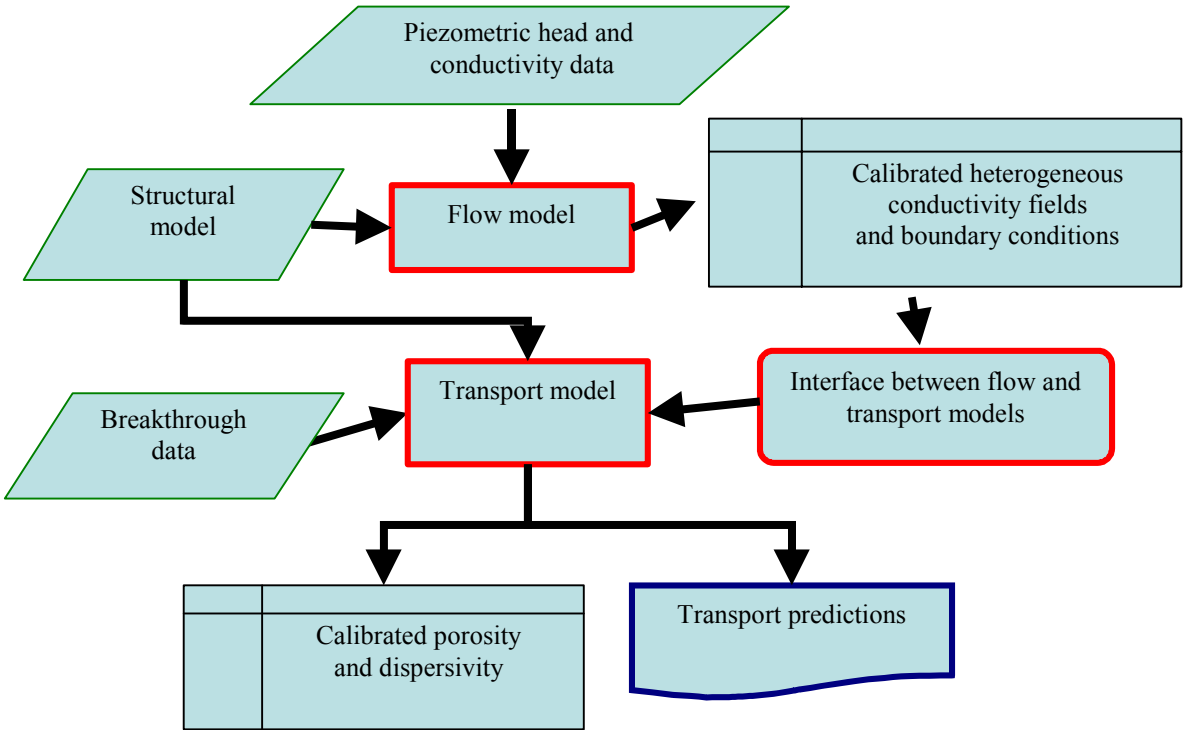

Figure 2-1. *Input data, process models, interface models and model results considered in the ENRESA SC approach.*

It should be stressed that as the SC approach aims to a stochastic characterisation of the transport predictions through the analysis of multiple realisations. An ensemble of predictions based on flow and transport representations – each of which is consistent with reality to the extent of reproducing the observational data – can be used for modelling the uncertainty in these predictions. In the present application within the TRUE Block Scale Project, it was only possible to build five such realisations, since it was not possible to make a sensible uncertainty analysis in this case.

2.4.4 Processes and model implementation

Transient fully saturated, three-dimensional flow is modelled. Conductivity is heterogeneous, with different degrees of heterogeneity for the discretisation blocks that are intersected by a feature and those that are not. Storativity is homogeneous over the whole domain. The flow boundary conditions are prescribed heads on the entire boundary, the values of which are taken from a regional model of the site. Given the observed steady-state and transient head data, the heterogeneous conductivity, homogeneous storativity and boundary conditions are calibrated to yield a set of values consistent with the data. This process is repeated for several realisations resulting in a set of conditional realisations, storativity and boundary conditions to be used by the transport model.

Due to the different discretisation of the flow and transport models, an interface tool was designed to transfer the finite difference conductivity values to the finite elements. This tool takes into account the geometries and relative sizes of the elements in both models and applies simple upscaling rules. The geometries of some of the features in the transport model are only approximate representations of their geometry in the hydrostructural model, this is due to some simplifications performed to ease the definition of the three-dimensional elements representing background fracturing.

Transient fully saturated, three-dimensional transport with steady state flow is modelled. The transport model evolved between the prediction and evaluation phases. In both phases, the processes considered are diffusion, advection, dispersion, decay and matrix diffusion. For the prediction phase, matrix diffusion was modelled as a retention process characterised by a linear isotherm, therefore it is represented by a single retention coefficient. For the evaluation phase, matrix diffusion was explicitly modelled through a one-dimensional diffusion equation with its own parameters for matrix porosity, matrix diffusion coefficient and matrix specific surface.

The size covered by the transport model is smaller than that of the flow model; the boundary conditions used by the transport model are readily taken from the piezometric steady-state head distribution predicted by the flow model. The additional parameters used by the transport model were: homogeneous, but different, porosities for the two-dimensional elements representing the features, the three-dimensional elements and the matrix; homogeneous values for the longitudinal and transverse dispersivities for the entire domain. Porosities and dispersivities are subject to calibration using the available breakthrough data, also differentiating between features, three-dimensional elements and matrix. The parameters describing matrix diffusion, either through a retention coefficient, or through the diffusion equation, are also considered homogeneous within the site.

2.5 Discrete Fracture Networks

2.5.1 Model description

In fractured crystalline rocks it is often assumed that the mobile or the advective component of groundwater flow takes place in the conductive fracture network. The Nirex-Serco[1] team has used a Discrete Fracture Network (DFN) approach to model the TRUE Block Scale tracer tests. This approach used:

- an accurate representation of the all of the key features characterised as part of the hydrostructural model,

- in-plane heterogeneity within the fractures of the hydrostructural model, to reflect the observed intra- and inter-variability in transmissivity attributed to structures,

[1] Known previously as AEA Technology Consulting.

- a model of one-dimensional transport, using path lines with the processes, advection, dispersion, and rock-matrix diffusion, included.

The overall objective of the Nirex-Serco approach is to build a sufficiently adequate, but broadly 'realistic', model of the fracture system in the TRUE Block Scale rock volume using the DFN approach.

The DFN model of the hydrostructural model is illustrated in Figure 2-2. A range of heterogeneous models were developed, from highly heterogeneous models on cm-scales, as illustrated in Figure 2-3, to variability on metre-scales, as illustrated in Figure 2-2. In the DFN model, every structure is treated as a rectangular feature, either unterminated or terminated against the boundary domain.

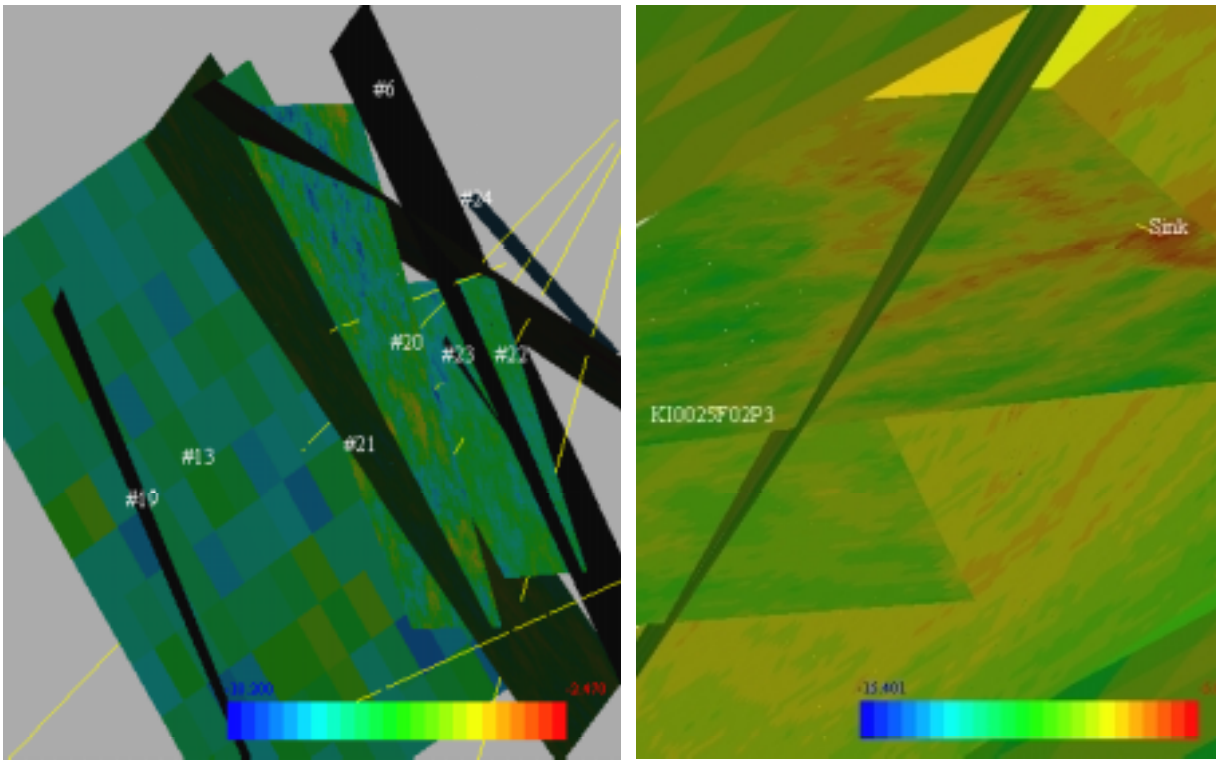

(a) (b)

Figure 2-2. *(a) The discrete fracture network model, using NAPSAC, of the Hydrostructural Model, coloured by log_{10} Transmissivity (m^2/s), with a range between –10.20 to –2.47. The yellow lines indicate the TRUE Block Scale borehole trajectories. Heterogeneity is applied to each numbered feature according to 2-3. However, to ensure there is sufficient accuracy, where it matters, only those structures actively involved in the transport are refined on a small scale (10–20 cm). The outer features are refined on a ten metre length scale. (b) A close-up view of the sink used for the Phase C tracer evaluation. It shows Structure #21' s Darcy velocity and channel-structure on a 20 cm length-scale.*

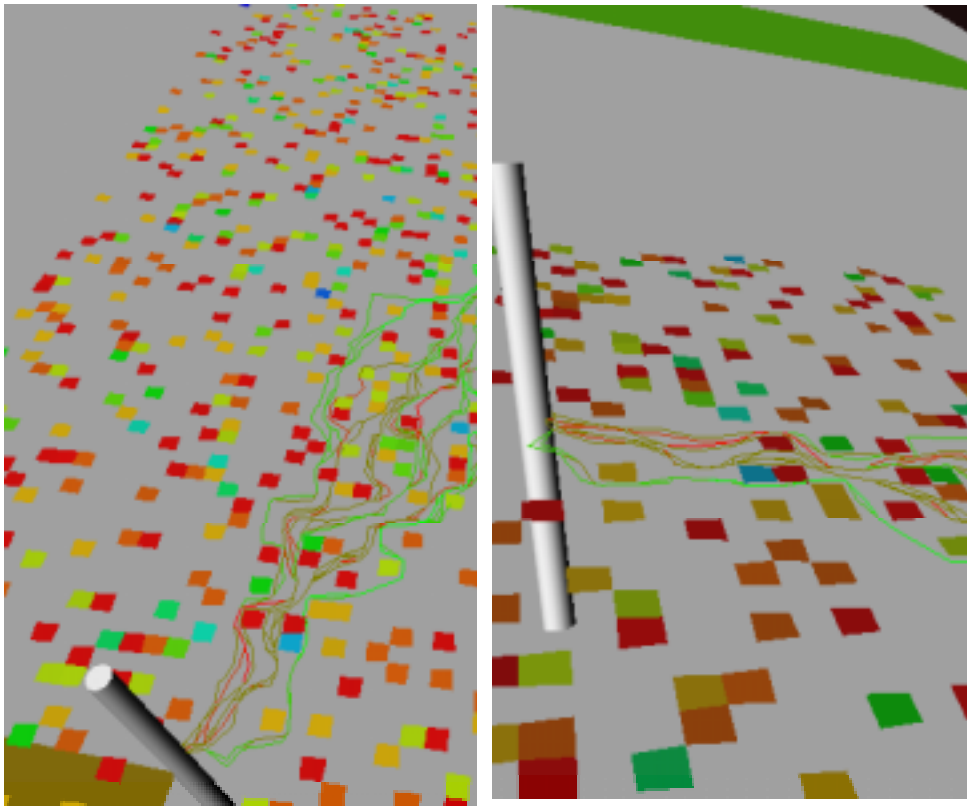

Figure 2-3. *An illustrative example of a series of flow-paths through a highly heterogeneous (Nugge Effect) transmissivity field. The conductive transmissive elements have been removed to show the capture of the pumping boreholes. Spatial correlation in this model is on a similar length-scale as the dimension of a borehole radius ~ 10 cm.*

In the Nirex-Serco DFN approach, each of the features of Figure 2-2 is represented by a discrete two-dimensional structure with spatially varying transmissivity. An example of this variability is illustrated in Figure 2-3. Groundwater flow through the features is controlled by variable transmissivity, connectivity, and boundary conditions (both at the borehole and the external boundary). The variable transmissivity is defined for each finite-element, with a correlation structure, using an exponential correlation function, with a fixed correlation length. The mean and a spread of the random variable are defined using a log-normal distribution sampled to produce the local transmissivity values.

Strategy and Hypotheses

The sufficiency of any modelling approach should be judged by the ability of the approach to be able to predict, reconcile or bound key characteristic features of groundwater flow and radionuclide retention. In particular, the DFN modelling was used to answer the basic hypotheses posed in Section 1.6. These basic hypotheses concentrate on understanding the conductive geometry of the target volume; the properties of fractures and fracture zones, such as in-plane heterogeneity and fracture intersection zones; and what key properties control transport in fracture networks.

The DFN approach aimed at an understanding the overall behaviour and adequacy of the hydrostructural model – the original hypothesis posed. However, the question of robustness and uniqueness of the hydrostructural model, cannot be so easily answered. Therefore, in addition to simulating multiple realisations (of the variable aperture), alternative variants were used to help address this question. A variant of the TRUE Block Scale hydrostructural model (i.e. an equally plausible structural model, in which an additional feature cross-connects the TRUE Block Scale rock volume, but does not intersect the borehole array) was used to investigate the robustness and uniqueness of the model results. That is to say, what are the important aspects of the hydrostructural model? Can we tell the difference between five structures being involved in the transport pathway and two? Is geometry important? This is of particular relevance for the C2 tracer test in which a number of structures are theoretically involved in the transport path. This variant to the hydrostructural model introduces an additional feature, which has been modelled as sub-horizontal (but equally could be sub-vertical), orientated broadly parallel to the TRUE boreholes with a size of the order of 20–30 m in extent. This additional feature has the effect of short-circuiting the transport pathway between KI0025F03:P7 and KI0023B:P6, without actually connecting these borehole intervals directly.

In addition, the DFN approach investigated whether introducing heterogeneity to the basic hydrostructural model is enough to 'understand' the results of the tracer testing, without the need to introduce additional layers of complexity, such as Fracture Intersection Zones (FIZ) or background fractures. A key aspect of the Nirex-Serco DFN modelling was to attempt to understand the possible role of in-plane fracture heterogeneity. Intuitively, this approach provides one possible conceptual model of flow in the TRUE Block Scale rock volume that includes the geometrical aspects,

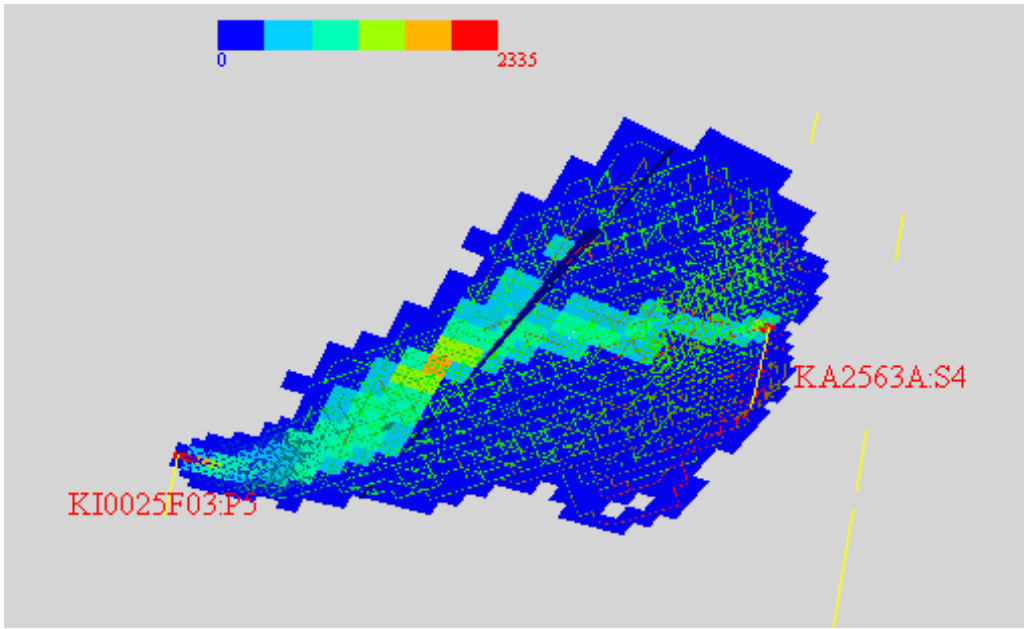

Figure 2-4. *A plot showing the path line density for tracer release from KA2563A:S4 for tracer test A5 /Andersson et al, 2000a/. It shows a shaded plot of the number of times a path passes through an element.*

the variability in interpreted transmissivity, and heterogeneity of flow paths. An advantage of this approach is that it can give rise to significantly different flow-path geometry if the boundary conditions (injection and abstraction rates) are modified.

A process related aspect addressed by the DFN modelling concerns process identification. In particular, how does the observed apparent dispersion arise? To address one aspect of this, path line calculations were computed, not only from a point release, but also from the neighbourhood of the borehole (a disc release), as illustrated in Figure 2-4, which is flux-weighted, to simulate a spread in flow velocities giving rise to increased hydrodynamic dispersion.

2.5.2 Concepts

Transport Equations

Radionuclide transport calculated for each particle path is modelled using an advection-dispersion-rock-matrix diffusion approach /Hoch, 1998/ as embodied in Equations (2-12a) and (2-12b). This uses the inversion of the closed-form Laplace transform solution of solute transport in a one-dimensional conductor /Lever et al, 1983/. In the heterogeneous, variable aperture models considered, the Laplace inversion is performed for each portion of each path through the hydrostructural model. The mean water residence time observed in the tracer testing can be matched to the DFN model by assuming a simple linear scaling relationship between transport aperture and the hydraulic aperture.

Pathways, Heterogeneity, and Dispersion

The DFN approach explicitly modelled heterogeneity within fracture planes. This approach was adopted to determine to what extent in-plane heterogeneity could result in:

- an appropriate spread of heterogeneous transmissivity and flux,
- hydrodynamic dispersion at a large-scale, and
- formation of transport pathways as a consequence of the heterogeneity.

This approach does not explicitly model micro-dispersion arising from small-scale heterogeneity that can result in potentially large contrasts in flow velocity. According to /Dagan, 1989/, for a log-normally distributed transmissivity, with variance σ^2 and dispersion length, I, the ergodic hypothesis will not be satisfied for a finite release of tracer of size l. For a release of solute aligned to the flow (i.e. with no width relative to the flow streamlines), the dispersion, D_L will be zero. In the case of a finite transverse release of tracer, of length, l, the ergodic limit (in which $D_L = \sigma^2 VI$, where V is the mean velocity) is only achieved if the ratio l/I is of the order of 100. The DFN models used, typically have correlation lengths of the order of 5 m and a scale of solute release of the order of one borehole diameter (~ 0.1 m), this implies an, l/I-ratio of the order of ~ 0.1/5 = 0.02, which is over three orders of magnitude different to achieve ergodicity. This condition of ergodicity (effectively not sampling enough of the heterogeneous

field) can only be satisfied if the dimension of the source release significantly exceeds the correlation length, which in practical terms, theoretically, could only be achieved for tracer to be injected, rather than passively released.

Spreading arising from variability in flow velocities resulting from small-scale heterogeneity was modelled using a standard dispersion length approach. Hence, it is erroneous, to assume that the computation of D_l depends on I only, but also on l as a ratio, l/I (and the geometry of the flow field). Therefore, the degree of in-plane heterogeneity sufficient to give rise to apparent dispersion cannot be so easily calculated.

In the DFN approach, transport paths between the injection and pumping sections are modelled as an ensemble of path lines.

Treatment of fault gouge and infilling materials

The presence of fault gouge, infilling materials, immobile zones either in the intact unaltered rock (or altered rock) or water, potentially result in an effective diffusive flux of solute from the mobile transport path. There is paucity of hard data concerning the spatial distribution of the fault gouge, infill or altered rock material. Consequently, this treatment considers an adequate modelling approach to assume that the effect of additional material is to enhance the effective diffusive flux. This is a pragmatic approach, because in practice there is currently limited scope for detailed process discrimination from the shape of the breakthrough curve.

2.5.3 Model Implementation

Overall and Input Data

The basic parameters used in the Nirex-Serco DFN model are summarised in Table 2-2 and Table 2-3. Table 2-2 gives the geometry used for the deterministic features[2] /cf Hermanson and Doe, 2000/ to model the Phase C tracer tests. Table 2-3 gives the stochastic parameterisation of each feature. The justification for the parameterisation using a Log-Normal distribution is demonstrated in Figure 2-5.

[2] The parameters and structures in Tables 2-2 and 2-3 are only strictly relevant to Phase C tests as minor modifications differentiated the earlier Phase A and B tests (because the hydrostructural model was evolving).

Table 2-2. The important structures used in the DFN modelling, taken from the hydrostructural model of /Hermanson and Doe, 2000/. The equations defining these planar structures is given by ax+by+cz+d=0 /Hermanson and Doe, 2000/. The coefficients for each equation, together with their orientation and extent are used as input to the DFN model.

Structure	a	b	C	d	Strike	Dip	Width	Length
#6	–0.8429	–0.5374	–0.0253	5487.00	327.5	88.6	118.60	118.63
#7	0.4404	0.8851	–0.1504	7299.84	116.5	81.4	112.25	113.55
#13	–0.7303	–0.5535	–0.4003	5172.72	322.8	66.4	106.66	145.49
#19	–0.8586	–0.5125	–0.0126	5285.73	329.2	89.3	163.04	163.05
#20	–0.7464	–0.6596	–0.0884	6129.78	318.5	84.93	120.11	120.58
#21	0.8698	0.3739	–0.3221	4504.55	156.74	71.21	87.08	91.98
#22	0.8437	0.3999	–0.3580	4672.57	154.64	69.02	49.80	93.34
#23	0.7337	0.6794	0.0000	6304.34	137.2	90.0	24.53	49.06
#24	0.6391	0.7552	–0.1457	6753.70	130.24	81.62	34.06	34.93
#10	–0.0916	–0.9458	–0.3117	6736.05	275.53	71.84	124.48	131.07
#XX								

Table 2-3. Summary of the mean and spread of transmissivity (m^2/s) derived from the interpretations given in /Hermanson and Doe, 2000/. These quantities have been estimated using all of the features taken together, and for each feature taken individually. As there is only one measurement of transmissivity estimated by Doe for Structure #24, it is not possible to estimate the spread. Therefore, for modelling purposes either infinite correlation (constant transmissivity) or a value for spread taken from consideration of all of the conductors ('All') is used to parameterise Structure #24.

Feature	Transmissivity (m^2/s) Geometric Mean (μ)	Standard Deviation (σ)	Correlation Length (m)
All	–6.78	1.05	5
#7	–5.46	0.96	5
#6	–7.16	0.65	5
#23	–8.01	0.21	5
#22	–6.93	0.69	5
#20	–6.36	0.41	5
#21	–7.52	0.81	5
#13	–7.49	0.64	5
#19	–6.07	0.78	5
#10	–6.47	0.87	5
#24	–7.53	0.00	–

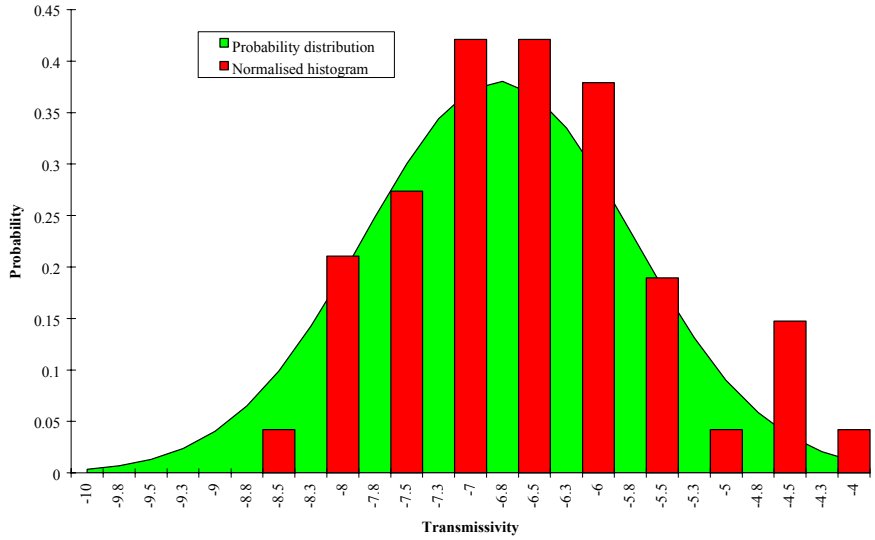

Figure 2-5. *Comparison between the Log-Normal distribution (μ, σ) (–6.78, 1.05) and a histogram of the measured transmissivity values.*

Geometric Implementation (Hydrostructural Model)

The DFN model used variable aperture features in the geometries as described in Table 2-2. A hypothetical Feature "#XX" was introduced to illustrate an alternative pathway between borehole KI0025F03:P7 and KI0023B:P6 in Test C2.

Boundary conditions

The DFN modelling was carried out either using the hydraulic head boundary condition derived by /Holton, 2001/ to the edges of the model or using a model with a constant head gradient, orientated so as to match the observed gradient towards the underground openings.

Figure 2-6 illustrates the adequacy of a constant head gradient applied across the model. The head gradient is applied as a vector quantity orientated along the borehole trajectory, with heads projected onto the boundary domain. This boundary condition was selected to allow sensitivity calculations to be more easily performed.

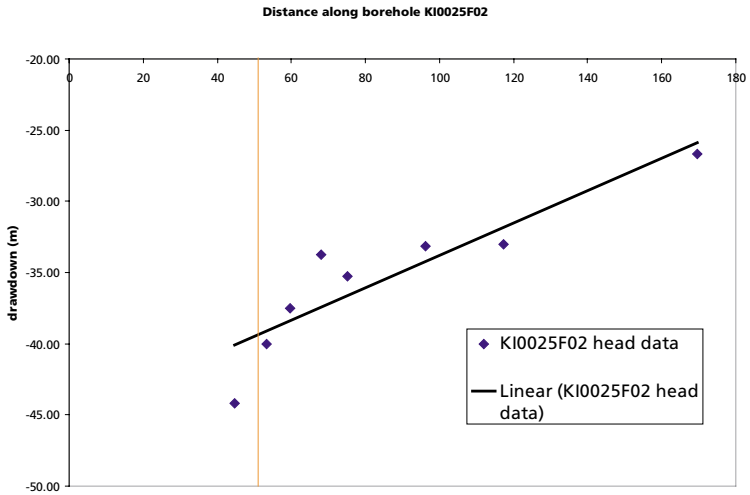

Figure 2-6. *An example of a linear head gradient boundary condition applied to the DFN model, the approximation appearing to be reasonable away from the Äspö HRL.*

Calibration strategy

The approach taken by the Nirex-Serco team was to modify the parameterisation of the structural model to match, as closely as possible, the results of the tracer testing. The models used were relatively complex and because a forward modelling approach was used it was not expected to produce 'precise' fits to the measured data. However, sensitivity calculations, for key parameters, were performed to provide some robustness to the parameterisation and conclusions. The geometry (and hence connectivity) of the hydrostructural model proposed by /Hermanson and Doe, 2000/ was strongly dependent on the conductive geometry and hence the modelling is ultimately predicated on a few fundamental assumptions. For example, little attention has been paid to the non-conductive geometry, i.e. the combination of boreholes (or pumping) that do not show good hydraulic responses or tracer breakthrough.

The basic postulate is that the logarithm of the transmissivity field can be modelled by a Gaussian spatial process. It is assumed that the correlation structure of the field can be characterised by an exponential variogram. Given the chosen variogram the next step was to produce many realisations of the transmissivity field with the required stochastic behaviour and to calculate the flow for each realisation, thus producing an ensemble of head fields. The realisations were produced using the Turnings Band method and conditioned on the measured values at the borehole intercepts using Kriging.

From the conditioned transmissivity fields, the 'best' fit to the head field was used as the basic flow model. Advective path line calculations were performed to estimate the mean water residence time. The simulated water residence time was modified using a simple linear scaling relationship between hydraulic aperture and transport aperture. It is expected that there is a weak correlation between hydraulic and transport aperture /Holton, 2001/. In addition to the advective component, other transport parameters for the conservative and reactive tracers were systematically adjusted to match the dispersion, sorption and diffusive fluxes. The initial parameter-set used for all

calculations were based on the tabulated laboratory measurements (K_a, K_d, φ etc). Effective transport parameters were derived based on obtaining adequate matches to the cumulative breakthrough curves. An analytical approximation to the source term solution was used to model the experimental input solute function. A convolution of the source term and the numerical simulation was used to evaluate the 'total' cumulative mass response.

Code description

The main tool used as part of the discrete fracture network modelling is the Serco Assurance software, NAPSAC version 4.2.

NAPSAC is a computer program used to model groundwater flow and transport in fractured rock. The models are based on a direct representation of the discrete fractures making up the flow-conducting network. A stochastic approach is used to generate networks of planes with the same statistical properties as those measured for fractures in field experiments. A very efficient finite-element method is used to solve the equations for flow in a network. A transport option in NAPSAC is designed to calculate the migration and dispersal of a tracer through a network for which the flow has been determined. The algorithm is based on particle tracking.

The basic technical details and mathematics of NAPSAC and the sorption and rock-matrix diffusion model (whose solution uses a semi-analytical method) in NAPSAC can be found in /Hartley, 1998/ and /Hoch, 1998/.

2.6 Posiva streamtube approach

The modelling concept is based on a simplistic representation of the streamtube (i.e. a collection of streamlines) that connects the source and sink of the tracer test. The transport model comprises two parts: the mobile part of the pore space where the advection takes place (streamtube) and the immobile part of the pore space that is adjacent to the streamtube (matrix, fault gouge, stagnant pools etc).

The geometrical simplification of the streamtube is called a flow channel. Groundwater flow in the flow channel is described by a distribution of the flow velocities that is calibrated against the available tracer test data. Tracer may be retarded by equilibrium sorption on the fracture surfaces or by diffusion to the immobile pore space.

The immobile pore space is adjacent to the flow channel and can be accessed only by diffusion. In the prediction phase, retardation caused by diffusion to the immobile zones is handled using grouped parameters, which are fitted using data from the earlier tracer tests. In the evaluation phase the immobile zones are parameterised using three alternatives: stagnant zones of the flow field, rock matrix and fault gouge.

2.6.1 Strategy and hypotheses

The TRUE Block Scale Project tests three hypotheses, concerning 1) the structural model of the TRUE Block Scale rock volume, 2) the influence of the heterogeneity on the flow and transport and 3) the network effects in the transport, cf Section 1.6. This modelling approach concentrates only on the transport aspects. Therefore the general hypotheses are reformulated to hypotheses that are connected to the retention in the fractured rock. Tested hypotheses in the Posiva approach are:

1. There is no fundamental difference in the tracer retention for transport through fracture network or single fracture flow paths.

2. The distribution of the flow rates determines the retention of the tracers.

These hypotheses are tested by applying data from single fracture transport experiments (TRUE-1) to predict transport through the fracture network at the TRUE Block Scale site. The conceptualisation of the transport modelling is presented in Figure 2-7. The transport path possibly goes through multiple fractures but it is simplified to single transport channel. The geometry of the transport channel is further simplified to the shape of a regular rectangular channel that is surrounded by immobile pore space.

2.6.2 Concepts

The transport channel is conceptualised by using a geometrical description. This does not mean that the flow channel is a geometrically constrained object or “tube” that is typical for the investigated rock mass and fracture system. In principle, the channel is characterised by material properties, boundary conditions and the size of the tracer test source area. Radially converging experiments in homogeneous fractures lead to straight streamlines that pass the source area and go to a sink forming a triangular flow channel. In this case, the width of the transport channel is not constant but it is equal to or smaller than the diameter of the injection borehole. Dipole flow fields make the shape of the flow channel more complicated. The injection flow rate pushes tracer into the fracture. This means that close to the injection point the streamlines diverge and locally the channel width can be larger than the width of the source area.

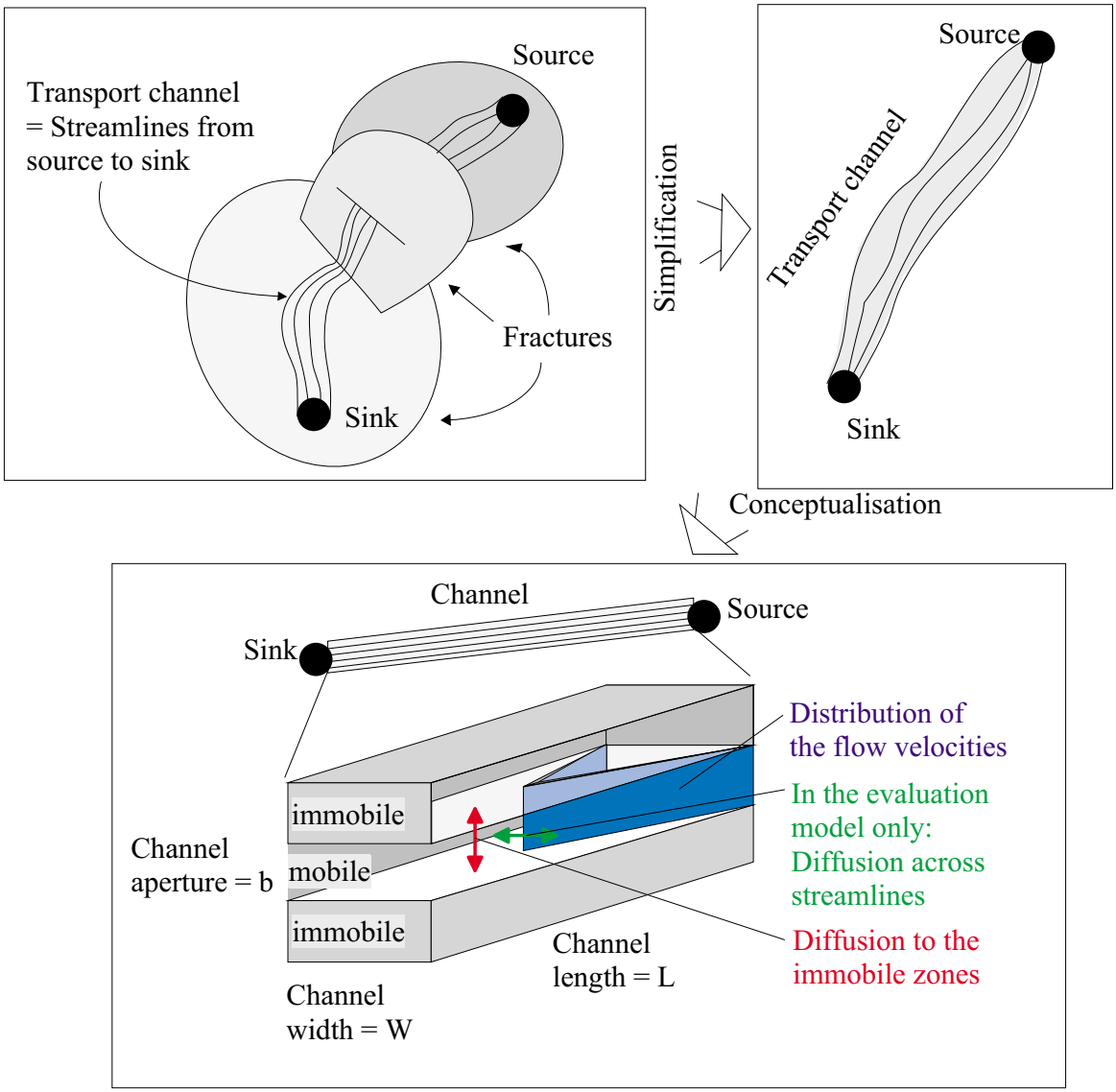

Figure 2-7. *Conceptual picture of the modelling approach applied in the Phase C predictions and evaluation.*

It is assumed that in solving the retention problem the complicated streamtube can be replaced by a homogeneous constant width transport channel. In practice, this means an homogeneous model that has the same effective retention properties as the real transport channel. In principle, heterogeneity of the immobile zone (lateral and longitudinal, not normal to the fracture surface) or of the flow field does not change the modelling concept. It can be shown /Poteri, 2002/ that the matrix diffusion parameters (u) and transit time (t_w) are additive along the transport path. This means that also heterogeneous cases can be modelled using the same approach, but replacing the varying properties by average properties. However, taking the heterogeneity into account may change the interpretation of the lumped effective retardation parameters.

Hydrodynamic dispersion in the flow field is modelled by utilising an appropriate distribution of flow velocities. In the predictions the non-sorbing tracer residence time distribution was explained entirely by varying flow velocities. In the evaluation phase, a spatially correlated velocity field and molecular diffusion in the mobile pore space of the transport channel have been applied.

An important retention process in the model is the diffusion of the tracer particles into the immobile pore space. The immobile pore space may be a stagnant pool, rim/altered zone of the matrix, fault gouge, fault breccia or rock matrix. Model calculations assign lumped retention parameters (u, R) to describe the measured retention in the tracer test. In the evaluation of the tracer tests the lumped parameters are explained by physical sorption, diffusion and flow field related parameters. The interpretation of the retention parameters is repeated for each of the immobile zones.

2.6.3 Processes

Modelling is based on advection, sorption and diffusion processes both in the predictions and in the evaluation. Although decaying tracers were used in the tracer experiments the radioactive decay has not been taken into account in the modelling and correspondingly the measured breakthrough curves are corrected for the decay. Variability in the flow field has been modelled by applying an appropriate velocity field. The prediction model includes only the advective field, which is the non-sorbing residence time distributions of the relevant Phase B experiments scaled by the difference in the flow field between Phase B and C tests and presented as a distribution of different flow velocities across the channel. In reality, the molecular diffusion between different streamlines averages the differences in the tracer particles residence times. This has been taken into account in the evaluation of the tracer tests by introducing transverse molecular diffusion in the flow field. This means that the evaluation model includes the dispersion process that arises from simultaneous advection and molecular diffusion. To model the dispersion process the spatial structure of the velocity field in the transport channel needs to be described by e.g. lateral correlation length of the velocity field. Correlation length is important because the capability of the molecular diffusion to average the differences in the flow velocities depends on the spatial structure.

The sorption model comprises equilibrium sorption on the fracture surface and sorption in the matrix. Both are modelled as linear and reversible processes.

The diffusion model includes retention due to the diffusion to the immobile zones. This is modelled analytically by assuming infinite depth of the immobile zone.

2.6.4 Model Implementation

Overview and input data

Phase C predictions and evaluation of the breakthrough curves are based on an analytical model. The model incorporates advection, unlimited matrix diffusion and sorption by applying a simple analytical advection-matrix diffusion solution to the non-sorbing tracer residence time distribution. The actual source term measured in the injection borehole is taken into account by convoluting the analytical solution of the delta function breakthrough curve with the measured source term.

Information from the TRUE-1 site plays an important role in the Phase C predictions. The sorbing tracer experiments performed during TRUE-1 (STT-1 and STT-1b) have been used to determine the retention parameters of the different tracers. In the predictions the retention properties were given in the form of lumped parameters for the matrix diffusion and sorption in the matrix (u) and for the surface sorption in the fracture (R). The retention properties of the different tracers were transferred unchanged from the TRUE-1 site to the TRUE Block Scale site.

For the predictions values of u and R were transferred from the evaluation of the TRUE-1 tests for application to the TRUE Block Scale Phase C tests. Applied parameters are presented in Table 2-4. In the evaluation phase the retention properties (u and R) of the tracers in the different Phase C tests were determined by fitting of the breakthrough curves (Table 2-4). The fitted retention properties were then further broken into physical parameters describing the diffusion, sorption and flow field properties. In this case the input data comprises laboratory measurements of the sorption and diffusion properties. For sorption and porosity values the laboratory measurements have been applied as constraints by not allowing porosity or sorption higher than the values measured in laboratory. The uncertainties in the overall retention properties have been attributed to the flow field properties.

Geometry Implementation (hydrostructural model)

The hydrostructural model was applied only to estimate the lengths of the transport paths. The estimated in-plane distances for different tests are 16 m in C1, 97 m in C2 and 35 m in C3 /Andersson et al, 2001c/.

Advective transport

The applied single transport channel approach does not need a flow solution. It takes the velocity field from previous tracer tests (prediction phase) or applies a linear velocity profile with transverse Taylor dispersion (evaluation phase). In the evaluation phase the advective transport of the non-sorbing tracer is described by Equation (2-23).

Table 2-4. Retention parameters (*u* and *R*) applied in the Phase C transport calculations. There is a distribution of the parameter u values corresponding to the non-sorbing tracer residence distribution in the mobile phase of the transport channel. This is represented by a linear relationship $u = U_t\, t_w$, where $U_t = \sqrt{D_w F \theta^2 \left(1 + \frac{1-\theta}{\theta} K_d \rho\right)} \Big/ 2b$ and *F* is the formation factor of the immobile zone, i.e. ratio between effective diffusion coefficient and diffusion coefficient in the free water (D_w). The retention parameters are given for both the predictions and the evaluation calculations.

		Prediction		Evaluation	
Test	**Tracer**	**U_t [$h^{-1/2}$] Corrected**	**R [–]**	**U_t [$h^{-1/2}$]**	**R [–]**
C1	Br-82	0.05	1.10	0.05 – 0.08	1.00 – 1.01
C1	Ca-47	0.18	2.10	0.17 – 0.23	1.30 – 1.31
C1	Cs-134	1.9	75.00	1.6 – 2.46	16 – 20
C1	K-42	0.38	1.90	0.27 – 0.39	1.4
C1	Na-24	0.07	1.35	0.08 – 0.16	1.05 – 1.21
C1	Rb-86	1.1	4.50	0.55 – 0.89	3.00 – 3.52
C2	Ba-131	0.5	5.00		
C2	Ca-47	0.18	2.10	0.1 – 0.25	2.4
C2	Cs-137	1.9	75.00		
C2	Re-186	0.018	1	0.05 – 0.13	1
C3	Ba-133	0.5	5.00		
C3	HTO	0.028	1	0.03 – 0.09	1
C3	Na-22	0.07	1.35	0.06 – 0.14	1.30 – 1.34
C3	Rb-83	1.1	4.50		
C3	Sr-85	0.15	1.80	0.09 – 0.24	1.50 – 3.40

$$C_m = \frac{1}{2}\left(erf\left[\frac{\frac{1}{2}X_S + X + \xi_1}{2\sqrt{\xi_2}}\right] + erf\left[\frac{\frac{1}{2}X_S - X - \xi_1}{2\sqrt{\xi_2}}\right]\right);$$

$$\xi_1 = -\frac{1}{2}\tau\,; \quad \xi_2 = \left(\frac{1}{(Pe)^2} + \frac{1}{120}\right)\tau - 8\sum_{n=0}^{\infty}\frac{1 - e^{-(2n+1)^2\pi^2\tau}}{(2n+1)^8\pi^8}\,; \,, \qquad \text{(2-23)}$$

$$\tau = \frac{D\,t}{a^2}; \quad X = \frac{D\,x}{a^2 u_0}; \quad X_S = \frac{D\,x_S}{a^2 u_0}; \quad Pe = \frac{a\,u_o}{D}$$

where *D* is the molecular diffusion in free water, *a* is the half lateral width of the channel (in fact, this is correlation length of the velocity field), u_0 is the maximum flow velocity (minimum velocity is zero) and *t* is the time. It is assumed that the tracer concentration is well mixed in the direction of the aperture and the aperture does not

have an effect on the advective transport. The advective residence time distribution above is the basis for the calculation of the retarded breakthrough curves.

Retention processes

The only retention processes in the model are sorption and diffusion to the immobile zones. Two types of sorption are considered: equilibrium sorption on the fracture surface ($K_\mathbf{a}$) and sorption in the immobile zone (K_d). Both sorption processes are modelled as linear and reversible processes. In addition, it is assumed that the properties of the immobile zone do not change as a function of the depth and that immobile zones are infinite depth from the transport point of view in the time scale of tracer tests. In this case if the non-sorbing and non-diffusive tracer residence time probability density function is $pdf(t_w)$ then the breakthrough curve in the case of delta function input is

$$k(t)=\int_0^t j(t,t_w,U_t t_w,R)\, pdf(t_w)\, dt_w \ ; \tag{2-24}$$

$$j(t,t_w,u,R)=H(t-Rt_w)\frac{u}{\sqrt{\pi}\left(t-Rt_w\right)^{3/2}}e^{-\frac{u2}{t-Rt_W}} \ ; \tag{2-25}$$

R, as noted previously, is the retardation coefficient due to the surface sorption. Retention due to the matrix diffusion to the immobile zone is determined by

$$u=\theta\sqrt{D_m R_m}\frac{WL}{Q} \ ; \tag{2-26}$$

where the definitions of θ, D_m and R_m are extended from "matrix properties" to "immobile zone properties", and W is the width, L the length and Q the flow rate through the channel. The breakthrough curve due to the measured injection function $s(t')$ is calculated using the following convolution

$$c(t) = \int_0^t s(t')\, k(t-t')\, dt' \tag{2-27}$$

Calibration strategy

Both in the prediction and evaluation phases the flow fields have been calibrated to give the measured non-sorbing tracers breakthrough curves. In the prediction phase the velocity fields of each test were calibrated using non-sorbing tracer breakthrough curves of the earlier Phase B tracer experiment. Velocity fields were scaled by the known difference in the pumping conditions between the Phase C and Phase B tests. This approach does not take into account that already in Phase B tests there might be retention due to the diffusion to the immobile zones.

In the evaluation phase the maximum flow velocity (linear distribution of the velocities across the channel) and correlation lengths of the velocity field have been fitted to give the measured non-sorbing breakthrough curves of Phase C tests.

Code description and evaluation procedure

The transport calculations were performed using analytical equations and the Matlab program /Mathworks, 1997/. The procedure applied during the evaluation of the Phase C tests is summarised below:

1. Calculate non-sorbing tracer residence time distribution. This is calculated using a linear velocity field with a given correlation length, and molecular diffusion. The residence time distribution is calculated using an analytical solution for the generalised Taylor dispersion that is based on the advection and transverse molecular diffusion.

2. Take the fitted matrix diffusion parameter u and surface retardation coefficient R. of the different tracers and different tests.

3. Calculate the breakthrough curve for a Dirac delta function input using an analytical solution of the advection – matrix diffusion equation, parameters u and R and the residence time distribution that was calculated in stage 1.

4. Convolute the breakthrough curve that was calculated in stage 3 with the actual injection source term to get the final breakthrough curve.

In order to fit the breakthrough curves, repeat steps 2, 3 and 4, changing u and R until the result of step 4 agrees with the measurement.

2.7 SKB KTH/WRE LaSAR approach

2.7.1 Background

The Lagrangian Stochastic Advection-Reaction (LaSAR) modelling approach, as applied to the TRUE Block Scale tracer tests, derives from the parallel plate diffusion/sorption model originally proposed for retention in crystalline fractures by /Neretnieks, 1980/. The model of /Neretnieks, 1980/ was extended as part of the TRUE program in two ways:

- The model was generalised to account for aperture variability, as well as for longitudinal heterogeneity in retention parameters /Cvetkovic et al, 1999, 2000/.

- The model was generalised from a single heterogeneous fracture to a network of heterogeneous fractures, where tracer particle trajectories extend over a series of fractures /Cvetkovic and Cheng, 2002/, see also /Painter et al, 1998/.

The LaSAR methodology was implemented for evaluating and interpreting the TRUE Block Scale tracer tests.

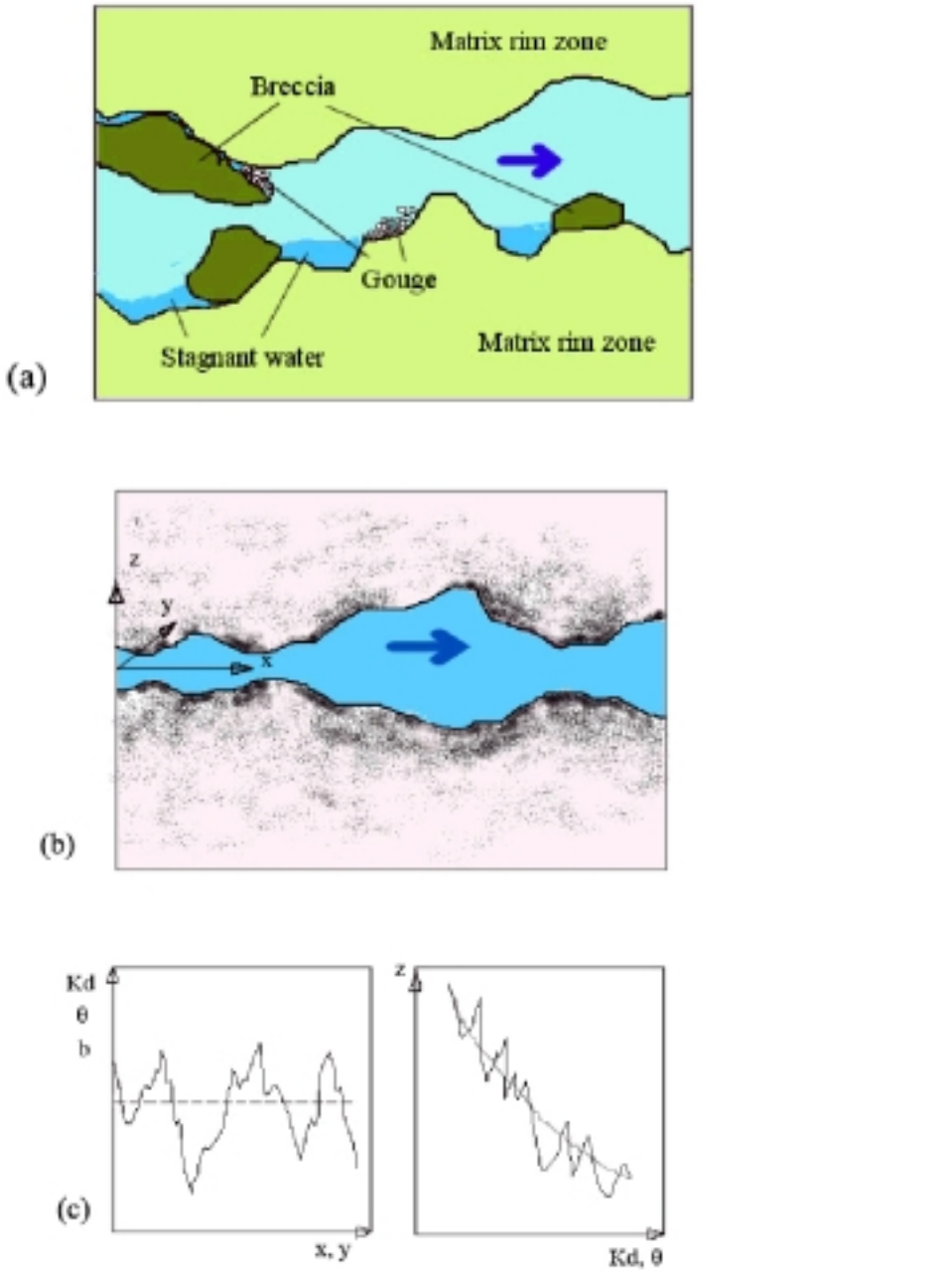

Figure 2-8. *Schematic illustration for LaSAR modelling approach to TRUE Block Scale tracer test evaluation and interpretation. (a) Four principle zone of retention. (b) Conceptualisation of retention zones for modelling; darker shading implies greater porosity, and even possibly K_d; retention in the four principle zones of a) are "lumped" into two mass transfer (retention) processes: kinetically controlled (diffusion limited) sorption in the rim zone and breccia, and equilibrium sorption on fracture surface, including gouge material. (c) Schematic presentation of variability in three dimensions; a trend is assumed in the z-direction, whereas no trend is assumed in the longitudinal direction.*

2.7.2 Conceptualisation and assumptions

Fractures of the TRUE Block Scale site are heterogeneous with a relatively complex microscopic structure. Based on available data, we identify four principle zones of retention: (i) rim zone of the matrix, (ii) breccia, (iii) gouge material, and (iv) stagnant water (Figure 2-8a). Our conceptualisation of the retention zones is given in Figure 2-8b. Matrix porosity is assumed heterogeneous in three dimensions, with a trend in the *z*-direction (normal to the fracture), decreasing from the rim zone toward the intact rock. Breccia is viewed as part of the microscopic heterogeneities with diffusion limited sorption, and the effect of fault gouge is viewed as part (equilibrium) surface sorption. The effect of stagnant water on retention (due to diffusion) is not explicitly accounted for.

The LaSAR for TRUE Block Scale modelling is based on the following assumptions:

- Flow is assumed to be steady state.
- Dominant hydrodynamic mode of transport in fractures is advection.
- Tracers are fully mixed in the fracture, in the direction normal to the fracture plane.
- Advective transport in the rock matrix is negligible.
- Tracer diffuses into the rock matrix in the direction normal to the fracture plane, i.e. diffusion into the rock matrix is one dimensional and unlimited.
- All mass transfer processes are linear.
- Sorption in the rock matrix is assumed to be at equilibrium.
- Sorption on the fracture surface is assumed to be at equilibrium.

2.7.3 Single particle transport model

The basic expression of our transport model is the probability density function for a single tracer particle arrival time from the injection to the detection (pumping) borehole which couples the processes of advection, diffusion and sorption (neglecting decay):

$$\gamma(t,\tau) = \frac{H(t-\tau)\,B}{2\sqrt{\pi}\,(t-\tau-A)^{3/2}} \exp\left[\frac{-B^2}{4(t-\tau-A)}\right] \tag{2-28}$$

where

$$B = \sum_{i=1}^{N} \kappa_i \beta_i \;; \qquad \beta_i = \frac{l_i}{V_i b_i} \;; \qquad \tau = \sum_{i=1}^{N} \frac{l_i}{V_i} \tag{2-29}$$

$$A = \sum_{i=1}^{N} K_a{}^{i}\ \beta_i \;; \qquad \kappa_i = \theta_i \left[D_i \left(1 + \frac{\rho_b K_d^i}{\theta_i} \right) \right]^{1/2} \tag{2-30}$$

and H is the Heaviside step function. The density γ [1/T] (2-28) is conditioned on the water residence time τ , and on parameters A and B. If there is no retention, then $\gamma(t,\tau) = \delta(t-\tau)$, i.e. particle residence time is equivalent to the water residence time through the fracture network. Note that the model (2-28) is obtained as a solution of the general model (2-18a)–(2-18b), by lumping all retention into one single "retention zone" (i.e. i=1), and setting D_l=0; also note that the index "i" has a different meaning in Equations (2-18) and (2-28); in the former it denotes a retention zone, in the latter it denotes a segment along a tracer particle trajectory.

The index "i" designates either a fracture (if the particle is transported through a series of fractures), or discretisation segments if we consider a heterogeneous fracture; N is the total number of segments, which could also cover transport through a few heterogeneous fractures. K_d [L^3/M] is the distribution coefficient in the matrix, K_a [L] is the sorption coefficient on the fracture surface, b [L] is the fracture half-aperture, D [L^2/T] is pore diffusivity and ρ_b [M^3/L] the bulk density of the rock matrix. All above parameters are in the general scale segment-dependent, hence index "i".

If the retention parameters θ , D, K_d are constant (effective) values for all segments, we have

$$B=\beta\kappa\ ; \qquad \kappa=\theta\ (1+K_d\ \rho/\theta)^{1/2}\ ; \qquad \beta = \sum_{i=1}^{N} \frac{l_i}{V_i b_i} \tag{2-31}$$

The parameter β [T/L] is dependent only on the advective (water) movement, i.e. on fracture hydrodynamics, which in turn is determined by the structure of the network (fractures) and prevailing boundary conditions. Our basic evaluation model is based on (2-31); however, we also used (2-29) and (2-30) in order to account for spatial variability in porosity.

2.7.4 Transport model for tracer tests

Let m_0 [M] denote the total mass (or activity) of a tracer released in the injection borehole with a rate $\phi(t)$ [1/T]. Let $g(\tau)$ [1/T] denote the joint probability density function of the water residence time τ from the injection to the detection borehole. If dispersion due to advection variability is neglected, then $g(t)=\delta(\tau-\tau_0)$ where τ_0 is the plug-flow water residence time for a given flow path.

Numerical simulations under various conditions have indicated that β is strongly correlated to τ . In general, the correlation between β and τ is a power-law. However, for the variability range encountered in TRUE Block Scale, a linear relationship appears sufficient. We thus approximate

$$\beta = k\ \tau\ , \tag{2–32}$$

where k [1/L] is an *in situ* parameter associated with a given flow path. Note that (2-32) simplifies the estimation problem significantly, since the entire distribution of β values is replaced by the distribution of τ and the parameter k; this parameter has been referred as "flow-wetted surface per unit volume of water" /Andersson et al, 1998/. A further simplification is to assume β constant for a given flow path.

Substituting (2-32) into (2-28), we get $A = \tau\,\zeta$ and $B = \tau\,\psi$ where the key parameter groups ζ [–] and ψ [$T^{-1/2}$] are defined as:

$$\zeta = k\,K_a\,; \quad \psi = k\,\kappa \tag{2-33}$$

The tracer discharge (or the breakthrough), Q, in the detection borehole is evaluated as

$$Q(t) = m_0 \int_0^\infty [\phi(t) * \gamma(t,\tau)]\, g(\tau)\, d\tau \tag{2-34}$$

where γ is given in (2-28) and "*" denotes the convolution operator. Thus to predict Q, we require the knowledge of all *in situ* retention parameters (assuming effective, uniform values), we require k, the water residence time density $g(\tau)$, the injection rate $\phi(t)$ and the total tracer mass m_0.

2.7.5 Calibration steps

The calibration procedure consists of two steps:

Determining $g(\tau)$ by "deconvoluting" breakthrough curves for non-sorbing tracers; the actual form of $g(\tau)$ is assumed to be inverse-gaussian, and the first two water residence time moments are calibrated for each flow path.

Calibrating the two parameter groups ψ and ζ on the TRUE Block Scale tracer breakthrough data, using the "deconvoluted" $g(\tau)$ from step 1.

Table 2-5 summarises the parameter groups ψ and ζ for the C1 tracer tests. The corresponding calibrated mean water residence time is 15 h and variance 50 h^2.

Table 2-5. Calibrated values of parameter groups ψ and ζ for the tracers used in the C1 test.

	Br-82	**Na-24**	**Ca-47**	**K-42**	**Rb-86**	**Cs-134**
ζ [–]	0	0.0042	0.24	0.432	3	9
ψ [$h^{-1/2}$]	0.04	0.12	0.29	0.504	1.44	5.03

2.7.6 Accounting for heterogeneity

Equations (2-28) through (2-30) directly account for lateral heterogeneity (i.e. in the *x,y*-direction of the fracture plane, Figure 2-8b and Figure 2-8c) for all parameters involved. As indicated by (2-29) and (2-30), the heterogeneity affects the transport in an *integrated* sense. Quantities A and B therefore correspond to averages along the flow path, and may be replaced by effective values, as is done in (2-31). However, the key problem is in relating the effective retention parameters in (2-31) to point measurements of say the porosity θ and K_d.

Retention parameters in (2-29) and (2-30) strictly assume that the parameters are constant in the direction normal to the fracture plane (*z*-direction, Figure 2-8b). Clearly there is spatial variability in all retention parameters from the fracture plane, through the rim zone, to the unaltered rock; there is evidence that porosity systematically decreases (as a trend) with increasing z and presumably so does K_d (Figure 2-8c). The key issue related to heterogeneity in the *z*-direction is the *penetration depth* for individual tracers. In particular, the values of say θ and K_d at any given point of the *x,y*-plane (which appear in Equations (2-29) and (2-30)), will depend on the extent a given tracer penetrates the rim zone.

Current data available is insufficient for constructing statistical models of retention parameter variability under TRUE Block Scale conditions. Thus attempts to expose potential effects of heterogeneity must be considered as qualitative. In particular, a log-normal distribution model is used for porosity in the *x,y*-plane (consistent with limited data available), and show that the lateral heterogeneity in porosity can significantly affect the *interpretation* of the effective porosity. Heterogeneity in the *z*-direction is accounted for indirectly, by estimating the penetration depth for different tracers, and using this estimate to define a depth-averaged, tracer-dependent porosity, again using the limited data available. It can be shown that accounting for the *z*-directional trend in porosity can significantly affect *in situ* estimates of the retention parameters.

2.7.7 Estimation of *in situ* retention parameters

If all effective *in situ* retention parameters were available, they could be inserted into (2-31) for each tracer. Based on (2-32), the calibrated ζ and ψ (cf Table 2-5) could be used to infer the parameter k. In this case, the estimation problem would be over determined, since there are a number of equations and only one unknown (k). In reality, the *in situ* retention parameters are unknown, and in fact, they are to be estimated. Since we only have calibrated ζ and ψ, the estimation problem is undetermined since we have more unknowns than equations (see /Cvetkovic et al, 2000/) for a discussion related to TRUE-1 evaluation). In fact, there are precisely two more unknowns than equations, and hence two additional constraints are required (or assumptions, or independent estimates) in order to close the system of equations and estimate all *in situ* retention parameters (including k).

Three possible, alternative constraints are summarised below:

Parameter *k*. Parameter *k* can be independently estimated in several ways; there are three possibilities:

- Numerical Monte Carlo simulations of particle transport in a discrete fracture network. Relevant DFN simulations were run, for instance, by JNC-Golder. These data include all tracer trajectories and necessary properties (velocities and apertures) along the trajectories. The parameter *k* is obtained through linear regression between τ and β. Based on the results from C1 test, and also combining the results from C2 and C3 tests, we estimated k=6000 1/m.

- Assuming a streamtube model, we have $\beta=2WL/q$ where W is the borehole diameter (0.056 m), *L* is the estimated distance between the injection and detection borehole (e.g. 14 m for C1) and *q* is the estimated injection flow rate (e.g. 45 ml/min for C1). The parameter *k* is then approximately $k=\beta/\tau$ where τ is the estimated mean water residence time (e.g. 15 h for C1).

- Following the definition of β , *k* can be interpreted as an inverse effective half-aperture. If we consider any particular value (obtained from hydraulic tests, or borehole imaging) as representative (say 1 mm as a representative aperture for TRUE Block Scale conditions), then we would estimate k=1/0.5 mm=2000 1/m.

Relationship between porosity and diffusivity. We can relate *D* and θ using "Archie's law" /Archie, 1942/ in the form $F=\theta^m$ where F [–] is the formation factor, cf Table 2-4 for alternative and equitable definition, and *m* is an exponent in the range say $1.2<m<1.6$. The limit 1.6 was obtained from a wide range of core data in petroleum engineering; the limit m=1 is for an ideal case of perfectly parallel microfissures, or micropores, from the fracture surface into the rim zone. Since we do not have *m* for TRUE Block Scale conditions, it is appropriate to consider sensitivity to the entire range 1.3–1.8.

Matrix sorption coefficient. We could assume that *in situ* K_d for any tracer is a particular value obtained in the laboratory, say from batch tests on 1–2 mm fraction. It would be appropriate in this context to consider a more strongly sorbing tracer, such as Cs, rather than a weakly sorbing tracer. For instance, the value for Cs is K_d = 0.053 m^3/kg for a 1–2 mm fraction from 36 days long batch tests /Byegård et al, 1998/.

Any two of the above three constraints/assumptions are sufficient to determine all other *in situ* retention parameters. Clearly, there are other possibilities for constraints. In our evaluation we have assumed Archie's law as the only constraint, and then generated tables of possible *in situ* retention parameter ranges. From these generated "estimation matrices", the implications of any additional constraint become apparent.

2.8 PA Works Channel Network

2.8.1 Model description

Strategy and Hypotheses

The JNC-Golder team used a Channel Network/Discrete Fracture Network (DFN/CN) approach for modelling the TRUE Block Scale Project. This approach combines

- direct implementation of the project 3D hydrostructural model,
- ability to control definition of flow and transport pathways (channels) within the fractures of the hydrostructural model,
- option to include stochastic background fractures representing the features not included explicitly in the hydrostructural model, yet known to occur within the rock block,
- option to include enhanced connectivity, transmissivity, or storage at fracture intersection zones (FIZ),
- ability to model transport including advection, dispersion, and diffusion (ADD) transport, with any number of interacting immobile zones.

The JNC-Golder approach was one of hypothesis testing rather than a inverse modelling – the goal was to understand the capabilities and limitations of the project hydrostructural model, rather than to produce a calibrated model capable of replicating the measurements. The JNC-Golder DFN/CN model directly addressed the project hypotheses, cf Section 1.6. Modelling the DFN/CN model directly reflected the accuracy and adequacy of the hydrostructural model, and the need to consider possible effects such as

- in plane heterogeneity,
- fracture intersection zones,
- incomplete connectivity within deterministic structures,
- importance of background fracturing,
- pathway properties within the discrete fracture network tested.

The DFN/CN model is illustrated in Figure 2-9 to Figure 2-11.

Figure 2-9 illustrates the DFN implementation of the hydrostructural model. In the current implementation, every structure is treated as a simple polygon. Terminations between structures are estimated based on the hydrostructural model.

In the JNC-Golder DFN/CN approach, each of the structures of Figure 2-9 is represented hydraulically by a set of connected pipe flow elements. These pipe flow elements are illustrated in Figure 2-10.

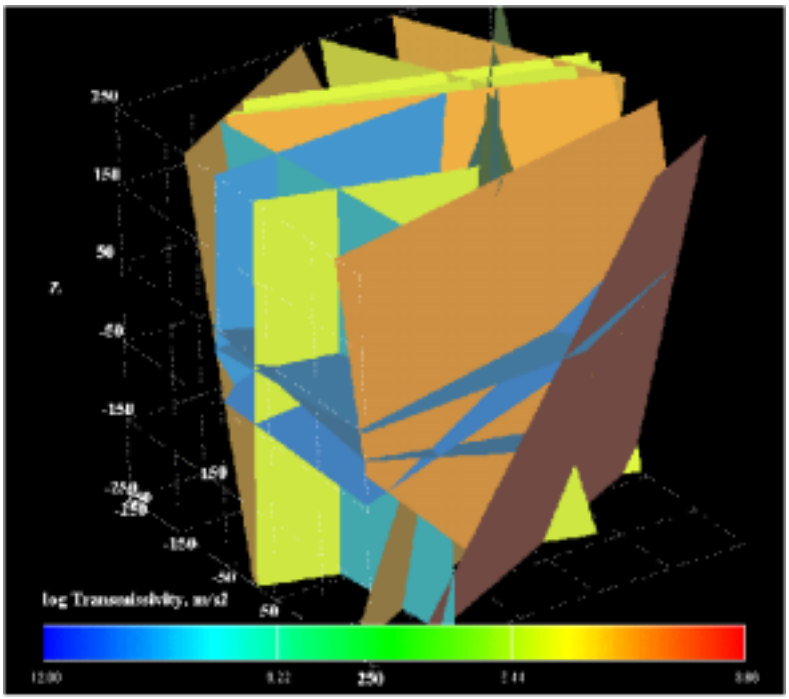

Figure 2-9. *Deterministic Structures of the Revised March 2000 Hydrostructural Model /Hermanson and Doe, 2000/, coloured by log_{10} Transmissivity (m^2/s). The cube is 500 m x 500 m x 500 m, centred at (7170 m, 1900 m, –450 masl) in Äspö local coordinates.*

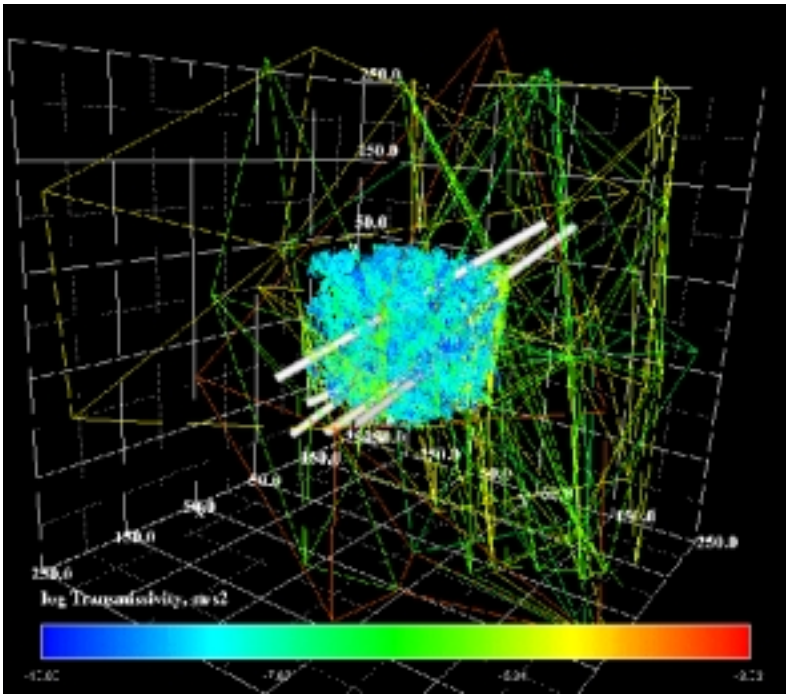

Figure 2-10. *Pipe Elements of the Revised March 2000 Hydrostructural Model /Hermanson and Doe, 2000/.*

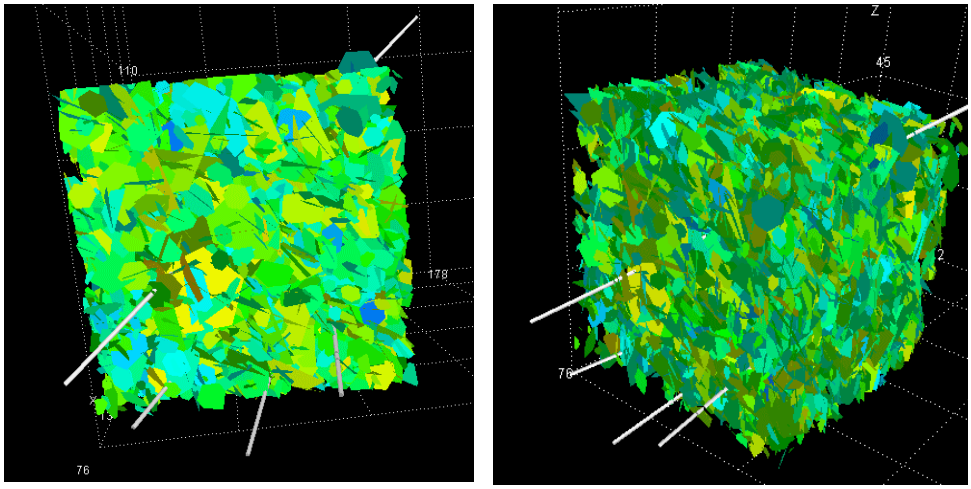

Figure 2-11. *Conductive background fractures (N=7415), coloured by log_{10} Transmissivity (m^2/s). Cube is 150 m x 150 m x 150 m, centred at (7170 m, 1900 m, –450 masl) in Äspö local coordinates. Approximate views: a) towards the north, b) towards northeast.*

2.8.2 Concepts

Transport equations and implementation

The JNC-Golder DFN/CN approach used conventional advection-dispersion-diffusion (ADD) transport equations /Bear, 1972/, with multiple immobile zones (Equations (2-18a) and (2-18b)). This was implemented using the Laplace Transform Galerkin approach of /Sudicky, 1989/.

Pathways, Heterogeneity, and Dispersion

The JNC-Golder DFN/CN approach did not consider heterogeneity within fracture planes directly. It is considered instead that in-plane heterogeneity results in

- apparent hydraulic dispersion, and
- formation of channelised transport pathways.

Apparent hydraulic dispersion relates the dispersion observed in breakthrough curves to the variability in velocity along the pathways due to heterogeneity according to the equation /Gelhar and Axnes, 1983/.

$$\alpha_L \approx \sigma^2 \lambda / \gamma^2 \qquad (2\text{-}35)$$

where α_L [L] is the apparent longitudinal disperison,σ^2 is the standard deviation of log transformed hydraulic conductivity in the heterogeneous field, λ [L] is the correlation length of the heterogeneity, and γ is a proportionality constant (frequently assumed to be 1.0). The above equation ignores the effect of molecular diffusion and pore-scale dispersion, since these are generally of a lower order than the heterogeneity effects on the velocity distribution.

Treatment of fault gouge and infilling materials

Fault gouge and infilling materials are the primary immobile zone in the JNC-Golder DFN/CN model. The immobile zone properties used in the transport modelling therefore should be most closely related to the physical properties of gouge and infilling, with some adjustment to reflect additional immobile zones in altered wall rock and the rock matrix. The JNC-Golder team based predictions of sorbing tracer transport on immobile zone properties based on those in the TRUE-1 sorbing tracer experiments STT-1, STT-1b, and STT-2 /Dershowitz et al, 2001/. In these experiments, gouge and infilling materials were found to have both a relatively high porosity and a relatively high reactive surface area. These values were used directly in the JNC-Golder modelling.

Fracture Intersection Zones

The channel network was enhanced to include possible “Fracture Intersection Zone” (FIZ) channels at the intersection of conductive features, cf Table 2-7. It was originally thought that these FIZ channels might produce detectible changes in breakthrough curves. However, generic FIZ studies reported in /Winberg, 2000/ indicate that the primary effect of FIZ channels is in reducing mass recovery by providing pathways to alternative sinks within the rock mass. Therefore, FIZ channels were implemented in the JNC-Golder model as pipe features with enhanced cross-sectional area, but also providing direct connections to the fracture zones surrounding the tracer experiment. These FIZ channel connections can then account for mass loss which is inexplicable based on any simple radial flow assumptions (Figure 2-12).

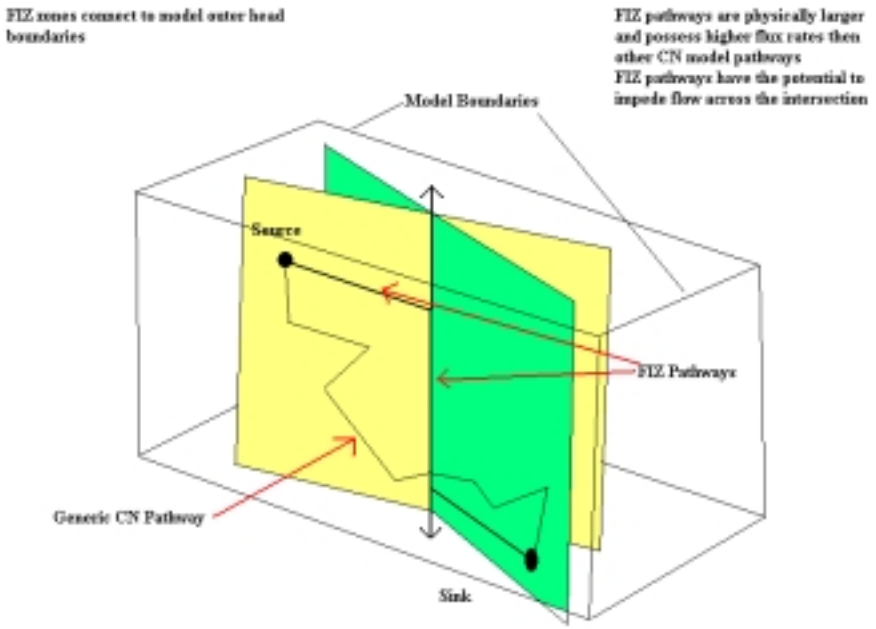

Figure 2-12. *Conceptual model of a fracture intersection zone (FIZ).*

Table 2-6. Properties of Background Fracture population(-s).

Parameter	Basis	Set #1	Set #2
Orientation Distribution	Two sets fitted to BIPS camera logs (NeurISIS)	Fisher Distribution Mean Pole (Trend, Plunge) = (211°, 0.6°) Fisher Dispersion = 9.4	Fisher Distribution Mean Pole (Trend, Plunge) = (250°, 54°) Fisher Dispersion = 3.8
Intensity P_{32}	Posiva Log Structures 0.29 m^2/m^3 total	0.16 m^2/m^3 (55.2% of fractures)	0.13 m^2/m^3 (44.8% of fractures)
Transmissivity	Posiva Log Structures, OxFilet Analysis of Packer Tests	Lognormal Distribution $\log_{10}$ mean = $-8.95\log_{10}$ m^2/s st.dev = $0.93\log_{10}$ m^2/s	Lognormal Distribution $\log_{10}$ mean = $-8.95\log_{10}$ m^2/s st.dev = $0.93\log_{10}$ m^2/s
Size Equivalent Radius	/Hermanson et al, 2001/	Lognormal Distribution mean = 6 m st.dev. = 3 m	Lognormal Distribution mean = 6 m st.dev. = 3 m
Spatial Pattern	Fractal and Geostatistical Analyses	Baecher Model in TTS Region. Fractal (D≈2.6) for larger scale blocks	Baecher Model in TTS Region. Fractal (D≈2.6) for larger scale blocks

Table 2-7. Characteristics of Fracture Intersection Zones (FIZ).

Fracture Intersection Zone properties	
Transmissivity	10 times larger then the Transmissivity of intersecting fractures
Boundary	FIZ pipes are extended to structures NE-2, and EW-1
Possible FIZ effects	1. provide a strong hydraulic connection to alternative sinks, decreasing tracer recovery 2. increase dilution 3. increase dispersion or travel time due to greater aperture or sorption properties 4. serve as a flow barrier due to infilling materials

Table 2-8. Transport parameters and relevant geometry.

Transport Aperture	0.17 to 2.7 mm
Path Width	10 to 26 cm
Rim / Infill Thickness	15 to 30 mm
Rim / Infill Porosity	1% to 4%
Altered Zone Thickness	15 to 37 mm
Altered Zone Porosity	0.5% to 3%

FIZ regions were assigned higher aperture and transmissivities than their associated features. Pipes along this intersection extend to features EW-1 and NE-2. A head gradient is established along the FIZ due to the natural gradient caused by the bounding features or by a head boundary explicitly placed at the FIZ end. Tracer tests crossing fracture intersection zones may experience mass loss due to enhanced retardation and/or diffusion, and by any head gradient along the FIZ.

Geometric implementation (Hydrostructural Model)

The model geometric implementation is described above in Section 2.8.1. Table 2-9 lists the details of the geometric implementation. The deterministic structures and FIZ pathways were implemented in the entire 500 m by 500 m by 500 m scale model region. The background fractures were only implemented in a 150 m scale detailed model region.

Table 2-9. DFN/CN Model Implementation.

	Deterministic Structures	Background Fractures*	FIZ Pathways
Number of Structures	29	7433	2
Intensity P_{32} (Area/Volume)	$2.61 \cdot 10^{-2}$ m^2/m^3	$7.74 \cdot 10^{-2}$ m^2/m^3	NA
Number of Pipes	5736	60219	2
Range of Pipe Lengths	2 m to 20 m	0.5 m to 20 m	290 m – 310 m

* detailed model region only.

Boundary conditions

The DFN/CN modelling was carried out directly applying the head boundary condition derived by /Holton, 2001/ to the edges of the 500 m scale model. These boundary conditions were derived using a continuum model, based on a structural model somewhat different from that adopted for the TRUE Block Scale transport experiments. In addition, the boundary condition does not directly consider the presence of the Äspö tunnels only 100 metres from the TRUE Block Scale transport experiments. The effect of the Äspö tunnels is treated indirectly in terms of the heads on the edges of the 500 m scale model.

Because the absolute values of head derive from the boundary condition applied, rather than being fundamental to the modelling carried out, the accuracy of the DFN/CN hydrogeological modelling is best evaluated in terms of drawdown rather than absolute head. The absolute head at any point in the DFN/CN model can be scaled directly by calibrating from the /Holton, 2001/ head fields.

For the purpose of DFN/CN modelling, the /Holton, 2001/ head field was applied as panels at the edge of the 500 m scale model region. A visualisation of the applied head field boundary condition is provided in Figure 2-13. These visualisations are in the model coordinate system, X(south), Y(north) and Z(up), centred on Äspö local coordinate 1900 m, 7170 m, –450 masl.

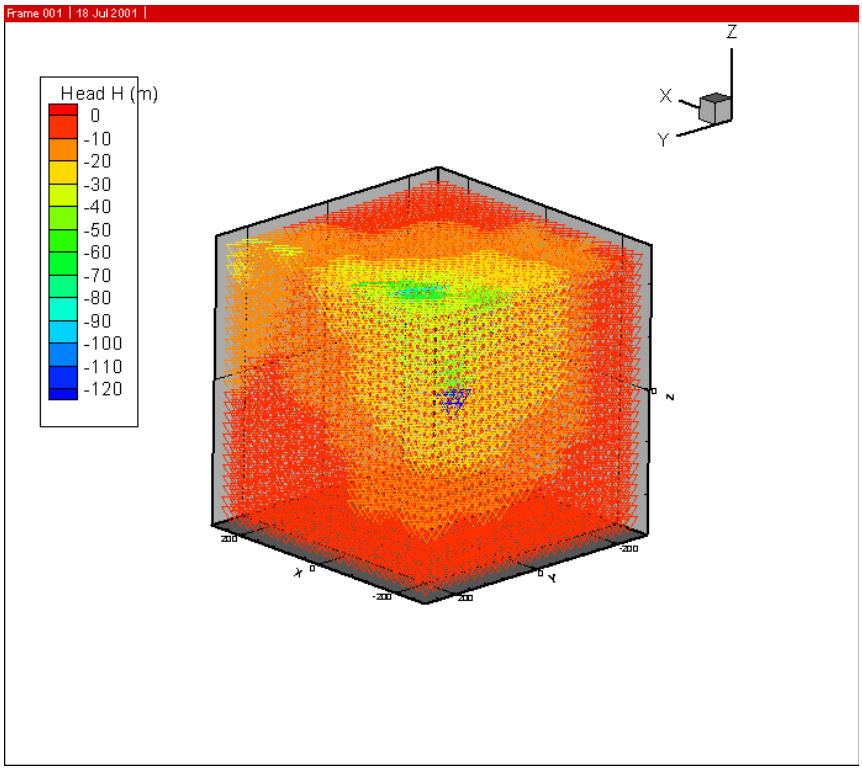

Figure 2-13. *Hydraulic Head Boundary Condition on 500 m Cube (masl).*

Calibration strategy

The strategy of the JNC-Golder team was one of hypothesis testing rather than calibration, and the models were therefore not calibrated through inverse modelling in the strict sense. The project hydrostructural model was implemented, and tested by comparison against interference and tracer transport responses. When comparisons between the hydrostructural model and measurements indicated deficiencies in the model, changes to the hydrostructural model were proposed.

The DFN/CN model requires three parameters for conservative tracer transport:

1. the correlation between transport aperture b_T [L] and fracture transmissivity T_f [L^2T^{-1}], generally assumed to be of the form, $b_T = c\ T^{\beta}$, where c is a proportionality constant, and β is an exponent, generally between 0.3 and 0.5,
2. the longitudinal dispersivity α_L *[L]*,
3. the effective porosity for immobile zones.

The values for these parameters were assumed based on the results of the TRUE-1 experiment calibrations, with the value of $c = 2$, and $\beta = 0.5$. Minor adjustments were made to these parameters to match the Phase A and Phase B tracer tests, but again this can only loosely be considered a "calibration".

Longitudinal dispersivity values are generally assumed to be on the order of 10% of the path length – which would be on the order of 3 to 10 metres for the tracer tests of Phase C. The longitudinal dispersivity was a calibration parameter, in that the values were adjusted to match the Phase A and pre-test tracer breakthroughs.

The effective porosity for immobile zones was also important for conservative tracer breakthrough, since increased matrix porosity has an effect even without sorption. The effective porosity for immobile zones was kept to small values (on the order of 0.01% to 0.1%) due to the lack of apparent dispersion in the Phase A and Phase B tracer tests.

Sorbing tracer transport properties are effective sorption K_d and K_a for each tracer. For predictive simulations, these values were taken directly from the values used in DFN/CN modelling of the TRUE-1 experiments. No calibration of these parameters was therefore carried out within the scope of the TRUE Block Scale Project for the Phase C predictions. However, these K_d and K_a values are not always taken identical to the laboratory measurements, which were also used in a set of simulations termed the "TRUE Block Scale sorption parameters".

In summary, calibration was not a major focus of the DFN/CN modelling. Such calibration as was carried out focused on longitudinal dispersivity $\alpha_{L,}$ which is a purely empirical parameter, and the matrix porosity for diffusion.

Numerical methods and discretisation

Groundwater flow was solved using the MAFIC flow solver based on a pipe element discretisation of the fracture network. The MAFIC flow solver /Miller et al, 1999/ uses Galerkin finite elements, with a pre-conditioned conjugate gradient solver. The finite element pipes range in length from 0.5 to 20 metres. There are, for example 6 pipes on the pathway between KI0025F03:P5 and KI0023B:P6 for Test B2g, cf /Andersson et al, 2002b/.

The Laplace Transform Galerkin solution for transport does not require time stepping, since calculations are carried out in the transform space. To produce breakthrough curves, results were output at intervals of 1 to 10 hours. The size of the interval does not influence the accuracy of the solution. The Laplace Transform Galerkin solution can be specified in terms of either mass rate (grams/hour), or concentration (percent solute/hour). The simulations reported here were carried out in mass rate.

3 Results of predictive modelling

During the TRUE Block Scale experiment, modelling groups were asked to provide predictions on the outcome of reactive tracer tests given the results of conservative tracer tests along the same flow paths. The majority of the modelling groups involved (JNC-Golder, Posiva-VTT, Nirex-Serco and SKB-WRE) had prior experience in modelling solute transport related to Äspö conditions. This included modelling the site scale transport experiment LPT-2 /Gustafson and Ström, 1995/ as part of Äspö Task Force Tasks 1-2 and modelling detailed scale transport in an interpreted single fracture related to the TRUE-1 experiments /Winberg et al, 2000/. The latter as part of Äspö Task Force Task 4 /Elert, 1999; Elert and Svensson, 2001; Marschall and Elert, in prep/. The ENRESA-UPV/UPC modelling lacked this site-specific Äspö experience.

Although a defined dataset for model prediction was provided prior to the predictions (part of Chapter 7 in /Andersson et al, 2002a/ the modelling groups were free to use their own experience and judgement is selection of the parameters that would go into their model predictions. Some groups decided to use the laboratory data provided related to TRUE Block Scale, and some groups decided to use the MIDS data set provided for TRUE-1 /Winberg et al, 2000/. Furthermore, based on the kinship between the investigated TRUE-1 some groups used their experience and evaluated *in situ* retention parameters from TRUE-1 for the prediction of the TRUE Block Scale Phase C experiments.

By comparing the conceptual positions taken by the groups, cf Chapter 2, and input data used in the predictions with the corresponding evaluated (calibrated) parameter groups and parameters presented in Chapter 6, a representation may be obtained of the evolution in understanding of transport/retention during the project.

In the following sections a brief overview of the different tracer test phases, the results of the model predictions of Phase C are presented and discussed.

3.1 Overview of the Tracer Test Stage

The TRUE Block Scale Tracer Test Stage was preceded by three successive site characterisation stages:

- **Scoping stage** (boreholes KA2563A and KA3510A),
- **Preliminary Characterisation Stage** (boreholes KI0025F and KI0023B),
- **Detailed Characterisation Stage** (borehole KI0025F02) /Winberg, 2000/.

Apart from drilling, characterisation and installation of multi-packer systems (5 to 10 sections) performed during all stages, cross-hole hydraulic interference tests, for the most part complimented by tracer dilution tests, were performed during the Preliminary and Detailed Characterisation stages. These successive experimental stages are documented in the first two volumes of the TRUE Block Scale final reporting /Andersson et al, 2002a,b/. We simply restate here the main characteristics of the Tracer Test Stage in order to facilitate understanding of the subsequent sections.

The Tracer Test Stage included drilling and characterisation of the final borehole, KI0025F03. This resulted in the final iteration and update of the hydrostructural model /Hermanson and Doe, 2000/. However, the main purpose of this stage was the subsequent series of three tracer tests /Winberg, 2000/. Phase A was focused on identifying the best sink section, Phase B was required to demonstrate sufficiently high mass recovery of non-sorbing species to allow the use of radioactive tracers. Finally, Phase C included performance of four injections with radioactive sorbing tracers in three sections (C1, C2, C3 and C4).

Phase A, with the aim of identification of the best sink, consisted of five test configurations /Andersson et al, 2000a/. A total of 53 point dilution tracer tests were performed in Tests A1 through A4, using successively sections KI0025F03:P5, KI0025F03:P4, KI0025F02:P5, and KI0023B:P6 as sinks, respectively. In addition, Tests A4 and A5 (sink section: KI0025F03:P5) were performed as radially convergent tracer tests, with tracer release in three sections for Test A4 and in five sections for Test A5. At the end of this phase, section KI0023B:P6 (Structure #21) was chosen as the optimal sink section for the subsequent phases.

Phase B concentrated mainly on selecting injection sections for the Phase C tests amongst the candidates already identified in tentative terms during Phase A /Andersson et al, 2000b/. The added constraint was that conservative mass recovery must be higher than 80% to allow usage of radioactive tracers. A total of eight injection sections located in boreholes KA2563A, KI0025F02 and KI0025F03 were employed during the two tests performed during this phase. From these eight flow paths, three were finally selected for Phase C, with mass recoveries above 80%. These paths correspond to the preceding tests B2g (release of tracer in section KI0025F03:P5), B2d (release of tracer in section KI0025F03:P7) and B2b (release of tracer in section KI0025F02:P3), These three flow paths are respectively named “flow paths I, II, and III” in volume 2 /Andersson et al, 2002b/ of this report and relate to injections/tests C1/C4, C2 and C3, respectively.

During Phase C, “cocktails” of tracers with various retention properties were injected in the selected flow paths when pumping in KI0023B:P6 at Q=1960 ml/min:

- Test C1 uses flow path I and tracers Uranine, ^{82}Br, ^{24}Na, ^{47}Ca, ^{42}K-, ^{86}Rb-, ^{134}Cs-. Forced injection at q=45 ml/min in Structure #20 (KI0025F3:P5).

- Test C2 uses flow path II and tracers Naphtionate, $^{186}ReO_4$, ^{47}Ca, ^{131}Ba, and ^{137}Cs. Forced injection at q=10 ml/min in Structure #23 (KI0025F03:P7).

- Test C3 uses flow path III and tracers HTO, ^{22}Na, ^{85}Sr, ^{83}Rb, and ^{133}Ba. Passive injection at q=1.8 ml/min (KI0025F02:P3).

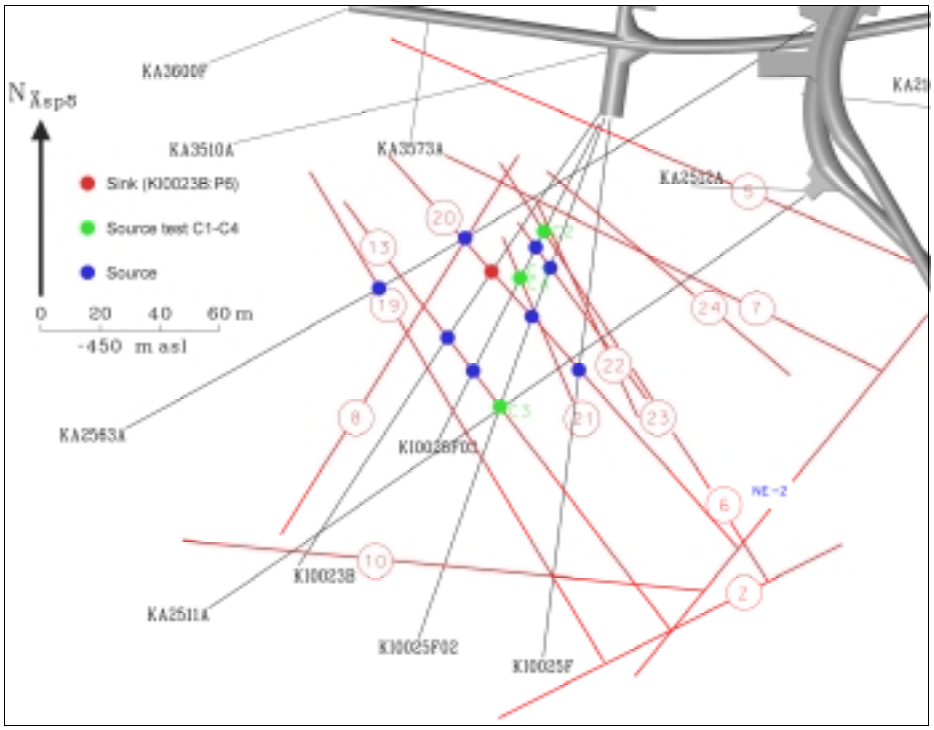

Figure 3-1. *Overview of the experimental geometry and packer locations for tracer tests using KI0023B:P6 as sink (flow paths I–XI). Position of sinks and sources are related to borehole intersections with the numbered structures and therefore represent different depths. Horizontal section at Z=–450 masl.*

- Test C4 uses flow path I again, with tracers ^{82}Br, ^{131}I, ^{47}Ca, ^{131}Ba, ^{54}Mn, ^{57}Co, and ^{65}Zn. Forced injection at q=45 ml/min (KI0025F03:P5).

Test C4 was not included as a defined component of the TRUE Block Scale prediction/evaluation process, for details cf /Andersson et al, 2002b/. An overview of the sink and source sections in relation to the hydrostructural model is given in Figure 3-1.

3.2 Predictive modelling

The modelling groups were given access to the results of the performed cross-hole interference tests, tracer dilution tests and results of relevant non-sorbing tracer tests performed in the flow paths at relevant pump rates. They were then asked to predict the reactive tracer breakthrough and associated mass recovery.

Tables A-1 through A-4 in Appendix A present the parameters used by the five modelling groups in their prediction simulations; pore space properties (porosity), diffusivities in the immobile pore spaces, and surface and volume sorption coefficients.

Tables 3-1 through 3-3 show the arrival times for 5%, 50% and 95% of the tracer mass in C1, C2 and C3, as well as the mass recovery as predicted by the 5 modelling teams. The tables also provide a comparison with the actual *in situ* results for the Phase C tests (corresponding *in situ* mass recovery given at times of termination of official sampling for Phase C, mass recovery not to be regarded as final, since some tracers kept arriving at the time when the last measurement was made).

The predicted and measured breakthrough and cumulative mass arrivals are plotted in Figures 3-3 through 3-17. For SKB-WRE the results related to evaluated *in situ* retention parameters from the TRUE-1 analysis are shown. In the figures, the presentation of "measured *in situ* data" is limited to what had been detected at the end of the first stage of the TRUE Block Scale Project. *In situ* monitoring was continued thereafter, so the curves for some of the most reactive tracers may be completed/updated as part the continuation of the project. Specifically, some of the more reactive tracers injected during tests C2 and C3 had not yet been detected when the last measurement presented herein was collected. This does not imply that these tracers will ever show up. Also, not all tracers were studied by all modelling groups.

A quick overview of the figures clearly shows that consideration of block scale reactive transport adds a significant "spread" in the range of predictions, becoming more pronounced with increasing path length (C2 and C3). The results for C1 in terms of bromide (Figure 3-3), show predictions which are in the same range. For K (Figure 3-6), Rb (Figure 3-7) and Cs (Figure 3-8), the differences in predictions span more than an order of magnitude. What should be remembered is that the conditions applicable to flow path I and the C1 injection very much resemble those met during the TRUE-1 experiments; the distance are in the same order and in addition there exists a geological and mineralogical kinship between Structure #20 of C1 and Feature A investigated as part of the TRUE-1 tests.

In the case of the C2 and C3 predictions, the span is more than an order of magnitude, cf Figures 3-9 through 3-12 and 3-13 through 3-17, respectively.

Two kinds of differences may explain the range of responses obtained by the groups: On the one hand, assuming that the differences between the conceptual models employed by the groups are unimportant, the variations in modelled responses must be due to the use of widely varying input parameters. On the other hand, if variations in responses do not appear consistent with the magnitudes of the parameters used by the groups, then they must be due to the differences in the conceptual models (including description of flow) employed by the modelling teams, cf Chapter 2.

If we scrutinise the parameters used by the modelling groups (see Tables A-1 through A-4 in Appendix A), a large range in the employed input parameters for the retention properties is noted:

- Porosities, not accounting for the Posiva-VTT value (see footnote in Table A-1) are in a range from 0.1% to 2%, i.e. within a factor of 20.

- Input diffusivity values are very much in agreement, with values in the 10^{-11} m^2/s order of magnitude applied by most teams, except for the case where the SKB-WRE team has employed their *in situ* evaluated parameters from the TRUE-1 tests ($1–5\ 10^{-10}$ m^2/s). Note that the values given for JNC-Golder cannot be directly compared to other ones. However, these values are fully compatible with the D_p values used by the other groups, given "reasonable" assumptions (see footnote).

- Input K_a values are within an order of magnitude for Ba, Cs and Rb. A two orders of magnitude difference (or more) is observed for Ca, K, and Na. Here, large values are applied by Posiva-VTT, while SKB-WRE employ the low values.

- The range of variability in applied K_d for various tracers is always large when comparing the groups with contrasts of two orders of magnitude for Ba and three orders of magnitude for all other tracers (exception being K, for which "only" a factor of 50 difference is noted). Low values are for the most part used by JNC-Golder, while Posiva-VTT and (to a lesser degree SKB-WRE) use values in the higher range.

Most of the variations discussed above may be summarised by computing the value of parameter κ [$LT^{-1/2}$], defined in Section 2.7.3 by:

$$\kappa=\theta\left[D_m\left(1+\frac{\rho K_d}{\theta}\right)\right]^{1/2}, \qquad (3\text{-}1)$$

where the notations are the ones given in Section 2.2, i.e.
θ is the porosity of the immobile zone [–];
D_m is the pore diffusivity into the immobile zone [L^2T^{-1}];
ρ is the density of the solid fraction [ML^{-3}];
K_d is the volume sorption coefficient [–].

Figure 3-2 below shows the values of κ as computed from the parameter values shown in Tables A-1 through A-4 in Appendix A.

In the following paragraphs, we try to ascertain the relationship between the ranges of input parameters used and the retentive responses obtained by the various modelling groups. Note that when we refer to the "range" of parameters, we simply mean the parameters used by the groups, as discussed above, and do not refer to what is the possible or plausible range of such parameters.

Nirex-Serco is one of the two groups which chose "mid-range" input parameters in all cases but one, but still consistently underestimate retention for the tracers used in the C1 and C2 tests. The explanation of the observed differences in output compared to the other groups in this case cannot be attributed to the choice of retention parameters.

The ENRESA-UPV/UPC group also chose "reasonable" mid range parameters for all but one case. This translates to breakthrough curves that are compatible with those of the other groups (possibly with the exception of Rb), despite the fact that surface sorption was not taken into account in the predictions.

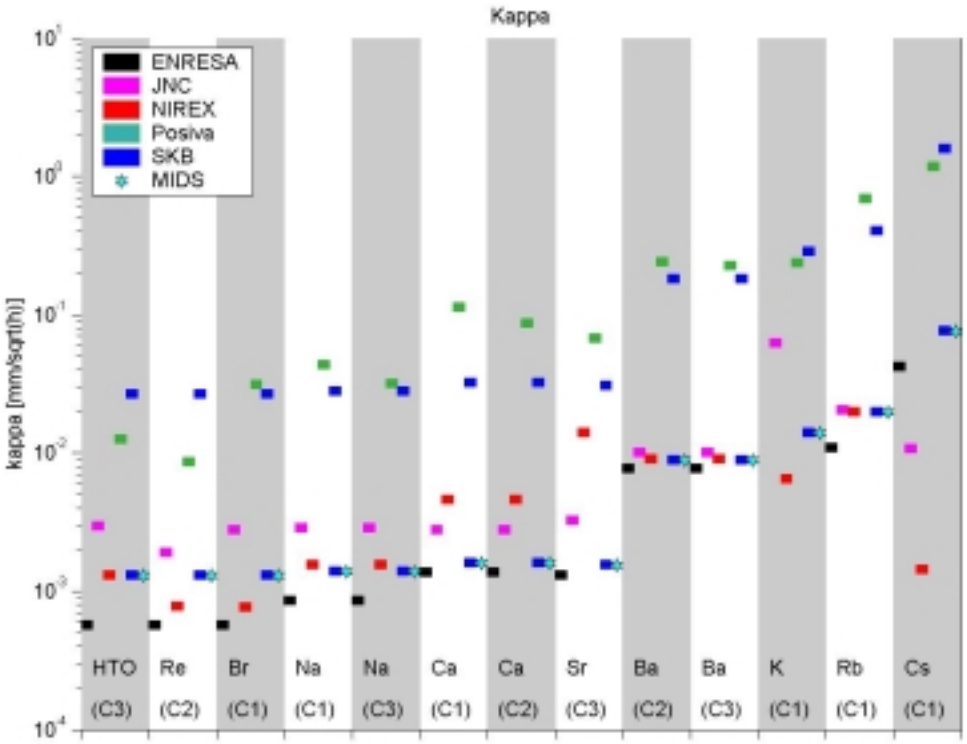

Figure 3-2. *Values of the κ (mm/h$^{1/2}$) material properties parameter used for the prediction of Phase C tracer experiment. Explicit numbers of the involved retention parameters are given in Appendix A.*

The JNC-Golder results also seem to be "in line" with the relative strengths of the selected retention parameters. Low K_d values (except for K) have been selected, while K_a values for the most part are "mid-range" (except for K again, with a large value). Therefore, retention should be expected in the lower end of the spectrum for most tracers (except for K which should be more retarded). A scrutiny of the breakthrough curves confirms this expectation, especially for the more reactive tracers where retention plays a large role.

The values provided by Posiva-VTT were not used in a direct fashion in the calculations. However, considering the global grouped parameter used, high porosities (see Table A-1 in Appendix A) combined with "reasonable" diffusivities and high K_a's and K_d's should yield a high retardation. This is in fact the case for most of the predicted breakthrough curves.

In Figures 3-3 through 3-17 the results of the SKB-WRE team predictions using evaluated *in situ* retention parameters from the TRUE-1 site are shown. For the C1 predictions the input evaluated *in situ* TRUE-1 retention parameters perform well, but less well for the C2 and C3 tests.

In summary, a full comparison of the prediction results of the modelling teams in relation to the input parameter data has to take into account the conceptualisation of the studied system (flow field and micro-structure/immobile zones). To the extent models with similar input data produce equitable output, the underlying conceptualisation of the flow field and description of immobile pore space (number of immobile zones, geometry and parameter values) produce a net effect which is nearly the same. In Section 6.2.3, attempts are made to evaluate the relative effects of the flow field on the evaluated retention. In Section 8.3 these results of the predictive modelling are revisited and discussed i.a. in the light of the results presented in Section 6.2.3.

Table 3-1. Measured and predicted characteristic times and recoveries, C1 injection. Times T_{xx} in hours, Recovery in % of total injected mass.

Tracer	Measure	Measured	ENRESA	JNC	Nirex	Posiva	SKB
Br-82	T_5	9	7.5	11	8	10	8.5
	T_{50}	20	16.5	26	12.4	43	23
	T_{95}	49	31.5	131	23.4	5,638	157
	Recovery	100 (160h)	100	100	100	96	95
Na-24	T_5	10	9	11	8.8	13	8.1
	T_{50}	27	23	24	12.1	37	20.5
	T_{95}	110	37	121	23.1	0	146
	Recovery	96 (110h)	100	100	100	94	93
Ca-47	T_5	14	10	11	9.8	25	8.8
	T_{50}	46	26	26	12.7	197	23.6
	T_{95}	260	65	131	25.5	0	333
	Recovery	98 (300h)	100	100	100	88	95
K-42	T_5	21		320	9.4	37	36
	T_{50}	100		750	13	645	377
	T_{95}	D		0	25.5	0	0
	Recovery	53 (110h)		92	100	80	23
Rb-86	T_5	66	34	45	40	196	77
	T_{50}	400	110	104	48	5,048	779
	T_{95}	D	330	660	68	0	0
	Recovery	67 (730h)	100	99	100	59	49
Cs-134	T_5	530		160	85	1,227	1072
	T_{50}	5000		450	103	0	11270
	T_{95}	0		2600	139	0	0
	Recovery	39 (3255h)		97	100	41	23

D=Short-lived isotope that had decayed before the specified mass recovery could be reached.

Table 3-2. Measured and predicted characteristic times and recoveries for the C2 injection. Times T_{xx} in hours, Recovery in % of total injected mass.

Tracer	Measure	Measured	ENRESA	JNC	Nirex	Posiva	SKB
Re-186	T_5	94	60	74	436	67	73
	T_{50}	260	180	200	568	263	191
	T_{95}	D	438	0	0	0	6211
	Recovery	80 (500h)	100	73	73	93	74
Ca-47	T_5	300	105	123	324	335	81
	T_{50}	D	330	370	380	6,324	241
	T_{95}	0	750	0	0	0	9428
	Recovery	29 (800h)	100	66	86	61	78
Ba-131	T_5	0		850	442	1715	642
	T_{50}	0		0	572	0	4,872
	T_{95}	0		0	0	0	0
	Recovery	0 (1900h)		7	79	33	27
Cs-137	T_5	0		0	2041	0	40136
	T_{50}	0		0	3390	0	4E+05
	T_{95}	0		0	0	0	0
	Recovery	0 (3197h)		0	91	1	0

D=Short-lived isotope that had decayed before the specified mass recovery could be reached.

Table 3-3. Measured and predicted characteristic times and recoveries for the C3 injection. Times T_{xx} in hours, Recovery in % of total injected mass.

Tracer	Measure	Measured	ENRESA	JNC	Nirex	Posiva	SKB
HTO	T_5	230	175	145	70	155	154
	T_{50}	820	0	330	118	953	441
	T_{95}	0	0	2000	298	0	14729
	Recovery	73 (3050h)	42	96	100	83	86
Na-22	T_5	340	190	152	73	301	154
	T_{50}	1500	0	380	147	3886	448
	T_{95}	0	0	0	0	0	15327
	Recovery	70 (3100h)	41	82	100	67	86
Sr-85	T_5	640	200	164	71	731	172
	T_{50}	3000	0	370	123	0	538
	T_{95}	D	0	1600	303	0	20066
	Recovery	52 (3100h)	44	99	100	47	83
Rb-83	T_5	0		500	352	0	6964
	T_{50}	0		1400	466	0	58857
	T_{95}	0		0	695	0	0
	Recovery	0 (3219h)		86	100	2	0.4
Ba-133	T_5	0		1100	114	5798	1538
	T_{50}	0		0	178	0	11526
	T_{95}	0		0	371	0	0
	Recovery	0 (3219h)		8	100	13	19

D=Short-lived isotope that had decayed before the specified mass recovery could be reached.

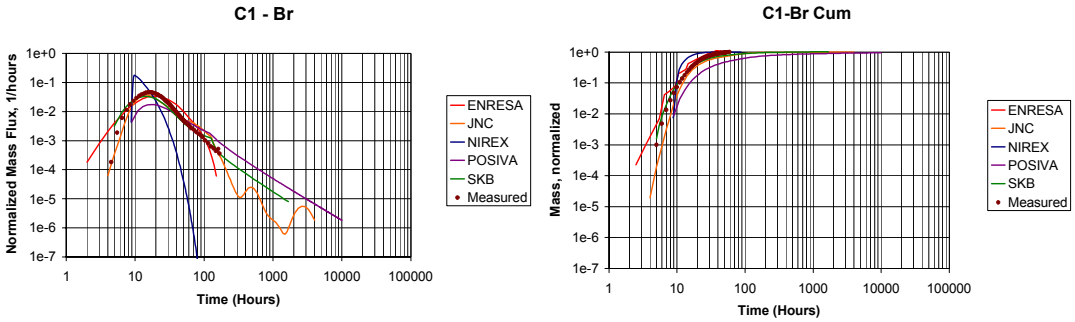

Figure 3-3. *Predicted and measured breakthrough curves for Bromide, test C1.*

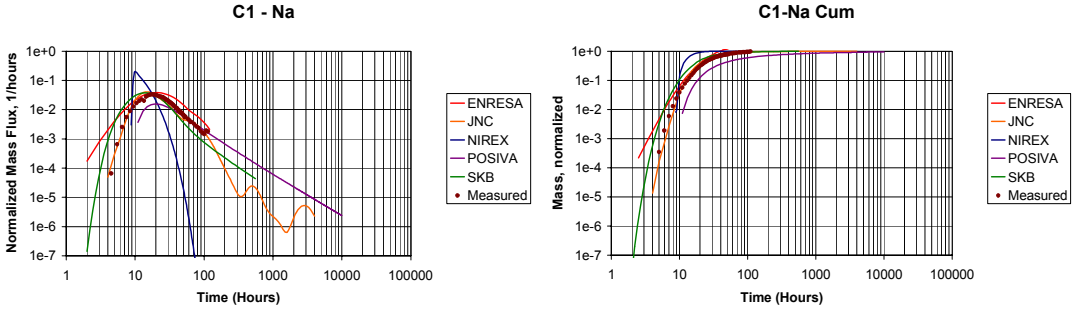

Figure 3-4. *Predicted and measured breakthrough curves for Sodium, test C1.*

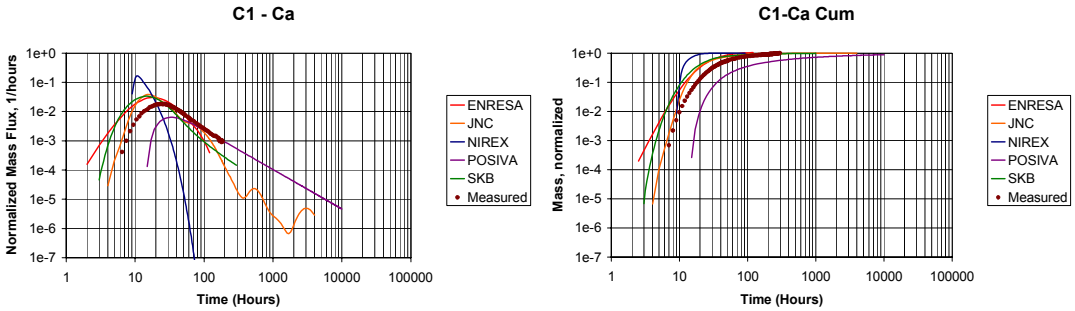

Figure 3-5. *Predicted and measured breakthrough curves for Calcium, test C1.*

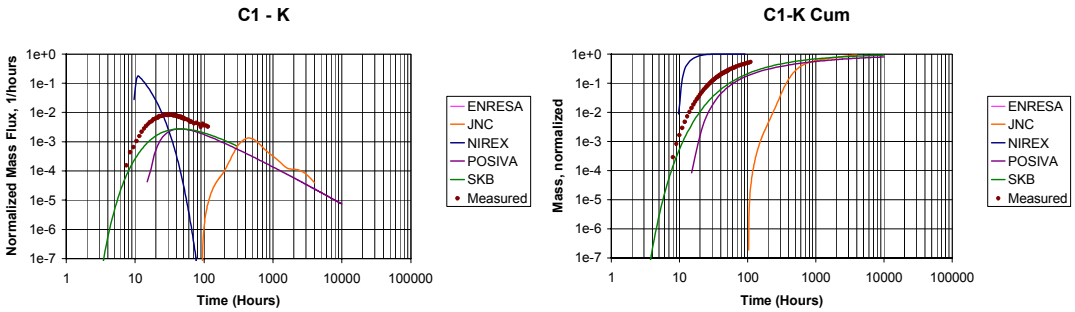

Figure 3-6. *Predicted and measured breakthrough curves for Potassium, test C1.*

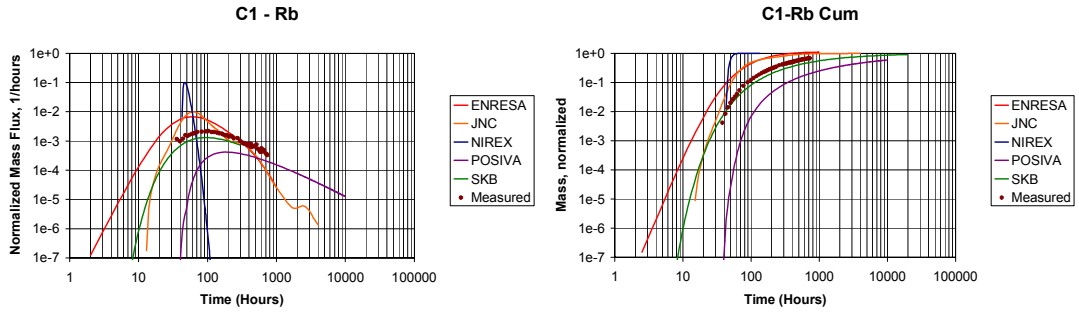

Figure 3-7. *Predicted and measured breakthrough curves for Rubidium, test C1.*

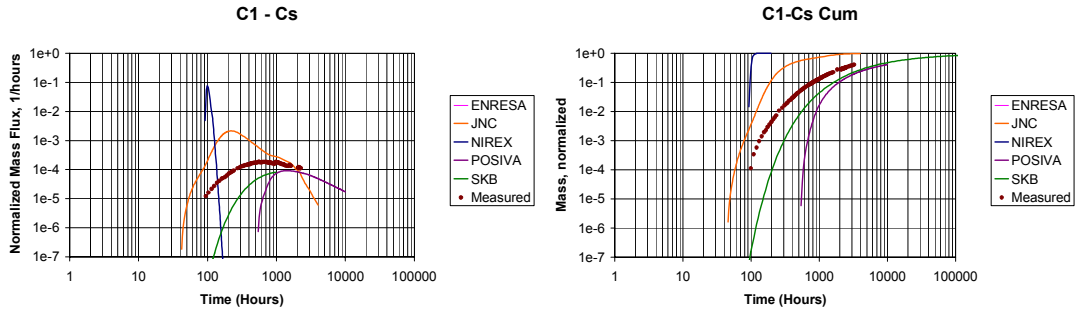

Figure 3-8. *Predicted and measured breakthrough curves for Cesium, test C1.*

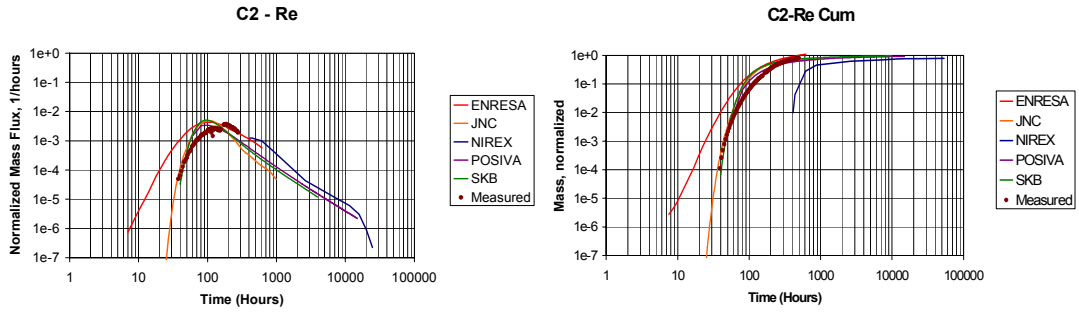

Figure 3-9. *Predicted and measured breakthrough curves for Rhenium, test C2.*

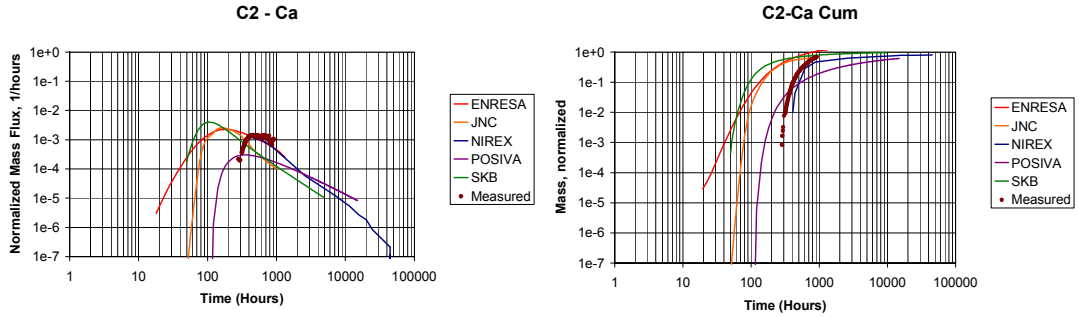

Figure 3-10. *Predicted and measured breakthrough curves for Calcium, test C2.*

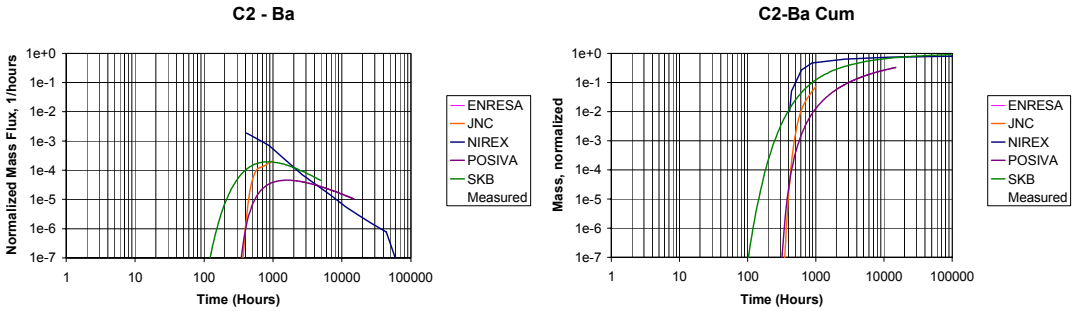

Figure 3-11. *Predicted and measured breakthrough curves for Barium, test C2.*

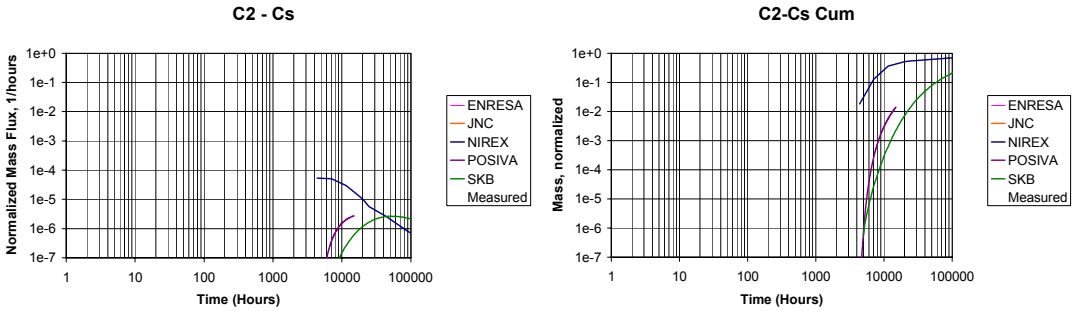

Figure 3-12. *Predicted and measured breakthrough curves for Cesium, test C2.*

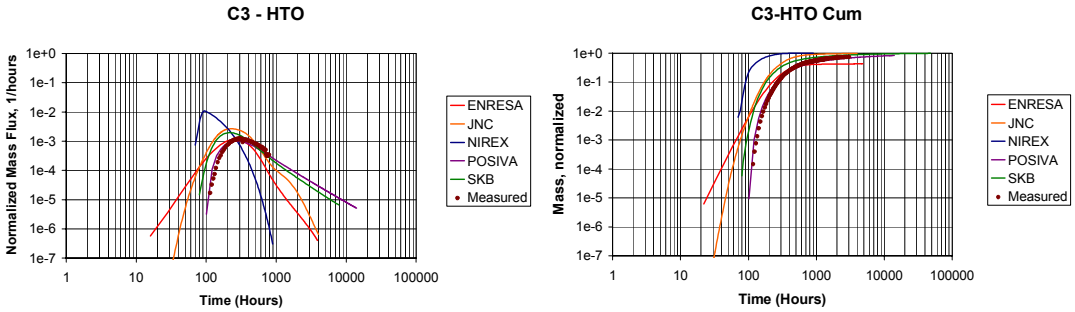

Figure 3-13. *Predicted and measured breakthrough curves for tritiated water, test C2.*

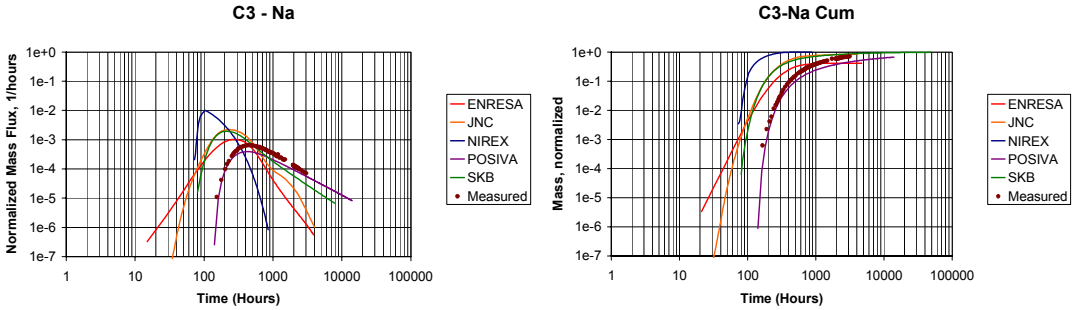

Figure 3-14. *Predicted and measured breakthrough curves for Sodium, test C3.*

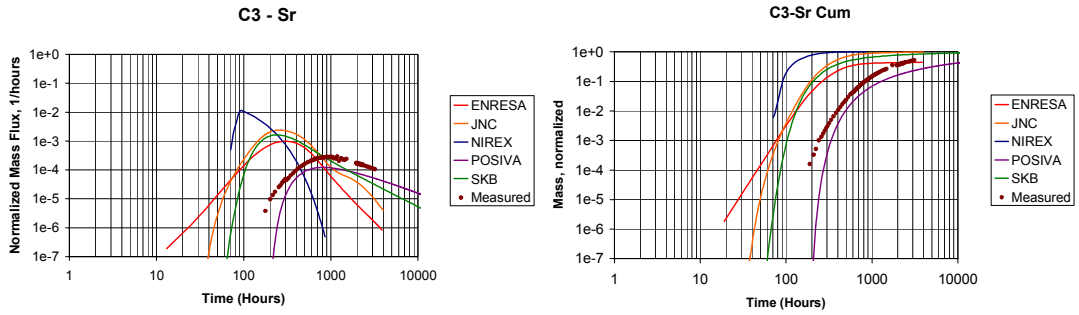

Figure 3-15. *Predicted and measured breakthrough curves for Strontium, test C3.*

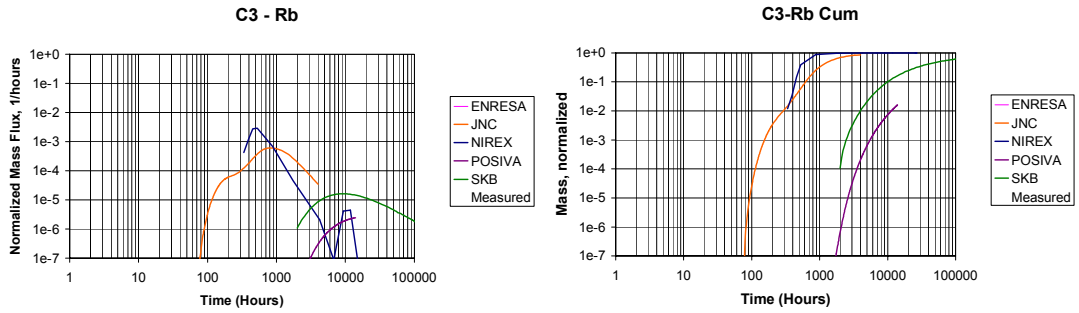

Figure 3-16. *Predicted and measured breakthrough curves for Rubidium, test C3.*

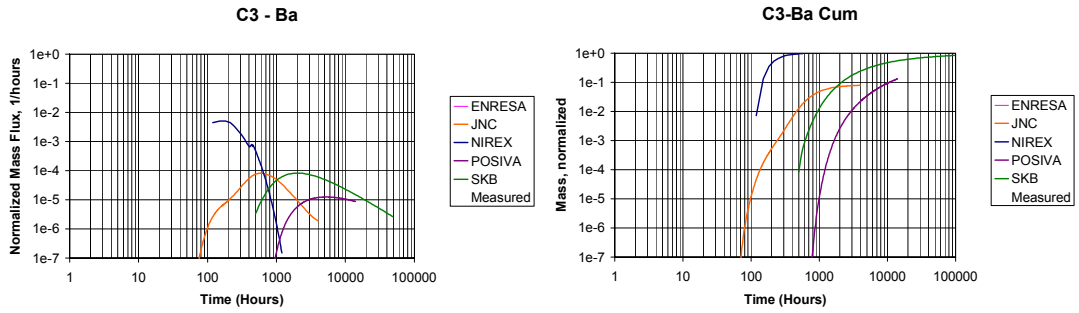

Figure 3-17. *Predicted and measured breakthrough curves for Barium, test C3.*

4 Testing of the hydrostructural model

The hydrostructural model, /Andersson et al, 2002a/, is principally a geometrical model of the TRUE Block Scale rock volume, designed to reproduce the overall connectivity of the 'major' conductors at the site. It is based on an integration of geophysical, geochemical, geological, and hydrogeological measurements and interpretations. One of the principal project hypotheses concerns whether the TRUE Block Scale rock mass can be represented by a 3-dimensional discrete feature hydrostructural model, cf Section 1.6. A great deal of information has been used in the construction of the hydrostructural model, therefore care must be taken when proving, or disproving this hypothesis, to avoid a potentially tautological approach. However, given the complexity of the connectivities, it is possible to at least determine whether the hydrostructural model is consistent with the measurements on which it is based.

This chapter describes the evaluation of the hydrostructural model hypothesis using stochastic continuum, discrete fracture network, and channel network techniques. The questions address include:

- does the hydrostructural model properly account for rock mass heterogeneity?
- is the hydrostructural model consistent with observed connectivity patterns?
- is the hydrostructural model consistent with the results of *in situ* tracer tests?

4.1 Evaluation based on conditioned hydraulic conductivity values

The self-calibrated algorithm for conditioning realisations of conductivity fields to piezometric head data used by the stochastic continuum (SC) modelling /Gómez-Hernández et al, 2002/ pinpointed some inconsistencies in the hydrostructural model in its preliminary versions. The self-calibrating SC algorithm conditions a heterogeneous realisation initially conditioned to measurements of hydraulic conductivity (but not to piezometric head data) by applying a perturbation to initial realisations. This perturbation is determined through a non-linear optimisation approach, and produces a conditioned hydraulic conductivity field. Comparison of the initial and final (conditioned) hydraulic conductivity fields can be used to determine which features become more permeable, and which become less permeable.

During the early modelling stages, using the October '97 hydrostructural model, all fractures had a log-conductivity average value of –6.5 log m/s. The conditioning to steady-state and transient piezometric heads introduced changes that modified, both locally and globally, the hydraulic conductivities within each fracture. Conditioning

results are shown in Table 4-1. Of these modifications, the increase of the average conductivities in Structures #8 and #16 by close to one order of magnitude were not consistent with the geological understanding of the site at the time. Structure #16 is subhorizontal and considered as not active, and Structure #8 is subvertical but it is also considered that it does not contribute to the hydraulic connectivity of the site. On the other hand, the hydraulic conductivity of Structure #5 decreased by two orders of magnitude, which is consistent with fact that this feature was grouted during the drilling of borehole KA2563A due to its large flow production.

The geologically inconsistent increase of conductivities in Structures #8 and #16 could be explained by the need to introduce some north-south connectivity to the site. Later, when Structures #21–#23 were added to the hydrostructural model, Structures #8 and #16 did not have to increase their hydraulic conductivities to match the piezometric head data.

Table 4-1. Testing of initial hydrostructural model by stochastic continuum modelling.

Structure	Initial Realisation	Conditioned to Steady State Heads	Conditioned to Transient Heads	Difference between Initial and Transient Head Conditioned
	Average hydraulic conductivity $\log_{10}$ m/s			Hydraulic conductivity $\log_{10}$ m/s
Background	–10.12	–9.83	–10.19	–0.07
#1	–6.47	–6.54	–6.54	–0.07
#2	–6.32	–6.22	–6.34	–0.02
#3	–6.47	–6.4	–6.46	0.01
#4	–6.44	–7.3	–7.32	–0.88
#5	–6.55	–4.98	–4.62	1.93
#6	–6.75	–8.18	–8.29	–1.54
#7	–6.39	–7.27	–7.37	–0.98
#8	–6.41	–4.78	–5.38	1.03
#9	–6.56	–8.05	–8.02	–1.46
#10	–6.29	–7.57	–7.41	–1.12
#11	–6.55	–7.93	–7.77	–1.22
#13	–6.48	–6.55	–6.59	–0.11
#15	–6.51	–7.75	–7.59	–1.28
#16	–6.27	–5.42	–5.32	0.95
#17	–6.28	–6.19	–5.9	0.38
#18	–6.22	–6.77	–7.04	–0.82
#19	–6.4	–5.98	–5.52	0.88
#20	–6.44	–6.35	–6.58	–0.14
#Z	–6.3	–7.2	–7.13	–0.83
EW-1	–6.3	–6.33	–6.32	–0.02

4.2 Evaluation based on hydraulic interference tests

Hydraulic interference and dilution tests are the most direct experimental measures of the hydraulic connectivity of the rock block, and therefore are an excellent approach for testing the hydrostructural model. The ability of the hydrostructural model to match the pattern of responses to hydraulic interference tests is a measure of the degree to which the connectivity of the hydrostructural model is consistent with *in situ* conditions. Simulation of hydraulic interference tests were carried out using the DFN/CN model, which directly implements both the deterministic structures and the background fracturing components of the hydrostructural model as homogeneous planes.

Interference tests typically show one of four main classes of responses:

1) **Network Response:** The greater the distance from the hydraulic source, the weaker the response. This is the classic distance-drawdown response. Experimental data showing network response are shown in Figure 4-1. Simulation results that display network response are shown in Figure 4-2.

2) **Compartment Response:** All points respond approximately the same, regardless of the distance from the hydraulic signal. This typically occurs within single structures of high transmissivity, with poor connection to hydraulic boundary conditions. Experimental data displaying compartment response are shown in Figure 4-3. Simulation results that show compartment response are shown in Figure 4-4.

3) **Flow Barrier Response:** Points show little or no hydraulic response, regardless of the distance from the hydraulic signal. This can be due to a lack of hydraulic connection, or due to a strong connection to a constant head boundary condition. Experimental data showing flow barrier response are shown in Figure 4-5. Simulation results that display flow barrier response are shown in Figure 4-6.

4) **Heterogeneous Response:** Responses are observed which are only poorly correlated to the Cartesian distance. This response is typical of cases where there are strong conductors which are connected to the hydraulic source and some of the monitoring sections, but are not connected into the overall fracture network. Experimental data showing heterogeneous response are shown in Figure 4-7. Simulation results that display heterogeneous response are shown in Figure 4-8.

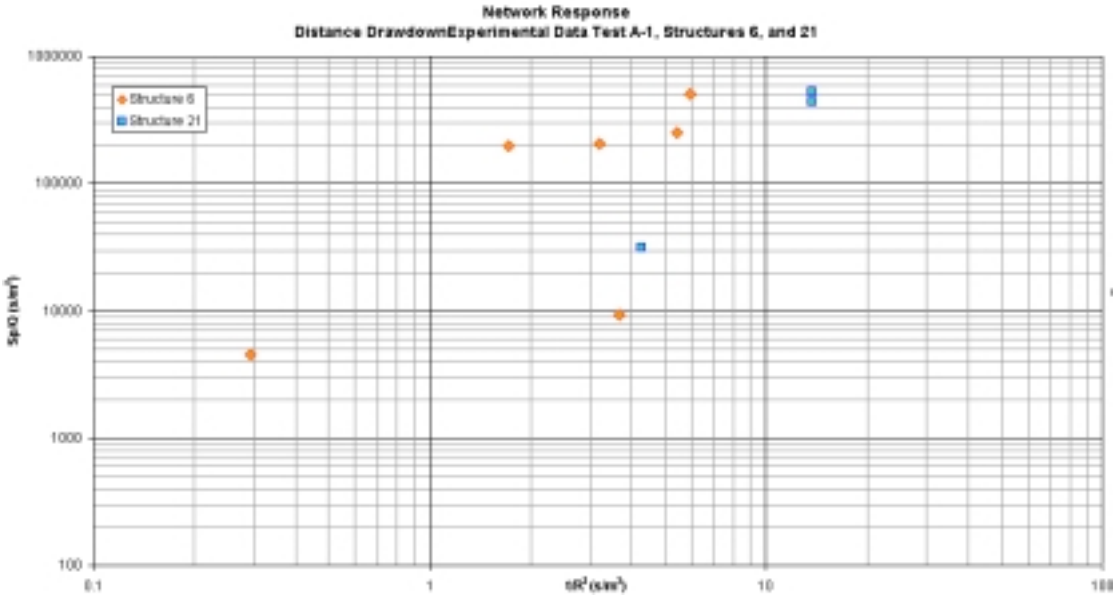

Figure 4-1. *Experimental data displaying Network Response.*

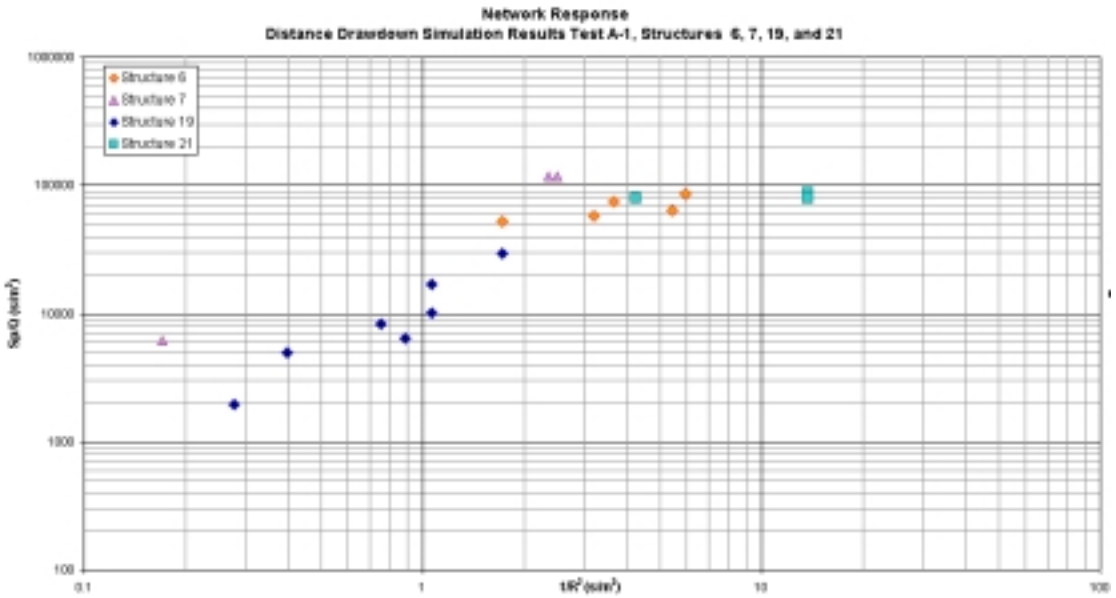

Figure 4-2. *Simulation results displaying Network Response (DFN/CN).*

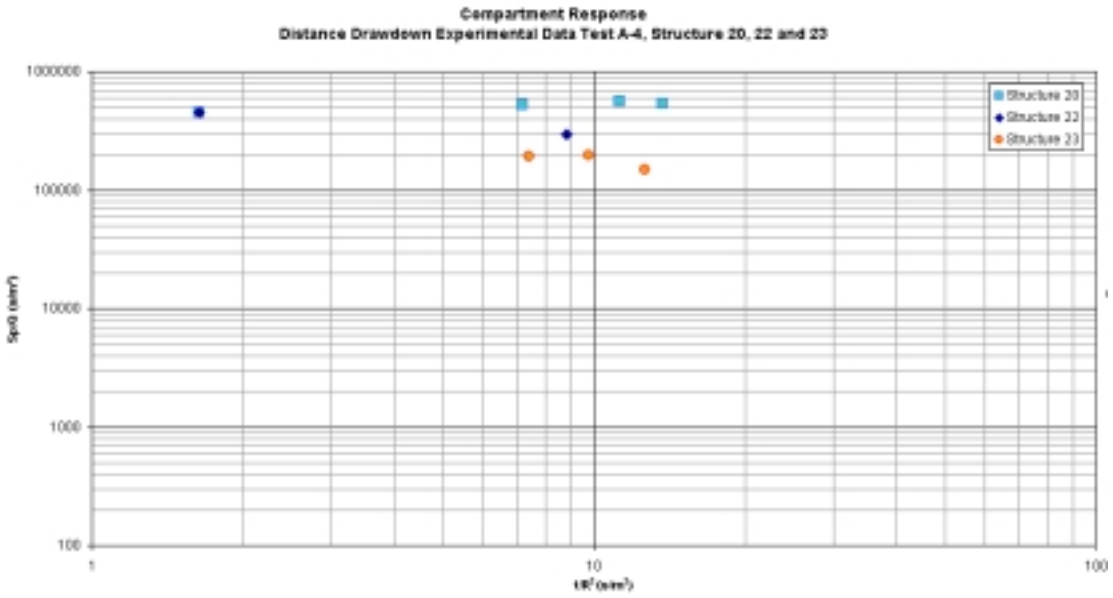

Figure 4-3. *Experimental data displaying Compartment Response.*

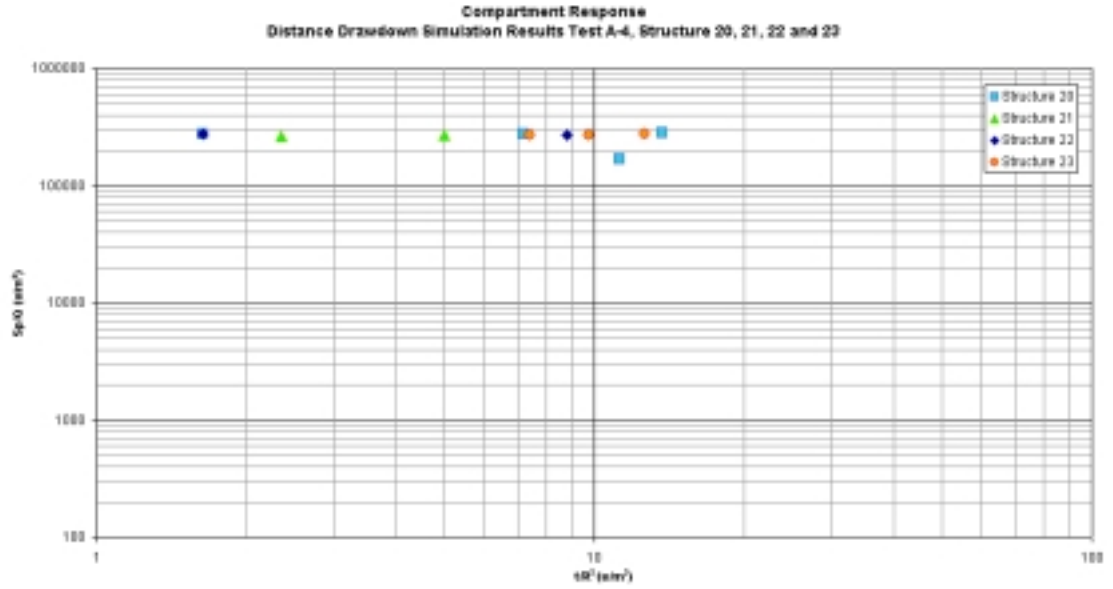

Figure 4-4. *Simulation results displaying Compartment Response (DFN/CN).*

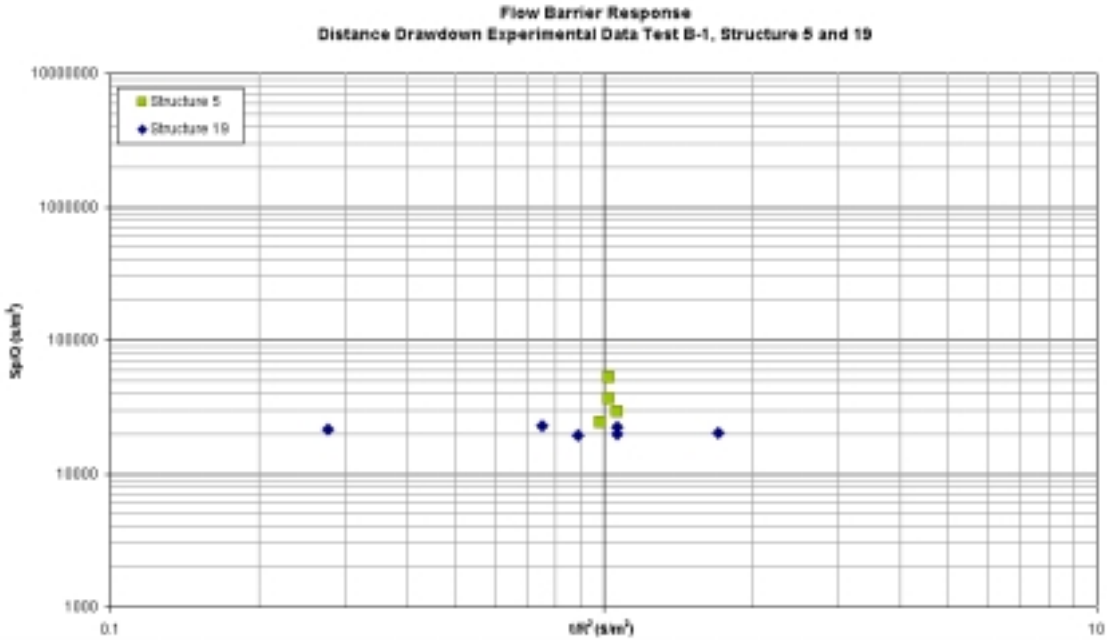

Figure 4-5. *Experimental data displaying Flow Barrier Response.*

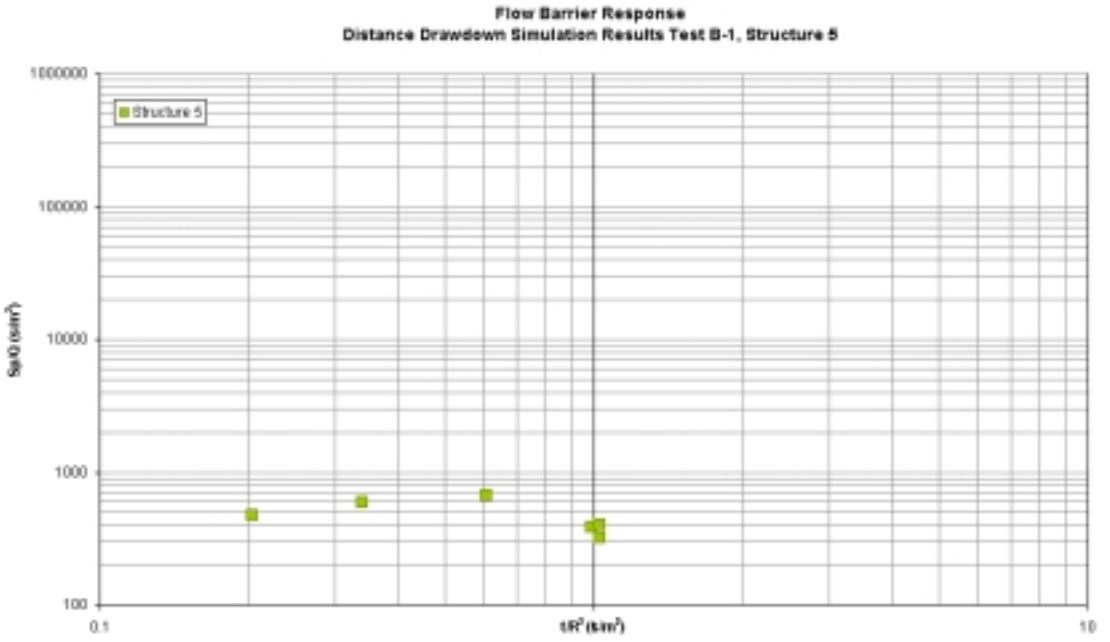

Figure 4-6. *Simulation results displaying Flow Barrier Response (DFN/CN).*

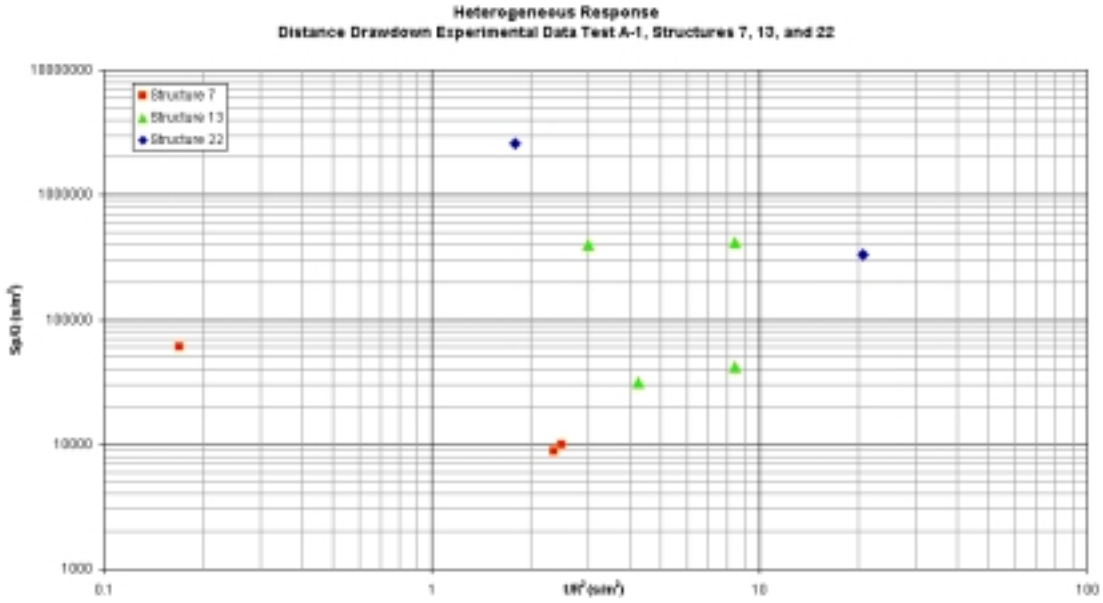

Figure 4-7. *Experimental data displaying Heterogeneous Response.*

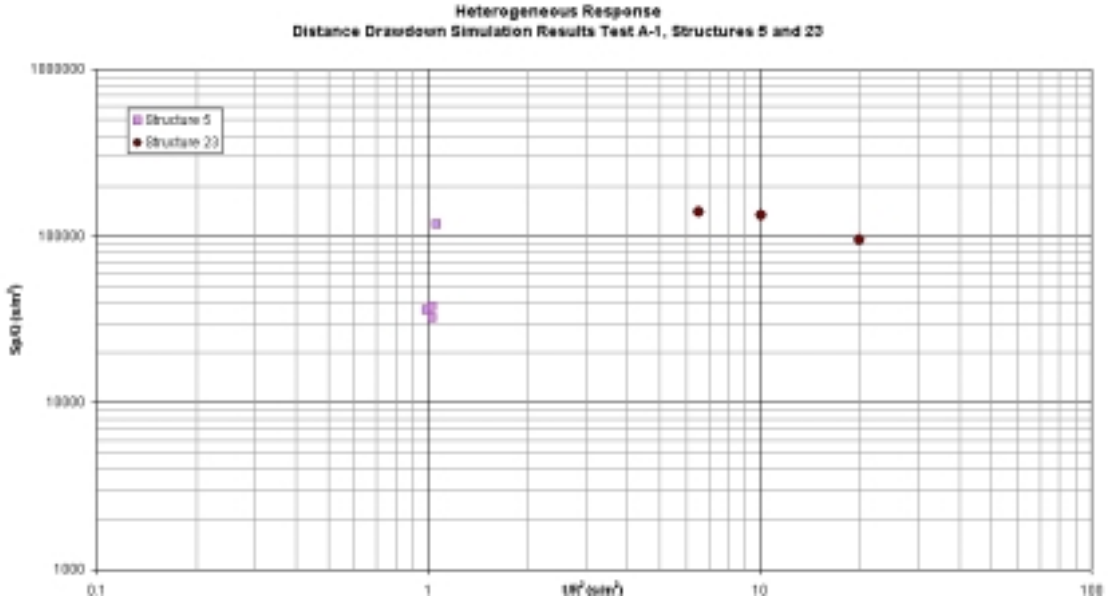

Figure 4-8. *Simulation results displaying Heterogeneous Response (DFN/CN).*

As can be seen from Figures 4-1 through 4-8 all four of these response classes have been seen in the field tests performed in the TRUE Block Scale rock volume, and these are also visible in the simulations based on the hydrostructural model. The ability of the hydrostructural model to reproduce the pattern of hydraulic response provides a direct comparison of the connectivity of the hydrostructural model against the *in situ* connectivity measurements.

Table 4-2 summarises the hydraulic responses observed in Phase A and Phase B testing, together with the results from simulations carried out using the DFN/CN model without background fractures. In Table 4-2, each of the measured responses to hydraulic interference testing is identified with the corresponding structure from the hydrostructural model, and the type of response seen. Although many of the responses observed *in situ* are correctly identified in the hydrostructural model as simulated in the DFN/CN model, there are several distinctive differences.

Interestingly, the type of response observed *in situ* is predominately a compartmental response, with the same normalised drawdown over orders of magnitude in normalised distance. This is inconsistent with the essential hydrostructural model, which provides a backbone for extensive interconnections throughout the rock mass, even without considering the additional connectivity provided by background fracturing. The level of connectivity of the hydrostructural model is evident in the fact that the simulations show generally network responses, even for the DFN/CN model implemented without background fractures.

Based on the results shown in Table 4-2, it is apparent that the hydrostructural model is overconnected, at least in a number of locations. The level of connectivity of the hydrostructural model could be decreased by applying an aperture or transmissivity field on the surface of each of the structures, then conditioning these transmissivities to obtain the a level of connectivity consistent with *in situ* measurements, as in the stochastic continuum modelling for example. Alternatively, a limited number of flow barrier structures within the model could explain the tendency toward compartmentalised responses.

Table 4-2. Hydraulic responses – experimental data and simulation results from DFN/CN model.

Test		**Network response** – Experimental – *Simulation*	**Compartment response** – Experimental – *Simulation*	**Flow barrier response** – Experimental – *Simulation*	**Heterogeneous response** – Experimental – *Simulation*
A1	20	6, 21 *6, 7, 19, 21*	20, 23 *13, 20, 22*	5, 19 –	7, 13, 22 *5, 23*
A2	21	6 *6, 7, 19, 21*	20, 22, 23 *20, 22, 23*	5, 19 –	7, 13, 21 *5, 13*
A3	20	– *6, 7, 13, 19, 20*	20, 21, 22, 23 *21, 22, 23*	5, 19 5	6, 7, 13 –
A4	20/21	6, 13, 21 *6, 7, 19*	20, 22, 23 *20, 21, 22, 23*	5, 19? –	7 *5, 13*
A5	20	6, 21 *7, 19, 22*	20, 22 *6, 21, 23*	5 *5*	7, 13, 19, 23 *13, 20*
B1	20/21	– *6?, 7, 19, 21*	6, 20, 22 *22, 23*	5, 19 *5*	7, 13, 21, 23 *13, 20*
B2	20/21	19? *6, 7, 19, 21*	6, 7, 22 *22, 23*	5 *5*	13, 20?, 21, 23 *13, 20,*

Although there are several exceptions, in general, the DFN/CN model drawdowns are lower than those in the measurements. This provides an additional indication that the DFN/CN implementation of the hydrostructural model is better connected to the hydraulic boundary conditions than the *in situ* rock mass. Alternatively, this error can be the results of the modelled boundary conditions. The average drawdown in the DFN/CN implementation of the hydrostructural model was increased to match measured values by adding a low hydraulic conductivity (K=10^{-10} m/s) skin zone where the structures/fractures of the 150 m model connect to the 500 m scale model.

The DFN/CN model was also used to evaluate whether specific changes to the hydrostructural model could improve the models connectivity as evidenced in the interference tests. Three DFN/CN models simulations were carried out for the A1 hydraulic interference test: The first (reference) simulation (Figure 4-9) considers the hydrostructural model, including the background fractures. The second simulation (Figure 4-10) removes the background fractures, as in the simulations reported in Table 4-2. The third simulation (Figure 4-11) attempts to improve the hydrostructural model to reduce the over-connectivity,

- Structure 21 was divided to reduce over-connectivity.
- Low permeability zones were introduced along the intersections between Structures 13 and 21 to reduce connectivity.
- The transmissivity of Structures 6, 13, 19, 20, and 21 was modified.

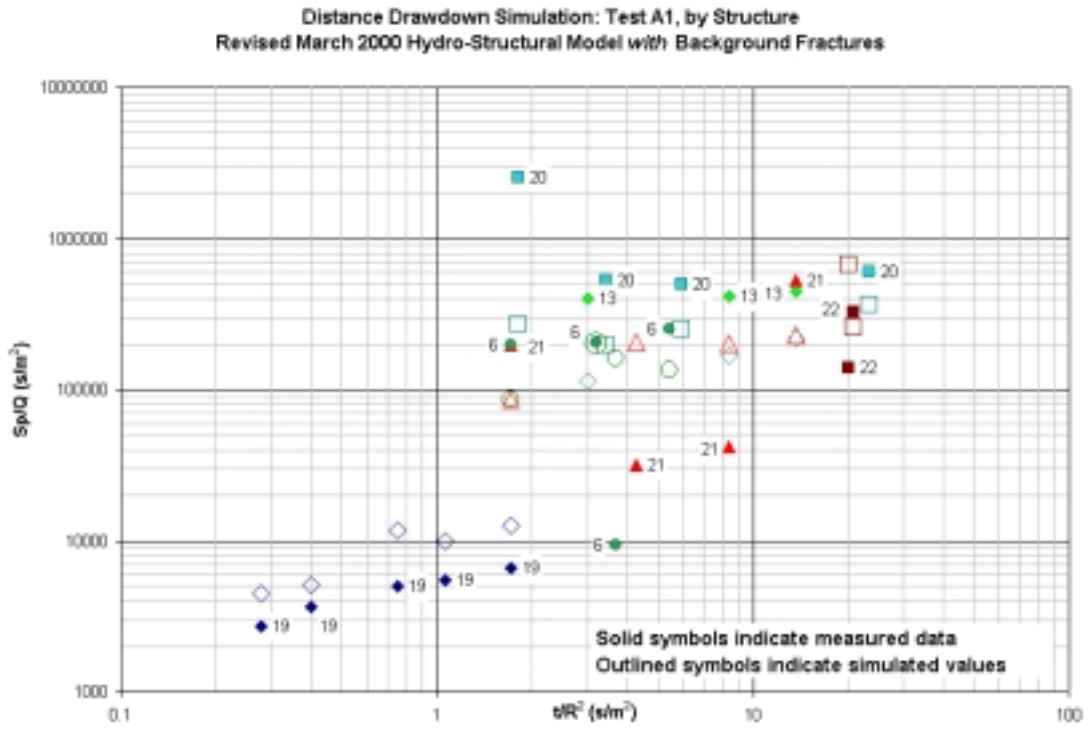

Figure 4-9. *Simulated distance-drawdown based on hydrostructural model with background fractures.*

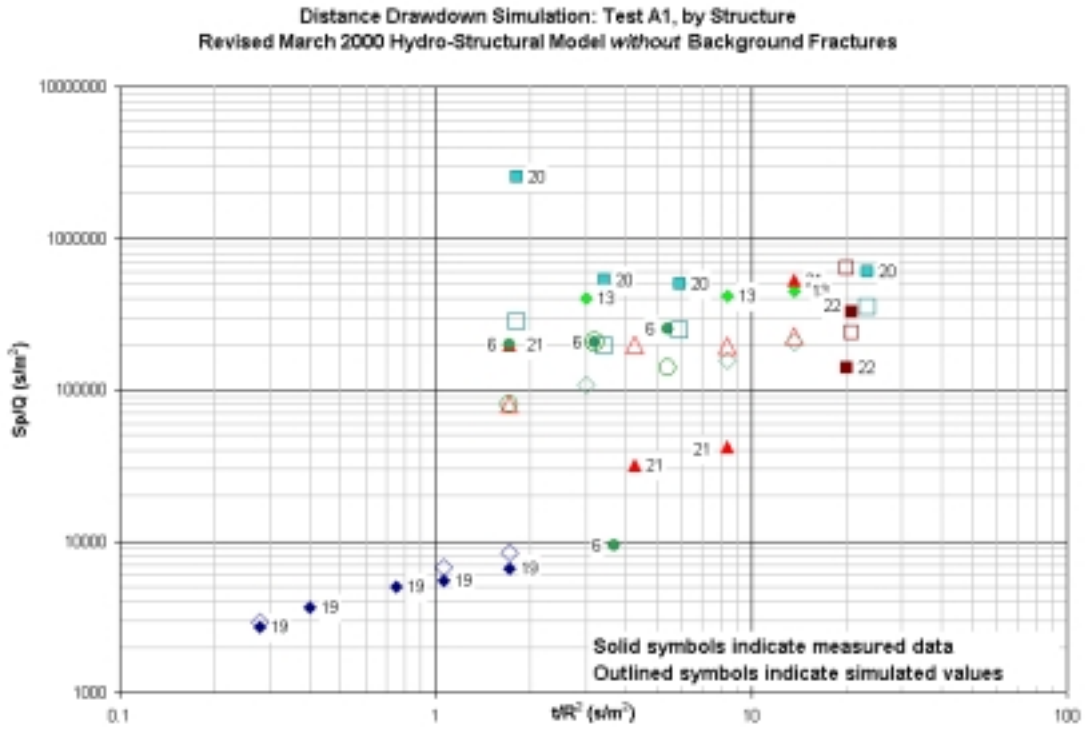

Figure 4-10. *Simulated distance-drawdown based on basic hydrostructural model.*

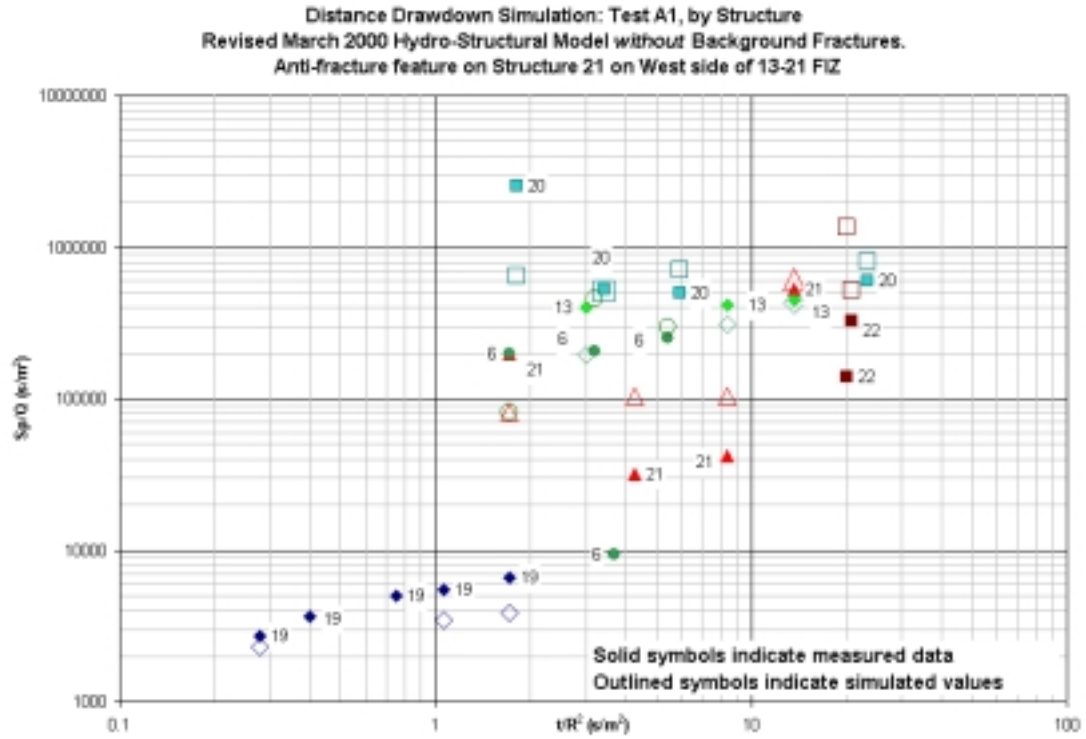

Figure 4-11. *Simulated distance-drawdown based on revised hydrostructural model.*

Most of the sampling points for the simulation of the hydrostructural model including the background fractures have too low a drawdown, consistent with the expectation for the hydrostructural model including background fractures. In the second simulation, with the background fractures removed, a much better match is obtained, but there are still a number of points with significant errors, particularly for Structures 13 and 21 indicating possible over-connection. The revised hydrostructural model used for the third simulation shows a clear improvement in the simulated interference test response. This indicates that the improvement of some form of heterogeneity in the plane of the structures may be appropriate. In addition, it provides support for the possible inclusion of flow barrier features within hydraulic structures.

4.3 Evaluation based on conservative tracer tests

The hydrostructural model was used directly to locate the boreholes, position packers, and determine sources and sinks for tracer tests. Tracer tests not carried out on pathways through the hydrostructural model were not expected to have sufficient recovery, and their intervals were therefore not tested. The importance of the hydrostructural model in the hydrotesting is therefore not an issue.

However, it is important to consider the extent to which the conservative tracer testing which was carried out can be considered to support or refute the hydrostructural model. This can be addressed in two ways:

- shape of breakthrough curve and degree of dispersion. The extent to which the tracer follows branching pathways rather than a single pathway defined by the hydrostructural model is a measure of the relative strength of the deterministically defined structures as compared to the stochastic fractures (or alternatively, the existence of multiple pathways within the structures),

- the percentage mass recovery. In theory, the ultimate recovery of mass for radially converging flow fields should be 100%. Any lack of mass recovery are generally an indication of branching pathways, which need to be explained by hydrostructural model components such as fracture intersection zones or branches in the network.

Table 4-3 summarises all of the conservative tracer tests carried out as part of the TRUE Block Scale Project, with their measured and projected ultimate recovery. Projected ultimate recovery for this table was calculated by graphically extending the measured breakthrough curve to at least 10,000 hours. Where projected ultimate recovery along pathways defined by the hydrostructural model is high (80–100%), this provides support for the hydrostructural model, since the high recovery would be unlikely in the absence of simple pathways through the hydrostructural model. Where the ultimate recovery is low (less than 30%) an explanation is needed as to whether this is due to the lack of pathways through the hydrostructural model, branching within the hydrostructural model, a failure of the hydrostructural model, or flows due to alternative sinks (i.e. the Äspö tunnels) through features not considered in the hydrostructural model.

Table 4-3. Ultimate recovery projected from conservative tracer tests.

Test	Pathway Source → Sink	Path Length[1] (m)	FIZ Crossings[1]	Effective Dispersion[2] (m)	Measured Recovery	Projected Ultimate Recovery[3]
A4a	KI0025F03:P5 → KI0023B:P6	17.9	0	1.5	38%	70%
A4b	KI00F03:P6 → KI0023B:P6	52.7	2	2	51%	90%
A4c	KI0025F03:P7 → KI0023B:P6	68.6	3	2.9	0	0
A5a	KA2563A:S4 → KI0025F03:P5	38.4	0	2.3	64%	72%
A5b	KI0025F02:P3 → KI0025F03:P5	55.9	1	4.5	0	0
A5c	KI0025F02:P5 → KI0025F03:P5	12.9	0	1	130%	100%
A5d	KI0025F02:P6 → KI0025F03:P5	41.1	1	4.1	43%	60%
A5e	KI0025F03:P6 → KI0025F03:P5	35	1	2.8	95%	100%
B1a	KI0025F03:P5 → KI0023B:P6	17.9	0	1.5	99%	100%
B1b	KI0025F03:P6 → KI0023B:P6	52.7	2	4.1	45%	65%
B1c	KI0025F02:P5 → KI0023B:P6	33.8	0	2	36%	38%
B2a	KI0025F03:P6 → KI0023B:P6	52.7	2	4.1	49%	60%
B2b	KI0025F02:P3 → KI0023B:P6	32.5	0	2	82%	85%
B2c	KA2563A:S1 → KI0023B:P6	169.2	2	13.5	3%	10%
B2d	KI00F03:P7 → KI0023B:P6	68.6	3	2.9	76%	80%
B2e	KI0025F03:P3 → KI0023B:P6	25.3	1	1.6	32%	36%
B2g	KI0025F03:P5 → KI0023B:P6	17.9	0	1.5	97%	99%
C1	KI0025F03:P5 → KI0023B:P6	17.9	0	1.5	111%	100%
C2	KI0025F03:P7 → KI0023B:P6	68.6	3	5.9	80%	100%
C3	KI00F02:P3 → KI0023B:P6	32.5	0	2	72%	80%

1. Path length and number of fracture intersection zone (FIZ) crossing calculated through the hydrostructural model.
2. Effective dispersion calculated using formula from /Domenico and Schwartz, 1992/, subtracting the dispersion in the injection curve calculated using the same formula.
3. Projected ultimate recovery (PUR) calculated by graphical projection of measured breakthrough curves to 10,000 hours.

Figure 4-12 presents the relationship between path length through the hydrostructural model and projected ultimate recovery for the conservative tracer tests summarised in Table 4-3. No clear relationship is visible between the path length and recovery, indicating that up to distances of at least 70 m, the paths as defined in the hydrostructural model are supported by the hydrostructural model. Only three of the 21 paths (14%) tested have projected ultimate recovery less than 30%, while ten of the 21 paths (48%) have projected ultimate recoveries of a least 80%. This again supports the hydrostructural model, although it does leave the open issue of where the missing tracer went, and whether the losses could be explained by adding features such as flow barriers to the hydrostructural model.

Figure 4-13 compares projected ultimate recovery for conservative tracers to the number of features intersections (FIZ) crossed along the pathway. Again, no clear correlation can be seen in an average sense. The pathways which have low recovery have one, two, and three FIZ crossings, indicating participation of two, three, and four fractures in the hydrostructural model. In addition, high recovery was also seen for several paths which included FIZ crossings. Perhaps this indicates some support for the hydrostructural model, since if the hydrostructural model were not correct, high recoveries would not be achieved for pathways of this level of structural complexity.

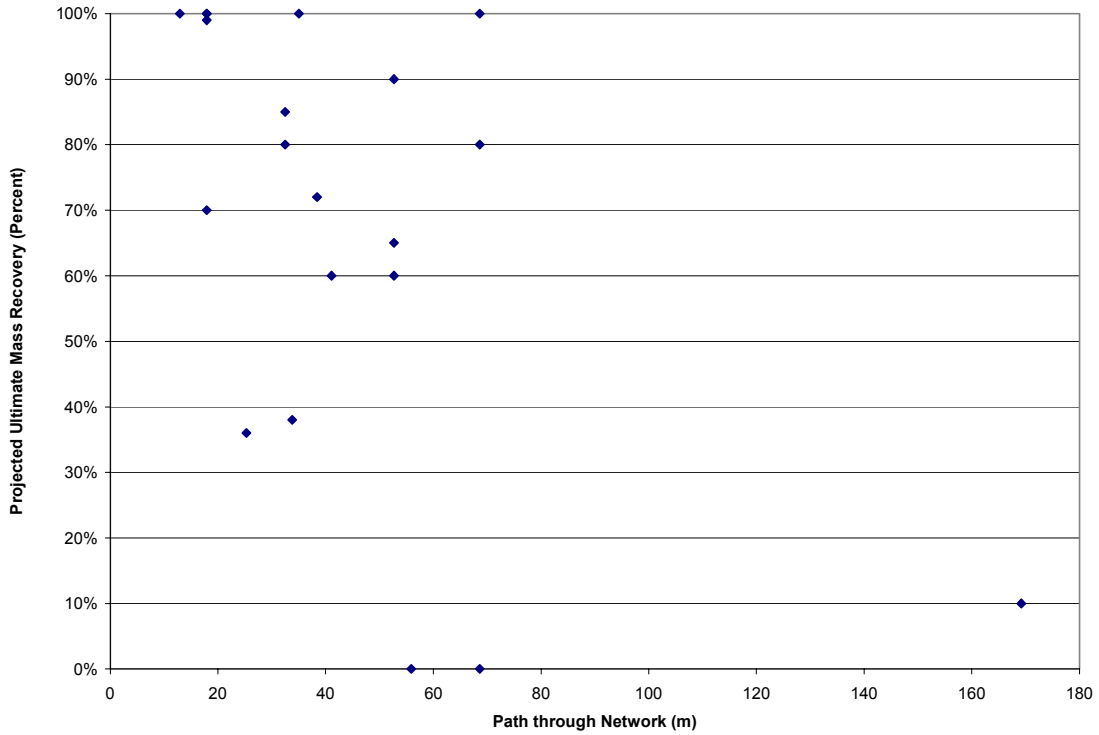

Figure 4-12. *Projected ultimate mass recovery as a function of the path length through the modelled fracture network representing the hydrostructural model.*

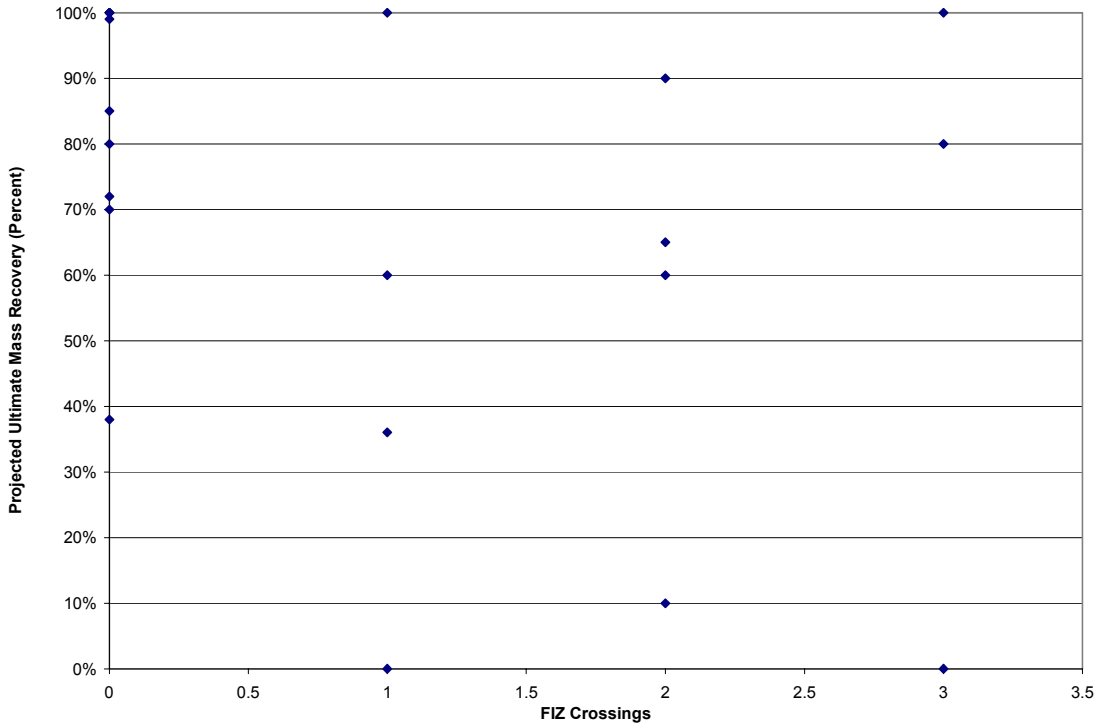

Figure 4-13. *Projected Ultimate Recovery as a function of number of FIZ crossings.*

An apparent dispersion α_L was calculated for each of the pathways using the formula,

$$\alpha_L = \alpha_{L\text{-}b} - \alpha_{L\text{-}i} \quad (4\text{-}1)$$

where $\alpha_{L\text{-}b}$ [L] is the apparent dispersion calculated from the breakthrough curve and $\alpha_{L\text{-}i}$ [L] is the apparent dispersion for the injection curve. Dispersion α_L for both breakthrough and injection was calculated according to /Domenico and Schwartz, 1992/,

$$\alpha_L = (L_p/8)(t_{84} - t_{16})^2/(t_{50})^2 \quad (4\text{-}2)$$

where L_p [L] is the path length through the hydrostructural model, and t_{16}, t_{50}, and t_{84} are the times [T] to 16%, 50%, and 84% mass recovery (or mass injection, in the case of injection curves).

Figures 4-14 and 4-15 illustrate the relationship between apparent dispersion α_L and the pathlength and number of FIZ crossings. A surprisingly clear linear trend is visible in both figures, most strikingly in Figure 4-14, with a slope of 7%. With due respect to the empirical nature of the relationship developed by /Gelhar, 1986/ and the wide variety in the origin of the data used therein, the consistent, although weak, relationship between dispersion and the path length through the TRUE Block Scale hydrostructural model provides support to the structural model hypothesis. The slope of 7% is about two thirds of the dispersion commonly cited in the literature, 10%. The lower level of

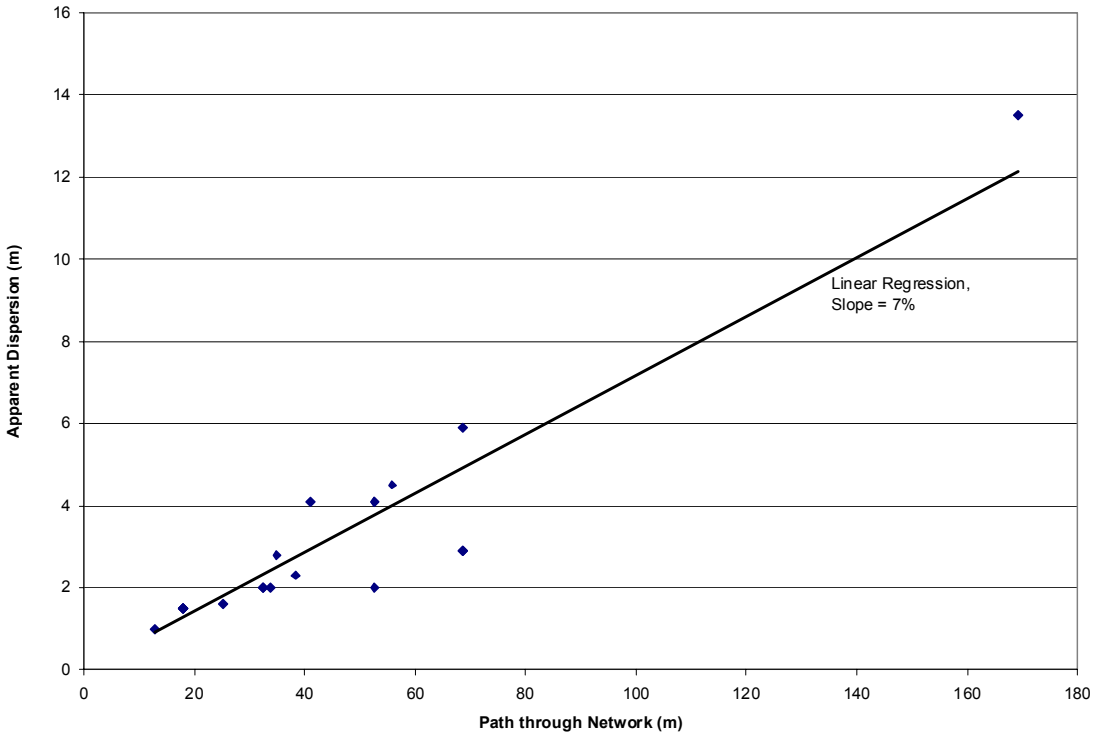

Figure 4-14. *Apparent dispersion for conservative tracers as a function of the path length through the fracture network.*

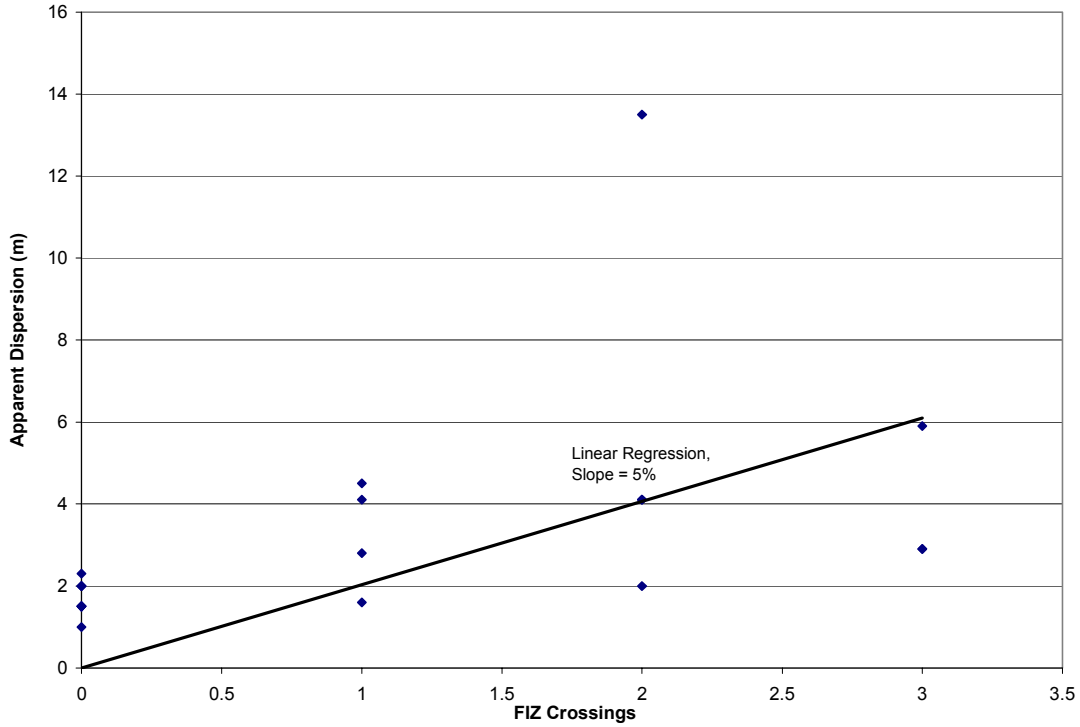

Figure 4-15. *Apparent dispersion for conservative tracers as function of number of FIZ crossings.*

dispersion is interesting, and may be due to the absence of network branching. It will be very useful to study whether this dispersion is consistent with tracer tests made at other areas in the Äspö Hard Rock laboratory.

4.4 Evaluation based on sorbing tracer tests

Sorbing tracer transport provides information about immobile porosities along the transport pathways, rather than about the geometry of the pathway itself, within the framework of the hydrostructural model. Sorbing tracer transport can provide information about the hydrostructural model to the extent that the geometry of the transport pathways can be isolated from the properties of the pathways. This is very difficult.

The strength of surface sorption and matrix diffusion are linearly proportional to the reactive surface area available along the flow path – the greater the reactive surface area, the greater the rate of diffusion.

$$(\partial C/\partial t)_{diffusion} \propto A_r\, n_i\, D_e\, K_d \qquad (4\text{-}3)$$

where A_r is the reactive surface area [L^2], n_i is the porosity [–] of the immobile zone, D_e is the effective diffusivity [L^2T^{-1}], and K_d is the effective distribution

coefficient[L^3M^{-1}]. The effect on a breakthrough curve, for example, would be the same for a doubling of the reactive surface area as for a doubling of the matrix porosity.

If n_i, D_e, and K_d are assumed constant, the reactive surface area A_r can be inferred from the change in the sorption rate with changes in the advective velocity. Several experiments were carried out at more than one pumping rate for the same experimental geometry. As a result, future evaluation will address the extent to which the hydrostructural model can be interrogated on the basis of sorbing tracer transport results.

4.5 Evaluation based on comparison between dilution and tracer tests

The lack of directly measurable information between a point of injection of a solute and its abstraction is at the heart of the non-unique interpretation of breakthrough curves arising from tracer tests. However, it is hoped that by combining these various strands of data: geological, geochemical, mineralogical, and fracture orientation data, together with hydraulic interference testing, will reduce this uncertainty. An understanding of this data, from the TRUE Block Scale site, is embodied in the hydrostructural model.

However, while the hydrostructural model specifies connectivity (the geometry), transport properties of specific structures, and heterogeneity within structures are derived separately based on interpretations of field and laboratory experiments. These properties include the spatial pattern of transmissivity, aperture, and immobile zones within structures, and immobile zone retention parameters such as thickness, porosity, and retardation coefficients.

The hydrostructural model consists of approximately 10 interpreted planar deterministic structures of finite extent, varying in size between 30 m and 150 m. The extent of each feature is controlled by a combination of the relatively limited spread of the boreholes (i.e. limited knowledge beyond the outermost influence of the TRUE Block Scale boreholes) and connectivity as measured in hydraulic interference and tracer dilution tests. Tracer experiments were carried out within the rock mass where the hydrostructural model would predict the occurrence of connected pathways. Consequently, a simulated tracer test, based on this model, is likely to result in very significant recovery (this does not necessarily follow if there is a significant head gradient). Therefore, it is important to check whether there is consistent flux through the injection interval (from dilution tests) and whether the shape of the tracer breakthrough is consistent with the transport pathway.

Figure 4-16 and Figure 4-17 illustrate the overall tracer pathway for two of the tracer tests, C3 and C2, performed as part of the Phase C testing. What is apparent in these cases is the tracer pathway for C3, shown in Figure 4-16, lies within one Structure (#21), whereas the tracer pathway C2, shown in Figure 4-17, depends on several interconnected features.

Structure #23 is of very limited extent (25 m scale), and as a consequence limited connectivity, cf Figure 1-3. Based on flow log information, this feature was originally given a lower transmissivity than other deterministic structures in the tracer tests region, with the exception of Structure #24. An example of simulated predictive results of tracer test C2 (Figure 4-18) show that the effect of poor connectivity and low transmissivity of Structure #23 gives rise to three problems. Firstly, the poor connectivity of Structure #23 results in a simulated flow in the injection interval being very low. The simulated flow is so low that when tracer is injected into this feature, as part of the C2 tracer test, it has the effect of locally dispersing the tracer much more widely. Secondly, because of this dispersal the total recovery of tracer at the abstraction borehole is not 100% as some of the tracer finds its way to the external boundary. This is consistent with the conservative tracer experiment B2d on the same pathway, which had only 75% measured mass recovery /Andersson et al, 2000b/, but not with the 100% recovery observed in the similar C2 experiment, cf Section 3.2. And lastly, the simulated breakthrough curves have multiple peaks, because there are multiple flow paths from this simulated injection.

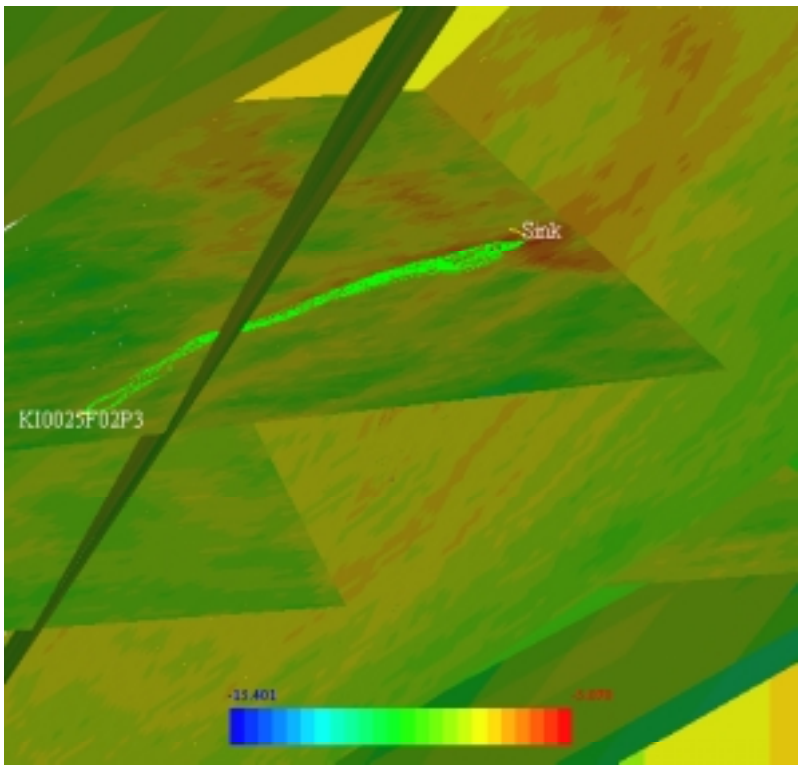

Figure 4-16. *The path of particles released from the injection interval KI0025F02:F3 is indicated in light green for the DFN simulation of tracer test C3.*

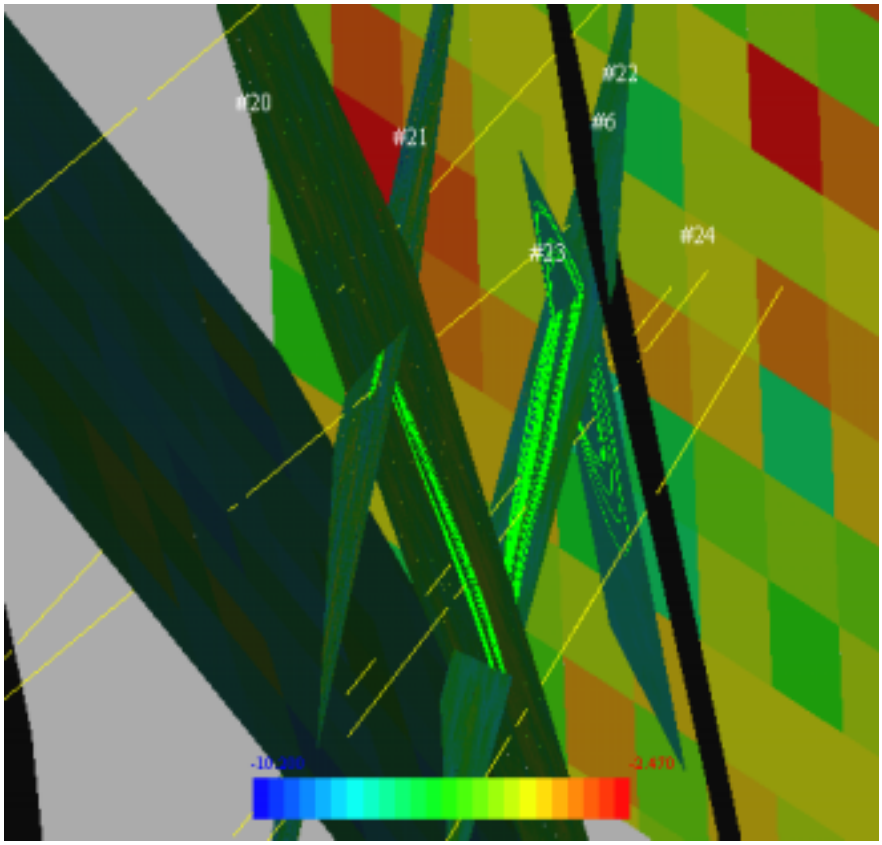

Figure 4-17. *The path of particles released from the injection interval KI0025F02:F3 is indicated in light green for the DFN simulation of tracer test C2. It shows that multiple structure are involved in flow, giving rise to distinct multiple flow paths.*

Figure 4-18 shows the initial predictive simulation in red, showing relatively low recovery and a multiple peaks as a consequence of the multiple flow paths The evaluation modelling remedied these problems by making Structure #23 more extensive and more transmissive, the resulting breakthrough curve shows a smoother breakthrough and greater mass recovery.

Additional simulations were performed using other modification to the basic hydro-structural model. One such modification consisted of introducing a new "hypothetical" Structure #"XX", which short-circuited the hydrostructural model, connecting Structures #23 and #20, without intersecting the TRUE Block Scale boreholes, this resulting in reduced the flow path length for tracer test C2. Calibration was performed on the transport model simulation resulting in a similar satisfactory fit to the breakthrough curves.

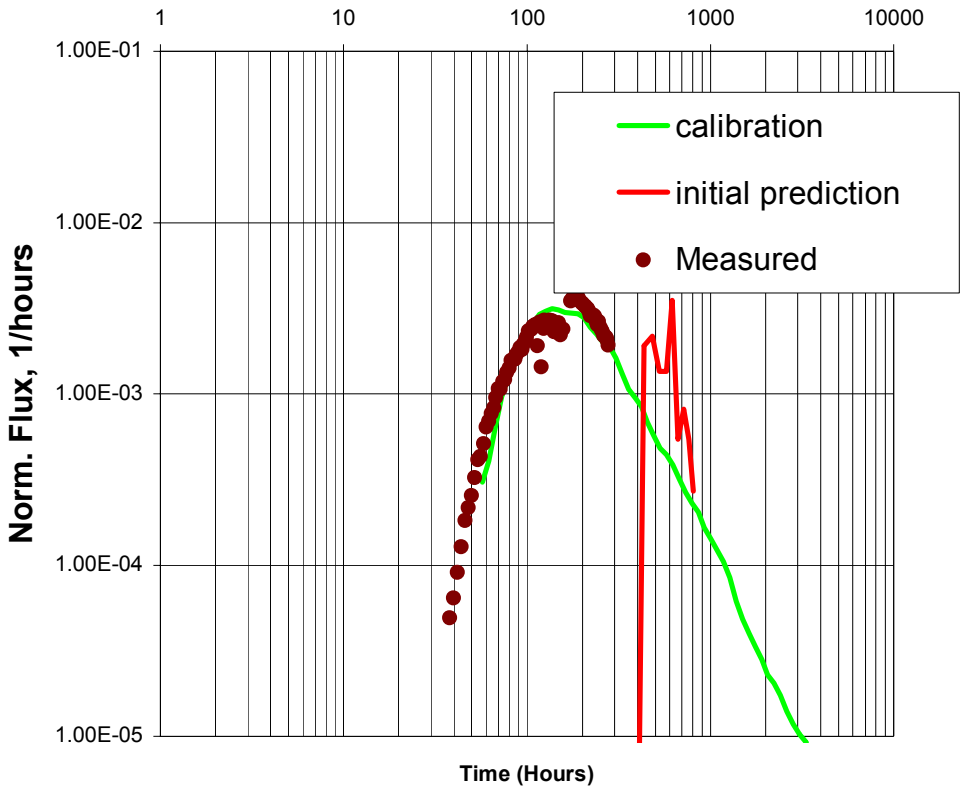

Figure 4-18. *Breakthrough curves for simulated prediction and evaluation results compared with the measured conservative tracer breakthrough curve for Re (tracer test C2).*

Figure 4-19 illustrates how the long C2 flow path involving multiple structures can be short-circuited by a structure not included deterministically in the hydrostructural model. Such a structure can be implemented without contradicting the hydrostructural model, for example as a background fracture which does not intersect any of the TRUE Block Scale boreholes (it can be either sub-horizontal or sub-vertical). The orientation of the hypothetical structure shown in Figure 4-19 is sub-horizontal. This demonstrates how background structures, not included deterministically in the hydrostructural model, may still play an important role as transport pathways.

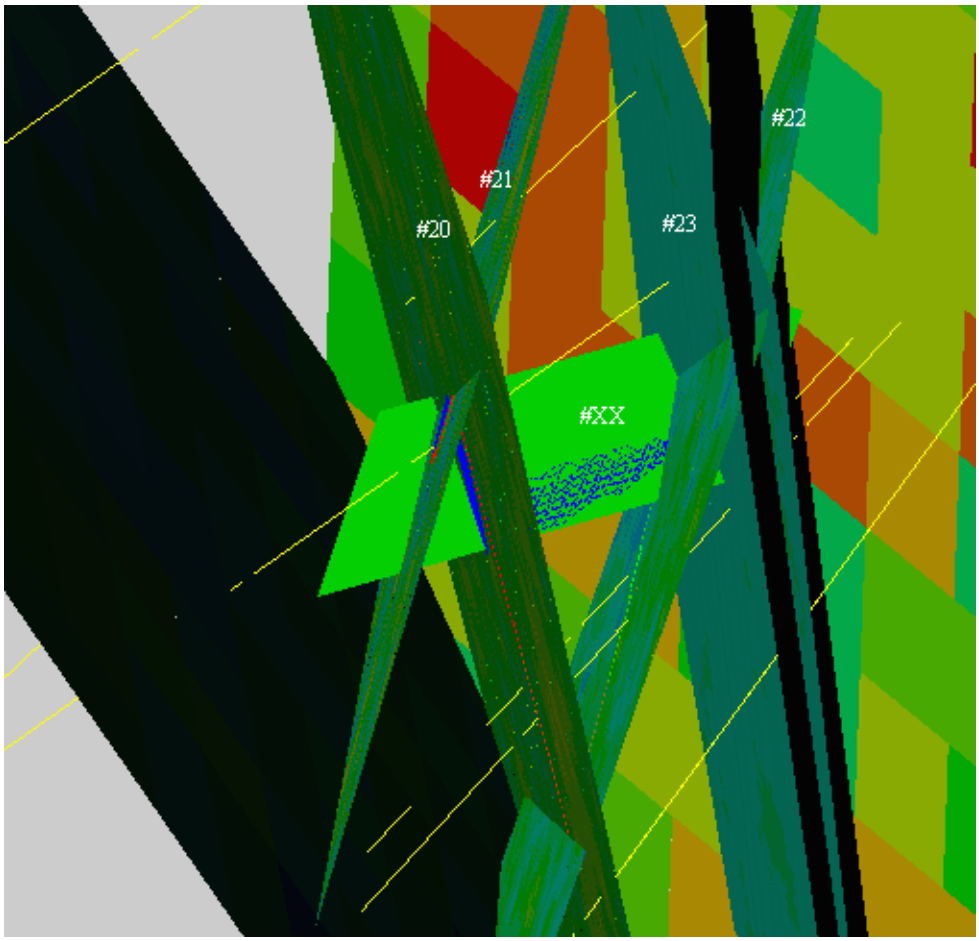

Figure 4-19. *The path of particles released from the injection interval KI0025F02:F3 is indicated in blue for the simulation of tracer test C2.*

4.6 Summary

The analyses presented in this section have provided empirical support for the TRUE Block Scale hydrostructural model as implemented, but have also demonstrated the difficulty of proving hydrostructural hypotheses.

The hydrostructural model combines a limited number of deterministic hydraulically active structures that explain the majority of the observed hydraulic responses. A background fracture population and/or an in-plane heterogeneity component is used to account for the remaining responses. The hydrostructural model is supported by multiple independent data sources, including head measurements, single borehole hydraulic tests, hydraulic interference, and hydrogeochemistry data /Andersson et al, 2002a/. It is therefore firmly believed that the hydrostructural model constitutes an accurate representation of the *in situ* pattern of discrete conductors within the TRUE Block Scale rock volume, particularly in the area where tracer tests were carried out during 1999 to 2001.

Subtraction of structures from the hydrostructural model results in inability to explain hydraulic connections, while the addition of structures to the model results in non-existent hydraulic connections.

With regards to breakthrough of non-sorbing solutes the following summary conclusions can be made:

1. breakthrough curves can only provide weak, empirical support to the hydrostructural model hypothesis, since tracer tests account for effective properties along pathways, without reference to where these pathways occur in space or within the context of a hydrostructural model.

2. the correlation between apparent dispersion and transport path length through the hydrostructural model is at least some empirical evidence that the hydrostructural model makes some sense,

3. a clearer (but still weak) test of the hydrostructural model can be made by looking at tracer recovery.

The hydrostructural model framework was shown to be "consistent" with steady state and transient hydraulic responses, and conservative and sorbing tracer breakthrough data. The following elements of the hydrostructural model were shown to be important:

- assignment of heterogeneous transmissivity (hydraulic conductivity) fields to structure planes,

- possible transport pathways involving undetected structures or background fractures,

- possible flow barriers (areas of low transmissivity) within specific structures,

- connectivity between structures and between structures and hydraulic boundaries.

Considered as an inverse problem, the hydrostructural model has not been found to be a unique or perfect model for the purpose of describing/explaining the hydraulic connectivity of the TRUE Block Scale rock volume. However, the hydrostructural model does provide a framework for integrating the available hydraulic, chemical and transport information. The degree of flexibility included in the hydrostructural model as implemented, appears to allow implementation of numerical models which are consistent with *in situ* measurements.

5 Evaluation of effects of heterogeneity

Heterogeneity is fundamental to the understanding of flow and transport in the TRUE Block Scale rock volume. Such heterogeneity is evident in a variety of guises and at a variety of scales, affecting both flow and transport. Heterogeneity is apparent in the variability of apertures, observed in the core; spatial distribution and composition of gouge material and rim zone structure; and structure of fractures (foliation, bifurcation, multiplicity of sub-parallel fractures making up the conductive structures at the TRUE Block Scale site).

The degree to which heterogeneity is explicitly modelled is the subject of considerable discussion. Generally, there is no right answer to how much heterogeneity to include, because this is a function of both the level of detail of the question posed and data to underpin or justify the approach. However, there are many modelling approaches used at various levels of detail to model flow and transport. Heterogeneities can be explicitly accounted for in some cases, while in others is replaced by equivalent parameter values that reflect an average property of the geological medium. In addition, sparse sampling (e.g. in hydraulic testing and in mineralogical analyses) provides only a limited knowledge about the spatially heterogeneous distribution of the parameters. Sparse knowledge results in an important source of uncertainty about the model and subsequent predictions based on it.

Treatment of uncertainty has not been a major goal during the TRUE Block Scale Project. A systematic methodology to treat this uncertainty could be approached using analytical or semi-analytical methods, as in the LaSAR model, or by Monte-Carlo, as in the DFN or SC model. It is likely that the treatment of uncertainty would consider the uncertainty at a variety of relevant scales. For example, the treatment of uncertainty in flow properties may be relevant to consideration of a longer length (macroscopic) scale. An appropriate instrument for this treatment would use the DFN or SC approach, in which there is an explicit representation of the flow path and the boundary conditions (Sections 5.1–5.2). The uncertainty in transport properties at a microscopic scale could be investigated using an analytical or semi-analytical approach (Sections 5.3 and 6.3).

This section discusses how heterogeneity has been considered by the different model concepts distinguishing between heterogeneity of flow parameters, mainly hydraulic conductivity or transmissivity, and heterogeneity of transport parameters.

5.1 Heterogeneity of the rock mass

The rock mass, which includes the background fracturing, has been explicitly considered in the SC model and the DFN/CN model. By background fracturing we refer to all joints and fractures that are not interpreted as numbered deterministic structures in the hydrostructural model, cf Figure 1-3. A deterministic structure is in this context possible to correlate hydraulically between at least two boreholes.

In the SC model, the TRUE Block Scale rock volume has been represented by deterministic structures of the hydrostructural model and the 'rock mass'. The hydraulic conductivities of these structures are spatially variable with an initial range of variability derived from the available measurements. An isotropic correlation range of 40 m has been assumed in the SC modelling, but there is not enough data for a reliable estimation. The variability of the rock mass conductivity overlaps that of the conductivity of the deterministic structures with some rock mass SC blocks being as permeable as the least transmissive structures.

When calibration is performed using the cross-hole tests there is an increase of the overall variability of the rock mass conductivities in each of the realisations. Figure 5-1 shows three cross-sections through the calibrated block of log-conductivities for one of the realisations. In the sections at –550 m and – 450 masl, it is apparent that the rock mass has reduced its conductivity by almost two orders of magnitude, within an important area in the western half of the model. It is also apparent that the spatial correlation of conductivity in the calibrated field is larger than initially estimated.

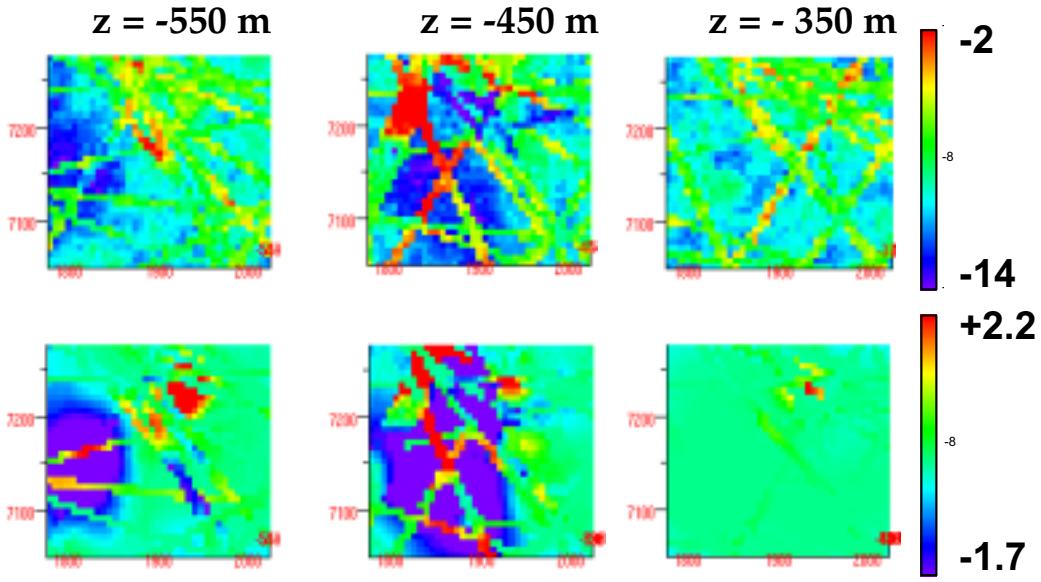

Figure 5-1. *Three cross-sections through a realisation of log-conductivities (log K) (m/s) calibrated to the cross-hole tests, along with the perturbation applied to the values prior to calibration. Notice the reduction of log hydraulic conductivity in the matrix in the lower western area.*

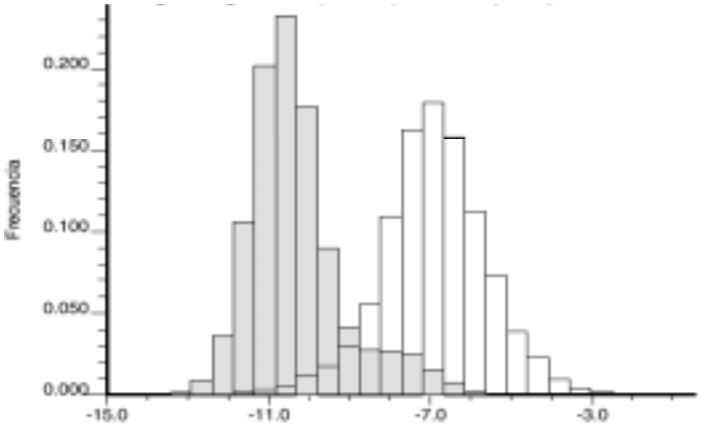

Figure 5-2. *Histograms of log hydraulic conductivity (log K) (m/s) obtained from a calibrated realisation, for the rock mass blocks (shaded) and for the blocks defining the conductive structures (white).*

Figure 5-2 shows the histograms of the final hydraulic conductivities in both the rock mass blocks and the structure blocks. It illustrates on average, that structures are four orders of magnitude more conductive than the rock mass (including background fracturing) and that there are areas of the model in which the background blocks are more conductive than some structure blocks.

5.2 Effect of in-plane heterogeneity on flow

In-plane heterogeneity for the main structures identified at the TRUE Block Scale has been implemented in the SC and DFN models. The DFN/CN model – the only other flow model – accounted for heterogeneity between fractures, but considered each fracture as homogeneous; this was the modeller's decision, not because of a limitation of the model.

There is observational and experimental evidence that fractures are heterogeneous. Much of the information used to characterise them are either on a very short length-scale (core dimensions) or arising from the measured variability derived from local transmissivity estimates. Hence as a consequence of the disparity in scale of supporting data the form of in-plane heterogeneity has to be postulated, however it must try to reconcile the observed variability

For the SC model a correlation length of 40 m was imposed for hydraulic conductivity, and a histogram based on the data collected from all structures was used to determine means and variances of individual structures. Initially, all structures display the same heterogeneity, that is, they share the same statistics. Although, all conductivities in the structure planes are spatially correlated, there is no correlation between structures or between any structure and the rock matrix.

For the DFN model the variability in transmissivity used a correlation length of 5 m. Although this is a shorter correlation length than used in the SC model, it was shown that this heterogeneity of transmissivity in the fracture planes is sufficient to produce multiple transport paths and flow channelling.

For the DFN/CN model in-plane heterogeneity was introduced at fracture intersections. It was hypothesised that fracture intersection zones (FIZ) may have very different characteristics from the fractures themselves, thus inducing a change in the flow field and consequently in transport results.

The SC model is initially conditioned to hydraulic conductivity data alone, but through a self-calibrating algorithm the heterogeneities both in the fractures as well as in the rock matrix are modified so as to match the available steady-state and transient piezometric head data. This updating has served two purposes, to highlight potential inconsistencies of the hydrostructural model and to analyse the relative importance of the different structures.

In the early stages of the hydrostructural model development (before the latest structures had been included), during the process of conditioning the heterogeneous realisations of conductivity, some of the subhorizontal fractures ended with average in-plane conductivities much higher than those expected from geological evidence and site data. Indeed, this result was inconsistent with geology, but in order to match the interference tests there was a need to propagate pressure in the north-south direction and, short of the subhorizontal fractures, there was no structure capable of doing so.

Figure 5-3 displays the evolution of Structures #9 (NB This structure is not included in March 2000 hydrostructural model, cf Figure 1-3) and #20. The top row shows the final conductivity values after conditioning to piezometric head data and the bottom row the variation with respect to the initial estimates. Note that conditioning to piezometric heads introduces substantial changes in portions of the fractures, for instance, Structure #20 appears to “close” over a large area while most of the flow will probably happen along the zone that suffers an important increase of conductivity.

An example showing the channelling that appears in the DFN model with in-plane heterogeneity is shown in Figure 5-4, in which a close-up of the Darcy velocity distribution around the intersection of section KI0023B:P6 and Structure #21, corresponding to the modelling of one of the dilution tests, is displayed. From the position of the intersection (at the centre of the picture) it is apparent that two channels of high velocities develop out of section KI0023B:P6. These two channels will result in two transport paths from this source to the corresponding sink.

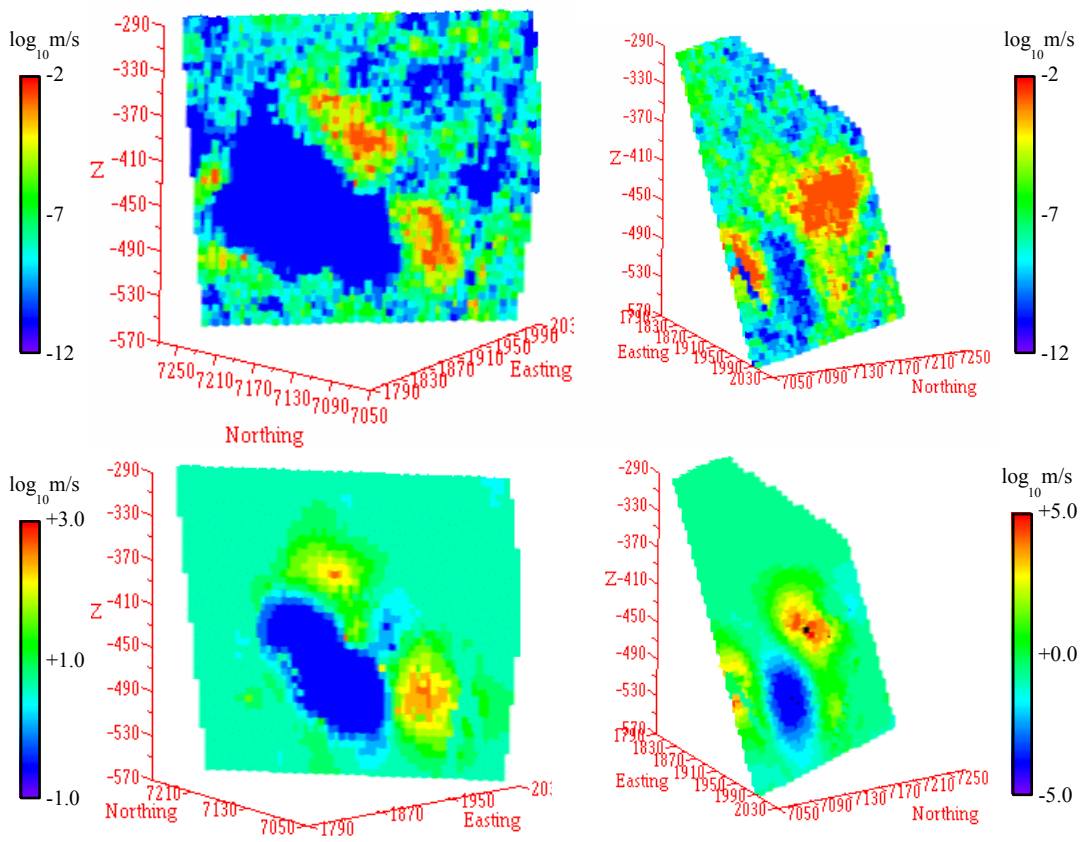

Figure 5-3. *Top row: Final distribution of hydraulic conductivity (log K) (m/s) within Structures #20 (left) and #9 (right) after conditioning to the interference tests. Bottom row: Perturbations applied to the initial hydraulic conductivity distributions, which were conditioned only to hydraulic conductivity measurements, but not to piezometric heads.*

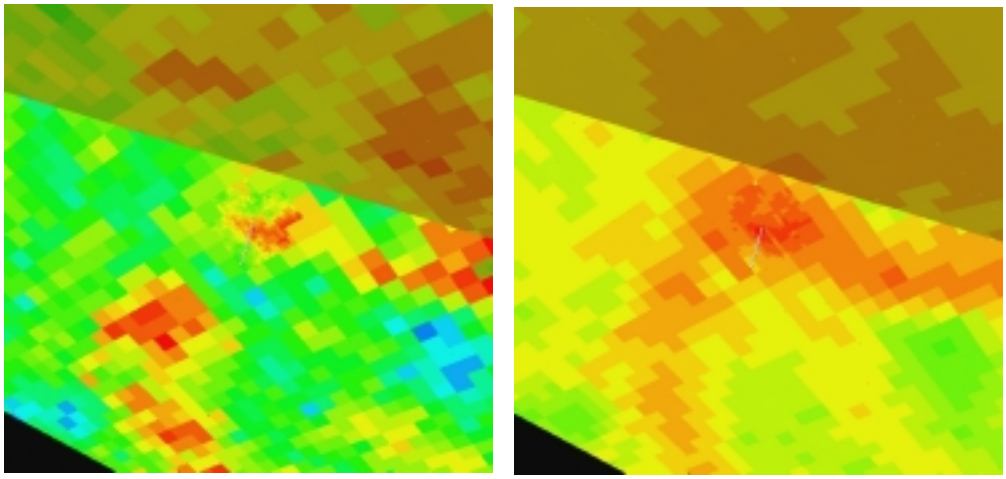

Figure 5-4. *Transmissivity distribution (left) and Darcy velocity (right after zooming in centre) from one of the realisations of the DFN model around the intersection of section KI0023B:P6 with Structure #21 (at the centre of picture). From the centre of the picture, two channels of high velocity appear to develop that will result in multiple transport paths to section KI0023B:P6 (main sink).*

Tracer transport calculations have been performed in both a predictive phase and an evaluation phase as part of the Phase C tracer testing. These have revealed a series of interesting observations.

The heterogeneity used in all model simulations were based on estimates of the mean transmissivity and variability in transmissivity derived from interpretations of packer tests. In addition, because of the interpreted extensive nature of the major structures, it was assumed that these structures have relatively long correlation lengths, on a scale of metres rather than centimetres. The modelling demonstrated that these two assumptions were generally inadequate to explain the dispersion observed in the tracer tests. This is especially apparent in the case where the transport path was interpreted by the structural model to be in a 'single' structure (with a relatively simple transport pathway). Hence, this observation holds for the C1 and C3 tests and most of the tracer tests of Phases A and B.

The reason behind this is inadequacy is that the heterogeneity used in the modelling gives rise to a relatively low degree of **variability** in flow velocity (and therefore spreading). In addition, the size of the source release is small compared to the scale of the correlation length, therefore the tracer does not sample the 'total' heterogeneity of the structures.

It was apparent in the DFN predictions, that the simulations showed an inadequate level of dispersion. This reflected the smoothness of the underlying geostatistical model for transmissivity with no explicit representation of micro-scale heterogeneity in the transmissivity (< 1 cm). The fit to the breakthrough data can be improved by introducing this additional micro-scale heterogeneity explicitly (using a multi-scale geostatistical model) or by using some phenomenological model that would naturally give rise to spreading. This could be based on an interpretation of flow distributions at a small scale or a more conventional 'dispersion' length based model.

With respect to the DFN/CN model and the heterogeneity induced by the fracture intersection zones (FIZ), it was concluded that they did not influence the breakthrough curves but that they provided pathways to alternative sinks in the rock mass with a net result of a reduction of the mass recovery, if connected to a boundary. The FIZ conceptual model is shown in Figure 5-5.

The importance of background fracturing has been tested by three flow models, the SC model incorporated both structures and rock mass, the DFN with structures only (although background fractures could have been added) and the DFN/CN model with both interpreted deterministic structures and background fracturing (rock mass). For all three flow concepts, the flow responses were modelled using background fracturing with given conductivity/transmissivity distributions and forcing the background fractures to be impermeable. For the SC model, in which there was no rock mass it was impossible to reproduce the piezometric head data. In the case of the DFN/CN model the match to piezometric head data was improved when no background fractures were included. For the DFN approach an adequate match to the drawdown response was possible using only the conductive structures.

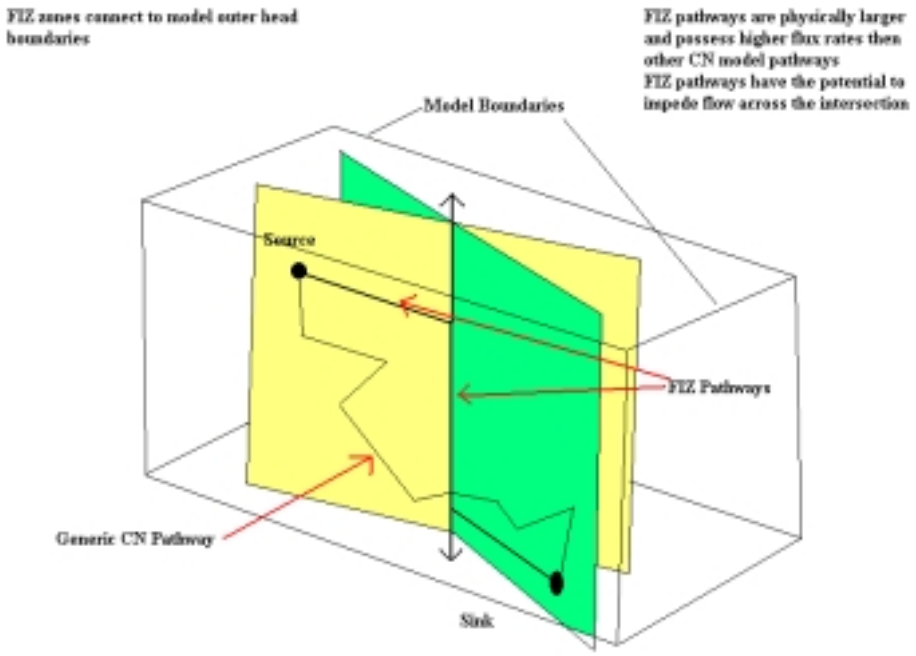

Figure 5-5. *Conceptual model of a fracture intersection zone as implemented in the DFN/CN model.*

.

5.3 Effect of micro-scale heterogeneity on transport

5.3.1 Description of microscale heterogeneity

Heterogeneity exists at a variety of scales. If one is able to track a solute particle it will be influenced by a variety of microscopic factors that influence whether it adheres to the surface of the fracture wall or gouge material (fault breccia) or diffuses into the rock mass, rim zone or stagnant water. It is however the detail of these factors that determines the degree of retention along a flow path.

Transport parameters determined for the TRUE Block Scale tracer tests were not based on site-specific laboratory diffusion and batch sorption measurements on site-specific materials from TRUE Block Scale, but from studies derived from the TRUE-1 experiments /Byegård et al, 1998/. The main reason for using this approach was the similarities in lithology, orientation and water chemistry between the TRUE-1 and TRUE Block Scale sites. However, an elaborate mineralogical and geochemical study was performed on material collected from structure intercepts of interest. In addition, fault breccia material has been analysed in the laboratory. Together with assessments of the cation exchange capacity, assessment of mineralogical distribution and site-specific hydrogeochemical data volumetric distributions coefficients K_d for the size fractions < 0.125 mm and 0.125–2 mm were estimated. Further, a comprehensive petrophysical programme has been performed with the aim to assess the porosity and porosity distribution/texture related to relevant structure intercepts.

Measurements were performed using both conventional water saturation/water absorption techniques and impregnation techniques using ^{14}C-labelled PMMA /Hellmuth et al, 1999/. In this context measurements were taken beyond measurements on wall rock samples alone in that porosity determinations were performed on 1–2 cm fault breccia pieces and even on 1–2 mm fault breccia fragments from the investigated target structures. The results show average bulk porosities for the fault breccia pieces (about 0.4–0.8%) which are comparable to that of wall rock samples. The fault breccia fragments, however, show porosities varying between 1–3% (with highs > 10%) /Kelokaski et al, 2001/, i.e. significantly higher than the corresponding altered wall rock.

These measurements formed the basis for the parameterisation of the microstructure models at the microscale, cf Section 6.3.

5.3.2 Model analysis of effects of microscale heterogeneity

The DFN analysis represented in-plane heterogeneity explicitly. The scale of discretisation of the key deterministic structures was approximately 10 cm. One of its aims was to study how far the dispersion 'measured' arose from the large-scale heterogeneity. As discussed in Sections 2.5 and 5.2 the dimensions of the release point (the borehole) is small as compared to the correlation lengths assumed. This gives rise to very little dispersion from the large-scale heterogeneity. There are two possibilities to account for this additional dispersion:

- microscale heterogeneity,
- 'observed' dispersion does not arise from the flow path heterogeneity, but from dispersal at the point of injection.

The fit to the breakthrough data can be improved by introducing additional dispersion, the explicit representation of the micro-scale heterogeneity is too computationally intensive.

Furthermore, evaluation of the breakthrough curves indicates that other processes than advection and dispersion alone are needed to explain the transport. There are strong indications that diffusion into the immobile pore space along the flow path together with sorption cause retention of the tracer breakthrough. In this process the retention is governed by a grouped property that depends on the flow field, immobile zone diffusivity, porosity and sorption. The retardation depends on the integral along the flow path and conclusions can be drawn on the average retention properties. Heterogeneity of the retention properties along the flow path influences the interpretation of the retention by different geological structures. It is also important to note that site-specific measurements indicate quite significant changes in porosity of the rock matrix close to the fracture surface. This heterogeneity affects the mean retardation and may partly explain the differences between the observed *in situ* retention and the material properties obtained from laboratory measurements of the relevant geological materials.

The theoretical basis and effects of micro-scale heterogeneity in retention parameters is discussed further in Chapter 6.

6 Quantification of processes through modelling

6.1 Concepts of processes

Crystalline rock is conceptualised as a dual porosity (mobile-immobile) system. Water flows through discrete fractures driven by ambient or applied boundary conditions and is effectively stagnant in the rock matrix. Indivisible tracer particles (e.g. radionuclide ions) enter the flow field at the injection borehole and are transported through one or several fractures to the detection (pumping) borehole. In fractured crystalline rock the mobile pore space is primarily the small portion of the total pore space that comprises the void space of the fractures. Water in the remaining majority of the pore space in the rock matrix and fracture filling material is in practice immobile. In the TRUE Block Scale experiments the tracer tests are carried out through a network of fractures that provides an opportunity to study both network effects in advective transport and mass transfer processes between the mobile and immobile pore space.

All TRUE Block Scale modelling approaches consider linear retention, motivated by the fact that TRUE Block Scale tracer tests are sufficiently diluted. As developed in Section 2.2, we can write the *common form* of transport equations used by TRUE Block Scale modelling teams as;

$$R\frac{\partial C}{\partial t}+V\frac{\partial C}{\partial x}=D_l\frac{\partial^2 C}{\partial x^2}-\sum_{i=1}^{N}\frac{\alpha^i\theta^i D_m^i}{b^i}\frac{\partial C_m^i}{\partial z}\bigg|_{z=0}, \qquad (6\text{-}1a)$$

and

$$R_m^i\frac{\partial C_m^i}{\partial t}-\frac{\partial}{\partial z}D_m^i\frac{\partial C_m^i}{\partial z}=0\,. \qquad (6\text{-}1b)$$

where notations are the same as in Section 2.2.

Equations (6-1) can in principle account for all types of heterogeneity, for which data are available, both in terms of flow and retention. Different modelling teams have used different simplifications of Equations (6-1), different techniques of solution, and different strategies to account for random/deterministic heterogeneity in flow and retention parameters. Details of different modelling approaches are provided in Chapter 2. A more comprehensive discussion on the effect of flow on retention is given in Appendix B, based on the streamtube approach. The streamtube concept is also used as a basis in Appendix C to illustrate typical cases of retention heterogeneity, which are envisaged to prevail under *in situ* conditions.

In the following, some key parameter dependencies for advection and retention in crystalline rock are discussed. To this end, Equation (6-1) is simplified such that an analytical solution is available. Tracer particles are assumed to be subject to two processes: (i) advection due to water movement, (ii) retention in the rock matrix and on rock surfaces due to diffusion and sorption. In other words, particle advective movement is retarded, relative to the flowing groundwater. Neglecting dispersion and focusing on plug-flow in a one-dimensional "channel", or streamtube, with the rock matrix as the single retention zone, Equation (6-1) reduces to the retention model for crystalline rock derived from the parallel plate model of /Neretnieks, 1980/, /Carslaw and Jaeger, 1959/, and with dispersion as given by /Tang et al, 1981/ and /Sudicky and Frind, 1982/. It was extended to a heterogeneous fracture by /Cvetkovic et al, 1999/ and to a network of fractures by /Painter et al, 1998/.

Rather than using the homogeneous model of /Neretnieks, 1980/, the parallel plate model is generalised below to a series of segments (fractures) in the spirit of /Painter et al, 1998/. The model couples the processes of advection, diffusion and sorption in parallel plate systems in series by the following expressions

$$\gamma(t,\tau) = \frac{H(t-\tau)B}{2\sqrt{\pi}(t-\tau)^{3/2}} \exp\left[\frac{-B^2}{4(t-\tau)}\right] \tag{6-2}$$

$$B = \sum_{i=1}^{N} \kappa_i \beta_i \quad ; \quad \beta_i = \frac{l_i}{V_i b_i} = \frac{2W_i l_i}{q} \quad ; \quad \tau = \sum_{i=1}^{N} \frac{l_i}{V_i} = \frac{2}{q} \sum_{i=1}^{N} W_i l_i b_i \tag{6-3}$$

$$\kappa_i = \theta_i \left[D_i \left(1 + \frac{\rho_b K_d^i}{\theta_i} \right) \right]^{1/2} \tag{6-4}$$

The solution can be summed up from the piecewise classical solutions (this can be shown easily e.g. in the Laplace domain).

In Equation (6-2) surface sorption can be included in τ if desired. The segments can be parts of a single fracture or segments representing several individual fractures. The total number of segments is N. In (6-3), b [L] is the half-aperture. The parameters θ, D, K_d characterise (microscopic) retention processes. θ [–] is the porosity of the rock matrix, D [L^2/T] is pore diffusivity, K_d [L^3/M] is the partitioning (distribution) coefficient and ρ_b [M^3/L] the bulk density of the rock matrix. The parameter W_i [L] is the width of the segment "i" of the flow path (streamtube). A more comprehensive discussion of the role of b, W and q is given in Appendix B.

The function γ (6-2) is in effect a probability density function (pdf) for particle residence time in the network, conditioned on the water residence time τ and on B. If there is no retention, then $\gamma(t,\tau)=\delta(t-\tau)$, i.e. particle residence time is equivalent to the water residence time through the fracture network. Tracer discharge into the pumping well is quantified using γ by performing two integrations: first a convolution with the input (injection) function as measured in the injection borehole, and then an integration with the residence time distribution which accounts for hydrodynamic dispersion.

If the retention parameters θ, D and K_d are constant for all segments, we have

$$B=\beta\kappa \quad ; \quad \kappa=\theta\,(D(1+K_d\,\rho/\theta))^{1/2} \quad ; \qquad \beta=\sum_{i=1}^{N}\frac{l_i}{V_i b_i}=\frac{2}{q}\sum_{i=1}^{N}W_i l_i \tag{6-5}$$

The parameter β [T/L] is dependent only on the water flux distribution, i.e. on fracture hydrodynamics, which in turn is determined by the structure of the network (fractures) and prevailing boundary conditions. For a tracer test where tracer is released from a borehole an estimation of the β near the source can be made by Equation (6-6) assuming that W_i is approximately equal say to the diameter of the borehole, W_0; then

$$\tau=\frac{2W_0 L b_0}{q} \qquad ; \qquad \beta=\frac{2W_0 L}{q} \quad , \tag{6-6}$$

where b_0 [L] is an "effective" half-aperture for the entire network, q [L^3T^{-1}] the flow rate through the injection borehole section and $L=\Sigma l_i$ is approximately the length of the transport path. In Equation (6-6), β is assumed to be constant for the whole flow path length and width, and the numerator ($2W_0L$) has been referred to as "flow-wetted surface" by I Neretnieks. An alternative representation of β where we can account for variability within the flow path is a distribution of β´s along different trajectories;

$$\beta=k\ \tau \ , \tag{6-7}$$

where k [1/L] is a parameter to be calibrated on breakthrough curve (BTC) data, or independently estimated. Note, that strictly speaking the β's of two streamlines are proportional to the τ's only if the apertures are the same. Equation (6-7) should be understood as a statistical relationship between β and τ for a large number of streamlines and given boundary/flow conditions.

Ideally, we would like to estimate all *in situ* retention parameters (β, or k, θ, D, K_d for all tracers). From the above expressions, we conclude the following:

- The controlling retention parameter B in (6-2) is an **integrated** quantity along the entire flow path; hence strictly we cannot determine its value from "local" (point) parameter values. This can be done only based on additional simplifications. If microscopic retention parameters θ, D and K_d are assumed uniformly distributed then only β needs to be integrated along the flow path.

- The macroscopic (hydrodynamic) retention parameter β controls retention jointly with the microscopic parameter group, i.e. the two parameters "act" as a group, or product $B=\beta\kappa$. Hence we cannot infer individual parameter values of the group B without invoking **additional constraints,** or independent estimates (i.e. independent of the measured BTCs); we require two constraints (or independent estimates) in order to infer all *in situ* retention parameters.

We can set the two constraints in different ways. One approach is to independently estimate β either based on (i) streamtube approximation, or (ii) Monte Carlo simulations. In the streamtube approach we would use Equation (6-6) with W_0 equal to say the borehole diameter, L the distance between the injection and detection boreholes, and q the flow rate in the injection borehole section estimated from tracer dilution tests. The second approach utilises structural and hydrogeological information (obtained from borehole logging, single-hole and cross-hole pumping tests, flow-meter measurements, etc) to construct a statistical discrete fracture network (DFN) model, as has been done by several groups. Monte Carlo DFN particle tracking simulations are carried out and τ and β are computed using (6-3) and (6-5). Based on the generated statistical database, we can establish a correlation between τ and β and in effect infer the slope k in (6-7); given τ, a deterministic relationship for computing β can be established.

Another possible constraint is on the microscopic parameters in form of the so-called Archie's law /Archie, 1942/, which provides a deterministic relationship between porosity and rock diffusivity. Still another possibility, is to use an independent estimate of K_d, say from batch experiments on 1–2 mm (or other size) fractions, and assume that this value is applicable *in situ.*

Prior to discussing and comparing different retention parameters as estimated by different groups, we provide an example of how the estimates based on the TRUE Block Scale tests could be extended to the performance assessment (PA) scale, in particular illustrating the significance of the parameter β.

In Figure 6-1 we show the BTC data [1/T] for Cs from the C1 test, cf Chapter 3, normalised with the total injected mass. The calibrated value of B in (6-2) that gives the best fit for Cs in C1 is B=75.45 $h^{1/2}$ /Cvetkovic and Cheng, 2002/. Neglecting dispersion, Equation (6-2) is plotted in Figure 6-1 with the best estimate of the water residence time as τ=15 h /Cvetkovic and Cheng, 2002/. Using the simple streamtube model Equation (6-6), we write B in (6-2) as B=(L/q) z where $z=W_0\kappa$. With the approximate value of L=14 m for test C1, and q=45 ml/min, we obtain $z=Bq/L=0.01455\ m^2/\ h^{1/2} = 1.36\ m^2/\ yr^{1/2}$. Thus we now have a straightforward means of **extrapolating** Cs transport to the PA scale, based on TRUE Block Scale C1 *in situ* retention data. This example also illustrates the difference between the *in situ* tracer experiment and PA scale application of the site-specific data. The retention processes are the same in both cases, but the differences in the flow conditions (through e.g. the boundary conditions) and in the retention properties of the rock matrix where retention takes place, may significantly augment retention. Namely, its not only the flow, its also the retention properties that are different: In one case it is the MIDS retention data /e.g. Winberg et al, 2000; Cvetkovic et al, 2000/ based on through diffusion data on samples of unaltered bedrock, and in the other its **calibrated** to *in situ* retention data from TRUE Block Scale, the latter assumed to be higher than for the MIDS data. This is why a quite significant effect is observed.

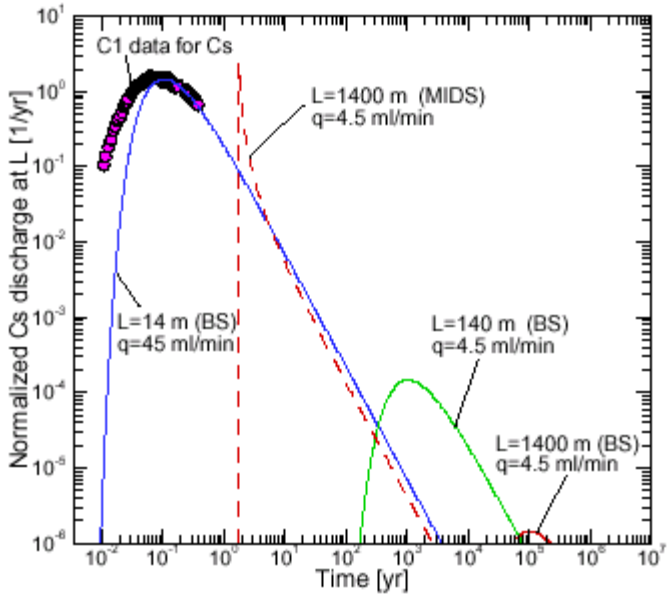

Figure 6-1. *Example of extrapolation to the PA scale for Cs from the C1 test of the TRUE Block Scale Phase C tests. The MIDS data can be found e.g. in Table 1-2 of /Cvetkovic et al, 2000/.*

In Figure 6-1, breakthrough curves for L=140 m (10 times the length scale for the C1 injection) and L=1400 m (100 times the length scale of the C1 injection) are compared, assuming an undisturbed flow rate of q=4.5 ml/min (10 times less than C1 injection flow rate). In the breakthrough curves presented in Figure 6-1, radioactive decay is included with $\lambda=0.23\cdot10^{-6}$ 1/yr. In this case without any notable effect. (Note that this decay rate is applicable to Cs-135, whereas in C1 the Cs-134 isotope was used with a considerably shorter half-life than Cs-135; we use here Cs-135 for illustration assuming identical retention properties as for Cs-134.)

In Figure 6-1, a prediction of the breakthrough of Cs at L=1400 m is included, however, using through-diffusion retention data from the TRUE-1 laboratory tests (MIDS), cf /Cvetkovic et al, 2000; Winberg et al, 2000/. Comparison of the curves in Figure 6-1 indicates several things. First, retention has a significant effect on reducing the discharge of Cs at distance L; the peak is reduced by almost six orders of magnitude from L=14 m (data) to L=1400 m. Second, there is a very significant difference in the peak value if we use the MIDS retention data for predictive purposes; in fact, the peak would not be reduced at all, relative to the data valid for experimental spatial scales. Third, we see that the simple pulse model (6-2), without accounting for dispersion or the actual injection, provides a reasonable "fit" with the data, viewed on the PA scale; clearly the simple model (6-2) does not capture early arrival (attributed to dispersive effects), however, it does reproduce the peak level and time of arrival, as well as the tail.

If the transport conditions for Cs would not change in space and time, from the conditions of the TRUE Block Scale C1 test, then Figure 6-1 would be a realistic estimate of discharge of Cs on the PA scale for a delta pulse release. Clearly when extending the transport conditions to the PA scale, there are several uncertainties and questions which have to be dealt with. We summarise these as follows:

(i) Hydrodynamic (macroscopic) retention parameter β: What is the most accurate estimate of β in the block scale? Is the simple streamtube estimate (6-5) conservative; is it sufficiently accurate for PA purposes? On which scale do Monte Carlo simulations provide more realistic estimates of β than the streamtube estimate; on the block scale of 20–30 m, or on the PA scale of 1000 m?

(ii) Are our *in situ* estimates of retention parameters K_d, D, θ as effective, flow path values, sufficiently accurate? It is apparent that one or several of these retention parameters are higher than the values for the unaltered rock (compare MIDS), however, are they "uniformly distributed" and representative for the PA scale? What role does heterogeneity play? If this role is significant, then what type of heterogeneity along the transport path is most important to account for, longitudinal (along the transport path) or transverse/vertical (i.e. normal to the fracture surface in the altered rim zone of the rock matrix)?

For real applications, say in a repository site selection program, we would need to estimate B in (6-2) by independently estimating β and the individual retention parameters K_d, D and θ from characterisation data. In view of the above uncertainties, the main goal of the modelling work is to infer/estimate individual retention parameters from the TRUE Block Scale *in situ* tracer test data, as accurately as possible.

6.2 Advection

Properties of the flow field are crucial for the transport and they have an important role in determining the retention properties, which are assigned to the different transport paths. The basic concept for fractured rock is a dual or multi-porosity medium that can be divided into mobile and immobile parts. Here we denote by advection the transport of an ideal non-sorbing and non-diffusive tracer through the mobile part of the rock. Retention processes, like sorption and diffusion to the immobile zones, are not taken into account in advection. The residence time distribution of this kind of ideal tracer should coincide with the groundwater transit time distribution.

The Phase C tracer tests of the TRUE Block Scale Project have been performed using three different injection points and one withdrawal point with separation distances (Euclidean) varying between 14–33 m /Andersson et al, 2002b/, cf Section 3.1. The measured breakthrough curves contain integrated information of the transport and retention processes that have been active in these tests along the respective pathways. It is, however, difficult to discriminate different processes based on the breakthrough data because many processes cause similar breakthrough behaviour. Different models

put emphasis on different characteristics/components of the problem and for this reason it is advantageous to have parallel modelling efforts using different approaches when evaluating the same test data.

The measured breakthrough curves are reproduced more or less equally well by different approaches, cf Section 3.2. The advantage is that comparison of the different approaches provides a wider view of retention in solute transport through fractured rock. Different structures of the transport and retention processes have different weights in alternative approaches and this way they can be regarded as alternative explanations (hypotheses) to the actual *in situ* retention process/-es. The comparison is made here through compilations of the parameterisation used to model the tracer tests. Emphasis is placed on the retention processes, not on transport *per se*. In the following a series of alternative evaluations will not be presented. Rather, various aspects of the interplay between different retention processes assumed active during the TRUE Block Scale experiments will be discussed and exemplified along the lines of the general formulation of the problem in Section 6.1.

It is clear that the advective flow field forms a basis, or a platform that determines the relative importance of the different retention processes. In a steady-state flow field, flow paths of the tracer particles coincide with the streamlines of the flow field. Advective transport is governed by the properties of the streamlines starting from the source and ending at the sink. If no diffusion processes are considered then the transport of the tracer particles is perfectly represented by the streamlines.

6.2.1 Flow in fractured rock

In fractured rock, the pore space can roughly be divided into the void space of the fractures (mobile zone) and the pore space in the rock matrix and fracture filling materials (immobile zones). If only the hydraulic head field is to be modelled, a first approximation may be a network of fractures, each attributed an effective transmissivity. The effective transmissivity may vary between fractures and it can be described only in a statistical sense, possibly locally conditioned at the measurement points (boreholes), by e.g. simulation of various hydraulic tests.

The geometrical structure of the hydraulic conductivity field in fractured crystalline rock is complicated and essentially random. Some degree of constraint may be enforced by the structure (foliation) of the rock and preferential fracture orientation resulting in hydraulic anisotropy. Only a small portion of the total pore volume of the rock belongs to the connected mobile pore space provided by conductive fractures. Spatial variation in hydraulic conductivity entails an uneven distribution of the groundwater flux. Heterogeneity in the flow properties is reflected in *in situ* experiments in that it is difficult to identify suitable injection and withdrawal points for the tracer experiments. In the experiments both the source and the sink sections should connect to the mobile pore space in such a way that the sink dominates relative to the ambient (background) groundwater flow conditions prevailing at the source point.

The division of the pore space into mobile and immobile zones is made primarily on the basis of the geology/mineralogy and material properties. This means that site characterisation data and associated understanding is applied to identify properties of the fractures (mobile), possible occurrences of mylonite, fine-grained fault gouge or fault breccia (immobile) and rock matrix (immobile). It is also possible that parts of the void space in fractures belong to the immobile pore space simply because of their small aperture, or due to boundary conditions that entail almost negligible groundwater flux in those regions. This affects advective transport (that can be based on the effective properties of fractures), but it may also be an important factor for the diffusive retention processes.

The flow problem has been treated differently among the five modelling approaches utilised in the evaluation of the Phase C tests. Three approaches actually model the flow problem explicitly applying 3D stochastic continuum (ENRESA-UPC/UPV, Section 2.4), DFN (Nirex-Serco, Section 2.5) or pipe network approaches (JNC-Golder, Section 2.8). Two approaches do not address the flow problem in a direct way. These models apply simple 1D connections between sink and source. The flow is conditioned to the measured flow in the injection section (Posiva-VTT, Section 2.6), or flow dependent transport properties are supported by separately calculated 3D particle tracking results and conservative tracer residence time distributions observed in the pre-tests (SKB-WRE, Section 2.7). The variety of different approaches applied to conceptualise the flow problem in the Phase C tests is illustrated in Figure 6-2.

The differences in approaches also implies that the question of heterogeneity have a different meaning for different models. Generally, if the flow problem is modelled the heterogeneity is calibrated and conditioned against the available hydraulic data. If the flow problem is not modelled then the heterogeneity in flow is taken into account indirectly in the groundwater transit time distribution using results from tracer pre-tests (prediction) or, in the evaluation phase, the breakthrough data for non-sorbing tracers.

6.2.2 Advective transport

Advective transport can be characterised by a distribution of advective velocities that results in the tracer transit time distribution. We may consider an ideal non-reactive tracer that is composed of indivisible particles. The lengths of the particle trajectories and the magnitude of flow velocities determine the transit time distribution. In practice, the trajectories of the individual tracer particles cannot be known deterministically and hence need to be treated statistically. Commonly, this is done by applying e.g. the advection-dispersion model, where the mean velocity determines the first, and dispersion the second temporal moment of the transit time distribution.

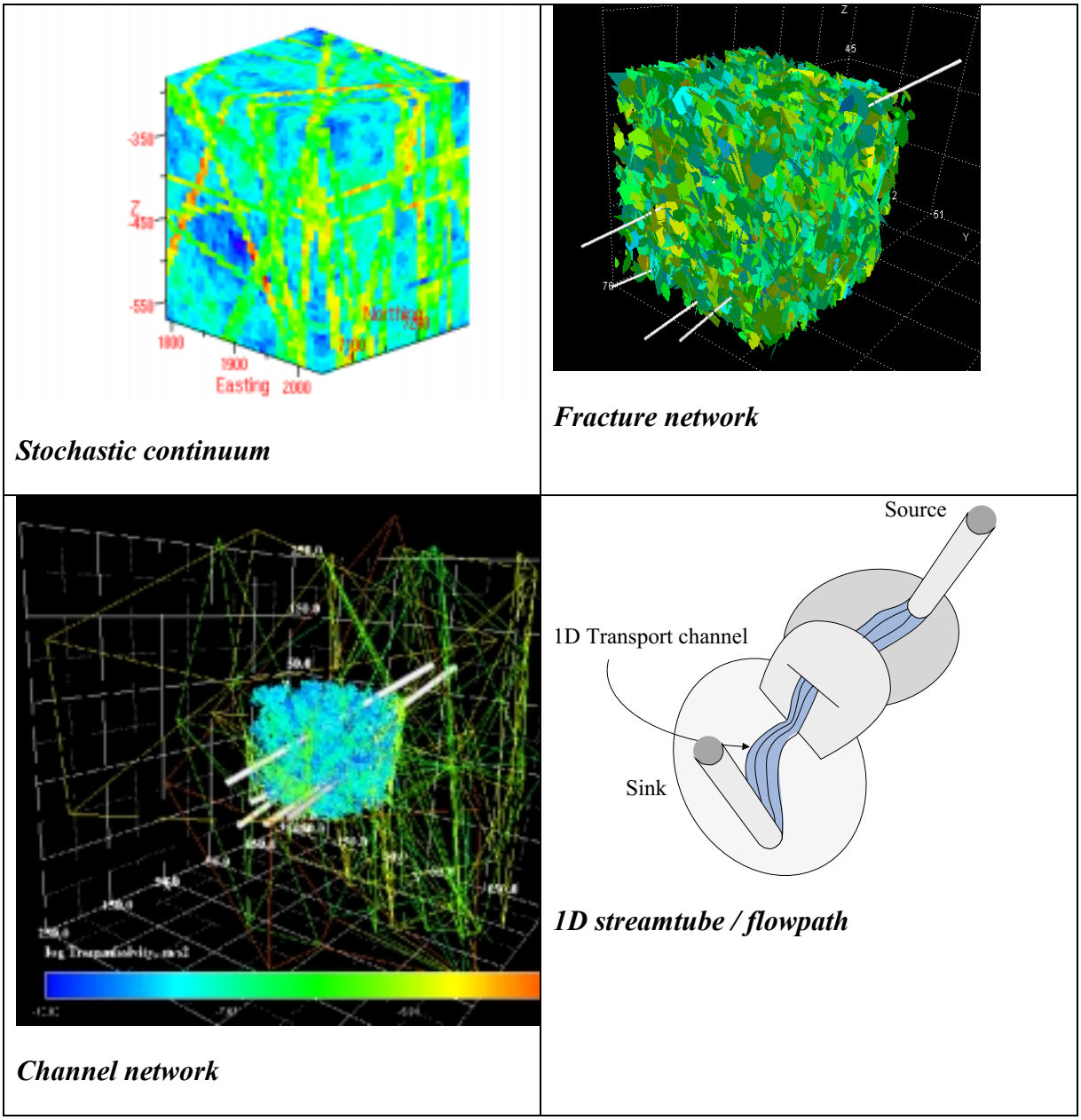

Figure 6-2. *Different conceptualisations of the flow problem that were applied in the prediction and evaluation of the Phase C tracer tests.*

Flow in fractured rock takes place in fractures, and the solution to the flow problem can be assessed with reasonable accuracy using effective transmissivities of the fractures, i.e. assigning constant effective apertures to individual fractures. In reality, the fractures are heterogeneous and the apertures are not constant, but vary from point to point. This means that the parallel plate fractures applied in the flow solution do not give accurate descriptions of the transport behaviour. In addition, the groundwater flux will be unevenly distributed over the fracture plane which entails channelisation of the groundwater flow and may have significant influence on the retardation if β decreases (see Section 6.1).

At a qualitative level there is ample evidence for correlation between the best hydraulic drawdown responses observed in borehole test sections in the TRUE Block Scale rock volume and corresponding anomalies in tracer dilution measurements, and ultimately, breakthrough of tracer between the same combination of borehole sections /Andersson et al, 2002b/. However, at a quantitative level this correlation is not obvious when the performance measures are more demanding. For example, when comparing the drawdown response (normalised to flow) with that of measurable transport performance measures such as; mean water residence time and mass recovery, also cf Section 7.4. This is of great relevance when trying to compare and understand the results of tracer test predictions and subsequent model evaluations.

The discrete fracture network models of flow and transport, as illustrated in Figure 2-2, are based on the intra- and inter-variability of the interpreted transmissivity of identified structures in the TRUE Block Scale rock volume, as given by /Andersson et al, 2002a/. In this way the models broadly reproduce the overall hydraulic behaviour observed within the context of the hydrostructural model.

Generally speaking it is not possible to explain the water residence time of the TRUE Block Scale tracer tests based purely on the sorts of smooth geostatistical models used to model variable aperture fractures using a relatively narrow range of transmissivity estimates as presented by /Andersson et al, 2002a/. For example, a four order of magnitude spread in transmissivity translates to just over an order of magnitude variability in aperture ($T \sim a_T^3$). Generally, this is insufficient to greatly affect the simulated water residence time, especially when there is significant spatial correlation in aperture (effectively behaving similarly to a constant aperture disc). A match to the water residence time can be achieved by introducing an effective transport aperture. There are many possible phenomenological models for the transport aperture, for example, making the effective transport aperture proportional to the equivalent hydraulic aperture ($a_{tran} = f * a_T$, where f is a scaling factor >1). In this sense, the cubic law appears to be conservative, predicting water residence times, which are too short. However, it may simply reflect the fact that the variability in aperture is insufficient to provide a large retardation in water residence time.

There are two completely different concepts that can explain the groundwater transit time distribution. Transit time distribution may follow from the particle trajectories that travel through different fractures and have clearly different lengths and flow velocities, i.e. due to **mechanical dispersion**. This may be a dominant process, especially when the source area is large compared to the mean distance between fracture intersections (along the fracture planes) and mean length of the fracture traces. This case is illustrated schematically by pictures in upper right and upper left in Figure 6-3. The flow field has a governing influence on the residence time distribution in this case. It is noted that in this case it is also impossible to have mixing between different trajectories, and the transit time distribution may easily contain multiple peaks.

If the source area is small relative to the scale of the fracture network then the particle trajectories tend to keep closer to each other during the migration. In this case the flow path has more of a one-dimensional nature (**streamtube**). This case also reflects more the conditions of the Phase C tracer test and it is illustrated by picture at lower left in Figure 6-3. Also in this case the distribution of the flow velocities and the variation in the lengths of the trajectories can be described statistically using dispersion. However,

the natural system does not usually show multiple peaks or substantial changes under small variation of the flow field. In the case of small source area it is also possible to have mixing across the streamtube.

In both cases above, under steady state and purely advective flow conditions, the tracer molecules follow the streamlines of the flow field. This means that the residence times of the ideal non-retarded tracer molecules are those of the streamlines. This residence time distribution can also be referred to as the "**groundwater residence time distribution**".

One characteristic of the fracture network transport compared to the single fracture transport, that has also been addressed in the TRUE Block Scale experiments, is the possible influence of the fracture intersection zones (FIZ) (cf Figure 5-5). The effects of FIZs cannot be/have not been connected to the measured *in situ* retention, but the FIZ may influence transport through the network by introducing branching points of potentially highly transmissive pathways. This leads to spreading of the tracer plume into different pathways, possibly resulting in tracer loss if a FIZ is connected to a hydraulic boundary. The simplistic fracture network shown in Figure 6-3 also contains FIZs, which in some cases constitute preferential flow paths. In Figure 6-3 red lines indicate the potential FIZs. In the tracer tests between two points in a fracture network a FIZ effect will show up as a tracer mass loss at the withdrawal point. JNC-Golder has performed simulations of potential FIZ cases among the TRUE Block Scale tracer experiments. There is statistical indication of the mass loss in the pathways that intersect FIZs but uncertainties connected to the ultimate recoveries makes this conclusion uncertain, cf Section 5.2.

6.2.3 Advective field in the different evaluation models

Transport, and also the retention, depends on the properties of the flow field. There is no sense comparing evaluated retention properties if the corresponding flow fields are not compared. A straightforward approach to compare the developed models is to make use of the calculated groundwater residence time distributions. In this way the comparison of the models is not complicated by the details of the simplifications made by each of the modelling teams to conceptualise the flow problem, e.g. channel network vs continuum approach etc. Comparison of the statistical parameters of the calculated groundwater residence time (mean and standard deviation of the breakthrough time), or representation of the advective field by basic transport parameters (mean velocity and dispersion coefficient) is not able to give a satisfactory description of all characteristics of the advective flow field which are of interest. The more interesting characteristics of the groundwater residence time distribution are e.g. the degree of symmetry/asymmetry and tailing.

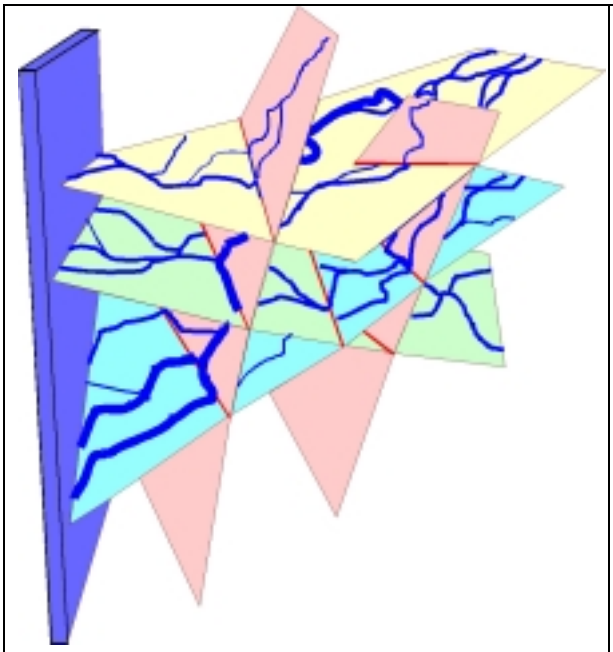

Ambient natural flow conditions. Large source marked with dark blue region on the left. Active flow paths indicated by dark blue.

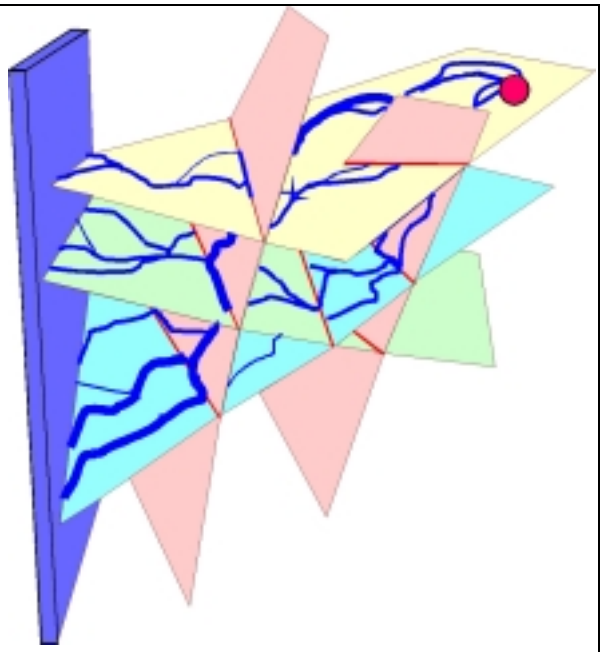

Sink in the model indicated by red circle. Large source area marked with dark blue region on the left. Active flow paths indicated by dark blue.

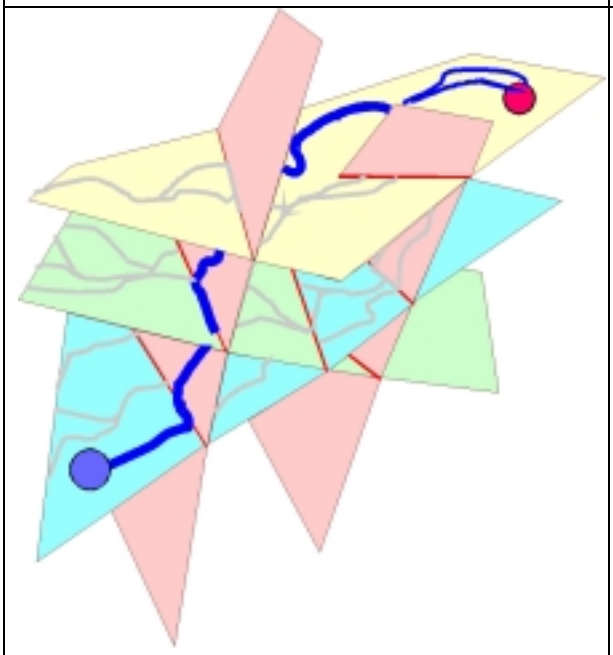

TRUE Block Scale Phase C conditions. Small source marked with dark blue circle and sink with red circle. Active flow path indicated by dark blue.

Note that FIZ are marked with red lines in the fracture network and in some cases the flow paths go along the FIZ.

Figure 6-3. *Schematic illustration of the influence of the boundary conditions and source and sink sizes on the fracture network transport.*

The comparison of the groundwater residence time distributions by means of the ideal non-diffusional and non-sorbing tracer breakthrough curve is not meaningful unless the breakthrough curves are calculated for the Dirac's delta function source (input) function (or a sufficiently short pulse). Application of other source functions (e.g. decaying pulse) may lead to ambiguous results because in the breakthrough curve the tailing of the early input (source term) are superimposed by the faster responses of the late time input (retention processes), i.e. the breakthrough curve will in this case not only carry information of the migration properties of the rock, but also of the source term itself.

A comparison of the advective fields is made between all five modelling groups that have predicted and evaluated the Phase C tracer experiments (Nirex-Serco, JNC-Golder, Posiva-VTT, ENRESA-UPC/UPV and SKB-WRE). In addition residence time distributions are presented also for 1D advection-dispersion model used by SKB-GEOSIGMA /Andersson et al, 2002b/. Simulated groundwater residence time distributions for all models and all three Phase C setups are presented in Figure 6-4. The evaluation models also apply different approaches to characterise the influence of the heterogeneity on the advective transport. The combined flow and transport models

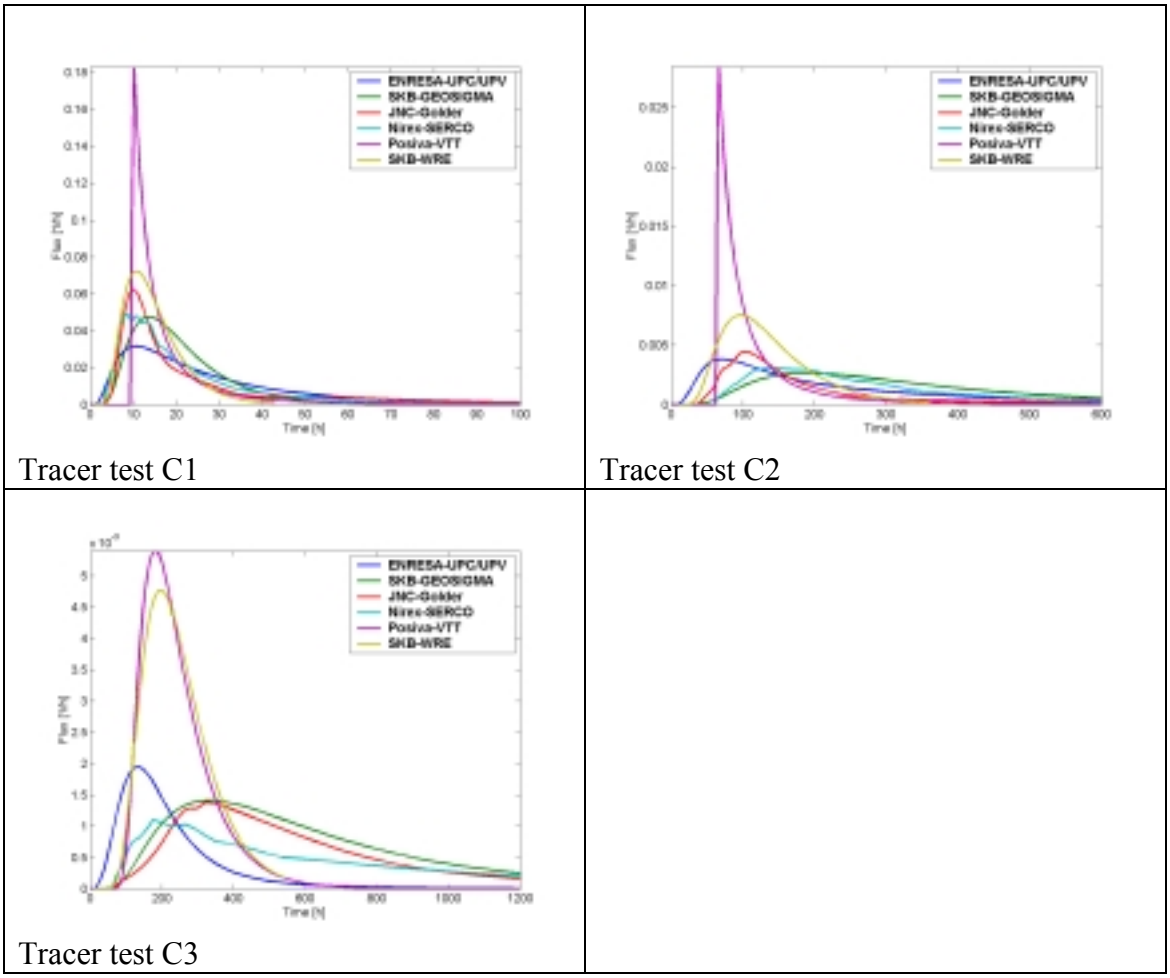

Figure 6-4. *Groundwater residence time distributions (no matrix diffusion/sorption) for the C1, C2 and the C3 tracer tests as provided by the different models.*

(ENRESA-UPV/UPC, JNC-Golder and Nirex-Serco) calibrate the transport aperture/porosity and dispersivity to obtain a correct advective behaviour. The two 1D models fit flow velocity and correlation length over the velocity field (Posiva-VTT) or groundwater residence time distribution directly (SKB-WRE).

When comparing the residence time distributions in Figure 6-4 it should be remembered that all curves calculated by the evaluation models, are conditioned to the measured breakthrough curves. This means that all advective fields in Figure 6-4 should produce similar tracer residence time distributions (i.e. measured breakthrough curves) if they are combined with the corresponding retention model. Considering e.g. the variability in width of the breakthrough curves it is clear from Figure 6-4 that different models have different emphasis on spreading due to the flow field relative to that imposed by retention processes. Models that produce narrow peaks in Figure 6-4 should have a retention model that produces more spreading in the breakthrough curve than the models that produce wide breakthrough already as a consequence of the advective field.

Posiva's model has the least amount of dispersion of all three tests and in the case of C1 this also causes delay in the first breakthrough time. Transit time distributions are also different when comparing 1D and 2D/3D models. Integration of the breakthrough curves in Figure 6-4 shows that the 1D models (Posiva-VTT, SKB-WRE and SKB-GEOSIGMA) show full recovery for all tests, as they should. However, the 2D/3D models (ENRESA-UPC/UPV, JNC-Golder) suggest presence of other sinks in the model for the C2 and C3 injections. Especially, C3 in the ENRESA-UPC/UPV model and C2 in the JNC-Golder model show low mass recovery, cf Table D-1 in Appendix D. The models can be roughly divided into three different groups according to the characteristics of the water residence time: stochastic continuum model shows early breakthrough and long tailing, 1D models produce narrow pulse type breakthrough and finally DFN and AD model seems to produce late peak time and long tailing. Behaviour of the channel network model varies depending on the flow path.

Hydrodynamic control of the retention (in terms of the parameter β, cf Equations (6-3) through (6-6)) in different models can be estimated based on the information on the groundwater transit times and retention apertures (cf Table D-1 in Appendix D). Figure 6-5 presents β's for different flow paths and different models. Flow path I (C1) shows a consistent grouping of most of the models showing values between 20 to 60 h/mm. It is noted, that flow path I gave breakthrough for the largest number of tracers and thereby the constraining power of the breakthrough curves is highest for this flow path. The retention parameter β should increase with increasing path length which is also clearly visible in Figure 6-5 (estimated path lengths C1<C3<C2). The complexity of the flow path may have increased the spread between different models in the case of flow path II (C2). However, tracer tests C1 and C2 were performed using forced injection that may have had an impact on the parameter β. Normalising the parameter β for different flow rates and path lengths ($W=\beta/2*q/L$, cf Equation (6-3)), indicating an equivalent transport width of a uniform channel representing the physical flow path, shows values of W for the models that are 2 m to 5 m for C1 and 0.2 m to 1.5 m for C2 and C3. Generally, W is a factor of 3–5 higher for C1 than for C2 and C3. It is also noted, that test C2 showed a breakthrough only for two of the tracers over the "official" monitoring time (3300 hrs).

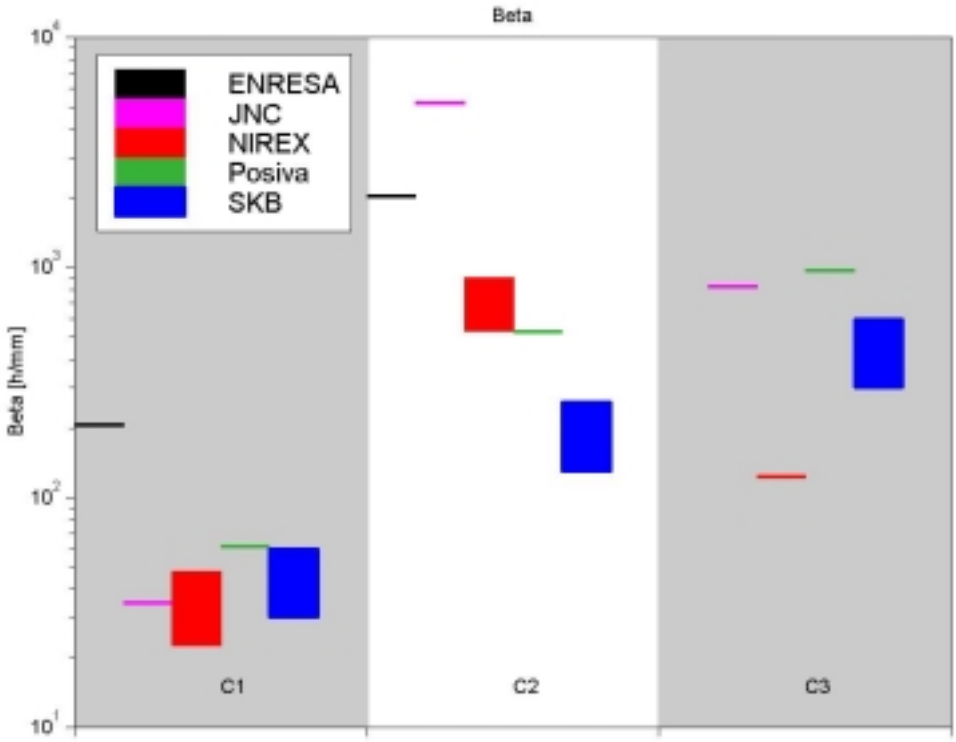

Figure 6-5. *Evaluated parameter β which describes the average flow geometry of the flow paths of the various models and flow paths (tracer tests).*

6.3 Retention due to diffusion

Diffusion to the immobile pore space, sorption in the immobile pore space and surface sorption on the fracture surfaces are interpreted to be the main retention processes in all prediction and evaluation models applied to the TRUE Block Scale experiments (see Chapter 2 for the different modelling approaches). The main support for this assumption are the residence time distributions associated with the TRUE Block Scale experiments (for both sorbing and non-sorbing tracers) which show tailing and spreading that may be indicative diffusive processes. This kind of behaviour can, for example, be indicated by a power-law tailing in the breakthrough curve. Diffusion to an infinite immobile zone should show a $t^{-3/2}$ tailing in the breakthrough curve. Figure 6-6 shows measured breakthrough curves scaled to the same injected mass. Reliable estimation of the characteristic tailing in log-log scale requires that the tailing of the breakthrough curves are measured for sufficiently long time. Clearly this is not possible for the strongly sorbing tracers, but the breakthrough curves of the non-sorbing tracers may give some indication of the behaviour. There is a spread in the measured tailings, but at e.g. Sodium, Calcium and Rhenium breakthroughs follow the $t^{-3/2}$ tailing.

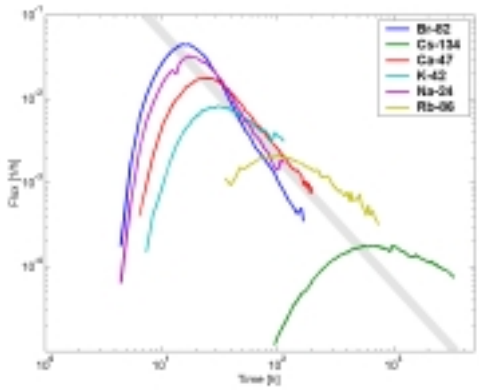

Phase C, Injection C1

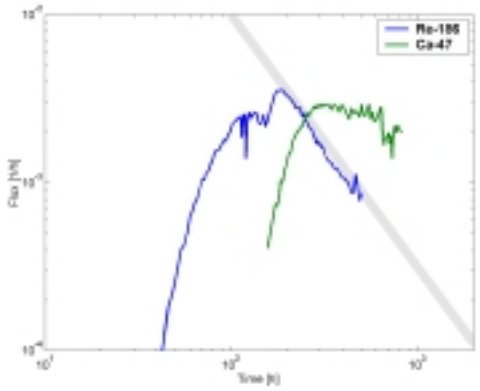

Phase C, Injection C2

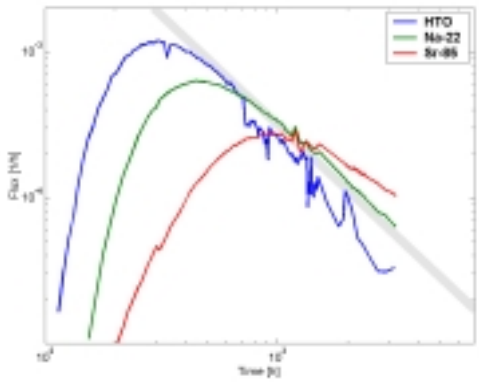

Phase C, Injection C3

Figure 6-6. *Measured breakthrough curves scaled to the same injected mass. Grey lines indicate $t^{-3/2}$ tailing.*

The importance of the diffusional mass transfer processes has also been examined using numerical modelling. JNC-Golder team has calculated the non-sorbing tracer residence time distribution using channel network modelling and by both a) taking the diffusional mass transfer into account and b) omitting it completely. Figure 6-7 illustrates how even for conservative tracers, matrix diffusion can flatten initial breakthrough, decrease early time recovery, and increase the relative amount of mass recovered during later time. The simulation results support the interpretation that diffusional mass transfer is important over the time scales employed in the TRUE Block Scale tracer experiments. The evaluation using different models also indicates that the measured residence time distributions can be reproduced more accurately with the diffusional mass transfer invoked, than without.

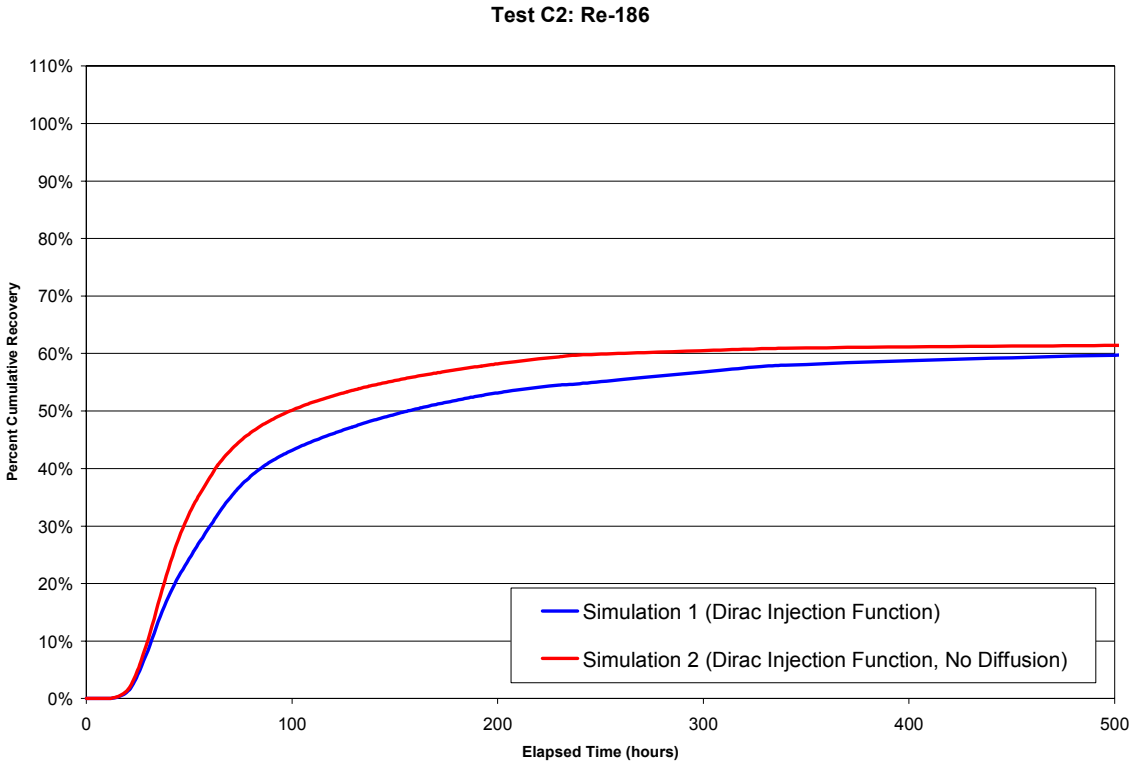

Figure 6-7. *Effect of matrix diffusion on conservative tracer transport (Example for pathway of tracer test C2 (Dirac Injection Function).*

Based on the geological evidence, a number of different immobile pore spaces are conceivable for diffusional processes along the studied flow paths; rock matrix (including altered rim zone), fault gouge, fault breccia and stagnant zones. Molecular diffusion is the crucial physical process that enables the mass transfer between mobile and immobile pore spaces. There is no discrimination between sorbing and non-sorbing tracers at this level of complexity. The advection and diffusion processes are acting in the same way on the sorbing and non-sorbing tracers and during the tracer test they spend the same time in the water phase. All tracer molecules of a given cocktail are collected when they arrive at the withdrawal point, that is, when they have spent the same groundwater transit time, or strictly the same pdf of time, in the mobile zone. The differences in the overall residence times arise from the differences in the time that the molecules have spent sorbed on the surfaces of the mobile and in the immobile pore spaces.

Molecular diffusion also takes place in the mobile pore space. In this process the tracer particles are not retarded because they remain all the time in the flow field. Instead, the tracer residence time distribution changes because particles in the low velocity areas may visit high velocity areas and vice verse. In this case diffusion evens out the advective tracer transit time distribution and attenuates the tailing of the breakthrough curve. Of course, the significance of this process depends on the properties of the advective flow field. In the case of multiple paths, diffusional mixing is not possible as in the case of a single (“one-dimensional“) flow path, and in a case strongly dominated by advection, this process have time to influence only over a short distance.

6.3.1 Pore spaces for the diffusion

Geological information from the TRUE Block Scale site support the assumption of multiple immobile zones /Andersson et al, 2002a/. There are pore spaces, like the altered rim zone, that have clearly higher porosity than the unaltered rock matrix. However, the total volume of the enhanced porosity, i.e. the **capacity**, is small. The limited capacity may be an important factor for some of the immobile pore spaces e.g. stagnant pools, fault gouge or altered rim zone. If the immobile pore space gets saturated it ceases to show kinetic diffusion mass transfer behaviour. In this case the saturated immobile zone shows equilibrium sorption behaviour. In practice this cannot be distinguished from other equilibrium sorption processes like surface sorption and interpretation of the breakthrough curves by surface sorption model will show enhanced surface sorption.

Possible indications of limited capacity of the immobile zone should be looked for in the non-sorbing tracer breakthrough curves. Breakthrough curves of non-sorbing tracers usually have long tailing for the tracer particles which have penetrated deepest into the immobile zones. The residence time distribution in the water phase of the immobile zones is the same for all tracers. Different sorbing/non-sorbing tracers have the same probability density to visit different depths in the matrix. However, for a sorbing tracer this means much longer overall residence time, and usually for practical reasons the long tailings of the strongly sorbing tracers are not measured. For the overall retardation the sorption within the immobile zone is an important process, cf Section 6.4. Present conceptualisation of the transport paths includes immobile pore space in the rock matrix (including altered rim zone and high porosity coating), fault gouge, fault breccia and stagnant zones. A conceptual illustration of a typical cross-section representative of flow paths/structures investigated as part of the TRUE Block Scale Project is presented in Figure 6-8.

The properties of the four different immobile environments are based on the following geological evidence:

- **Rock matrix.** The rock that bounds the fractures including the altered rim zone and a high-porosity coating on the actual fracture surface. The pore structure (and porosity) of the rock matrix may change as a function of the depth in the matrix. Measurements close to the fracture surfaces indicate higher porosity in the vicinity of the fracture surface compared to at depth in the unaltered rock matrix /Andersson et al, 2002a; Kelakoski et al, 2001/.

- **Fault breccia.** Millimetre to centimetre (> 2 mm) sized pieces of altered wall rock/cataclasite and/or mylonite. The chemical and mineralogical composition is usually similar to that of the (altered) wall rock. Observable in the BIPS log /Andersson et al, 2002a/.

- **Fault gouge.** Fragments and mineral grains (≤ 2 mm) of altered wall rock and secondary minerals (clay minerals and calcite). The smaller fractions (< 0.125 mm) are to a variable degree enriched in clay minerals, calcite, pyrite and FeOOH. Not possible to identify from BIPS log /Andersson et al, 2002a/.

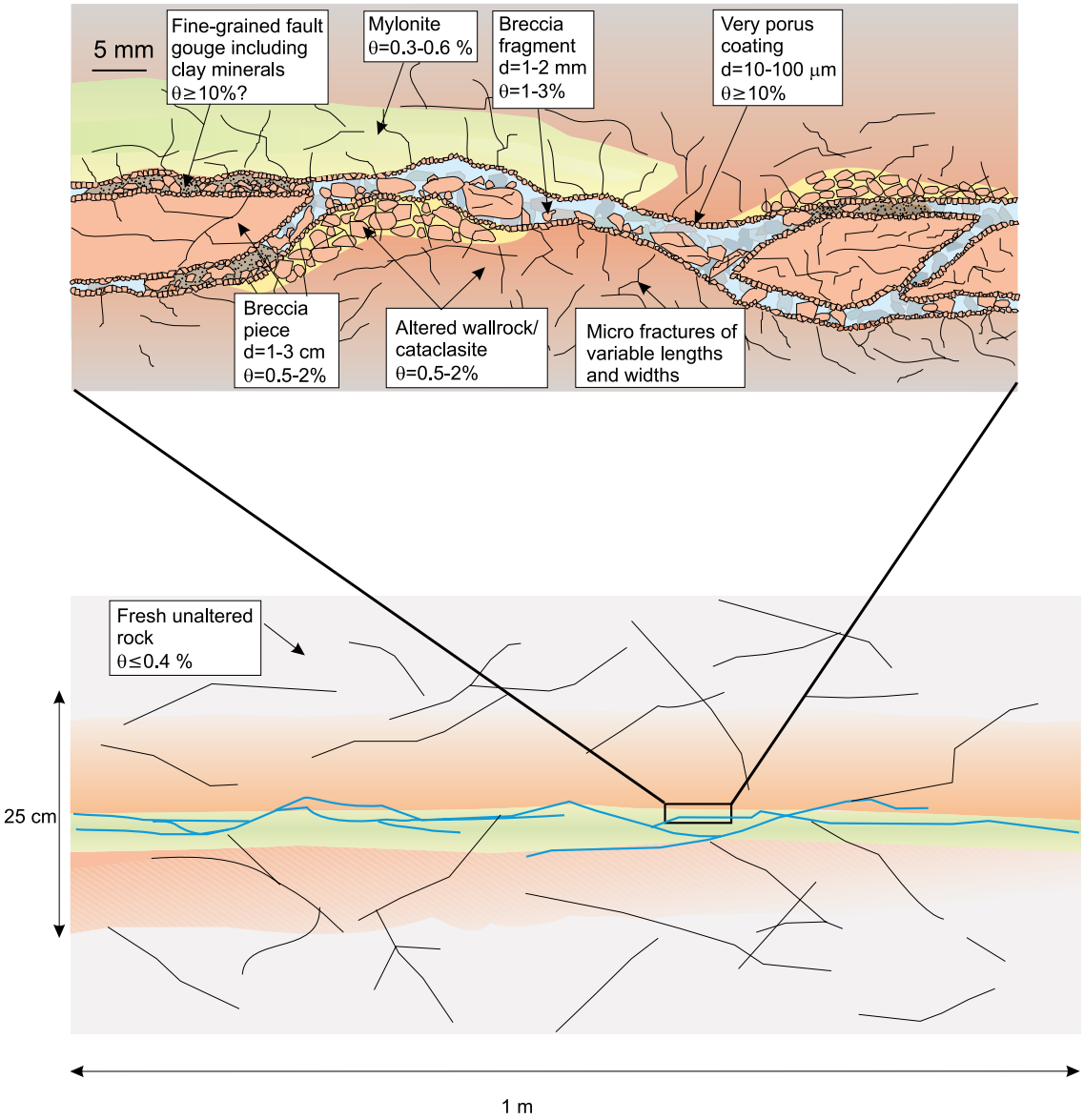

Figure 6-8. *Conceptual figure model of the pore spaces available for diffusion. The figure is based on the conceptual model of the TRUE Block Scale fractures presented by /Andersson et al, 2002a/. Stagnant zones are found normal to the plane of the figure.*

- **Stagnant zones.** There are two different origins of stagnant zones. First, they can be part of the pore space that is immobile (or have extremely low flow rate) due to the boundary conditions. Under different boundary conditions these pores can be part of the mobile pore space (e.g. due to groundwater flowing in another direction). Second, stagnant zones can be regions of small aperture in the fracture, or dead end pools. In both cases the stagnant zones are part of the void space of the fracture.

6.3.2 Interpretation using matrix diffusion models

The four immobile zones presented in Section 6.3.1 exhibit differences that may influence the retention properties e.g. the total volume or thickness of the available pore space. It is obvious that the rock matrix has infinite capacity in practically any *in situ* tracer experiment. Contrary to the rock matrix, the fault gouge is composed of small particles that have very limited capacity. It is thus possible that in the fault gouge the effects of the matrix diffusion dissipate and the retardation can be modelled as a part of the equilibrium surface sorption. The latter approach is adopted by the SKB-WRE team /Cvetkovic and Cheng, 2002/. The tracer behaviour in the stagnant zones is probably similar to that in the fault gouge, although the capacity may be higher. The capacity of the fault breccia is somewhere in between that of the fault gouge and rock matrix. Probably, within the time scale of the tracer tests the capacity of the fault breccia pieces do not differ much from that of the infinite medium. In addition to the variable pore space capacity, the multiple and parallel appearance of the available immobile pore spaces cause superposition of similar response characteristics in the breakthrough curves. This means that it is not possible to distinguish the contribution of diffusion to the different pore spaces using the breakthrough data alone.

Retention processes in different immobile zones follow the same basic mechanisms. Diffusion controls the mass exchange between the mobile and immobile pore spaces. The characteristic $t^{-3/2}$ tailing of the matrix diffusion breakthrough curve results from the diffusion process to the infinite immobile zone. However, an internal boundary in the immobile zone, or changes in diffusion properties as a function of depth in the immobile pore space will change the slope of the tailing. Tracer retardation depends on the integrated (effective) retention property along the flow paths. This integrated property is composed of the porosity and pore diffusivity of the immobile zones together with the sorption properties of the tracer and properties of the flow field (parameter B in Equation (6-3)). It is not possible to back-calculate values of the individual physical retention parameters, or at least, it is not possible to obtain unique solutions. The interpretation of the retention properties from the breakthrough curves is also strongly linked to the underlying assumptions of the dispersion (i.e. advective flow field) and equilibrium surface sorption. Both of the latter processes can produce similar characteristics in the breakthrough curves as the matrix diffusion.

Heterogeneity in the immobile zone properties can influence the interpretation of the retention. For example, site-specific measurements indicate that the porosity of the rock matrix changes quite significantly close to the fracture surface (cf Figure 6-9). The porosity immediately adjacent to the fracture is much higher than the average porosity in the intact unaltered rock. The high porosity zone of limited extent adjacent to the fracture (including a very thin high-porosity coating) indeed has influence on the tracer retardation over experimental time scales, and it may partly explain the noted differences between the retention observed in the laboratory and that observed *in situ*.

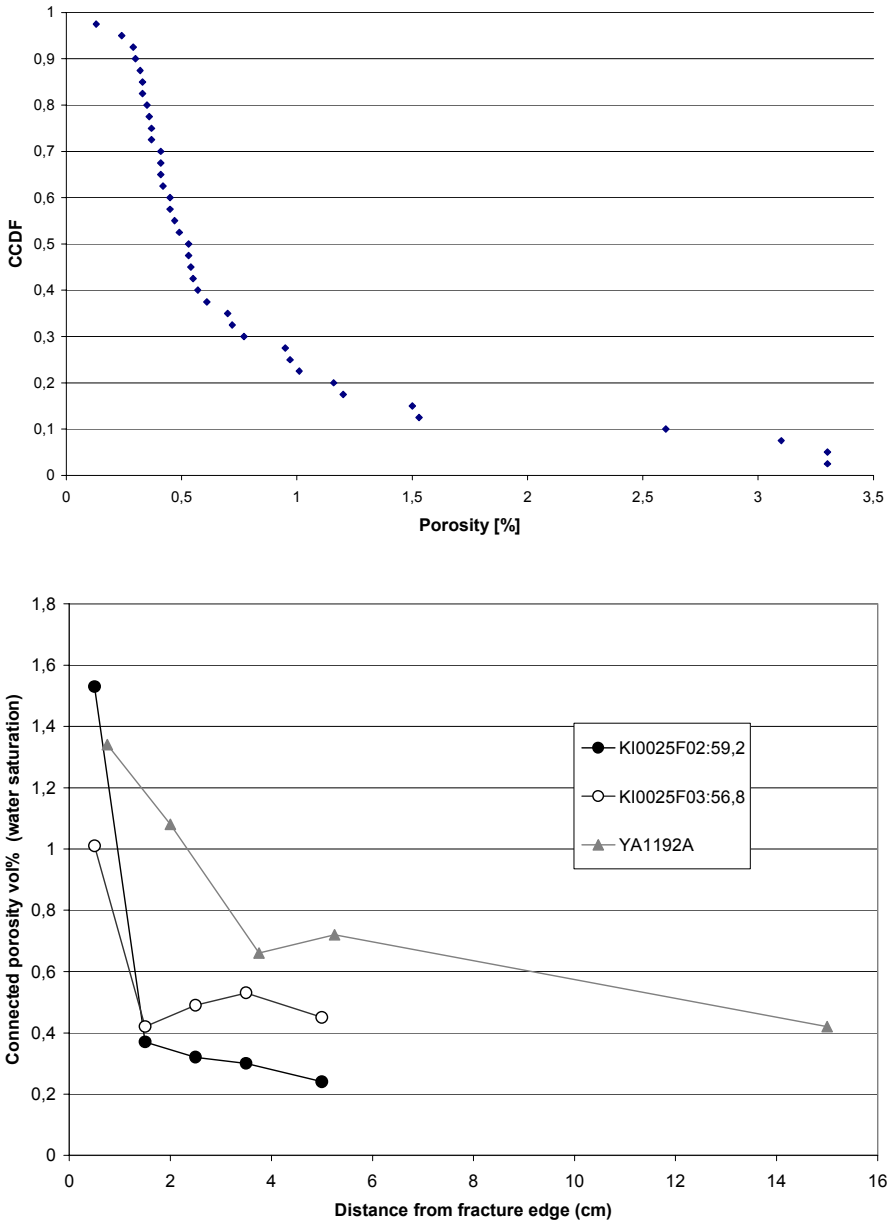

Figure 6-9. *Observed porosity values show heterogeneity. (a) Complementary cumulative density function (CCDF) of the measured porosity at the TRUE-1, TRUE Block Scale and REDOX sites show range of porosity values up to 3%. (b) Examples of observed heterogeneity in the porosity profiles from the fracture wall into the altered wall rock matrix /Andersson et al, 2002a/. Profiles from Structure #23 established on core samples from boreholes KI0025F02 (L=59.2 m) and KI0025F03 (L=56.8 m).The sample YA1192A represents a profile from a fracture surface exposed in the tunnel /Landström et al, 2001/.*

6.3.3 Comparison of the modelling approaches

Diffusion from the mobile part of the pore space to the immobile part is modelled in all models as a one-dimensional process. This leaves some freedom to the geometrical definition of the structure of the pore spaces. Immobile pore spaces can be conceptualised as separate zones that have different properties and which are accessed from the mobile pore space by diffusion in different directions and to different locations along the flow path. The conceptualisation of a typical flow path into different diffusion sub-processes is presented in Figure 6-10. In the direction normal to the fracture plane the tracer experiences (altered) rock matrix and possibly high porosity coating at the surface of the fracture. Stagnant pools, fault gouge and fault breccia may also be located in the fracture planes in the lateral direction and normal to the extension of the flow path.

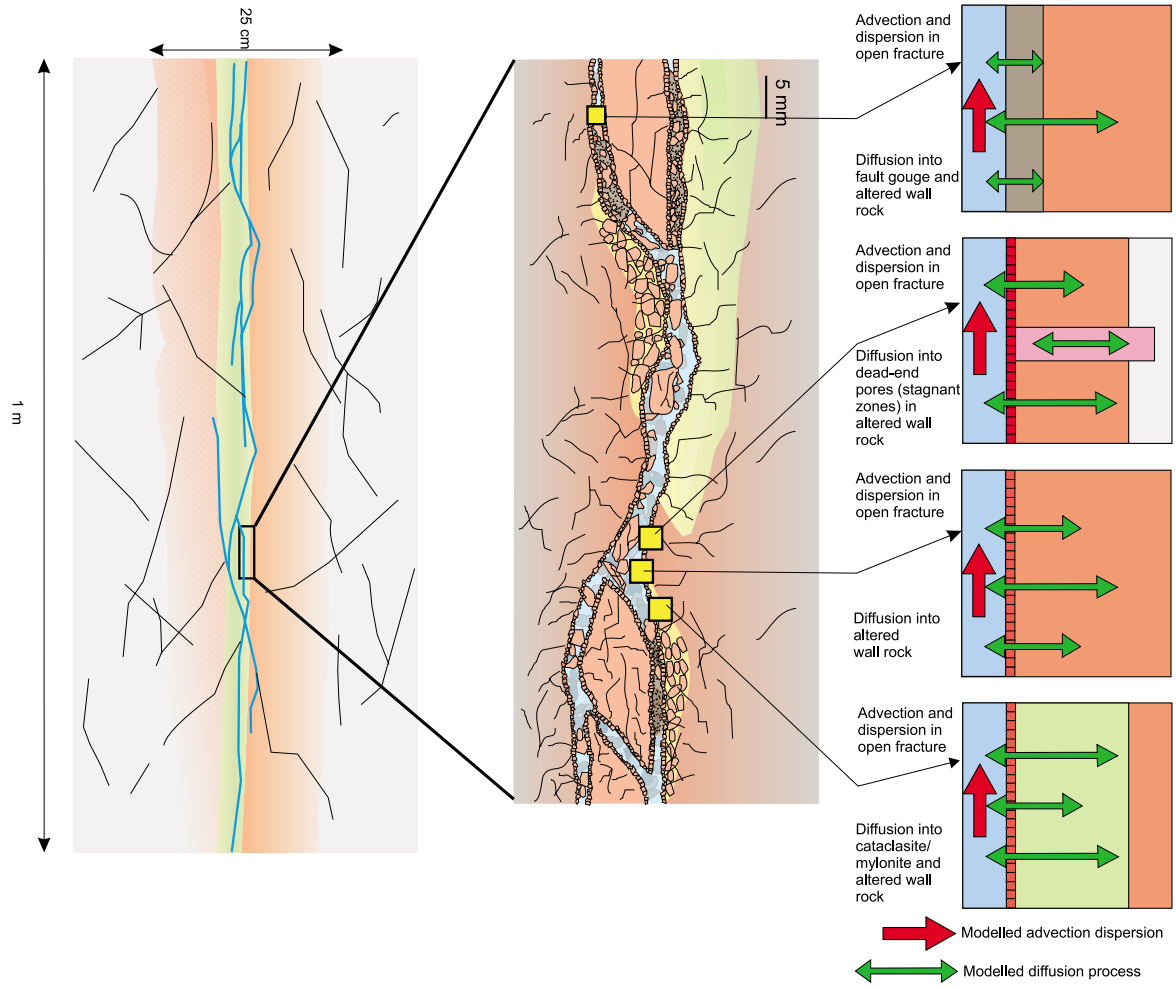

Figure 6-10. *Simplification of the pore space structure as applied in the evaluation models.*

All the five modelling approaches used to predict/evaluate the Phase C tracer tests include diffusion into the immobile pore space as a retention process (see Chapter 2). Most of the approaches account for the limited depth of the immobile zone, but the thickness of the immobile zone vary from 0.1 mm to 1 m and in one model (SKB-WRE) a depth-dependent porosity has been applied. The immobile pore spaces included by the different modelling teams are summarised in Table 6-1. The corresponding properties of the different immobile pore spaces and associated diffusivities are presented in Tables E-1 and E-2 in Appendix E, respectively.

Commonly, the immobile zone properties are presented in models as effective properties that integrate the effects of the rock matrix, fault gouge and fault breccia. In one case three alternative immobile zones are used (Posiva-VTT). The porosities assigned by the teams are not all that different and are also close to the laboratory values established for rock matrix, fault breccia pieces and fault breccia fragments /Andersson et al, 2002a/. One exception is the high porosity assigned to the stagnant zones by Posiva-VTT, but in the latter case no supporting data exist. It seems that the immobile zone diffusion properties are mainly adjusted by changing the pore diffusivity. The spread in the assigned values of pore diffusivity for all tracers is from about 10^{-11} m^2/s (ENRESA-UPC/UPV) to $5 \cdot 10^{-10}$ m^2/s (SKB-WRE) (see also Figure 6-14). Only in one case (SKB-WRE) a non-constant pore diffusivity (function of distance) has been considered. It is noted, however, that the porosity measurements indicate enhanced porosity adjacent to the fracture and that heterogeneity in porosity could be important feature that need to be considered in the modelling.

Table 6-1. Type and number of immobile pore spaces and surfaces used by the modelling teams in the evaluation of the TRUE Block Scale Phase C tracer experiments.

	ENRESA-UPC/UPV	JNC-Golder	Nirex-Serco	Posiva-VTT	SKB-WRE
Number of different pore spaces	One	One	One	three alternative models: rock matrix, fault gouge, stagnant zones	One
Number of different adsorption "surfaces"	No surface	One	One	two: fracture surface, stagnant zone	One, fault gouge integrated in surface sorption.

Diffusion-coupled retention in different models is compared by using the retention time T ($T=\beta^2\kappa^2=B^2$, cf Equation (6-5)) and material parameter group κ (Equation (6-5)). The comparison of evaluated retention time B^2 is shown in Figure 6-11 and the comparison of evaluated κ is shown in Figure 6-12.There is clear separation between the models as to how they apply material properties in retention, cf Figure 6-12. The majority of the models apply material properties that are clearly higher than the MIDS values, the latter which indicate properties of the unaltered rock matrix. Only the stochastic continuum model (ENRESA-UPV/UPC) applies material properties that are comparable to the MIDS values. In the evaluated retention time this is compensated by the higher β values (cf Figure 6-5).

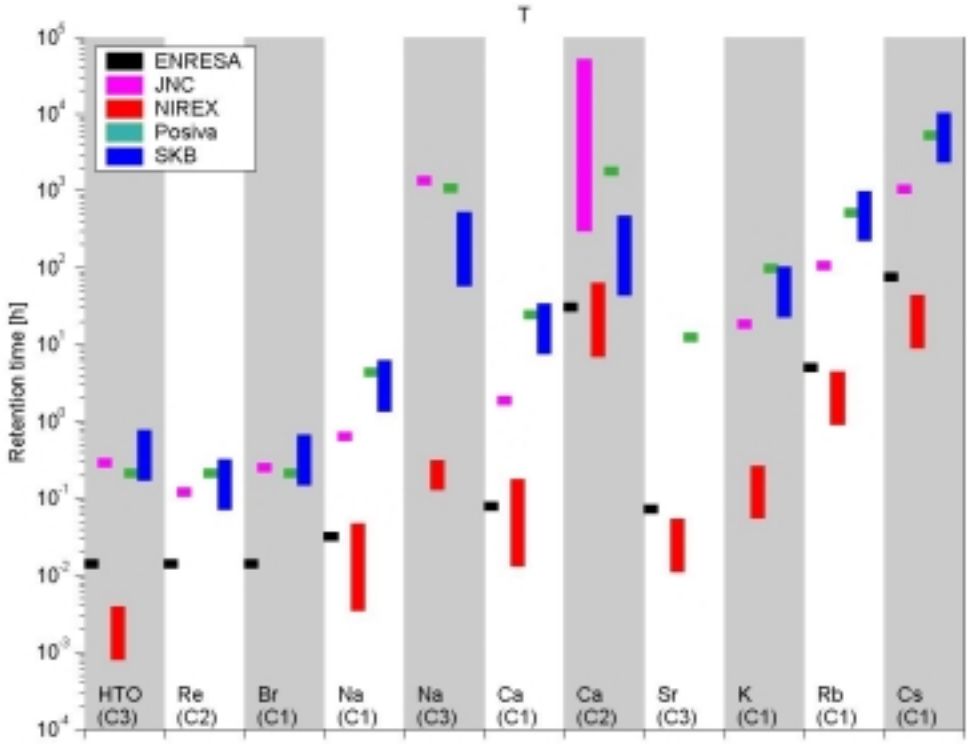

Figure 6-11. *Evaluated retention times (B^2) from Equation (6-5) for the different models and tests (C1, C2 and C3).*

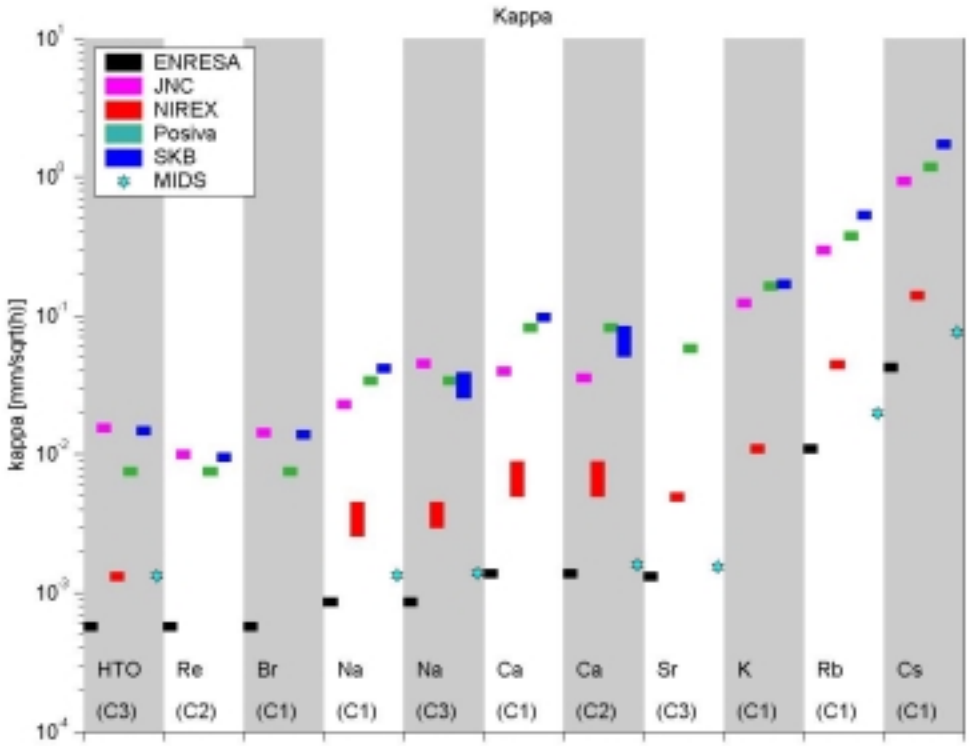

Figure 6-12. *Evaluated retention material parameter group κ (cf Equation (6-5)) for the respective evaluation models and tests (C1, C2 and C3). Compare Figure 6-2 for corresponding visualisation of input κ used in model predications.*

6.4 Retention due to sorption

Transport of selected tracers and radionuclides in crystalline bedrock is reactive. This means that the tracer particles interact with the groundwater-rock system by various chemical reactions during transport along the flow paths. In transport modelling, all the various reactions, such as adsorption and ion exchange, are referred to as “sorption”. Usually, these reactions retard the transport of the tracers, but there are also rare cases where sorbing tracer particles may migrate faster than a non-sorbing tracer. Such a situation may be caused e.g. by anion exclusion coupled with hydraulic and chemical heterogeneity /EPA, 1999a/ or presence of colloids.

The sorption models that have been applied by the modelling groups in the analysis of the TRUE Block Scale experiment are based on considerably simplified representations of the real system being studied. All models have reversible and instantaneous equilibrium sorption (cf Section 2.2); limitations of the latter assumption for the tracers used are discussed by /Byegård et al, 1998/. Fixed distribution coefficients, either by a volume-based distribution coefficient K_d, or a surface-based distribution coefficient K_a

parameterises sorption of the different tracers. The latter two parameters depend only on the tracer used, the geological material being interacted with and the groundwater composition, cf Section 2.2.

Depending on the modelling approach, the applied sorption values are based either on the fitting of breakthrough curves from previous *in situ* experiments at Äspö HRL and/or laboratory measurements that have been interpreted using the K_d approach. However, it should be noted that it is also possible to fit the breakthrough curves by changing other parameters than the values of sorption parameters. This emphasises the need to evaluate assignment/estimation of sorption values alongside with the porosity and pore diffusivity of the immobile zones, and the properties of the flow field (see Equation (6-4)).

6.4.1 Sorption environments

Sorption may take place onto any geological material that is available along the transport path. Potential sorption sites along the flow paths investigated in the TRUE Block Scale experiments are located in the pore space of the (altered) rock matrix (rim zone), fault breccia, fault gouge and on the surfaces of the fractures making up the mobile pore space, cf Figure 6-10.

In conjunction with the TRUE-1 experiments /Winberg et al, 2000/ the sorptivity of various geological materials was investigated in the laboratory /Byegård et al, 1998/. The investigations included experimentation on non-site-specific unaltered rock material (Äspö diorite and Fine-grained granite) and altered matrix material from the Feature A mylonitic rim zone. The general conclusions of the investigations are that Äspö diorite is more sorptive than Fine-grained granite. The investigations also indicated that alteration and mylonisation causes reduction in the sorptivity. On the other hand, higher concentrations of biotite cause higher sorptivity. Sorption on the pure biotite is much higher than any of the rock types investigated (p 39 in /Byegård et al, 1998/).

The sorptivity of the fault gouge material collected from the borehole intercepts of the interpreted deterministic structures involved in the TRUE Block Scale Phase C experiments has not been determined experimentally. However, estimates of K_d for the fine-grained fault gouge have been calculated based on the cation exchange capacity (CEC) using the mineralogical composition of the material of a grain size smaller than 125 μm /Andersson et al, 2002a/. By applying a cation exchange sorption model combined with the groundwater composition associated with a given intercept and literature values of selectivity coefficients, the sorption distribution coefficient (K_d) can be calculated. For the fault gouge/fault breccia material of the size fraction larger than 0.125 mm, sorption coefficients have been estimated using the investigation of the altered Äspö diorite from the TRUE-1 site /Andersson et al, 2002a/. CEC-based estimates of the K_d for the fine-grained size fraction of the gouge material show K_d values that are substantially higher (a factor of about 20 to 60) than those based on the investigated larger size fraction from the TRUE-1 site.

6.4.2 Sorption in different models

In the modelling of solute transport a distinction of the retention processes can be made between equilibrium and kinetic sorption. Sorption on the fracture surfaces can usually be handled by *equilibrium sorption*. However, matrix diffusion to the immobile pore space and subsequent sorption in the immobile pore space causes retardation that is time dependent (kinetic effect), which is mechanistically similar to the sorption influenced by chemical kinetics. A division between equilibrium and kinetic types of the retention needs to be sorted out in the evaluation phase by deciding how much of the tracer retention that can be attributed to the equilibrium sorption, and how much is attributed to kinetic sorption. This division is not trivial, and it may eventually have an influence on the interpreted matrix diffusion properties.

All sorption sub-models applied in the modelling of the TRUE Block Scale Phase C tracer tests are based on linear reversible equilibrium sorption, both in the immobile pore space (volume-based distribution coefficient, K_d) and on the fracture surfaces (surface-based distribution coefficient, K_a), cf Table 6-2 and Appendix F. Generally, the sorption properties are based on model fits to available and relevant breakthrough curves. However, many approaches also apply laboratory-derived estimates, or CEC-based estimates as initial values, or constraints, of the K_d. All model approaches apply K_d based sorption for the immobile zones, and all but the ENRESA-UPC/UPV team have also included surface sorption. The final evaluation models are conditioned to the measured breakthrough. This means that different choices made for the advective field, or diffusion properties need to be compensated, or balanced, by the selected sorption properties. In practice, small dispersion in advection, low pore diffusivity and/or porosity require high sorption coefficients to fit the *in situ* test data, and vice versa. This kind of interplay can also be seen in the parameters used.

The material parameter group κ is divided into porosity, diffusivity and K_d values in Figures 6-13 through 6-15. In general, the applied material properties in the evaluation models are higher than the MIDS data /Winberg et al, 2002/, which is derived for the unaltered rock matrix. The greatest contribution to elevated (enhanced) material properties comes from the K_d values, which are 50 to 200 times higher than MIDS values. Diffusivities are up to 50 times higher than MIDS and porosities may be 10 times higher than MIDS.

The spread in the used K_d values is smaller for the strongly sorbing tracers than for weakly sorbing tracers. This may indicate the influence of the differences in the advection-dispersion transport between the models. Transport of the strongly sorbing tracer does not depend on the advective transport as the weakly sorbing does. This diminishes the spread in the required K_d values for the strongly sorbing tracers.

The spread in the material property group κ is not that large as the spread in the individual parameters may suggest. This follows from the fact that individual models compensate the emphasis of one parameter by attenuating other parameters. However, this does not provide explanation for all models. The stochastic continuum model emphasises hydraulic control of the retention and advection-dispersion transport. This is reflected by clearly lower values of the material retention group. Similarly, the DFN

model emphasises surface sorption (cf Table F-1 in Appendix F) that also is seen as lower diffusion-coupled retention and in that way a lower value of the material property group κ.

Table 6-2. Sorption models applied by the modelling teams to the different geological materials in the evaluation of the TRUE Block Scale Phase C tracer tests.

Team	Geological material	Sorption model	Source of the sorption data
ENRESA-UPC/UPV	Immobile zone	K_d	Table 6-1 in /Byegård et al, 1998/
JNC-Golder	Rock matrix	K_d	Primarily run using MIDS data /Winberg et al, 2000/. Range of additional sensitivity studies based on Phase C tracer test results
	In-fracture immobile zones(fault breccia/gouge/stagnant zones)	K_d	Se above!
	Altered wall rock	K_d	See above!
Nirex-Serco	Rock matrix	K_d /K_a	Breakthrough curves. Initial estimates based on laboratory data
Posiva-VTT	Rock matrix	K_d	Fits to breakthrough curves, constrained by Table 6-3 in /Byegård et al, 1998/
	Fault gouge	K_d	Fits to breakthrough curves, constrained by Table 7-4 in /Andersson et al, 2002a/
	Stagnant zones	K_a	Fits to TRUE-1 breakthrough curves
	Mobile zone of the Fracture	K_a	Fits to TRUE-1 breakthrough curves
SKB-WRE	Rock matrix, fault gouge integrated in to surface sorption and matrix and fault breccia integrated into matrix	K_d /K_a	Inferred from TRUE Block Scale breakthrough curves

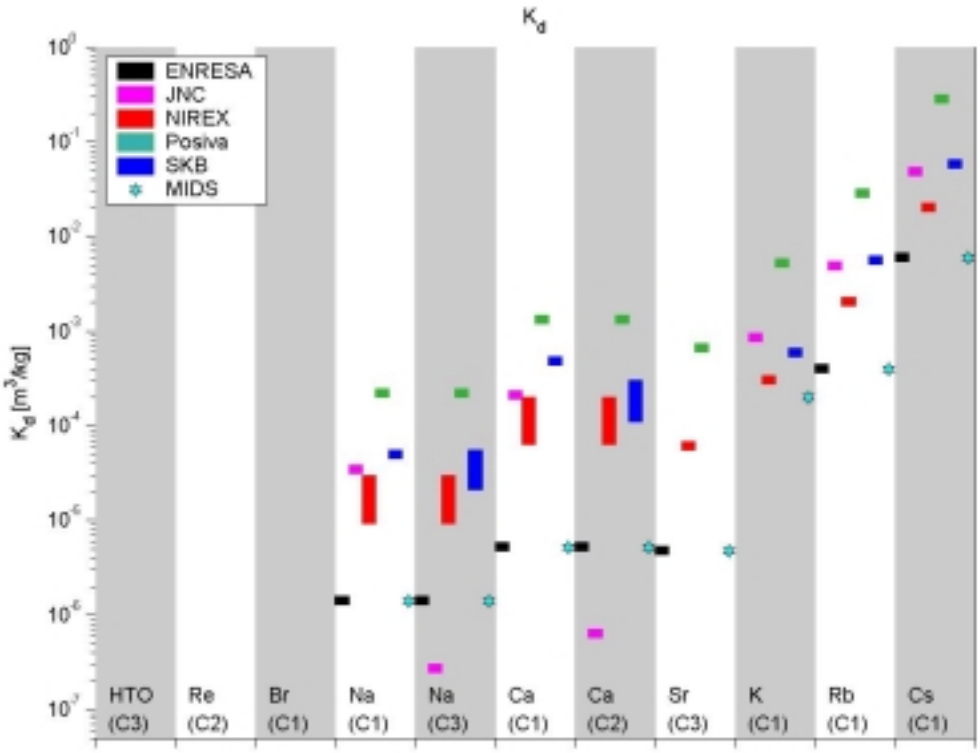

Figure 6-13. *K_d values used in the respective evaluation models.*

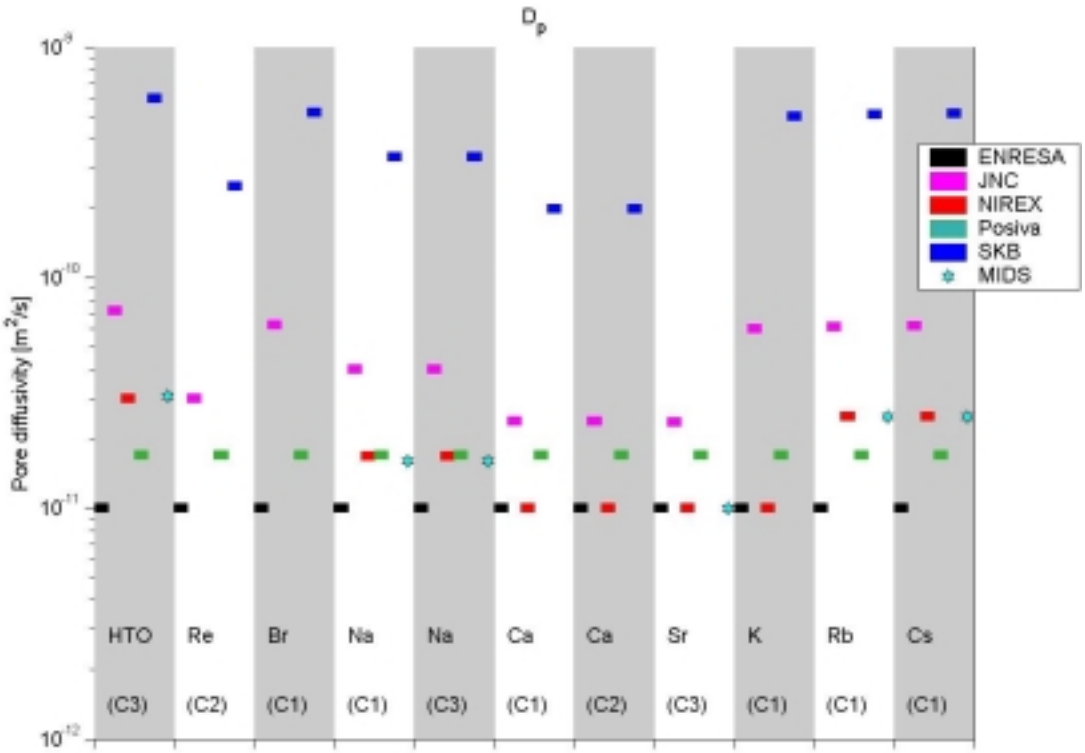

Figure 6-14. *Pore diffusivities used in the respective evaluation models.*

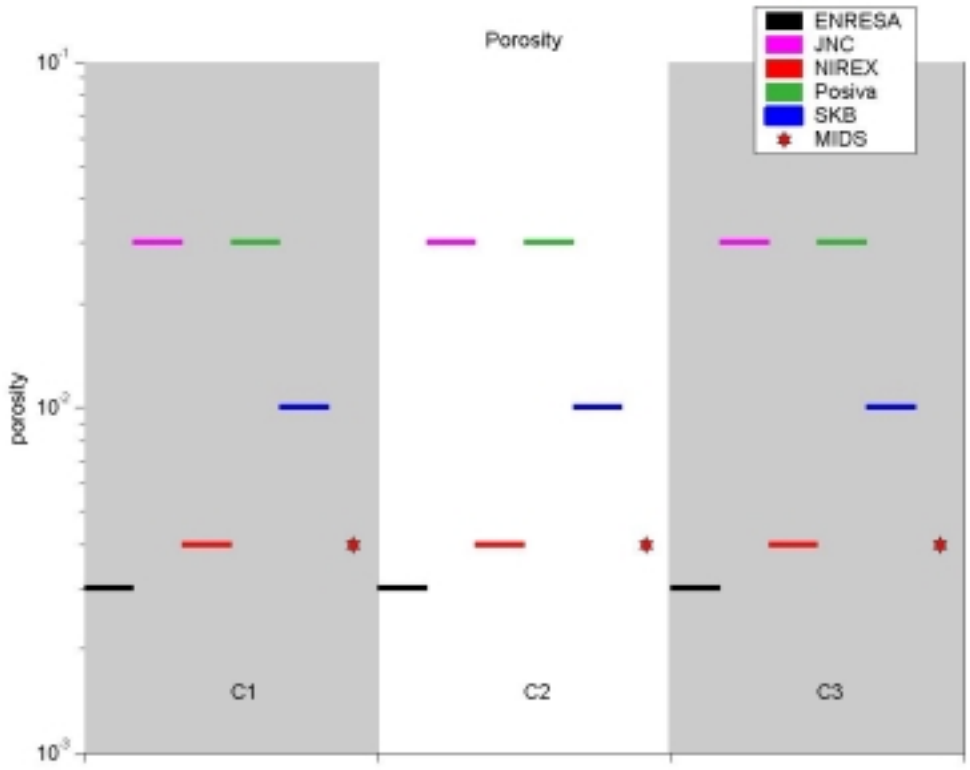

Figure 6-15. *Porosity of immobile zone used in the respective evaluation models.*

6.4.3 Uncertainties in sorption models

Modelling of the sorption may include substantial uncertainty that can influence the interpretation of the results. Sorption models are based on constant (time/chemistry and space invariant) sorption values resulting from direct measurements of the partitioning of a given tracer between the solid and aqueous phases. This is an empirical procedure to account for various chemical and physical retardation mechanisms that are influenced by a large number of different variables. Sorption mechanisms that can be well described by the K_d/K_a approach are e.g. the adsorption/desorption processes. Adsorption/desorption (and ion exchange) will likely be the key process in areas where chemical equilibrium exists.

The most significant uncertainty in the applied sorption models is probably associated with the kinetic effects. The approach based on the distribution coefficient assumes no kinetic effects in the adsorption/desorption processes. These processes are assumed to take place through instantaneous equilibrium. An example of extreme disequilibrium sorption is the adsorption that is irreversible within the time frames of the experiments.

Irreversible characteristics in the tracer adsorption/desorption properties (e.g. fixation of Cs) may have significant influence on the retention and the interpretation of the breakthrough curves. In the standard linear-reversible-equilibrium sorption model the effects of the irreversible sorption are reflected in the recovery of the tracer, and therefore there is a risk that indications of possible irreversible sorption are used to explain, or interpret/evaluate totally different properties associated with the transport or the flow field.

One assumption related to the applied sorption modelling is connected to the applicability of the concept of the distribution coefficient. It is not completely clear that this concept can explain sorption of all tracers equally and sufficiently well. Inherent in the "linear isotherm" adsorption model is the assumption that adsorption of the tracer is independent of its concentration in the aqueous phase. The Freundlich isotherm, for example, has been used to describe the sorption of Cesium for a wide range of Cesium concentration. These kinds of calculations show e.g. a decrease of the Cesium K_d by an order of magnitude when the Cesium concentration increases from about 10^{-9} mol/l to 10^{-6} mol/l. However, at low concentrations the sorption isotherm follows the linear relationship very well /EPA, 1999b/. In modelling, the application of non-linear models complicates the modelling process and linear models are more favourable. First of all, application of the non-linear models requires more parameters that cannot always be supported/constrained by the available data. In the TRUE Block Scale experiments the tracers are used with sufficiently high dilution, such that one can argue with great confidence that there is no need for an application of a concentration-dependent sorption coefficient.

All evaluation models apply constant (space and time invariant) distribution coefficients. This means that the models do not address sensitivity to changing hydrochemical and geological conditions with time. In reality, sorption processes do depend on the chemical environment. If the groundwater properties (e.g. pH) change, a different sorption value should be used in the model. From the modelling point of view, the solution is simply to apply the parametric model, which changes the sorption value according to the evolving chemistry and mineralogy of the system at the node being modelled. The deficiencies of this approach are related to the collection of the necessary input data for this model. In practice it is very difficult, if not impossible, to determine the mineralogy or groundwater chemistry along a transport path in space and time. On the other hand, from the transport point of view, it is not necessary to know the detailed local variation of the sorptivity but only the integrated effect along the flow paths.

6.5 Partial conclusions

The measured breakthrough curves show retention behaviour that can be explained by diffusional mass transfer processes to immobile pore spaces. At the same time, it is not possible to consistently fit all breakthrough curves using a standard advection-dispersion-sorption model. This also supports the finding that diffusional mass transfer is an important process during the phase C tracer tests.

Geological evidence shows that in addition to the (altered) rock matrix there are also other possible immobile zones along the flow paths, cf Section 6.3.1. These include fine-grained fault gouge, fault breccia and stagnant zones of the flow field. According to the field data (both from the TRUE Block Scale and TRUE-1 sites) the porosity of the altered rock zone adjacent to the fracture is clearly higher than the porosity of the unaltered intact rock matrix on average. Over tracer test temporal scales the diffusional mass transfer to the altered rock zone is thus much stronger than is expected based on the data of the unaltered rock matrix.

A grouped (or pooled) property that depends on the flow field, immobile zone diffusivity, porosity and sorption, cf Equation (6-4), governs diffusional mass transfer to the immobile pore spaces. Retardation along a flow path depends on the integral of this parameter along the flow path. Conclusions can be drawn on the average retention properties of the immobile zones. Lateral heterogeneity in the retention properties of the immobile zones influences the interpretation of the average retention by different geological structures. However, when explaining the outcome of the tracer tests it is important to appreciate the implications of the heterogeneity of the immobile pore space normal to the fracture, e.g. the observed decreasing trend in porosity from the fracture surface towards the virgin rock matrix. This heterogeneity may partly explain the differences between the observed *in situ* retention and the material properties obtained from laboratory measurements on the relevant geological materials.

The TRUE Block Scale experiments do not show conclusive indications of new transport phenomena in the block scale, partly because of the one-dimensional nature of the flow paths that will tend to attenuate possible network effects. One potential network effect is loss of mass due to e.g. fracture intersection zones (FIZs). A statistical correlation has been noted that indicates a possible higher tracer mass loss associated with flow paths that intersect possible FIZs.

6.6 What have we learned?

The evaluations made indicate that diffusional mass transfer is required in order to explain the *in situ* retention observed in the TRUE Block Scale Phase C experiments. There is one example of calculations, which have been carried out without diffusional mass transfer, i.e. SKB-GEOSIGMA's advection-dispersion model presented in Section 6.1. SKB-GEOSIGMA's results show that the asymmetry in the breakthrough curves requires, e.g. for the C3 injection, a dispersivity amounting to 26% of the projected path length (L=33 m) (assuming path lengths are calculated using the hydrostructural model). This also indicates that other processes than advection and dispersion alone are needed to explain the transport.

The large variability between different models in the selected/evaluated pore diffusivity indicates that there is no single immobile zone, which dominates the retention. It also shows that the retention depends on different physical properties in a grouped (or pooled) way and in the evaluation emphasis can be put on different properties. It appears evident, however, that the unaltered rock matrix as investigated in laboratory cannot provide sufficient retardation to explain the results of the *in situ* tracer tests. Indirectly this provides support for the conceptualisation of a significant layer of altered rock, characterised by increased porosity (and diffusivity?!) along the fracture walls of the flow paths which is important over the time scales of the tracer tests.

The immobile pore spaces are heterogeneous in all directions. Ultimately, this heterogeneity shows up as limited capacity of the enhanced retention observed in the tracer tests. The SKB-WRE evaluation has addressed the question of heterogeneous immobile zone properties and the results indicate that this may explain some of the observed discrepancy between laboratory-derived and *in situ* retention properties.

7 Supporting modelling

7.1 Overview

Various types of supporting modelling activities have been performed during the course of the TRUE Block Scale Project which have not been directly coupled to the predictions and evaluations associated with the cross-hole pressure interference tests, tracer dilution tests and tracer tests.

Early in the project it was identified that there was a need for a site scale model which could provide boundary conditions in a flexible manner to boundaries positioned in an arbitrary way. A decision was taken to update the existing UK Nirex-AEA DFN model which had previously been employed in the analysis of Tasks 1 and 3 within the scope of the Äspö Task Force /Gustafson and Ström, 1995/, cf Section 7.2. Further, given the location of the Äspö island in relation to the Baltic, and given that saline waters are found at depth at Äspö HRL, it was decided to use the Nirex–AEA DFN model to assess the effects of salinity on ground water flow, cf Section 7.3.

One of the original objectives stated for TRUE Block Scale was to explore means of correlating hydraulic data (parameters) with transport data (parameters). If such a relationship could be established, it could possibly play a role in making tentative predictions of transport on the basis of (hopefully less expensive) hydraulic tests. The results of this study performed with the ANDRA-Itasca 3FLO code /Itasca, 2002/ is found in Section 7.4.

Testing of the hydrostructural model is discussed in Section 6.2. It should be mentioned in this context that no consistent study/evaluation of the various hydrostructural model updates in relation to performed tracer tests was undertaken during the course of the characterisation programme. However, after completing the tracer tests this was revisited using the 3FLO code /Itasca, 2002/ where a selected set of tracer injections were made in series of model updates to evaluate the impact of the hydrostructural model on the ability to reproduce the tracer tests in the model, cf Section 7.5.

7.2 Boundary conditions for local models from a site-scale DFN model

7.2.1 Introduction

This section contains a description of the modelling used to understand site-scale groundwater movement in fractured crystalline rock at the Äspö Hard Rock Laboratory (HRL) site as part of Serco Assurance's modelling participation on behalf of Nirex in the Äspö TRUE Block Scale Project.

The approach adopted for this work uses the discrete fracture network software NAPSAC, to construct a detailed site-scale groundwater flow model. From this site-scale model various modelling tasks were designed to advance the design, interpretation and understanding of tracer tests planned as part of the TRUE Block Scale Project. In particular, a number of prediction and evaluation modelling exercises were planned on a local scale (i.e. a sub-scale of the site-scale) and hence require boundary conditions as part of their input. The intention of this site-scale model was to provide boundary conditions on a smaller sub-scale, 500x500x500 m (and smaller), centred at Äspö coordinates (1900 m, 7170 m, –450 masl).

7.2.2 Site-scale structural model

The modelling used the SKB conceptual model for the hydrogeology of the Äspö site.

A structural model of the Äspö region, shown in Figure 7-1a, produced by /Svensson, 1997/ and /Rhén et al, 1997/ identified the water-bearing fracture zones in the Äspö area. The subsurface was divided into two sub-units; a set of extensive deterministic fracture zones determined by a series of geophysical and hydrogeological investigations and a lower hydraulic conductivity, averagely fractured rocks whose properties were inferred from /Svensson, 1997/. The fracture zones are the main conductors for groundwater flow, but the fractures in the background averagely fractured rock may also be conductive.

Figure 7-1a shows a schematic representation of water-bearing conductive structures for the Äspö area at ground level. The solid line means that a fracture zone has been confirmed by a borehole or surface geophysical investigation, a dashed line indicates possible hydraulic continuity of the fracture zone, derived by extrapolating the known fracture zones. The transmissivities of the fracture zones are defined according to /Svensson, 1997/.

The piezometric level on the Äspö island is governed by the brackish Baltic sea and the natural recharge provided by precipitation incident on the island. As Äspö is an island, fresh groundwater near the ground surface lies on stratified stagnant saline water at depth.

7.2.3 Data used to parameterise the Discrete Fracture Network Models

Away from the fracture zones there are less extensive fractures that represent relatively minor hydrogeologically significant features. These features are fully characterised both geometrically and hydraulically by ascribing orientation, transmissivity, length, and density of the fractures. As these features are in greater numbers as compared to the fracture zones a complete deterministic characterisation of them is clearly not possible. However, an estimation of typical effective properties is possible.

The TRUE Block Scale experiments focus on transport over a length scale representing the distance between the repository and the closest major fracture zone. As the TRUE Block Scale Project has progressed it has become apparent that a hierarchy of hydraulically active structures exist in the investigated rock volume. Investigations has focused on the identification of flowing features that either may have a role in controlling the flow within a subregion of the block or are features of direct relevance to performing well controlled tracer tests. The hydrostructural model of the TRUE Block Scale rock volume has evolved throughout the project. It is the scale of these structures that is represented in much of the predictive modelling.

To simplify the approach the 'background' fracturing has been represented as a regular array of features. The form of the array of features allows the possibility of introducing anisotropy very easily, see /Rhén et al, 1997/.

Figure 7-1b shows a discrete model with a combination of regional features and background fracturing.

The transmissivity data for the Äspö site come from two distinct sources; a) pump tests based on a 3 m packer setting and b) pump test data based on a 30 m packer setting, these data has been summarised by /Rhén et al, 1997/ and /Svensson, 1997/. For the purposes for consistency those values used by /Svensson, 1997/ as they have been derived through a combination of raw data and a certain amount of calibration of the equivalent continuum model used for that work.

A very simple model for the transmissivity of the background fracturing was assumed- that of a constant 'background' hydraulic conductivity. This comprised of taking an average of the background permeabilities that /Svensson, 1997/ used for his work. In addition, to this it is important to check the consistency of parameter values used for the background permeabilities and that of 'upscaling' the TRUE Block Scale rock volume based on a parameterisation of the structural model. An approximate background hydraulic conductivity has been derived from Svensson by taking the geometric average of SRD1 to SRD5 given in Table 2-3 of /Svensson, 1997/. This is approximately $1.8 \cdot 10^{-8}$ m/s. For comparative purposes the hydraulic conductivity derived from a TRUE Block Scale rock volume (based on a parameterisation of the 'September, 1998' model) is $5.0 \cdot 10^{-9}$ m/s.

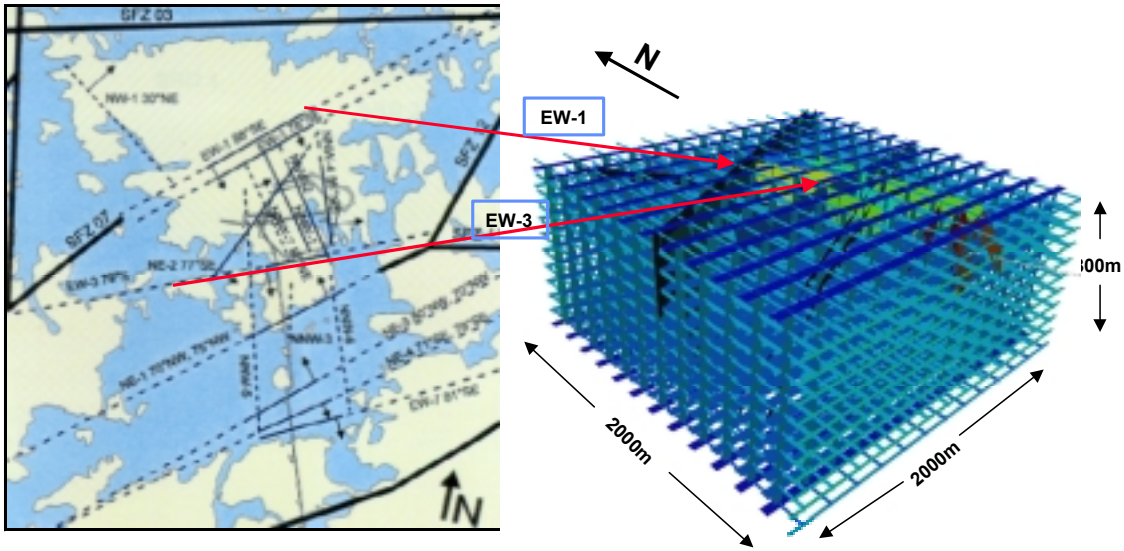

(a) (b)

Figure 7-1. *(a) A schematic plan view of the site-scale structural model of Äspö island; (b) discrete implementation of the site-scale structural model, with both regional structures and background features included.*

7.2.4 Important internal boundaries

In this study the boundary condition applied to the tunnel system is the prescribed flow rates to segments of the tunnel taken from /Rhén et al, 1997/ and /Svensson, 1997/. A schematic plan view of the weirs is shown in Figure 7-2. The flow rates and total chloride concentrations are given in Table 7-1. In the vicinity of the TRUE Block Scale rock volume it is the drainage to the underground openings of the Äspö HRL that is the dominating sink in the system.

In general the values in Table 7-1 should be taken to be indicative, as the measured observed chloride concentrations experience significant fluctuation and are not recorded at the same time. Some values quoted may have the residue of fluctuation following tunnel construction.

Table 7-1. Weir flow rates observed as a result of inflow from the tunnel wall, the actual measurements have significant variability. The weirs occupying the TBM in the lowest part of the HRL have been aggregated into a single flow rate. The measured chloride concentration in mg/l are also given where appropriate.

Weir Name	Approximate observed inflow rates (m^3/s)	Approximate observed inflow rates (l/min)	Salinity [Cl] (mg/l)
MA682G	$1.66\ 10^{-3}$		2801
MA1030G	$9.68\ 10^{-3}$		3366
MA1232G	$3.21\ 10^{-3}$		3152
MA1372G	$7.50\ 10^{-3}$		3613
MA1584G	$1.05\ 10^{-3}$	63	2969
MA1745G	$4.65\ 10^{-4}$	28	
MA1883G	$5.00\ 10^{-4}$	30	5119
MA2028G	$5.83\ 10^{-4}$	35	4545
MA2178G	$8.33\ 10^{-4}$	50	3053
MA2357G	$9.60\ 10^{-5}$	58	4932
MA2496G	$6.60\ 10^{-5}$	4	
MA2699G	$9.30\ 10^{-4}$	56	6330
MA2840G	$3.83\ 10^{-4}$	23	8977
MA2994G	$1.12\ 10^{-3}$	68	
MA3179G	$2.12\ 10^{-3}$	127	
MA3384G MA3411	$1.60\ 10^{-3}$	96	
MA3426G MF0061G			
Shaft	$3.77\ 10^{-3}$	226	

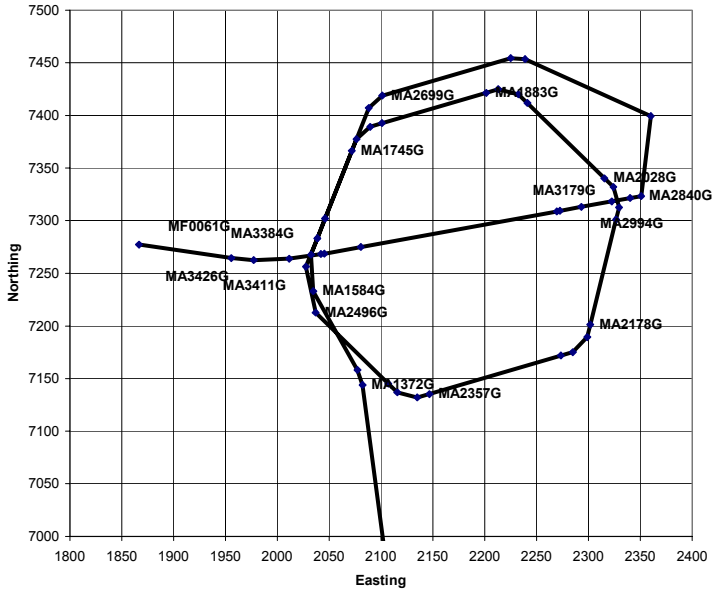

Figure 7-2. *A plan view of the locations of measurement weirs along the tunnel. The number indicates the name of the weir in the section of tunnel where it is situated.*

7.2.5 Results and boundary conditions for the local-scale

Calibration of the site-scale model was performed to match both drawdown and salinity distributions. An illustration of these results is given in Figure 7-3. On a 500 m scale, boundary conditions were taken from this site-scale model. The salinity distribution for a block of 500 m^3 is shown in Figure 7-4.

The importance of providing the boundary conditions at the TRUE Block Scale is that the external boundaries provide the driving force that competes directly with the local abstraction boreholes used in the tracer tests. In this case as the weir flow rates have been applied directly to the site-scale model domain the overall flux through the model will be correct, except when there have been significant changes in drainage patterns.

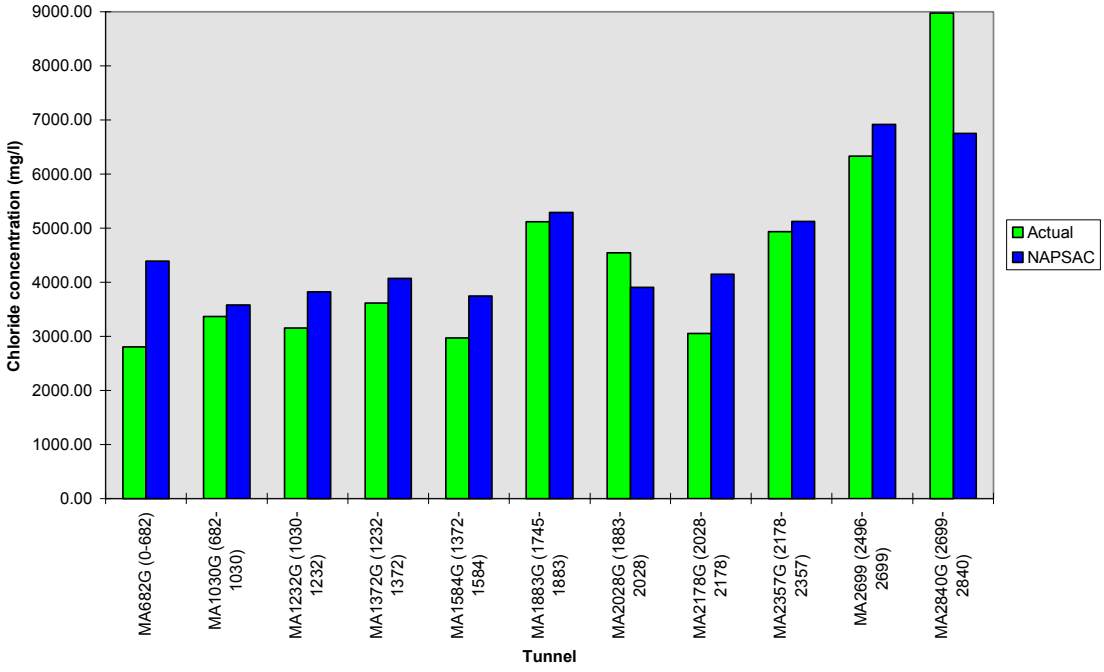

Figure 7-3. *Measured chloride concentration (mg/l) of measured inflows to weirs (green) compared with the simulated NAPSAC results (blue).*

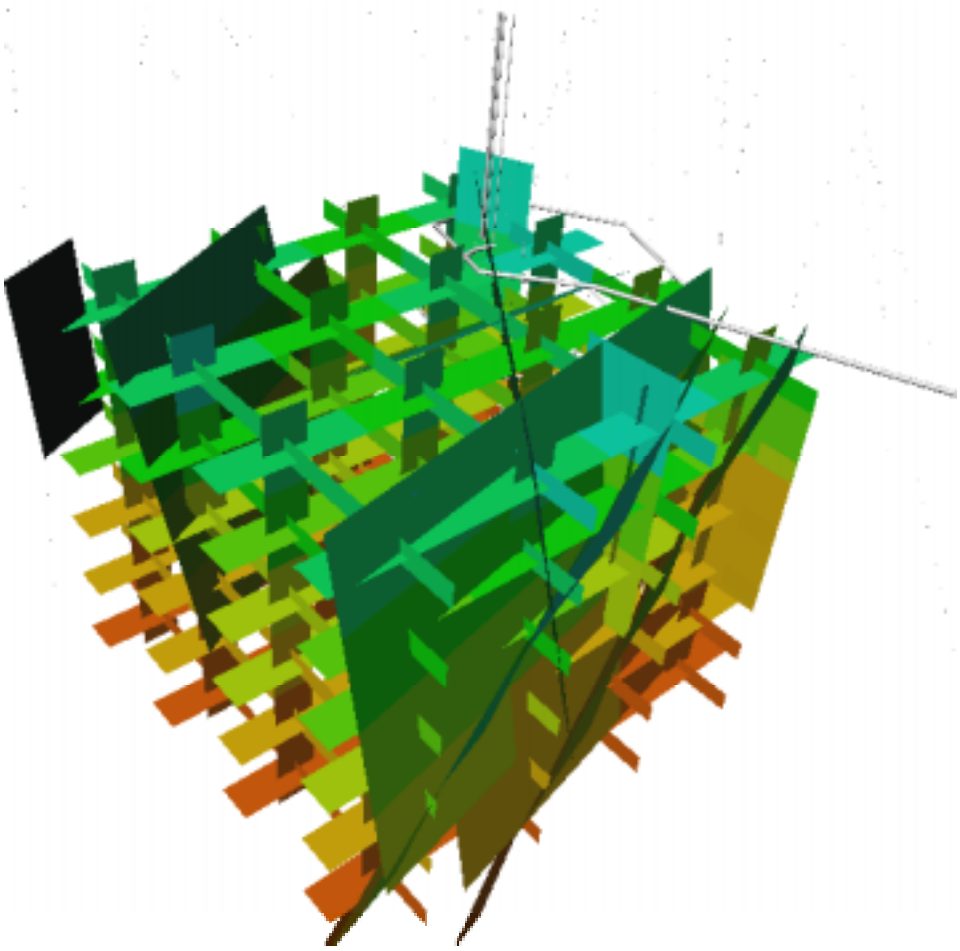

Figure 7-4. *A 500x500x500 m sub-region of the regional scale discrete model, viewed from the south-west, was used to provide boundary conditions for the TRUE Block Scale flow and transport modelling. It shows the spiral of the HRL and the access tunnel, a regular array of fractures used to represent effective rock mass hydraulic conductivity (or more accurately could be described as a representation of the fractures on the sub-scale), as a representation of the regional scale high conductivity fracture zones. To aid with visualisation, the discrete features have been removed from the regional model outside this sub-region to give a clearer impression of the density variation on the local TRUE Block Scale. The colours indicate the distribution of salinity in the block. The density of the groundwater varies from* $\rho = 1003 kg / m^3$ *(less saline) at the top of the sub-region to* $\rho = 1013 kg / m^3$ *(more saline) at the bottom of the sub-region.*

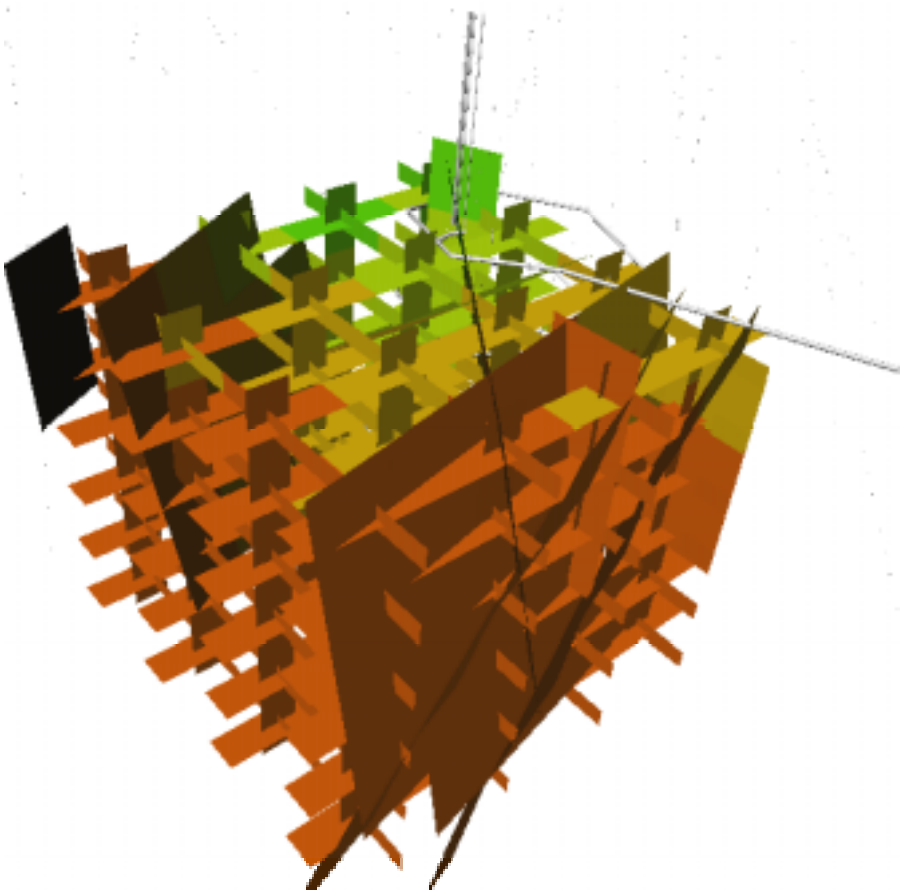

Figure 7-5. *A 500x500x500 m sub-region of the regional scale discrete model, viewed from the south-west, was used to provide boundary conditions for the TRUE Block Scale flow and transport modelling. The figure shows the spiral of the HRL and the access tunnel, a regular array of fractures used to represent effective rock mass hydraulic conductivity (or more accurately could be described as a representation of the fractures on the sub-scale), and a representation of the regional-scale high conductivity fracture zones. To aid with visualisation, the discrete features have been removed from the regional model outside this sub-region to give a clearer impression of the head variation in the local TRUE Block Scale rock volume. The figure clearly shows the effect of drawdown due to the presence of the underground openings. The colours vary linearly according to the magnitude of drawdown, from 60 m drawdown in green to a few metres (1–5 m) shown in red.*

7.3 Importance of salt concentration

The density of the groundwater in the 500 m block model varies between 1003 kg/m^3 and 1013 kg/m^3, which is equivalent to a freshwater head difference of approximately 5 m due to the variability in the salt concentration. At the site-scale the presence of the tunnel can give rise to a drawdown as high as 60 m (measured in the HMS). At the block-scale the drawdown is not expected to be this high, but still significant when compared with the influence due to the presence of the salt. At the scale in which one may want to perform a tracer experiment (say less than 50 m), the density variation is considerably less (< 0.5 m) and as a consequence constant density models would be adequate to describe the flow. The influence of the presence of variable salt concentrations should also be compared to the level of uncertainties in the modelling at this scale.

7.4 Correlation between hydraulic response and tracer breakthrough times

A major difficulty in experiments such as the ones carried out as part of the TRUE Block Scale Project is dimensioning tracer tests so that time scales are:

- Long enough for retention to take place (become a measurable process).
- Short enough for the experiment to be feasible in a time perspective.

Being able to assess transport time scales before performing a full-scale experiment is therefore valuable. This may be possible by assessing the correlation between the early time response to hydraulic pumping tests (which may be obtained in a short time) and tracer breakthrough times. /Herweijer, 1996/ claimed such a correlation for heterogeneous porous media. The author explained this by the fact that pumping test data reveal high conductivity inter-well pathways, which also dominate the solute transport in the aquifer he was considering. In other words, heterogeneity, by forcing solute in relatively well defined pathways, was the cause of the correlation observed. In fractured rock, where the hydraulic properties of the flow path generally are highly variable, this is also likely to be the case.

The existence and relevance of this correlation in fracture networks was investigated using numerical simulation using 3FLO /Itasca, 2002/, focusing on the understanding of the response of the system modelled, in order to check the robustness of the "drawdown-breakthrough time" relationship. The objective was to assess if this concept can be of use to help dimensioning transport experiments. All the simulations /Paris, 2002/ used the TRUE Block Scale hydrostructural model and borehole array as the base case reference.

A constant-head test (50 m drawdown at pumping well) and advective tracer tests in various fracture networks were simulated, changing both network geometry and conductor hydraulic properties. Subsequently the breakthrough time for a 0.5 cm drawdown (1/1000) was compared with the arrival time for 1% of the tracer mass.

The influence of the scale of heterogeneity on the correlation between the pumping test response and the tracer breakthrough times was accessed. The response of six networks, with various fracture densities and fracture mean radii were computed, all other parameters kept constant. For all the networks, the product of the fracture density times the mean square fracture radius was kept constant. This fixes the average number of fractures a borehole would cut (line density, or "fracture area per unit volume of the medium"). Therefore, all the networks used should look identical if probed by boreholes; they conform to the most robust type of data accessible.

Figure 7-6 shows log-log plots of the relationship between the characteristic transport and flow times for four runs, with fracture mean radii varying from 3.2 m to 200 m. The figures show very clearly how the degree of correlation depends on the respective scale of the fractures and the volume of rock tested. In other words, the correlation we are investigating may be of practical interest if the flow paths tested include only a few fractures. In a system with many interconnected small fractures, the pathways between the injection and recovery wells may branch in a lot of different ways, adding some extra tracer dispersion to the transport process, compared to a system with a few large fractures. This means that for a fracture field with a given "linear density" measured in boreholes, looking at the degree of correlation obtained between well test responses and tracer breakthroughs should yield information on the scale of observation of the fracture network. This, in itself, would be quite useful, since fracture size are quite difficult to measure in the field, with size distributions from fracture trace surveys often truncated because of the inadequate size and shape of the available sampling areas (tunnel walls, outcrops).

The effect of varying conductor hydraulic properties was then investigated, using networks with fairly large radii. Figure 7-7 shows a horizontal slice through one of these networks, with a mean radius of 70 m, as well as some of the correlation plots obtained with this network when varying the hydraulic properties. In summary, geometry is by far the most important factor. An attempt was also made to incorporate matrix diffusion in a series of runs and only minor effect was observed. This may be attributed to the fact that early time pressure and early tracer breakthroughs were tracked. This conclusion would certainly be very different if instead, for example, a 50% tracer recovery was monitored.

In terms of a direct field application of the concepts discussed here (i.e. "predicting" tracer breakthrough time scales from well tests), good results can be expected if the distance between the monitoring and the pumping wells is not large compared to the size of the fractures. Besides increasing the test durations, increasing distances between wells may add fracture intersections and complexity into the flow and transport system,

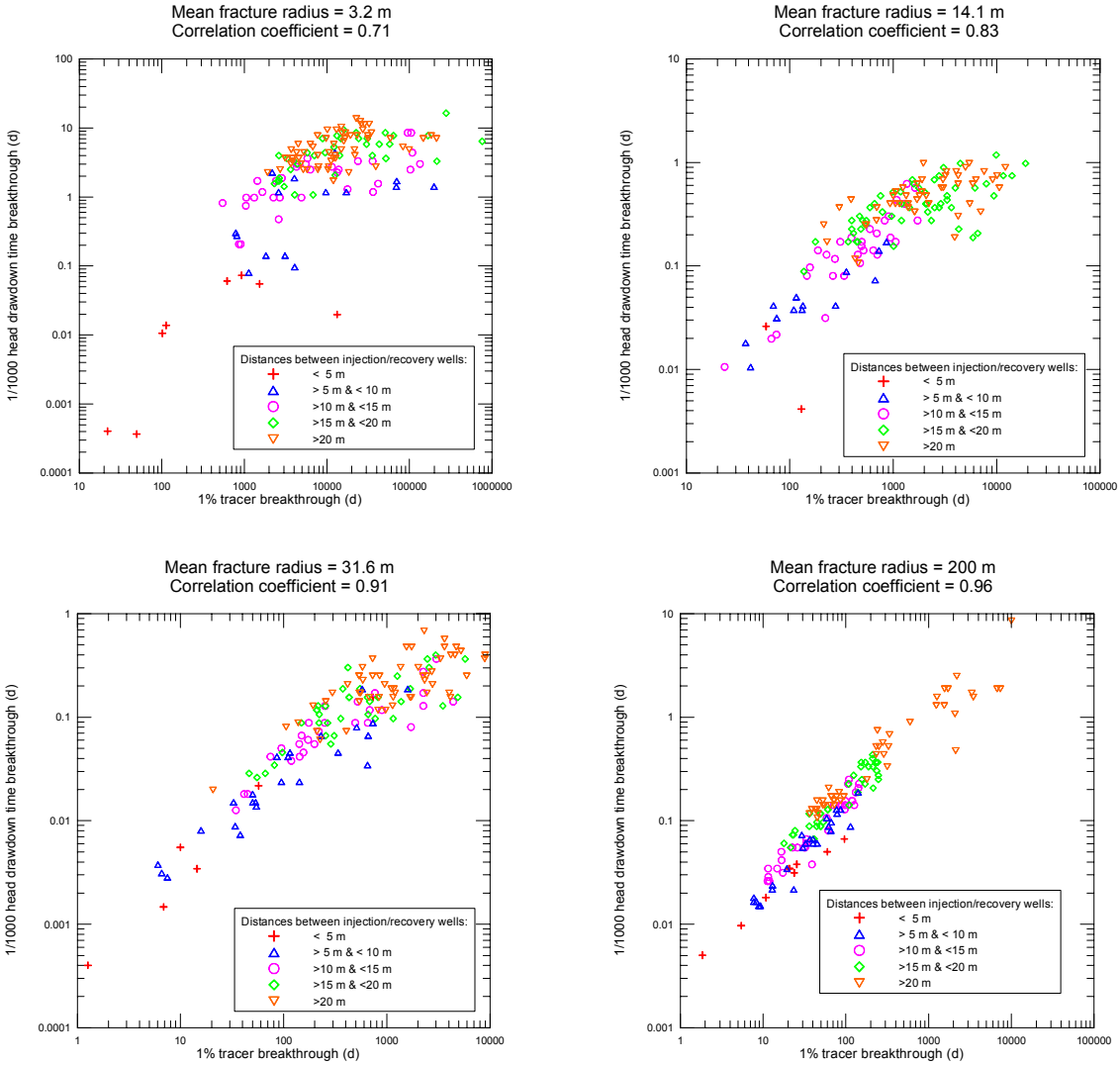

Figure 7-6. *Time for 1% head drawdown versus time for 1‰ tracer breakthrough, for various mean fracture radii.*

and result in poorer correlation. It is hoped that future adequate well test analysis techniques, using for instance a variable flow dimension approach, will allow us to better understand the system geometry. The information gained from well test analysis would be the key for predicting the correlation between tracer and head drawdown breakthrough times and therefore help for designing tracer tests in complex systems.

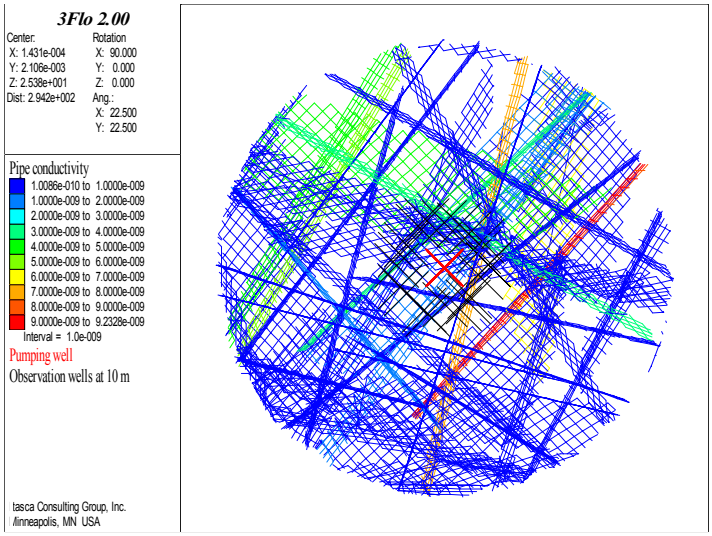

a) 10 m thick horizontal slice through the model

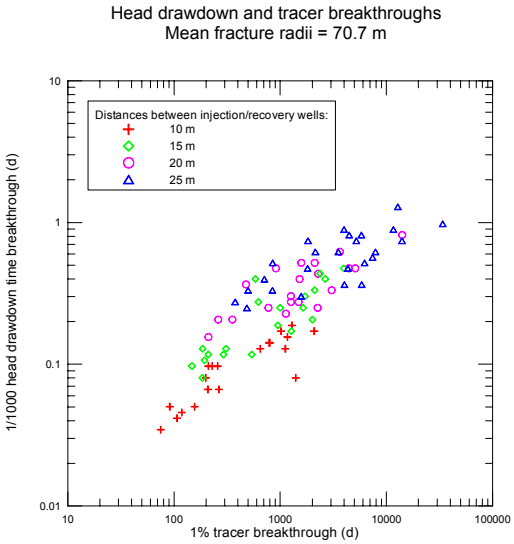

b) constant aperture and conductivity

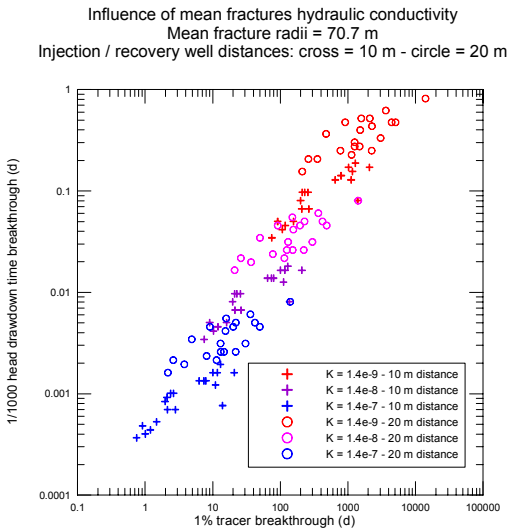

c) constant aperture, variable conductivity

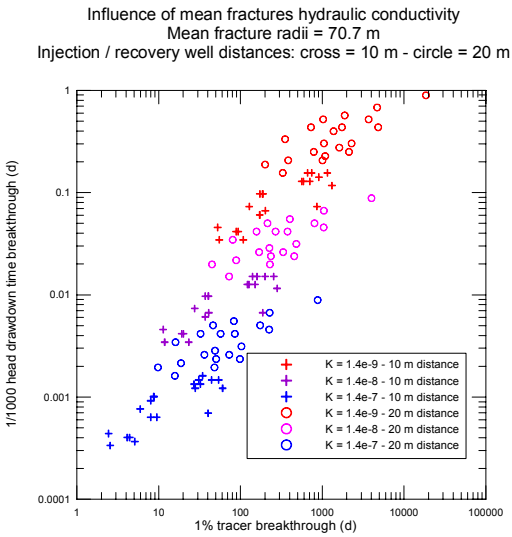

d) variable aperture and conductivity

Figure 7-7. *Effect of conductor hydraulic properties – Time for 1% head drawdown versus time for 1‰ tracer breakthrough.*

7.5 Tracer response dependence on evolution of hydro-structural model

7.5.1 Introduction

The TRUE Block Scale Project has employed an iterative approach to characterisation: one borehole is drilled, characterisation data is obtained from this borehole and integrated into the hydrostructural model of the block, and then the objectives of a new borehole is discussed, along with its geometry. Is it needed? If yes, where should it be drilled?

This approach, together with reprocessing of previously acquired data with new characterisation data from testing in existing boreholes, has resulted in a number of successive updates of the hydrostructural model of the block. This, in order to accommodate incompatibilities between the new incoming data and the "old " model. One may question how much the model upgrades have contributed to enhancing the predictive power of the models with regards to tracer transport. Suppose one had to produce a blind prediction of an experiment to be performed later. What would the prediction have been for this experiment at each stage of model upgrading? How much would this have changed? Finally, how much better would a prediction turn out based on our current knowledge, embodied in the latest model, compared to ones made using prior versions of the model?

In order to tackle these questions, numerical simulations of real experiments using 3FLO /Itasca, 2002/ and employing the successive model updates were performed and interpreted /Rachez and Billaux, 2002/, and then compared with the *in situ* results. These simulation runs use "a priori" information on geometry and material properties as described by the respective model, without attempting calibration. Subsequently, after transport properties had been calibrated to obtain a realistic representation of tests using the latest hydrostructural model, repeated runs using these calibrated properties and the older hydrostructural models were used to evaluate the eventual degradation of the tracer transport simulations in relation to the calibrated results using the most recent model.

Four successive hydrostructural models were analysed. The first model embodied the prior knowledge of the site before onset of TRUE Block Scale (i.e. used for scoping calculations before the Preliminary Characterisation Stage), the second one is the output of the Preliminary Characterisation Stage, the third one is the "March 1999 model", which embodies the outcome of the Detailed Characterisation Stage results, and the fourth model is the "March 2000 model" from the Tracer Test Stage. Figure 7-8 illustrates the similarities and differences between the interpreted structures included in the four models. Note that all models also encompass the background fracturing, taken as known at the time of each model generation.

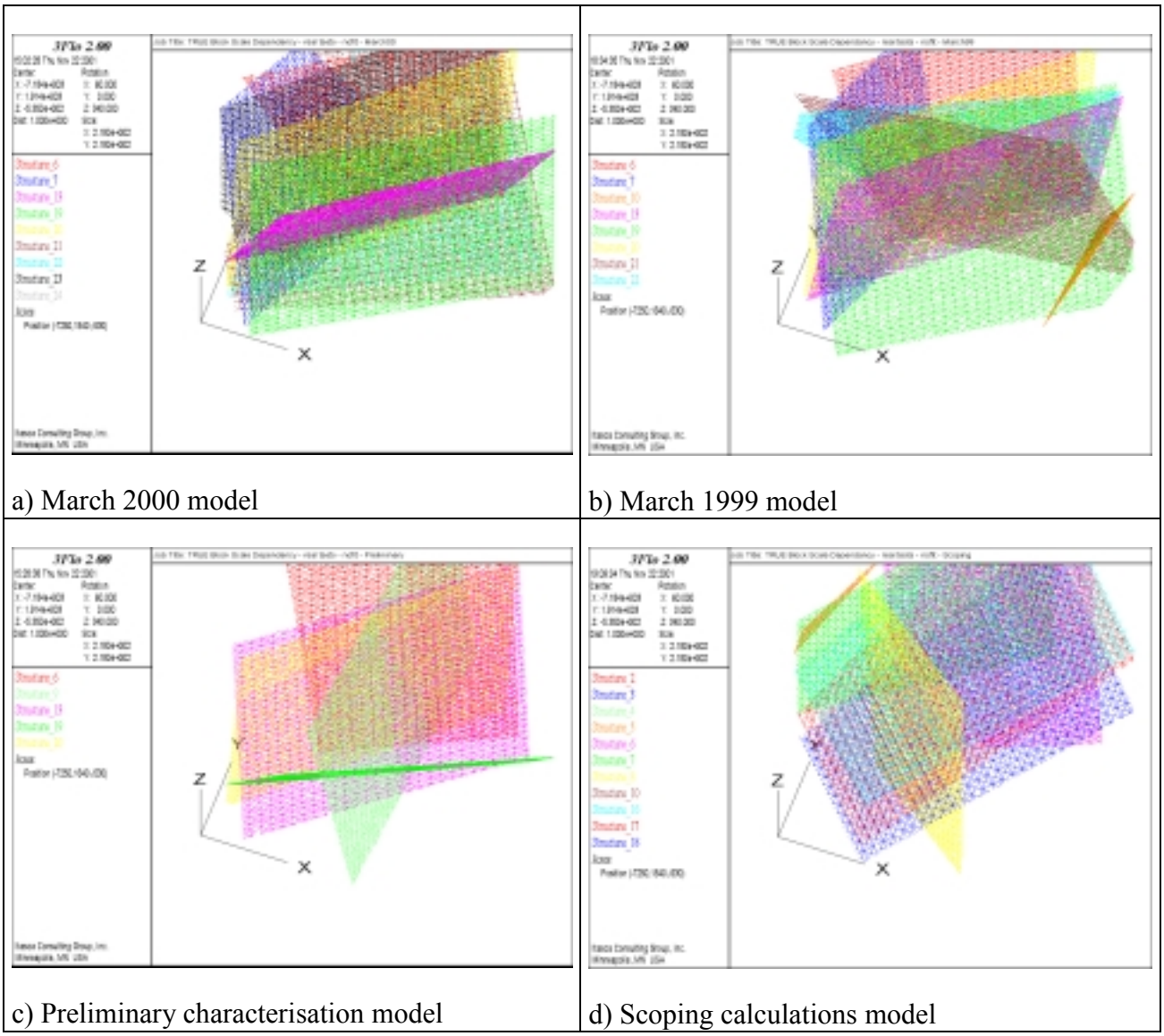

a) March 2000 model

b) March 1999 model

c) Preliminary characterisation model

d) Scoping calculations model

Figure 7-8. *The four structural models considered.*

Three tracer tests, chosen from the Phase B2 tracer tests /Andersson et al, 2000b/, were analysed in each model. One of the tests (B2d) was conducted in a strongly asymmetrical dipole flow geometry, while the other two (tests B2c and B2b) were run in a radially converging geometry. These three tests correspond to the same sink location (KI0023B:P6, located in Structure #21), and to three different injection locations, in KI0025F03:P7 (Structure #23) for test B2d, in KA2563A:S1 (Structure #19) for test B2c, and in KI0025F02:P3 (close to intersection of Structures #13 and 21) for test B2b.

7.5.2 Injection test simulations

Figure 7-9 shows the mass fluxes computed by the forward simulations, without calibration. One can observe that while the response is not significantly modified from the March 2000 to the March 1999 model, it becomes totally different when going back further in time. This is illustrated by Figure 6-5 showing the transport paths along involved structures for test B2c. Note that for legibility, background fractures contributing to the transport path are omitted from the plot. While the geometry is roughly consistent between the two most recent hydrostructural models, the earlier ones produce strikingly different transport paths.

After these forward simulations, the transport parameters (porosity and transmissivity) of the March 2000 structural model were calibrated simultaneously to the three tracer tests, concentrating on reproduction of the first arrival and peak arrival times.

Essentially, the forward simulations produce too fast breakthroughs for tests B2d and especially B2c, and somewhat too slow breakthrough for test B2b. The material properties were modified; Structure #13 (porosity divided by 10, mean transmissivity multiplied by 10 to 10^{-6} m^2/s), #19 (porosity divided by 10) and Structure #23 (transmissivity multiplied by 10 to a mean of 6.10^{-9} m^2/s).

Calibration improves the match of the above defined arrival times (cf Table 7-2). However, when using the new transport parameters together with the former hydro-structural models, very little improvement is seen. For example, when using the March 1999 structural model, the calibrated parameters barely modify results for test B2d. For test B2c, the first arrival and peak arrival times are reduced, but the reduction is less than in the March 2000 model (Figure 7-11). They are still overestimated by a factor of 7 to 10 compared to the measured travel times. For test B2b, the "calibration" modifies slightly the first arrival and peak arrival times with a shift in the wrong direction: particles accelerate, increasing the gap with the measured experimental times.

A comparison of the "calibrated" March 1999 and March 2000 structural models shows that the addition of Structures #23 and #24, and removal of Structure #10, changes considerably the response to the three simulated tracer tests. By comparing the responses of these two models, before and after calibration (Figure 7-9 and Figure 7-11), we can conclude that the change in the parameters resulting from calibration have a small effect compared to the modifications of geometry implemented from one model to the other.

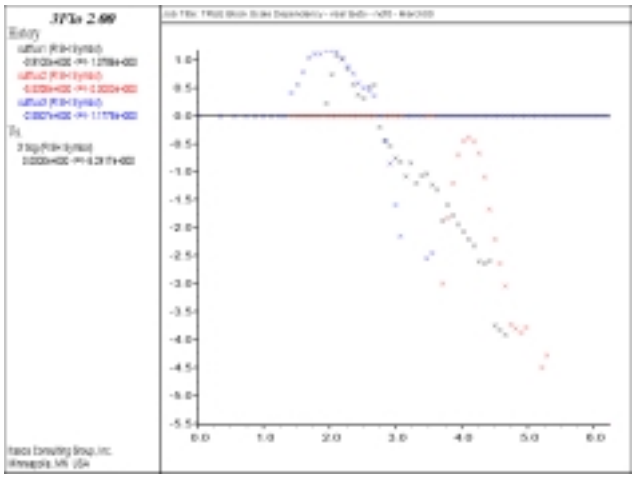

a) March 2000 model

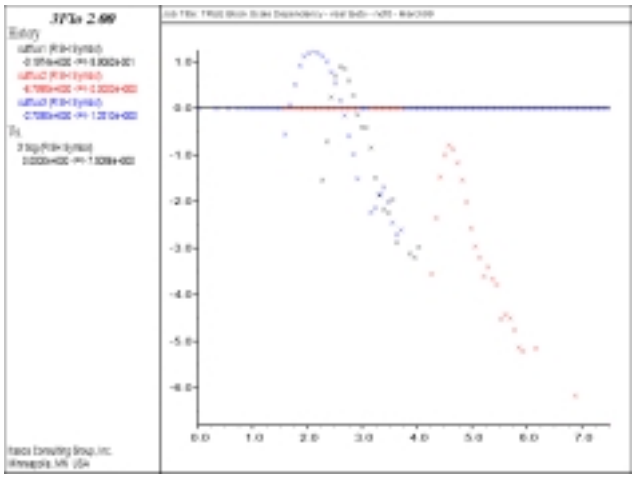

b) March 1999 model

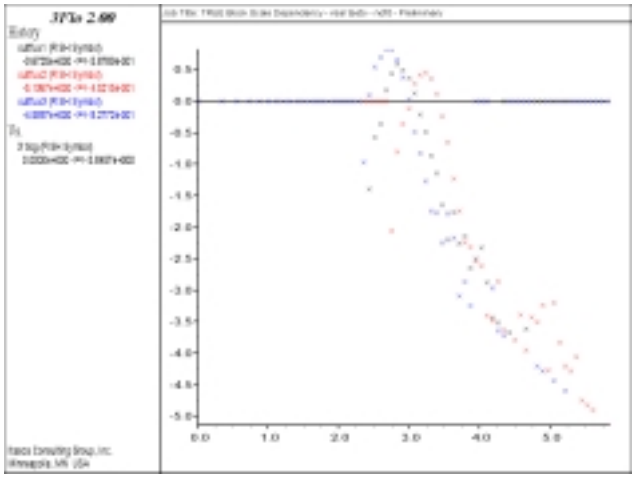

c) Preliminary characterisation model

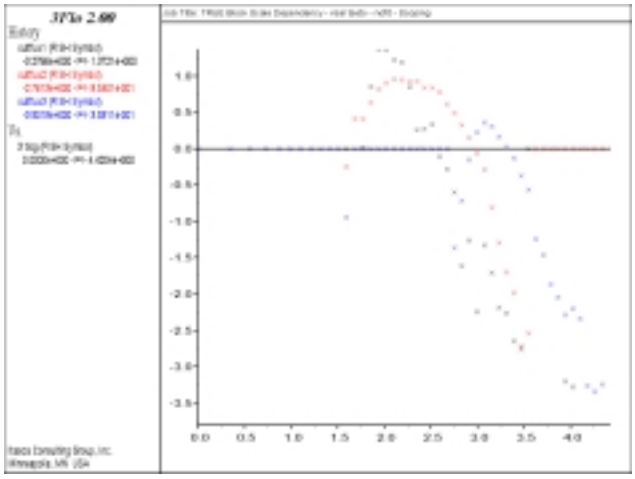

d) Scoping calculations model

Figure 7-9. *Log-log plot of mass fluxes at pumping well (mg/h) vs time (h). Black is Test B2d; red is Test B2c; blue is Test B2b.*

Table 7-2. First arrivals and Peak breakthrough values for real injection tests and for the March 2000 structural model simulations before calibration and after calibration.

Test number	Test Name	First arrivals (time in hours)			Peak breakthrough (time in hours)			Mass flux at peak (mg/h)		
		In situ	*3FLO*		*In situ*	*3FLO*		*In situ*	*3FLO*	
			no fit	fit		no fit	fit		no fit	fit
1	B2d	*30*	100	70	*100*	250	150	*14*	10	10
2	B2c	*300*	6000	600	*1800*	16000	2500	*1*	0.4	1
3	B2b	*40*	25	20	*300*	100	100	*18*	12	8

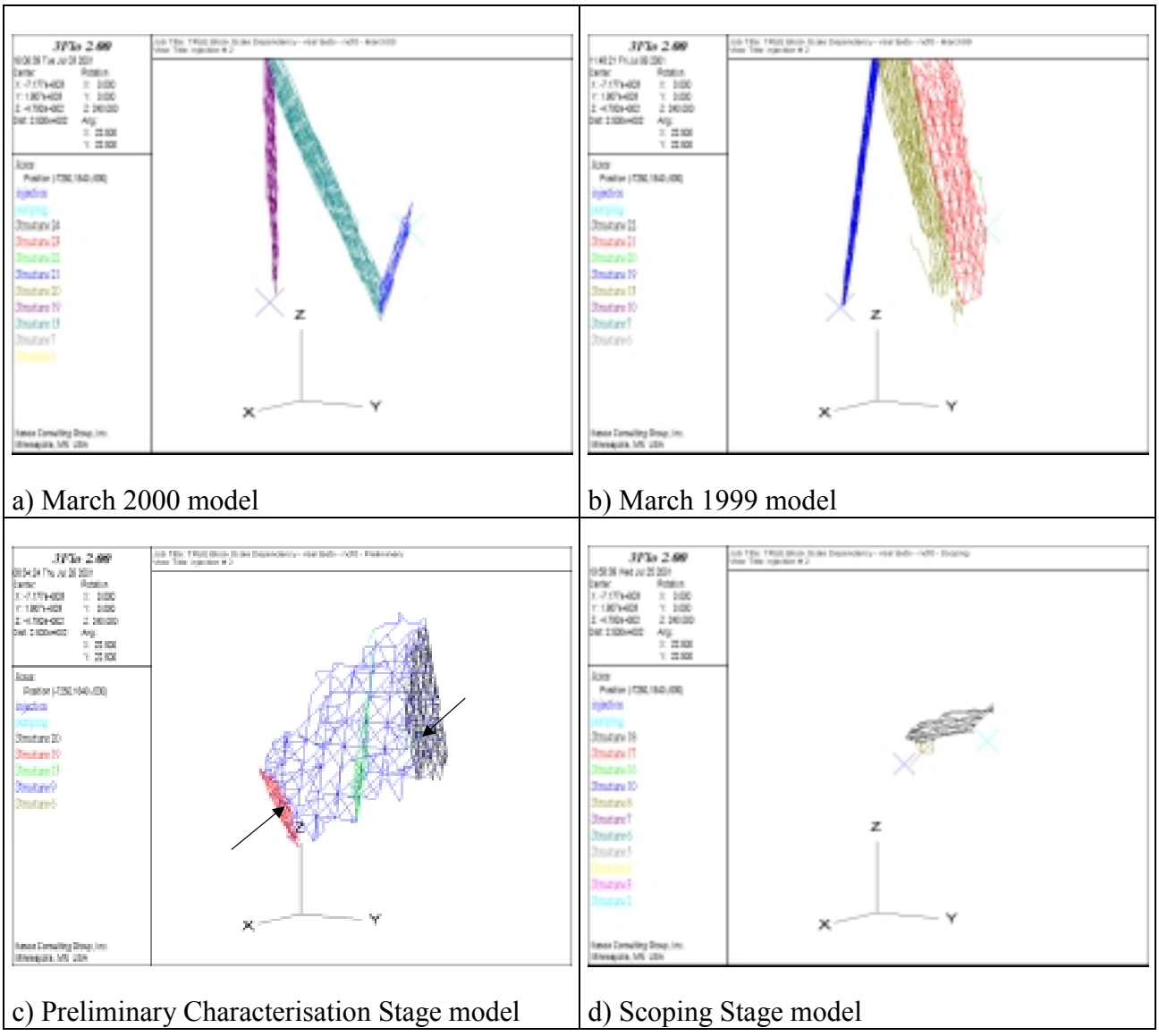

Figure 7-10. *Transport paths through structures, Test B2c, forward simulations.*

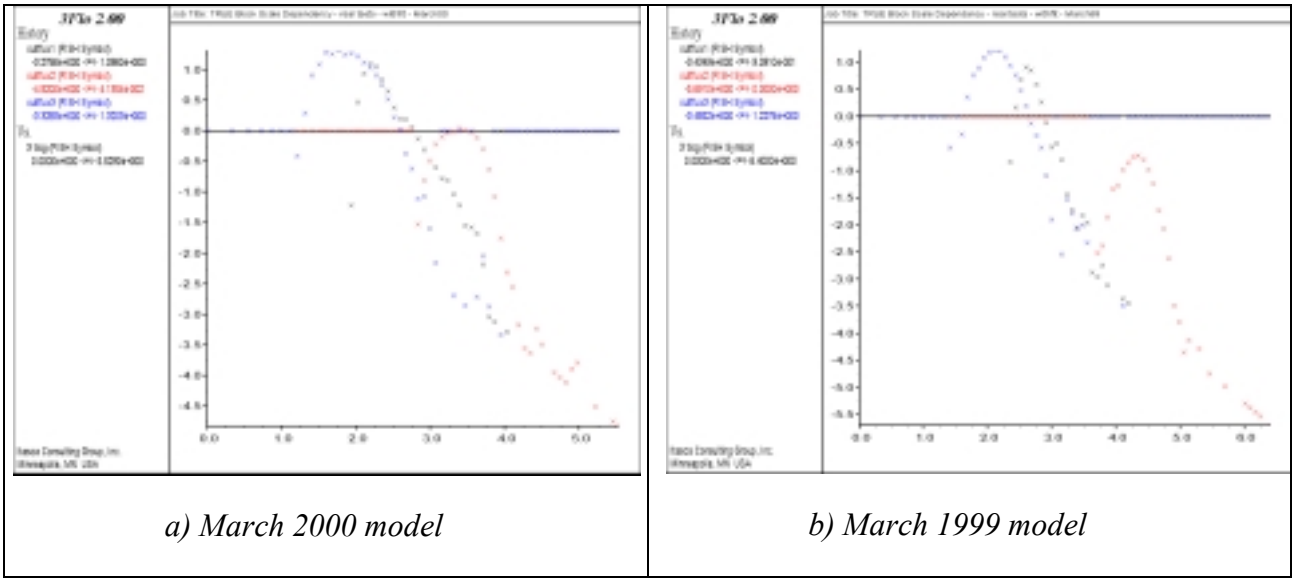

a) March 2000 model | *b) March 1999 model*

Figure 7-11. *Calibrated simulations. log-log plot of mass fluxes at pumping well (mg/h) vs time (h). Black is Test B2d; red is Test B2c; blue is Test B2b.*

7.5.3 Conclusions

Twelve "forward" simulations (three tracer tests per hydrostructural model generation), were made using the properties specified by the hydro-structural models available at each stage (March 2000, March 1999, Preliminary Characterisation, and Scoping), cf /Andersson et al, 2002a/. The injections points, in the earlier models, were selected to represent the real injection points as closely as possible. In these tests, we could see how the variation of the transport path geometry, from model to model, and progressively deteriorated the similarity between the simulated and *in situ* breakthrough curves.

Transport parameters of the March 2000 network were simultaneously calibrated to the three tests, by changing the properties of three structures (#13, #19 and #23). This resulted in a significantly improved, if not perfect, fit between the simulated and measured tracer recoveries. On the other hand, using the calibrated properties from the most recent model in the older models essentially did not improve their response.

Through this work, it was clearly demonstrated how, in the Äspö HRL environment, the prediction of response to tracer tests is strongly conditioned by the hydro-structural model used. Because most of the tracers travel along a limited number of deterministic features, proper knowledge of their geometry is a requisite for being able to represent the network behaviour realistically.

8 Discussion of important findings

8.1 Introduction

The TRUE Block Scale series of experiments capitalises on about 20 years of development in the description and understanding of flow and transport in fractured rock. This development is mainly associated with issues related to storage of nuclear waste in deep geological formations. However, this development has in turn benefited from developments in e.g. the oil industry, where today oil recovery from heterogeneous and fractured reservoirs is common.

The TRUE Block Scale experiments are preceded by experimental work in underground laboratories and test sites world-wide, performed with various objectives, performed in various geological and chemical conditions, and performed at variable scales and variable flow configurations. An account of relevant flow and transport experiments and associated characterisation work is given by /Andersson et al, 2002b and 2002a/, respectively. The past two decades have witnessed a rapid development in computing resources which has facilitated a more realistic approach to flow and transport problems associated with fractured heterogeneous rock formations, and the uncertainty associated with their assessment.

The modelling and analysis work performed within the TRUE Block Scale Project has i.a. benefited from developments made in international fora for exchange of information and experience related to performance assessment (PA) of geological repositories for nuclear waste run under the auspices of e.g. OECD/NEA, cf Section 1.3.

In the TRUE Block Scale Project, a large effort has been made to integrate expertise from various geoscientific disciplines to realise and perform the best possible flow and transport experiments for the given conditions and length scales. Performed flow and transport experiments have for the most part been preceded by model predictions. Three hypotheses, cf Section 1.6, related to the hydrostructural model, effects of heterogeneity and radionuclide retention, respectively, constituted guides for design and performance of the experiments and also for their evaluation. A number of alternate model concepts and approaches were employed in the analysis of the experiments (predictions and post-experiment evaluation). These model concepts include typical site characterisation approaches (stochastic continuum (SC), discrete feature network (DFN) and channel network (DFN/CN) models). Complementary to the latter approaches, two approaches have been employed (LaSAR and Posiva streamtube approach) which are closely related to repository performance assessment. To this list should also be added the advection-dispersion approach used for performing the basic evaluation of each *in situ* tracer test. Despite the apparent differences between the modelling approaches employed, it is demonstrated in Section 6.1 that the transport models employed share one common conceptual transport model. The differences between the approaches lie in

how they account for heterogeneity in transport properties, i.a. in how many immobile zones for retention which are included and how heterogeneity is treated.

In the following sections the main components and contributions of the model analysis of the TRUE Block Scale experiments are reviewed. The various model concepts, with emphasis on description of transport/retention are discussed in Section 8.2. Section 8.3 discusses the outcome of model predictions and the applicability of the models for prediction of transport processes at different spatial and temporal scales. The outcome of modelling of groundwater flow and testing of the hydrostructural model and effects of heterogeneity are discussed in Section 8.4. Section 8.5 covers discussion of modelling of transport followed by Section 8.6 which deals with radionuclide retention, including a discussion of relative importance of processes. The feasibility of models and their applicability to modelling of future *in situ* experiments are discussed in Section 8.7. The concluding sections 8.8 and 8.9, discuss implications for performance of future block scale experiments and implications for PA modelling, respectively.

8.2 Approaches to modelling of transport and retention

The model representations of fractured crystalline rock used in the TRUE Block Scale Project at first glance are seemingly very different, cf Sections 2.3–2.8. This is very much inherent in the way the various components of the fractured rock are represented, which spans from porous blocks to concepts where discrete features are represented either as discrete discs, or as interconnected pipes/channels. However, these differences for the most part affect the way in which the flow problem is parameterised and solved, cf Section 2.1. Despite the obvious difference in how macro elements of the studied domain are included, it is shown that the approach to the transport problem does not differ all that much between the various concepts. This is demonstrated in Section 6.1 where a common conceptual transport model is presented. The difference lies how the various approaches treat heterogeneity in flow and retention properties.

8.2.1 Modelling steps

The characterisation strategy employed in the TRUE Block Scale Project was an iterative one /Andersson et al, 2002a/. This implied that each borehole was drilled on the basis of an updated hydrostructural model with the objective of improving the hydrostructural model and facilitating planned tracer tests in the block scale. At the onset of the characterisation a DFN model was utilised to integrate the hydrostructural model at a given point in time with available experimental results (mainly cross-hole interference tests and ultimately tracer dilution and cross-hole tracer tests). However, it was found that the early immaturity of the hydrostructural model, in combination with the speed at which it developed, made it difficult to keep the more time-consuming development of the DFN model in parallel. The latter mainly attributed to the more

cumbersome effort needed to build the numerical model, run model simulations and draw relevant conclusions in due time to provide guidance to the continued characterisation. Towards the end of the characterisation work modelling on a much broader front was initiated, including the SC and DFN/CN approaches. The Posiva streamtube and LaSAR approaches were introduced as part of the predictions of the Phase C tracer tests, cf Section 8.2.3. The full suite of approaches, five in all, were also used for the evaluation of the Phase C tracer tests.

8.2.2 Conceptual and theoretical frameworks

Not all models include an explicit solution for flow, i.e. the LaSAR and Posiva stream tube approaches, whereas the SC, DFN and DFN/CN approaches include solutions of the diffusivity equation, cf Section 2.1.

All concepts used for transport involving matrix diffusion assume that fractured crystalline rock can be conceptualised as a dual porosity (mobile-immobile) system where water flows through the fractures (advection) driven by induced or natural boundary conditions, and where water is effectively stagnant in the rock matrix adjacent to the fractures. The mobile pore space (fractures and major structures) constitute only a very small fraction of the total pore space. Water in the remaining pore space is regarded as immobile. The TRUE Block Scale tests which have been run in interpreted networks of fractures/structures allow study of network effects on advective transport as well as mass transfer between the mobile and immobile pore spaces.

8.2.3 Implementation

The various models developed as part of the TRUE Block Scale modelling include complex 3D stochastic continuum /Gómez-Hernández et al, 2002/, discrete feature network /Holton, 2002/ and pipe channel network models /Dershowitz and Klise, 2002; Dershowitz et al, 2002a,b/, plus two approaches which are more performance assessment-related; the Posiva streamtube /Poteri, 2002/ approach and the LaSAR concept /Cvetkovic et al, 1999/ extended to the block scale /Cvetkovic and Cheng, 2002/. The three-dimensional models have been used to simulate flow (including responses to various cross-hole hydraulic tests) and transport (prediction and evaluation of parts/components of the tracer test program).

A common form of the transport equations used by the modelling teams involved in the analysis of the TRUE Block Scale experiments is given by Equation (6-1). In their analysis, the teams have used different simplifications of Equation (6-1), different solution techniques as well as different strategies to account for random/deterministic flow and retention heterogeneity.

8.3 Predictions of sorbing tracer tests

8.3.1 Background and scope

Efforts were made during the early stages of characterisation to use the developed DFN model for the prediction of hydraulic pressure responses and natural/induced flow rates in packed off sections. The model was also used to predict the outcome of a set of preliminary tracer tests. The success of these predictions was limited and to a large extent reflected the immaturity of the hydrostructural model.

The components of the Tracer Test Stage which have been subject to model prediction were the Phase A tests /Andersson et al, 2000a/ where the DFN/CN approach was used. The Phase B tests /Andersson et al, 2000b/ were not subject to model predictions, but the results of Phase B were used as a calibration set prior to making predictions of the Phase C tests /Andersson et al, 2001c/, cf Section 3.2.

The predictions of the Phase C tests, cf Chapter 3, were carried out using all five approaches used in the evaluation TRUE Block Scale Phase C tracer tests. Full accounts of processing of the Phase A/Phase B tests and Phase C prediction/evaluation are given by /Gómez-Hernández et al, 2002/, /Holton, 2002/, /Dershowitz et al, 2002a,b/, /Dershowitz and Klise, 2002/, /Poteri, 2002/ and /Cvetkovic and Cheng, 2002/. In the following discussion, the focus is placed on the Phase C predictions, which focus on transport and retention.

8.3.2 Prediction of Phase C tracer tests

The data base of transport parameters for the Phase C predictions was based on the compilation of laboratory data included in /Andersson et al, 2002a/. However, the modelling groups were free to use their own judgement and experience in the selection and usage of the parameter data. This is also reflected in Tables A-1 through A-4 (Appendix A) where the parameter values used, and their origin are presented. One important component to keep in mind when discussing the outcome of the prediction of the sorbing tracer transport is the underlying prediction of the non-reactive (conservative) tracer, which introduces an important constraint on subsequent predictions of the sorbing species in the same flow field/flow path.

8.3.3 Discussion of results

One can argue whether the TRUE Block Scale predictions were truly “blind” or not. Some of the modelling groups (JNC-Golder, Posiva-VTT, SKB-KTH and Nirex-Serco) had prior experience from analysis of the TRUE-1 tests at a length scale of 5 m. Given the general geological and mineralogical kinship between the TRUE-1 Feature A and

Structure #20 (tested by test C1 in flow path 1), the prediction can equally well work as a "validation exercise" relative to the understanding gained in the TRUE-1 analysis. Models, to a variable degree calibrated to data from one site are used to predict the outcome of experiments at a nearby (but geographically different) site, at a similar length scale (factor 3 or more longer). When the same models and parameter settings (NB no groups used different parameter sets for the three different flow paths/tests which were subject to prediction) were used to predict the outcome of a test on a longer spatial scale (C2 and C3) the simulated results compared to the *in situ* results (where breakthrough was noticed) were not as successful. Above all, the differences between the various teams are more profound than for C1. We know that the individual retention processes/parameters form parameter groups, cf Section 8.5.1, and in the case of C1, cf Section 3.2, despite variable magnitude of the different parameters of the groups, similar net results are noted. Given the above, why are the predictions more comparable for C1 (between different models, and relative to the *in situ* results) and more different in the case of C2 and C3?! Why is the retention for Ca (C2) and Na (C3) generally underpredicted by models?! One possible explanation for the different shapes of the C2 breakthrough curves is the disturbances introduced in the injection flow rate for these tracers introduced by a few inadvertent pump stops.

In Chapter 6 efforts were made to elucidate the effects of the underlying non-reactive breakthrough on the overall transport on the basis of the final evaluation models developed by the different teams. From Figure 6-4 a general consistency for C1 is observed for all modelling teams, although with slightly different spreading (dispersion) exerted by the underlying flow description (NB A similar analysis was not performed for the "prediction models"). In the case of the corresponding non-reactive pulse simulations for C3, a much higher variability and difference between the models emerge. The two 1D models (SKB-WRE and Posiva-VTT) show breakthroughs characterised by high and sharp peaks, whereas the models which have an underlying description of flow in three dimensions show a higher dispersion. This finding is even more profound for the corresponding simulation of injection C2.

A picture emerges where the modelling philosophy adopted (including description of flow and micro-structure and associated retention parameters), when applied to prediction of test C1 produces an equitable net effect. The reason for the noted compatibility is for the most part attributed to the prior experience from TRUE-1 paired with geological and mineralogical resemblance between the C1 flow path and that of Feature A (TRUE-1). The same modelling philosophy applied to prediction of the longer flow paths (C2 and C3) is, with some exceptions, not as successful. Possible explanations for this difference could be existing geological/mineralogical differences compared to flow path I (C1). For example, Structure #22 interpreted to be involved in the C2 test is, unlike Structure #20, characterised by mixed-layer clay with a high cation exchange capacity, cf /Andersson et al, 2002a/. Alternatively, the longer flow paths can be more heterogeneous and complex than initially assumed/interpreted. This is exemplified in the case of flow path III (C3), which despite a shorter path length given by the hydrostructural model, 33 m compared to 97 m for C2 shows a two times longer travel time, cf Tables 3-2 and 3-3. Support for a more complex flow path in the case of C3 is also provided by the basic evaluation of the C3 test /Andersson et al, 2002b/ which indicates high dispersivity paired with indications of lower diffusion (compared to flow paths I and II), cf Section 8.4.4. A possible third explanation is that the

modelling philosophies, as defined above, are not able to fully describe transport and retention over the longer distances with the information available.

A more thorough deliberation of the individual modelling philosophies and the relative contributions of the flow field and retention heterogeneity (number of, and description of microstructure of immobile zones) to overall retention is planned for the TRUE Block Scale Continuation Project. The latter also includes further analysis of the continued Phase C breakthrough collected from November 2000 through October 2002.

Despite the noted discrepancies discussed above the following partial conclusions can be drawn;

- Predictions of the breakthroughs resulting from the C1 injection were generally successful over the complete spectrum of used tracers of variable sorption capacity.

- Poorer performance was observed with increased length scale/complexity and sorption capacity of tracer (injections C2 and C3). The observed *in situ* retention is generally underpredicted for those sorbing tracers which show breakthrough within the monitoring time (3300 hrs).

Of interest is to note that the non-existing *in situ* breakthrough (at 3300 hrs) of some of the more strongly sorbing tracers is correctly predicted by some groups, and "nearly" by others (long travel times predicted).

8.4 Conductive geometry and heterogeneity

8.4.1 General

The principal objective with the work related to testing of the hydrostructural model is to assess whether the most recent hydrostructural model, which includes a set of interpreted deterministic conductive structures, is consistent with available results from hydraulic and transport tests/experiments. Is the model of the deterministic structures sufficient to allow planning, performance and evaluation of performed tests? Does the background fracture population have to be invoked in order to explain the observed results? Implicit in the preceding issues/questions is also whether the observed transit times are in accord with the hydrostructural model and the interpreted transport paths (and the structures involved).

Intimately coupled to the validity of the hydrostructural model is the heterogeneity in hydraulic and transport properties which is introduced by the variability in constitution (i.a. genetic aspects) of the structures involved. It should in this context be emphasised that heterogeneity is present also in, and along individual structures at Äspö HRL. This has previously been demonstrated by /Mazurek et al, 1997/ and has also been shown e.g. for the deterministic Structures #20 and #13 /Andersson et al, 2002a/.

An additional characteristic of a fracture network which has been addressed within the limitations present in this project is the possible role of fracture intersection zones (FIZ) for flow and transport. The FIZ constitutes a 1D object which connects two intersecting fractures in a 3D fracture network. Assessment/characterisation of FIZs with boreholes (1D objects) is regarded as essentially futile. The challenge thus lies in assessing the importance of FIZs from indirect data (e.g. crosshole interference and tracer test data) and possibly distinguishing its effect from other 1D (channelised) porosities in the planes of fractures/structures along the transport path.

The testing of the hydrostructural model through modelling and coupled assessment of various aspects of heterogeneity does not provide or represent the ultimate understanding of transport and retention which can be achieved from available data. However, it still warrants interest, as reflected in the two related Hypotheses #1 and #2, cf Section 1.6, in that the outcome of this part of our analysis reflects our ability to build and inform the geometrical lattice of conductive structures which forms the basis for carrying out successful *in situ* tests, and subsequent evaluation through modelling.

Calibration has shown that the three groups analysing flow in three dimensions (Stochastic continuum, Discrete Feature Network and Channel Network) all succeed in producing acceptable fits to the available cross-hole hydraulic interference test data.

8.4.2 *In situ* hydraulic responses and connectivity

The developed hydrostructural model for the TRUE Block Scale rock volume provides ample opportunity for extensive interconnections throughout the investigated rock mass. However, this is inconsistent with the noted *in situ* responses which for the most part reflect compartmentalised hydraulic responses. This in turn indicate a rock volume featured by a poorly connected fracture network.

In situ network responses are primarily seen in the larger Structures #6 and #19 for tests with sinks in the "Structure #20/#21/#13 system", cf Table 4-1 and Figure 1-3, but also in the "#20/#21/#13" system itself. However, although compartmentalised responses dominate, a full suite of different types of responses are evident in the *in situ* data, including flow barrier responses and heterogeneous responses, cf Section 4.2. This variability very much reflects the poor connectivity of the investigated fracture network in combination with acting (and sometimes complex) boundary conditions.

8.4.3 Testing of the hydrostructural model using hydraulic data

Testing of the hydrostructural model using the existing DFN/CN model indicates that differences exist between simulated and experimental drawdown when employing background fractures, cf Section 4.2. Generally, the calculated drawdowns in the DFN/CN model are much smaller than measured in the field. This indicating that the

model is too well-connected to the hydraulic boundaries compared to the *in situ* bedrock. The correspondence is improved when performing simulations without background fractures, and is further improved when strategic changes are made, including changes of transmissivities of Structures #6, #13, #19, #20, #21 and #22. In addition Structures #13 and #21 were disconnected at their geometrical intersection to reduce overconnection /Dershowitz and Klise, 2002/.

The self-calibrating algorithm employed in the SC modelling early on indicated a need to increase the hydraulic conductivity of a northeast subvertical structure and also of included subhorizontal structures. These components of the hydrostructural model were attributed low hydraulic conductivity on the basis of the site characterisation and thus provided an early indication of a need to identify near northsouth trending structures which could account for the hydraulic connection noted in the *in situ* test data. Such structures, Structure #21 and #22, were identified as apart of the Detailed Characterisation Stage. This can effectively be regarded as an elevation of two former members of the background fracture population to numbered deterministic structures. The overall hydraulic significance of subhorizontal structures is considered to be low /Andersson et al, 2002a/.

8.4.4 Testing of the hydrostructural model using conservative tracer data

In the TRUE Block Scale rock volume, there exists high-conductive zones/channels (e.g. Structure #5 in (KA2563A). Due to the poor connectivity and low hydraulic gradient the connectivity from the Tracer Test Volume, cf Figure 1-2, to the underground openings is low, which paved the way for successful performance of well-controlled block scale tracer experiments with associated high mass recovery.

The majority of the measured breakthroughs exhibit single peaks, with significant apparent dispersion. However, networking effects have been identified for some of the tracers test responses in terms of noticeable multiple peaks which are indicative of network effects, although in some cases the appearance of the breakthrough may be caused by the input function. Observed low mass recovery for conservative tracers can be due to networking effects in combination with a boundary condition effect. As a result, it is not possible to conclusively state that intersecting background fractures are unimportant for transport along the investigated pathways. However, in the JNC-Golder simple pipe model, a need was identified to use much more dispersion (longitudinal dispersion α_L) than was required in a corresponding transport model which included background fractures /Dershowitz and Klise, 2002/. This indicates that there are multiple pathways providing the multiple velocities that are mapped along the pathways by performed tracer experiments. These multiple pathways may be interpreted as some combination of pathways due to fracture microstructure and complex fracture pathways (e.g. effects of fault breccia), or alternatively due to background fractures, or a combination of both. However, no conclusive evidence could be provided by the JNC-Golder team on the basis of their comparison of a DFN model with a simple pipe pathway DFN/CN model. It should in this context also be mentioned that a single peak

in the breakthrough curve may imply that there really is only one path, or that multiple pathways form a continuous distribution of velocities, which can be represented in general as a dispersion coefficient.

With regards to the conservative tracer tests performed as part of Phase C, some conclusions can be drawn on the basis of available breakthrough times and evaluated dispersivities from the basic evaluation /Andersson et al, 2002b/ and modelling results presented therein. The modelling approach is tentatively described in Section 2.3. The evaluated dispersivities in this case are 16.4% of the projected Euclidean transport path, cf Table 8-1. In the case of injection C2 the evaluated dispersivity is 24.7% of the projected Euclidean transport path length. The dispersivity value for C3 (L=33 m) is 9.0 which corresponds to 27.3% of the flow path length. As a very rough consistency check for dispersivities, *D/v* should empirically be about 10% of the transport path length. The above compilation suggests that the associated transport paths should/could be somewhat longer, or alternatively slightly more complex. In the case of C2 the evaluated *D/v* suggests that the actual transport path length is somewhere in the interval 17–97 m. If effects of complexity/heterogeneity are discarded the actual transport path length should be some 40–45 m. In the case of C3 the evaluated dispersivity, given that the interpreted flow path constitutes a single structure flow path (in Structure #21), suggests that the flow path is more complex that anticipated. This could be attributed to interaction between Structures #21 and #13 making the flow path longer. To this should be added a possible more complex constitution (sandwiching) of Structure #21 itself.

Table 8-1. Compilation of dispersivities for different interpreted path lengths evaluated using the basic 1D Advection-Dispersion model. Compiled from results presented by /Andersson et al, 2002b/.

Flow path/ injection	**Path distance (m)** ***Euclidean***	**Evaluated dispersivity *D/v* (m)** ***Euclidean***	**Path distance (m)** ***Along interpreted structures***	**Evaluated dispersivity *D/v* (m)** ***Along interpreted structure***
I :C1	14	2.3	16	2.7
II :C2	17	4.2	97	24
III :C3	33	9	33	9

The modelling teams have assessed the validity of the hydrostructural model in terms of arrival time/transport path length compared to the pre-test transport path lengths given on the basis of the hydrostructural model. The JNC-Golder team in their simulations presumed the March 2000 hydrostructural model and therefore the path lengths are consistent with the hydrostructural model. Path lengths do vary somewhat where, for example, the path travels to the nearest FIZ, along a FIZ segment for some time, then into the next fracture towards the pumping well. As a result the "average" length is somewhat longer – the length given by the Euclidean distance is the minimum path length possible. The length given by the connected structures of the hydrostructural model length is longer than the Euclidean, but should not be regarded as a definite distance. Detours and deviations involving background fractures could either add or subtract from the length of the transport path projected by structure geometry.

8.4.5 Assessment of effects of macro-scale heterogeneity

Macroscale heterogeneity is manifested in the hydrostructural model, and in numerical model representations thereof, in terms of existence of background fractures, heterogeneity within structures and fractures (intraplanar) and heterogeneity imposed by intersections between structures/fractures.

It is noted that in the DFN/CN representation of the hydrostructural model the (stochastic) background fractures model play an insignificant role for the specific performed hydraulic and transport experiments. Therefore they could effectively be eliminated since they also provide an over-connectivity to the model which is not seen in the *in situ* data. This despite the size, density and transmissivity distributions of the background fractures as inferred from borehole data and tunnel mapping /Andersson et al, 2002a/. Although the deterministic hydrostructural model accounts for most of the identified hydraulic conductors and hydraulic and connections, it should be pointed out that the hydrostructural model does not include all physical hydraulic connections in the investigated rock volume. These connections unaccounted for include the significant background fractures. The extent to which background fractures are significant depend on the nature of the connection (or the pathway). If the pathway is dominated by radial flow in a deterministic structure, the role of background fractures will not be significant. In the event an experiment is performed between background fractures, or from a background fracture to a deterministic structure, the involved background fractures will become significant.

In the case of the stochastic continuum model, contrary to the DFN/CN model, it was found necessary to include the rock mass (corresponding to background fracture population) with a rock mass hydraulic conductivity to obtain a reasonable inversion using the available hydraulic information, cf Section 4.1. No attempt was made in this study to test calibration of the SC model including only the deterministic structures of the hydrostructural model.

Spatial variability in hydraulic conductivity was introduced in the rock mass and deterministic structure units of the SC model, in both cases with a correlation length of 40 m. The SC model is initially conditioned to hydraulic conductivity. Through the use of a self-calibrating algorithm the heterogeneity in the deterministic structures as well as in the rock mass were modified to match the available steady state and transient head data.

The Nirex-Serco DFN model included a correlation length of 5 m for the transmissivity data in individual structures. Despite the relatively short correlation, multiple transport paths and channeling were observed.

One component of Hypothesis #2 related to heterogeneity was whether evidence of effects of fracture intersection zones (FIZ) could be detected through the analysis of available breakthrough curves. This implying, that this effect also could be differentiated from effects of heterogeneity within individual planar structures.

It is noted that the constitution of FIZs in essence could resemble those of channels developed in fracture planes. This primarily attributed to the fact that FIZs most likely do not exhibit a clear-cut characteristic, but rather can show a combination of those related to a barrier and a structure with enhanced conductivity.

Performed modelling studies indicated that simulated (synthetic) tracer tests cannot distinguish effects of fracture intersection zones on evaluated pathway transport parameters. However, it appears to be possible to distinguish FIZ effects in terms of tracer mass lost to alternative sinks along FIZ-related pathways if being hydraulic contact with the alternative sink /Dershowitz et al, 2002a/. A correlation has indeed been noted between tracer mass loss and flow paths passing fracture intersection zones. However, and not surprisingly, the tests concerned are all representative of longer paths, such that connections to other alternative sinks apart from the pump section are plausible.

8.5 Modelling of transport and retention

It is noted that the same basic (conceptual) model used for modelling transport (and retention) in single structures/fractures (e.g. TRUE-1) also is applicable to networks of structures/fractures. This is evident in the good correspondence between model predictions of the C1 breakthrough, cf Section 8.3.3. This finding is attributed to the integrating nature of the matrix diffusion process along the transport path (possibly in combination with the configuration of the flow field employed during the tests) in combination with similar geological/petrophysical conditions/properties.

8.5.1 Parameter groups

Retention is governed by parameter groups that include the parameters accounting for the flow field, immobile zone diffusion and sorption properties. With the available data it is difficult to fully discriminate between the basic retention processes, and perhaps more which of the available immobile zones that dominate. It is hence difficult to come up with unambiguous values of evaluated *in situ* retention parameters, cf Section 8.6. For example, an interpreted low sorption coefficient may be compensated/balanced by a high diffusivity with a resulting equitable net effect, cf Sections 6.1 and 8.6.

Notwithstanding, the results of the performed evaluation employing various modelling concepts/approaches show that reasonable parameter values can be retained/estimated, although different approaches are used.

8.5.2 Calibration – Data usage, adequacy and relative importance

Calibration related to transport/retention only provides values of parameter groups which relate to flow and retention as shown in Section 6.1. Deliberation of individual retention properties related to diffusion and sorption can possibly be made using independent data and previous knowledge, by which the uncertainty range of transport properties is reduced.

8.5.3 Assessment of role of micro-scale heterogeneity

Effect of micro-scale heterogeneity in porosity was addressed in two ways by the KTH/WRE group; 1) by studying at the effect of the microstructure conceptual model (i.a. trend in porosity in the direction normal to the fracture plane), and 2) by allowing the porosity to vary laterally along the flow path in accordance with a log-normal distribution. /Cvetkovic and Cheng, 2002/ show that the estimated *in situ* slope k, cf Sections 6.1 and 2.7, decreases with increasing porosity variability, whereas the estimated *in situ* K_d for strongly sorbing tracers, like Rb and Cs, increases. Likewise, if a depth-dependent variability (trend) in porosity is neglected, then the estimated *in situ* K_d for Rb and Cs become too large with increasing lateral variability in porosity along the flow path. With regards to lateral heterogeneity, the available data are derived from relatively minute core sections /Byegård et al, 1998, 2001/. The variability along the entire flow path may thus be even higher than projected /Cvetkovic and Cheng, 2002/.

Heterogeneity in immobile zone properties may have an important influence on interpretation of the results. The most important heterogeneity is that experienced normal to a fracture surface (effect on kinetics, effective properties (porosity and diffusivity)) and may also furnish partial explanation to the observed difference between retention observed in the laboratory and that observed *in situ*.

8.5.4 Assessment of effects of test configuration

It should be pointed out that despite the statement made in Section 8.6.1 that no additional transport processes are required to interpret the performed tests, it cannot be ruled out that the configuration of the tracer tests to a variable extent biases this conclusion. Embedded in the existing borehole instrumentation and the strong unequal dipole character of the flow field, are a resulting small source area and a slight overpressure injection which entails 1D flow paths. This has generally produced single peak breakthrough curves. Notwithstanding, it is considered that the employed test procedure probably is the only feasible one since it provides a basis (necessary control) for understanding the flow field during a given test.

8.6 Retention in the block scale

8.6.1 General on processes, retention and scaling

No additional transport phenomena (processes) were added/required when taking the step from modelling of detailed scale (TRUE-1, L=5 m) to modelling block scale (TRUE Block Scale, L= +50 m) transport phenomena and retention. In this context it was observed that the explicit new block scale heterogeneity component, the fracture intersection zone (FIZ), was not found to be crucial, neither for explaining the hydraulic responses, nor for explaining the transport results, cf Section 8.4.5.

The parameter groups for retention (and where applicable, also individual retention parameter values) obtained from the calibration of the block scale tests with radioactive sorbing tracers were for the most part found to be in the same order of magnitude as those found for the analysis of the corresponding TRUE-1 tests. In fact, the C1 results (L=15 m) could be predicted fairly well by combining the conservative tracer test results obtained in earlier phases of the TRUE Block Scale tracer tests and the retention properties deduced from the TRUE-1 experiments /Byegård et al, 1998, 2001/ and compilations of characteristics related to fault breccia and fault gouge materials /Andersson et al, 2002a/, cf Section 3.2.

8.6.2 Comparison of block scale and detailed scale retention

Comparison of retention can be done in various ways and taking various aspects of retention into account. A basic measure, which only reflects the material properties that govern diffusion and sorption, is the parameter group κ as defined and discussed in Sections 6.1 and 6.3.3, respectively. An alternative measure, which also accounts for the hydrodynamic control, is the retention time T as defined in Section 6.3.3. The latter measure is dependent on the flow path length/residence time and the injection flow rate. A "scaled retention time" T_s, with flow path length and injection flow rate filtered out, provides a measure of an average characteristic retention along a given flow path. Yet an alternative measure is the "diffusion time" t_d (defined e.g. by Equation (9-27) in /Cvetkovic and Cheng, 2002/) which is independent of the path length/residence time and similarly to T_s also accounts for the hydrodynamic control[3]. /Andersson et al, 2002b/ introduced a measure of retention (or rather a measure of "apparent retardation") as part of the basic evaluation of the tracer tests. This measure, defined as $R_{50\%}$= time at which 50% of the sorbing tracer has been recovered divided by the time at which 50% of the non-sorbing tracer has been recovered effectively accounts for "advective travel time"+ "retention time" normalised by the "advective travel time".

[3] The A parameter [$T^{1/2}$] in Section 2.3 is related to κ, K_a (surface sorption coefficient) and k (from $\beta=k\ \tau$) as $A=1/(k\cdot\kappa) + K_a/\kappa$. The A parameter can also be related to diffusion time t_d as $A=(t_d)^{1/2}+ K_a/\kappa$). Thus, the A parameter contains information on the hydrodynamic control and both sorption-diffusion and surface sorption. In this sense it differs from the parameters T, T_s and t_d which do not account for surface sorption.

Looking at the retention in terms of the κ parameter group employed in the evaluation of the TRUE Block Scale Phase C tests, cf Figure 6-12, it is seen that retention for the non-sorbing conservative tracers used in the C1, C2 and C3 injections is similar. It is also noted that the κ used in the evaluation of Na (C1 and C3) and Ca (C1 and C2) are similar. A comparison with κ values used in the evaluation of the TRUE-1 STT-1 and TRUE Block Scale C1 tests used by the Posiva-VTT /Poteri, pers comm/ and the SKB-WRE /Cvetkovic, pers comm/ teams shows similar values and hence similar retention in terms of the material properties group.

No rigorous comparison of retention in terms of T_s or t_d (both including effects of the hydrodynamic control) has been carried out between TRUE-1 and TRUE Block Scale as part of the TRUE Block Scale Project. However, tentative analysis indicates similar *in situ* retention when comparing the TRUE-1 and TRUE Block Scale flow paths e.g. when strongly sorbing Cs is considered /Cvetkovic and Cheng, 2002/. These findings are also supported by independent analysis /Poteri, pers comm/.

The above indication of similar retention on the two length scales is based on a comparison between the Phase C tests performed using three block scale source receiver pairs, of variable length and variable interpreted complexity, with results based on two source-receiver pairs in the detailed scale (TRUE-1). The finding is therefore indicative for crystalline rock similar to that found at the Äspö HRL. The result is potentially significant for performance assessment, as it implies spatial scaling effects in the "near zone" (corresponding to the distance from the repository to the nearest major (local) fracture zone) of a deep geological repository may not be important. It should however be pointed out that the temporal scaling, taking the step from experimental to performance assessment time scales, may have a strong impact on the result for a given microstructural model and its parameterisation. The above indications will be subject to continued analysis in subsequent phases of the TRUE project.

8.6.3 Visualisation of relative retention and importance of processes

This section attempts to integrate the information on parameters related to retention used by the different modelling teams as presented and discussed in Sections 6.2 through 6.4. The objective is to illustrate the relative contributions to retention from the various processes/parameter groups included in the evaluation of the Phase C tracer tests. These are the material parameter group κ (Section 6.3), the hydraulic control parameter β (Section 6.3), surface sorption (Section 6.4) and advection-dispersion (Section 6.2), cf Figure 8-1. In producing the illustration a simple weighting scheme was employed which indicates the relative importance put on a given process in a given model approach. It should be emphasised that the weights have been given subjectively by looking at the different processes included in the individual models. No direct and objective calculation method was employed to assess the relative importance of the processes. Nevertheless, the presented figure by and large indicates the relative importance of the different retention and transport processes included in the final models used to evaluate the TRUE Block Scale Phase C experiments. The different approaches are ordered vertically in descending order in terms of the overall retention.

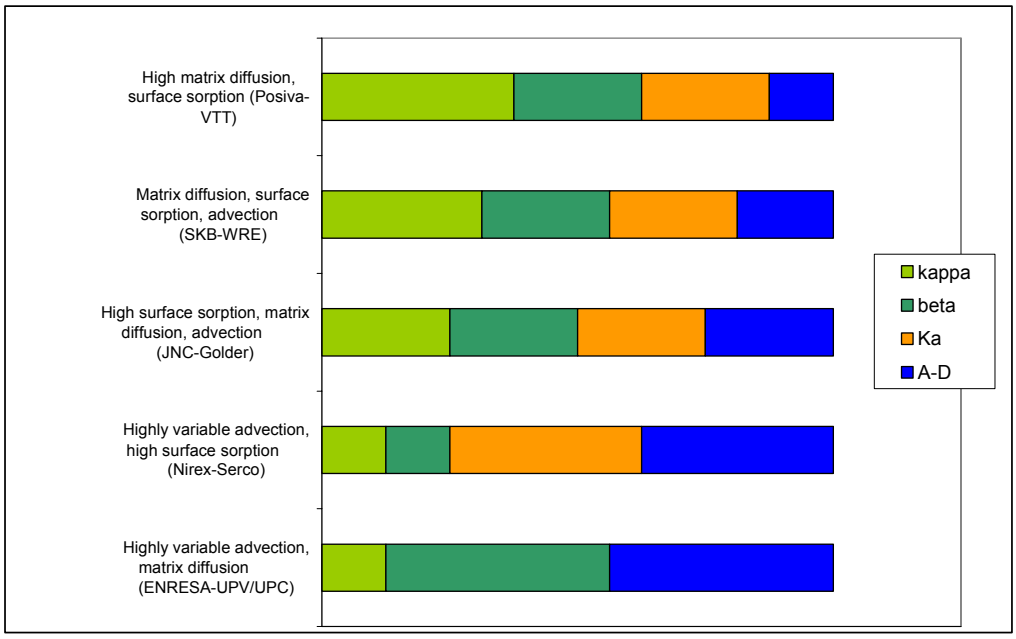

Figure 8-1. *Visualisation of subjective ranking of relative importance of retention and transport processes in models used to evaluate the TRUE Block Scale Phase C tracer tests.*

For the most part the noted differences in mapped contribution to retention between models are explained by the differences in the modelling of the advective field. Continuum models (ENRESA, Nirex) give more variable advective transport than one-dimensional models (Posiva, SKB). The channel network model (JNC) is located somewhere in-between these two groupings. Hydrodynamic control of the retention (β) is largest in the continuum model (ENRESA) where the flow may be divided between several fractures. The hydrodynamic control in the case of one-dimensional models (Posiva and SKB) and channel network model (JNC) is equitable. The diffusional coupling of the retention is adjusted by also adjusting the material properties group (κ).

8.6.4 Summary on block scale retention

The following partial conclusions regarding block scale retention can be drawn from analysis of the TRUE Block Scale tracer experiments;

- It is necessary to include diffusional mass transfer to explain the observed *in situ* retention.

- It is not possible to fully discriminate the relative importance of conceptualised immobile zones with available data.

- The heterogeneity in immobile zone properties may have an important influence on interpretation of the results (cf Section 8.5).

- There is no need to include additional phenomena/processes in the interpretation of the TRUE Block Scale tracer tests (in networks of fractures/structures) in order to explain the observed *in situ* retention.

- The observed *in situ* retention of the TRUE Block Scale flow paths is similar to that observed in the flow paths investigated as part of the detailed scale TRUE-1 experiments.

8.7 Revue of the TRUE Block Scale modelling

A revue has been made of the TRUE Block Scale modelling work in relation to the outcome of the international model inter-comparisons conducted during the past two decades with in the framework of the OECD/NEA INTRACOIN, HYDROCOIN, INTRAVAL and GEOTRAP studies. In particular in relation to some of the demands/requests raised in the most recent GEOTRAP study and associated workshops. The following accomplishments have been identified associated with the modelling of the TRUE Block Scale tracer experiments in relation to stated GEOTRAP conclusions and demands;

1) Structural variability (heterogeneity) in flow models

TRUE Block Scale offers three numerical groundwater flow models (SC, DFN, DFN/CN) which all can provide realistic, although different, representations of the structural variability (heterogeneity) of the studied rock volume. GEOTRAP II /OECD/NEA, 1998/ identifies the availability of data as the most important constraint on usage of heterogeneity.

Comment:

In TRUE Block Scale, i.a. the lack of hydraulic conductivity/transmissivity data, particularly from identified deterministic structures, makes it difficult to infer relevant statistics and description of spatial correlation. For the SC modelling a correlation length of 40 m was assigned based on expert judgement /Gómez-Hernández et al, 2002/. Likewise, in the case of the DFN analysis /Holton, 2002/ a correlation length of 5 m was employed.

2) Usage of different model approaches

GEOTRAP II /OECD/NEA, 1998/ considered use of different model approaches as an important premise in order to deal with conceptual model uncertainty.

Comment:

In TRUE Block Scale, a wide range of approaches and codes have been considered which, to a variable degree, are consistent with available information from site characterisation and model-testing exercises.

3) Model “blind” predictions

GEOTRAP II /OECD/NEA, 1998/ identified blind predictions as an important premise for narrowing the range of conceptual model uncertainty. It was also identified that calibration and testing of models should be performed at a range of scales.

Comment:

TRUE Block Scale included model predictions made in advance of tracer experiments and selected measurements made as part of the site characterisation work. The TRUE Block Scale experiments cover a range of interpreted distances between 14–97 m and comprise a balanced blend of interpreted single structure and multistructure fracture network pathways. The predictions cannot be considered fully “blind” given the prior TRUE-1 experience.

4) Usage of effective parameters

GEOTRAP II /OECD/NEA, 1998/ identified that simplified models employing effective parameters are likely to remain important, especially for the purpose of modelling transport problems. It was also emphasised that quantification and use of effective parameters require careful justification.

Comment:

The TRUE Block Scale effort has resulted in progress regarding understanding as well as in quantifying “effective” parameters (one may refer to these as “equivalent” parameters, for reasons explained by /Cvetkovic and Cheng, 2002/). Further, the entire TRUE effort so far has indicated that usage of retention data from the intact unaltered rock (close to what was e.g. used in SR 97 /SKB, 1999/) is conservative. This while the altered rim zone and fault gouge introduces an extra safety “margin” which has not been accounted for in previous safety studies. This is of course applicable for sites such as Äspö where most fractures are altered and assumed partially infilled with fault gouge. It may not necessarily be applicable to all sites/geological environments.

5) Process discrimination

GEOTRAP II /OECD/NEA, 1998/ identified that progress was being made to unravel the associations between the different (variable) properties which influence radionuclide migration over a range of scales.

Comment:

The TRUE Block Scale experiments offers a wide range of flow paths, tracers of variable sorption capacity, variable flow rates and supporting hydrochemical and laboratory data which principally allow the possibility to make distinctions between the relative strength of retention processes. Notwithstanding the above premises, it is identified in Chapter 6 that different processes/retention parameters come into play in parameter groups where e.g. matrix diffusion is balanced by matrix sorption, cf Sections 6.1 and 6.5. Furthermore, variable contribution and overlap of the immobile zones available is assumed to occur along the pathways. Given that the transport pathways

only are known at a few intercepts, a major uncertainty is associated with the actual distribution of immobile zones along the transport pathways, and hence also in the relative contribution of processes.

8.8 Model feasibility and implications for modelling of future experiments

Despite the apparent complexity of the TRUE Block Scale deterministic hydrostructural model, it has been identified that is possible to successfully model the conducted experiments (particularly the Phase C1–C3 tests) using single channel flow path models (Posiva-VTT, JNC-Golder and SKB-WRE). It should however in this context be acknowledged that the TRUE Block Scale experiments were biased towards creation of channelised single flow paths through the employment of essentially radially converging flow fields. This drive was very much dictated by the search for source-sink combinations featured by high mass recovery (> 80%) and necessary radiation protection measures in relation to other activities in the Äspö tunnels.

The model concepts are shown to provide consistent matches to available data,
- using variable complexity,
- with variable usage of the available databases.

This finding is not new or surprising. The same (unfortunate) finding came out of the INTRAVAL (Geoval 94) and TRUE-1 studies as part of the Äspö Task Force work on the TRUE-1 experiments /Elert and Svensson, 2001/. This is attributed partly to the integrating nature of the mass transfer process. One goal of the planned TRUE Block Scale Continuation (BS2) is to bring assessment and comparison of effects of conceptual models and approach-specific assumptions further, hopefully allowing an improved assessment of the relative importance of retention processes and available immobile pore spaces.

8.9 Implications for performance of future block scale experiments

What are the requests from the modellers with regards to performance of future tracer tests in order to improve understanding of transport/retention (in general, and specifically for the block scale):

Type of flow geometry for tracer tests

Despite the limited sampling of fracture surfaces which results from unequal dipole flow fields, this flow geometry is still preferred since this configuration provides the best ability to control and characterise the advective flow field.

Variable flow rates

Ideally tests with sorbing tracers should be performed with variable flow rates to improve the possibility to identify retention processes. This demand is most often in conflict with practical constraints and other priorities. However, inherent heterogeneity in the immobile zone/-s may result in changes in evaluated retention parameter values if the boundary condition (pumping flow rate) is changed.

Shape and duration of injection pulse

It is well known that the tailing of a tracer input pulse makes interpretation of the tail of tracer breakthrough curve difficult. In TRUE Block Scale attempts have been made to make the tracer pulses as short and square-shaped as possible. In cases where tracer dilution indicated low induced flow due to pumping during a preceding tracer dilution test, a slight overpressure was applied in conjunction with the tracer injection.

Site characterisation data

Given that the hydraulic characterisation of the investigated rock volume has been targeted on the major conductive structures, only limited hydraulic conductivity and transmissivity data are available for the rock mass. This means that data to infer representative and site-specific univariate statistics and spatial correlation of the rock mass are scarce. For the SC approach this means that the utilised spatial correlation is assigned on empirical basis with a correlation scale of 40 m, in the rock mass and in the modelled deterministic structures. For the DFN/SC approaches however, ample data are available from flow logging, borehole imaging/core logging and tunnel mapping to determine the fracture statistics of the background fracture population.

Data from the laboratory

Sorption data are not available for fine-grained fault gouge and fault breccia materials. In addition pore diffusivity data are missing for fine-grained fault gouge as well as for fault breccia pieces/fragments. In the case of fault gouge it is identified that a useful estimation of diffusivity and porosity only can be obtained by *in situ* experimentation under (at least near) natural ambient rock stress conditions. The estimation of diffusivity is considered a more difficult challenge than that of porosity. It is foreseen that an acrylic or epoxy resin injection in a fault gouge-filled structure in a near-tunnel situation and subsequent overcoring and analysis can be one way of getting reasonable estimates of the *in situ* porosity of the fault gouge.

8.10 Implications for performance assessment modelling

Difference between retention in the detailed and block scales

Tentative evaluation of retention seen in the detailed scale TRUE-1 and TRUE Block Scale experiments indicate similar retention in terms of the material property group, κ, and alternative measures also accounting for the hydrodynamic control, cf Section 8.6.2. It is also noted that the breakthrough from the C1 injection, performed on a similar length scale, was generally well predicted by the modelling teams. In the case of TRUE Block Scale, similar values of the material property group κ was used for the flow paths tested by the C1, C2 and C3 injections. The finding of similar retention is independently supported by the similarities in geology/mineralogy/geochemistry and hydrogeochemistry observed at the two sites. In addition, also the constitutions of the conductive structures participating in the respective tests show a high degree of kinship. It is noted that firm confirmation of the existence of fault breccia (pieces/fragments) and fine-grained fault gouge is presently unavailable from the TRUE-1 site, /Winberg et al, 2000/.

The indication of similar retention in the detailed scale (< 10 m) compared to the block scale (< 100 m) at Äspö (TRUE-1/TRUE Block Scale) (TRUE Block Scale tests with sorbing tracer effectively cover the length scale < 50 m) constitutes a point statistic. This indication could potentially be highly useful if it can be generalised, in that it suggests that there is no need for any elaborate spatial scaling of parameters governing *in situ* retention parameters when taking the step from the detailed to the block scale. For both scales, however, there exists a need to firmly link laboratory derived retention parameters with the retention seen *in situ*. There also exists a need to improve the description of heterogeneity in retention parameters of the immobile zones in the vicinity of flow paths. This includes variability in porosity in the (altered) matrix rock and in the fault breccia (pieces/fragments/faulty gouge), see below. It should however be pointed in this context that in the case of taking large steps in time, i.e. from experimental (1–2 years) to PA time scale (10^4–10^5 years), the corresponding temporal scaling effects are not as simple to assess. It is anticipated that the choice of microstructural model and its associated parameterisation may have a strong impact on long-term performance. This is presently addressed as part of the analysis of Task 6 of the Äspö Task Force.

Heterogeneity (macro- and micro scale)

The analysis of macro heterogeneity within the context of the available experimental data from TRUE Block Scale rock volume show no significant effects on retention which can be attributed to the effect of fracture intersection zones. This attributed to inability to distinguish any measurable FIZ effect from that exerted by channelisation developed by in-plane heterogeneity in transmissivity in combination with applied boundary conditions. Effects are however noted indirectly in terms of reduced mass recovery correlated to flow paths that involve multiple fractures and interpreted FIZs

connected to hydraulic boundaries. However, the noted effects are for the most part associated with longer flow paths and longer transport times. This finding implies that the tracer mass loss may be related to secondary sinks (underground excavations or points with low pressure in the Äspö HRL borehole array) which may entail diversion of the injected tracer mass. In relation to PA the observations made are positive in that characterisation of fracture intersection zones are not called for.

The TRUE programme has emphasised the importance of the minute rim zone of altered fracture wall rock on retention over experimental time scales. This zone is featured by an increased porosity which is reduced gradually away from the fracture. Lateral heterogeneity in the retention properties of the immobile zones influences the interpretation of the average retention by different geological structures. When assessing effective parameters it is important to appreciate the heterogeneity of the immobile pore space normal to the fracture, e.g. the observed decreasing trend in porosity from the fracture surface towards the virgin rock matrix. This heterogeneity may partly explain the differences between the observed *in situ* retention and the material properties obtained from laboratory measurements on the relevant geological materials. The properties of the immobile zones adjacent to the fractures (including the altered rim zone and fault gouge) have not been taken into account in previous safety analyses (e.g. SR 97 /SKB, 1999/). The rim zone and available fault gouge infilling contributes an additional retention margin, although with limited capacity.

Modelling tools

TRUE Block Scale has involved model analysis (prediction and evaluation) of the performed tracer tests using five different model approaches (SC, DFN, DFN/CN, LaSAR and Posiva streamtube approach), cf Chapter 2. Additional supporting modelling is provided by the 1D AD basic evaluation modelling /Andersson et al, 2001c, 2002b/ and the 3D DFN/CN model 3FLO /Paris, 2002; Rachez and Billaux, 2002/.

It is demonstrated that the five approaches used for modelling transport and retention can be reduced to one common conceptual transport model as presented in Section 6.1. This is an important finding in that it dedramatises the apparent difference between the models which lies more in how the macro heterogeneity and conductive structures are included; porous blocks (SC), discrete fractures (DFN) and conductive pipes (DFN/CN). The difference between the approaches is in how the small-scale retention heterogeneity is included, if it is included at all. In part the difference lies in how many immobile zones which are included in the analysis.

It is noted that overall the modelling approaches have been provided with the necessary input data. The following exception is identified (apart from the important data needs identified above):

Hydraulic conductivity data for the rock mass in the TRUE Block Scale rock volume is scarce. This means that it is difficult to assess univariate statistics and spatial correlation (e.g. in terms of a variogram) for application in stochastic continuum and therefore expert judgement has to be employed. The scarcity in data is due to the fact that the

characterisation has been focused primarily on interpreted deterministic conductive structures. Also the number of hydraulic conductivity/transmissivity data per interpreted deterministic structure is limited. This implies that assessment of spatial variability of transmissivity of individual structures is associated with uncertainty.

It should be noted that all modelling teams implicitly make use of a correlation length. In the case a finite correlation length is not selected, the correlation is implicitly set as infinite. It can be argued that the wealth of data from the TRUE Block Scale rock volume suggests widespread heterogeneity. Thus it could be argued that a finite correlation length is better posed than an implicit infinite assumption.

9 Summary conclusions

In the following the major conclusions regarding radionuclide retention drawn from the performed modelling analysis of the TRUE Block Scale tracer tests are presented in condensed form:

Sufficiency of hydrostructural model (Hypothesis #1, Objectives #1/#2)

- It is concluded that the hydrostructural model developed of the TRUE Block Scale rock volume has provided a satisfactory geometrical basis for the evaluation of the TRUE Block Scale tracer tests.

- The DFN/CN model analysis indicates that it is not necessary to invoke the background fracture population along the modelled transport paths to explain the hydraulic or transport results. In contrast, the SC model used explicit representation of the rock mass to provide the necessary description.

- Access to a well-developed hydrostructural model is considered vital for providing a geometrical basis for modelling the performed tracer experiments. This is i.a. demonstrated by the supporting DFN/CN transport modelling (Section 7.4) where the most recent hydrostructural model is shown to perform better than previous (older) versions of the hydrostructural model, based on a smaller number of boreholes.

Immobile zones and their characteristics (Hypothesis #2, Objectives #1/#2)

- Geological evidence indicates that other immobile pore spaces than (altered) rock matrix are likely to exist along the studied flow paths (fault gouge/fault breccia and stagnant zones).

- Porosity is considered high in the outer fracture rim zone, and decreases away from the fracture surface to attain its background value (representative of unaltered intact rock) a few millimetres to a few centimetres away.

- Heterogeneity in immobile zone properties may have important influence on the interpretation of the *in situ* test results. Possibly most important is heterogeneity normal to the fracture surface (effect on kinetics, effective properties, and may provide partial explanation of differences between laboratory and *in situ* retention (parameters).

Relative importance of processes (Hypothesis #3, Objectives #1/#2)

- The observed retention of radioactive sorbing tracers cannot be explained by equilibrium sorption alone.

- All modelling groups assign matrix diffusion as an important (and dominant) retention mechanism. The inclusion of matrix diffusion is also supported by characteristic $t^{-3/2}$ slopes in the breakthrough curves for most of the tracer tests run over sufficient time scales for the tailing to develop. Soft data support for matrix diffusion is provided by the impregnation studies which indicate increased porosity in the altered fracture rim zones as well as in the fault breccia (cm-sized pieces and mm-sized fragments). Evidence of existence of fine grained fault gouge in the investigated structures exists. Its relative abundance and distribution is unknown, as is its *in situ* porosity and diffusivity.

- Retention is governed by parameter groups (flow field, immobile zone diffusion properties and sorption). It is difficult to fully discriminate between the basic retention processes, and hence it is difficult to come up with unambiguous *in situ* values on retention parameters. For example, low sorption coefficients may be compensated with high diffusivities. Still, the modelling results show that reasonable parameter values are retained/estimated using different assumptions/hypotheses.

Retention in the detailed and block scales (Hypothesis #3, Objectives #1/#2)

- It is demonstrated that the various transport approaches share the same conceptual basis for transport. The ability to demonstrate this kinship is important for dedramatising differences between the modelling approaches. The actual differences between the transport approaches lie mainly in how many immobile zones that are included in the analysis, and the way heterogeneity in retention parameters is accounted for.

- No new phenomena/processes are required in the block scale (network of fractures/ structures) in order to explain the measured breakthrough curves. The same basic model used for single structures is also applicable to the studied network of structures (attributed to the integrating nature of matrix diffusion process). It should be pointed out that it cannot be ruled out that the configuration of the tracer tests biases this conclusion (small source area, slight overpressure injection – > 1D flow paths, single peak breakthrough curves). Still, the employed test procedure probably is the only feasible one (provision of necessary control to facilitate understanding of the flow field).

- The results from the tracer tests with (radioactive) sorbing tracers performed at the TRUE Block Scale and TRUE-1 sites at the Äspö HRL indicate similar *in situ* retention for the flow paths tested as part of (TRUE-1, 5 m) and Block Scale (15–100 m). The implications of this finding suggests that transport modelling over block scale distances (equivalent to the safety distance between the repository and the closest major fracture zone) may not be overly complicated by needs for spatial scaling of properties governing retention. It should however be pointed out that temporal scaling resulting from taking the step from experimental to performance assessment time frames may be more complicated and dependent on the processes and immobile zone configuration employed, and their parameterisation.

Correlation between hydraulic and transport parameters (Objective #3)

A semi-generic model study using the DFN/CN model 3FLO shows that a reasonable correlation between time of early drawdown in observation a well (0.1% of drawdown in pump well) is near linearly correlated with the time of first arrival (1% relative mass), if the distance between the two wells is not large compared to the average size of the fractures which make up the pathway.

10 References

Andersson J, Elert M, Hermanson J, Moreno L, Gylling B, Selroos J O, 1998. Derivation and treatment of the flow wetted surface and other geosphere parameters in the transport models FARF31 and COMP23 for use in safety assessment. Swedish Nuclear Fuel and Waste Management Company. SKB Report R-98-60.

Andersson P, 2000. Personal communication.

Andersson P, Ludvigsson J-E, Wass E, Homqvist M, 2000a. Interference tests, dilution tests and tracer tests, Phase A, Swedish Nuclear Fuel and Waste Management Company, International Progress Report IPR-00-28.

Andersson P, Wass E, Holmqvist M, Fierz T, 2000b. Tracer tests, Phase B. Swedish Nuclear Fuel and Waste Management Company, Äspö Hard Rock Laboratory, International Progress Report IPR-00-29.

Andersson P, Ludvigsson J-E, Wass E, 2001a. Preliminary Characterisation Stage – Combined interference tests and tracer tests – Performance and preliminary evaluation. Swedish Nuclear Fuel and Waste Management Company, Äspö Hard Rock Laboratory, International Progress Report IPR-01-44.

Andersson P, Ludvigsson J-E, Wass E, Holmqvist M, 2001b. Detailed Characterisation Stage – Interference tests and tracer tests PT-1 – PT-4. Swedish Nuclear Fuel and Waste Management Company, Äspö Hard Rock Laboratory, International Progress Report IPR-01-52.

Andersson P, Byegård J, Holmqvist M, Skålberg M, Wass E, Widestrand H, 2001c. Tracer Test Stage – Tracer test, Phase C. Swedish Nuclear Fuel and Waste Management Company, Äspö Hard Rock Laboratory, International Progress Report IPR-01-33.

Andersson P, Byegård J, Dershowitz W, Doe T, Hermanson J, Meier P, Tullborg E-L, Winberg A, 2002a. TRUE Block Scale Project. Final report. 1. Characterisation and model development. Swedish Nuclear Fuel and Waste Management Company. SKB Technical Report TR-02-13.

Andersson P, Byegård J, Winberg A, 2002b. TRUE Block Scale Project Final Report 2. – Tracer tests in the block scale. Swedish Nuclear Fuel and Waste Management Company (SKB), Technical Report TR-02-14, in prep.

Archie G E, 1942. The electrical resistivity log as an aid in determining some reservoir characteristics. J. Pet. Technol., 5:1-8.

Bear, 1972. Dynamics of fluids in porous media. American Elsevier, New York.

Byegård J, Johansson H, Skålberg M, Tullborg E-L, 1998. The interaction of sorbing and non-sorbing tracers with Äspö rock types. Sorption and diffusion experiments in the laboratory scale. SKB Technical Report TR-98-18. ISSN 0284-3757.

Byegård J, Widestrand H, Skålberg M, Tullborg E-L, Siitari-Kauppi M, 2001. Complementary investigation of diffusivity, porosity and sorptivity of Feature A-site specific geological material. Äspö Hard Rock Laboratory International Cooperation Report ICR-01-04.

Carslaw H S, Jaeger J C, 1959. Conduction of heat in solids, second edition. Oxford: Clarendon press.

Cvetkovic V. Personal communication.

Cvetkovic V, Cheng H, Selroos J O, 1999. Transport of reactive tracers in rock fractures, J. Fluid Mech., 378, 335–356.

Cvetkovic V, Cheng H, Selroos J O, 2000. Evaluation of tracer retention understanding experiments (first stage) at Äspö, Swedish Nuclear Fuel and Waste Management Company. Äspö Hard Rock Laboratory. International Cooperation Report ICR-00-01.

Cvetkovic V, Cheng H, 2002. Evaluation of block scale tracer retention understanding experiments at Äspö HRL. Swedish Nuclear Fuel and Waste Management Company. Äspö Hard Rock Laboratory. International Progress Report IPR-02-33.

Dagan G, 1989. Flow and Transport in Porous Formations, 465 p, Springer-Verlag Heidelberg Berlin New York, 1989.

Dershowitz W, Foxford T, Sudicky E, Shuttle D A, Eiben Th, 1998. PAWorks: Pathways analysis for discrete fracture networks with LTG solute transport. User Documentation, Version 1.5. Golder Associates, 1998.

Dershowitz W, Lee G, Geier J, Foxford T, Ahlstrom E, 1999. FracMan Interactive Discrete Feature Data Analysis, Geometric Modeling, and Exploration Simulation. User Documentation, Version 2.6. Golder Associates Inc.

Dershowitz W, Cladouhos T, Uchida M, 2001. Äspö Task Force, Task 4E and 4F – Tracer tests with sorbing tracers. Swedish Nuclear Fuel and Waste Management Company. Äspö Hard Rock Laboratory. International Cooperation Report ICR-01-02.

Dershowitz B, Klise K, 2002. Evaluation of fracture network transport pathways and processes using the Channel Network approach. Swedish Nuclear Fuel and Waste Management Company. Äspö Hard Rock Laboratory. International Progress Report IPR-02-34.

Dershowitz W, Klise K, Fox A, 2002a. Evaluation of Phase A and Phase B tracer tests using a channel network model with fracture intersection zones. Swedish Nuclear Fuel and Waste Management Company. Äspö Hard Rock Laboratory. International Progress Report IPR-02-28.

Dershowitz W, Klise K, Fox A, Takeuchi S, Uchida M, 2002b. Channel Network and discrete fracture network analysis of hydraulic interference and transport experiments and prediction of Phase C experiments. Swedish Nuclear Fuel and Waste Management Company. Äspö Hard Rock Laboratory. International Progress Report IPR-02-29.

Doe T, 2001. TRUE Block Scale Project – Reconciliation of the March'99 structural model and hydraulic data. Swedish Nuclear Fuel and Waste Management Company, Äspö hard Rock Laboratory, International Progress Report IPR-01-53.

Domenico P, Schwartz F, 1998. Physical and Chemical Hydrogeology. Second Edition. J. Wiley and Sons, NY.

Elert M, 1999. Evaluation of modelling of the TRUE-1 radially converging tests with conservative tracers, The Äspö Task Force on Modelling of Groundwater Flow and Transport of Solutes., Tasks 4C and 4D. Swedish Nuclear Fuel and Waste Management Company (SKB), Technical Report TR-99-04.

Elert M, Svensson H, 2001. Evaluation of modelling of the TRUE-1 radially converging tests with conservative tracers, The Äspö Task Force on Modelling of Groundwater Flow and Transport of Solutes., Tasks 4E and 4F. Swedish Nuclear Fuel and Waste Management Company (SKB), Technical Report TR-01-12.

EPA, 1999a. United States Environmental Protection Agency. Understanding variation in partition coefficient, Kd, values, Volume I. EPA 402-R-99-004A.

EPA, 1999b. United States Environmental Protection Agency. Understanding variation in Partition coefficient, Kd, values, Volume II. EPA 402-R-99-004B.

Fox A, Dershowitz W, 2002. Channel Network Model – Predictions for Phase A tracer tests. Swedish Nuclear Fuel and Waste Management Company. Äspö Hard Rock Laboratory. International Progress Report IPR-02-27.

Gelhar, Axnes, 1983. Three-dimensional stochastic analysis of macrodispersion in aquifers. Water Resour. Res. 19 (1), 161–180.

Gelhar L W, 1986. Stochastic subsurface hydrology from theory to applications. Water Res. Res. (22), pp 135S–145S.

Gómez-Hernández J-J, Sahuquill A, Capilla J E, 1997. Stochastic simulation of transmissivity fields conditioned to both transmissivity and piezometric data, 1. Theory. Journal of Hydrology (203)162–174.

Gómez-Hernández J-J, Franssen H-J, Medina Sierra A, Carrera Ramirez J, 2002. Stochastic continuum modelling of flow and transport. Swedish Nuclear Fuel and Waste Management Company. Äspö Hard Rock Laboratory. International Progress Report IPR-02-31.

Gustafsson E, Klockars C-E, 1981. Studies of groundwater transport in fractured crystalline rock under controlled conditions using non-radioactive tracers. KBS Technical Report TR-81-07.

Gustafson G, Ström A, 1995. The Äspö Task Force on modelling of groundwater flow and transport of solutes. Evaluation report on Task no 1, the LPT2 large scale field experiments. Swedish Nuclear Fuel and Waste Management Company. Äspö Hard Rock Laboratory. International Cooperation Report ICR-95-05.

Hartley L, 1998. NAPSAC (release 4.1) Technical Summary Document, AEA Technology Report AEA-D&R-0271.

Hellmuth K-H, Siitari-Kauppi M, Klobes P, Meyer K, Goebbels J, 1999. Imaging and Analyzing Rock porosity by Autoradiography and Hg-Porosimetry/X-ray Computertomography-Applications, Phys. Chem.

Hendricks-Franssen H-J, Gomez-Hernandez J-J, Medina A, Amaranta M, 2002. Phase A predications. Swedish Nuclear Fuel and Waste Management Company. Äspö Hard Rock Laboratory. International Progress Report IPR-02-31.

Hermanson J, Doe T, 2000. March'00 structural and hydraulic model based on borehole data from KI0025F03. Swedish Nuclear Fuel and Waste Management Company (SKB), Äspö Hard Rock Laboratory, International Progress Report IPR-00-34.

Hermanson J, Follin S, Wei L, 2001. Structural analysis of fracture traces in boreholes KA2563A and KA3510 and in the TBM tunnel. Swedish Nuclear Fuel and Waste Management Company, Aspo Hard Rock Laboratory, International Progress Report IPR-01-70. SKB, Stockholm.

Hermanson J, Nilsson P, Stenberg L, Follin S, Nyberg G, Winberg A, 2002. TRUE Block Scale – Updating of the structural-hydraulic model and compilation of scoping data set. Swedish Nuclear Fuel and Waste Management Company, Äspö Hard Rock Laboratory, International Progress Report IPR-02-13.

Herweijer J C, 1996. Constraining uncertainty of groundwater flow and transport models using pumping tests, in Calibration and Reliability in Groundwater Modeling, IAHS Publ., 237, 473–482.

Hoch A R, 1998. Implementation of a Rock-Matrix Diffusion Model in the Discrete Fracture Network Code NAPSAC. United Kingdom Nirex Limited Science Report S/98/005.

Holton D, 2001. Boundary conditions for sub-models at the Äspö TRUE Block site. Äspö Hard Rock Laboratory International Progress Report IPR-01-50.

Holton D, 2002. Evaluation of the Phase C tracer tests using the discrete fracture network approach. Swedish Nuclear Fuel and Waste Management Company. Äspö Hard Rock Laboratory. International Progress Report IPR-02-30.

Itasca, 2002. User's Manual 3FLO Version 2.0

Jakob A, Mazurek M, Heer W, 2002. Solute transport in crystalline rocks at Äspö – II: Blind predictions, inverse modelling and lessons learnt from test STT1, J. of Cont. Hydrology (61), pp 175–190.

Kelokaski M, Oila E, Siitari-Kauppi M, 2001. Investigation of porosity and microfracturing in granitic rock using the 14C-PMMA technique on samples from the TRUE Block Scale site at the Äspö Hard Rock Laboratory. Swedish Nuclear Fuel and Waste Management Company (SKB), Äspö Hard Rock Laboratory, International Progress Report IPR-01-27.

Landström O, Tullborg E-L, Eriksson G, Sandell Y, 2001. Effects of glacial/post-glacial weathering compared with hydrothermal alteration – implications for matrix diffusion. Results from drillcore studies in porphyritic quartz monzodiorite from Äspö, SE Sweden. SKB Report R-01-37.

Lever D A, Bradbury M H, Hemmingway S J, 1983. Modelling the Effects of Diffusion into the Rock Matrix on Radionuclide Migration, Prog. Nucl. Energy 12, 85–117.

Marschall P, Elert M, (in prep). Äspö Task Force. Overall evaluation of the modelling of the TRUE-1 tracer tests – Task 4.

Mathworks, 1997. Matlab version 5.1. The MathWorks, Inc., www.mathworks.com.

Mazurek M, Jakob A, Bossart P, 2002. Solute transport in crystalline rocks at Äspö – I: Geological basis and model calibration, J. of Cont. Hydrology (61), pp 157–174.

Miller I, Lee G, Dershowitz W, 1999. MAFIC: Matrix/Fracture Interaction Code with heat and solute transport. User Documentation Version 1.6, Golder Associates Inc.

Neretnieks I, 1980. Diffusion in the Rock Matrix: An Important Factor in Radionuclide Retardation? Journal of Geophysical Research, Vol 85. No B8, pp 4379–4397.

Neretnieks I, 2002. A stochastic multi-channel model for solute transport—analysis of tracer tests in fractured rock, J. of Cont. Hydrology, 55, 175–211.

Nordqvist R, 1994. Documentation of some analytical flow and transport models implemented for use with PAREST – Users manual. GEOSIGMA Internal report GRAP 94 006, Uppsala.

OECD/NEA, 1992. The International HYDROCOIN Project. Groundwater hydrology modelling strategies for performance assessment of nuclear waste disposal. Summary Report, OECD/NEA, Paris 1992.

OECD/NEA, 1995. GEOVAL '94 – Validation through model testing, Paris, Oct 11–14, 1994, OECD/NEA, Paris 1995.

OECD/NEA, 1996. The International INTRAVAL Project. Developing groundwater flow and transport models for radioactive waste disposal. Six years of experience from the INTRAVAL Project – Final Results, OECD/NEA, Paris 1996.

OECD/NEA, 1998. GEOTRAP – Modelling of the effects of spatial variability on radionuclide migration. Workshop proceedings, Paris, June 9–11, 1997. OECD/NEA, Paris 1998.

OECD/NEA, 2002. GEOTRAP: Radionuclide migration in geologic, heterogeneous media – Summary of accomplishments. OECD/NEA, Paris 2002.

Ogata A, Banks R, 1961. A solution to the differential equation of longitudinal dispersion in porous media. U.S. Geological Survey Prof. Paper 411-A, Washington D.C.

Paris B, 2002. Investigation of the correlation between early-time hydraulic response and tracer breakthrough times in fractured media, Results of Phase II. Äspö Hard Rock Laboratory International Progress Report IPR-02-16.

Pickens J F, Jackson R E, Inch K J, 1981. Measurement of distribution coefficients using radial injection dial-tracer test. Water Resour. Res., 17, no 3, pp 529–544.

Poteri A. Personal communication.

Poteri A, 2002. Predictive modelling and evaluation of the Phase C tracer tests. Äspö Hard Rock Laboratory International Progress Report IPR-02-32.

Painter S, Cvetkovic V, Selroos J O, 1998. Transport and retention in fractured rock: Consequences of a power-law distribution for fractured lengths, Phys. Rev. E, 57, 6917–6922.

Rachez X, Billaux D, 2002. Investigation of effect of structural model updates on response to simulated tracer tests. Äspö Hard Rock Laboratory International Progress Report IPR-02-26.

Rhén I (ed), Gustafson G, Stanfors R, Wikberg P, 1997. Äspö HRL – Geoscientific evaluation 1997/5. Models based on site characterisation 1986–1995. SKB Technical report 97-06.

SKB, 1999. Deep repository for spent nuclear fuel. SR 97 – Post-closure safety. Swedish Nuclear Fuel and Waste Management Company (SKB), Technical Report TR-99-06. ISSN 1404-0344.

SKB, 2001. First TRUE Stage – Transport of solutes in an interpreted single fracture. Proceedings from the 4th International Seminar, Äspö September 9–11, 2000.

SKI, 1984. INTRACOIN – International Nuclide Transport Code Intercomparison Study. Final Report Level 1 – Code verification. Swedish Nuclear Power Inspectorate. Technical Report SKI 84:3, September 1984.

SKI, 1986. INTRACOIN – International Nuclide Transport Code Intercomparison Study. Final Report Levels 2 and 3 – Model validation and uncertainty analysis. Swedish Nuclear Power Inspectorate. Technical Report SKI 84:3, September 1984.

Sudicky E A, Frind E O, 1982. Contaminant transport in fractured porous media: Analytical solutions for a system of parallel fractures, Water Resour. Res. 18, 1634–1642.

Sudicky E A, 1989. The Laplace transform Galerkin technique: A time-continuous finite element theory and application to mass transport in groundwater. Water Resour. Res., 25(8), 1833–1846.

Svensson U, 1997. A site scale analysis of groundwater flow and salinity distribution in the Äspö area. SKB Technical report TR-97-17.

Tang D H, Frind E O, Sudicky E A, 1981. Contaminant transport in fractured porous media: Analytical solution for a single fracture. water Resources Research, Vol 17, No 3, 555–564.

Van Genuchten M Th, Alves W J, 1982. Analytical solutions of the one-dimensional convective-dispersive solute transport equation. U.S. Dep. Agric. Tech. Bull., 1661.

Winberg A, Andersson P, Hermanson J, Stenberg L, 1996. Results of the SELECT Project – Investigation Programme for Selection of Experimental Sites for the Operational Phase. Swedish Nuclear Fuel and Waste Management Company. Äspö Hard Rock Laboratory Progress Report PR HRL-96-01.

Winberg A, 1997. Test plan for the TRUE Block Scale Experiment. Swedish Nuclear Fuel and Waste Management Company. Äspö Hard Rock Laboratory. International Cooperation Report ICR 97-02.

Winberg A (ed), 1999. Scientific and technical status. Position report prepared for the 2nd TRUE Block Scale review meeting, Stockholm, Nov 17 1998. Swedish Nuclear Fuel and Waste Management Company. Äspö Hard Rock Laboratory. International Progress Report IPR-99-07.

Winberg A (ed), 2000. TRUE Block Scale Project, Final Report of the Detailed Characterization Stage. SKB International Cooperation Report ICR-00-02. SKB, Stockholm.

Winberg A, Andersson P, Hermanson J, Byegård J, Cvetkovic V, Birgersson L, 2000. Final report of the first stage of the tracer retention understanding experiments. Swedish Nuclear Fuel and Waste Management Company (SKB), Technical Report TR-00-07. ISSN 1404-0344.

Winberg A, Hermanson J, 2002. TRUE Block Scale Experiment – Allocation of experimental volume. Swedish Nuclear Fuel and Waste Management Company. Äspö Hard Rock Laboratory. International Progress Report IPR-02-14.

Winberg A, Andersson P, Byegård J, Poteri A, Cvetkovic V, Dershowitz B, Doe T, Hermanson J, Gómez-Hernández J-J, Hautojärvi A, Billaux D, Tullborg E-L, Meier P, Medina A, 2002. TRUE Block Scale Project. Final Report – 4. Synthesis of flow, transport and retention in the block scale. Swedish Nuclear Fuel and Waste Management Company. Technical Report TR-02-16 (in prep).

Zuber A, 1974. Theoretical possibilities of the two-well pulse method. In: Proc. Of Sympon on Isotope Techniques in Groundwater Hydrology, 1974, Vienna, IAEA, Vienna.

Appendix A

Parameters used in numerical model predictions of the TRUE Block Scale Phase C tracer tests

Table A-1. Pore space properties used in numerical model predictions of the Phase C tracer experiments.

	ENRESA-UPC/UPV	JNC-Golder	Nirex-Serco	Posiva-VTT [4]	SKB-WRE	
					MIDS	TRUE-1
Porosity, %	0.3	0.1–1	0.4	3–13	0.4	2
Thickness, mm	100		1000	infinite	infinite	infinite
Depth dependence	no	no	no	no	no	no

Table A-2. Pore diffusivities of the immobile pore space used in the numerical model predictions of the Phase C tracer tests.

D_p [m^2/s]	ENRESA-UPC/UPV	JNC-Golder [5]	Nirex-Serco	Posiva-VTT [6]	SKB-WRE	
					MIDS	TRUE-1
Ba	10^{-11}	$8.3\ 10^{-10}$	$1.05\ 10^{-11}$	$1.7\ 10^{-11}$	$1.0\ 10^{-11}$	$1.7\ 10^{-10}$
Br	10^{-11}	$2.1\ 10^{-09}$	$1.00\ 10^{-11}$	$1.7\ 10^{-11}$	$3.0\ 10^{-11}$	$5.0\ 10^{-10}$
Ca	10^{-11}	$7.9\ 10^{-10}$	$1.00\ 10^{-11}$	$1.7\ 10^{-11}$	$1.0\ 10^{-11}$	$1.6\ 10^{-10}$
Cs	10^{-11}	$2.1\ 10^{-09}$	$2.50\ 10^{-11}$	$1.7\ 10^{-11}$	$2.5\ 10^{-11}$	$4.2\ 10^{-10}$
HTO	10^{-11}	$2.4\ 10^{-09}$	$3.00\ 10^{-11}$	$1.7\ 10^{-11}$	$3.0\ 10^{-11}$	$5.0\ 10^{-10}$
K	10^{-11}	$2.0\ 10^{-09}$	$1.05\ 10^{-11}$	$1.7\ 10^{-11}$	$2.5\ 10^{-11}$	$4.2\ 10^{-10}$
Na	10^{-11}	$1.3\ 10^{-09}$	$2.18\ 10^{-11}$	$1.7\ 10^{-11}$	$1.7\ 10^{-11}$	$2.8\ 10^{-10}$
Rb	10^{-11}	$2.0\ 10^{-09}$	$2{,}50\ 10^{-11}$	$1.7\ 10^{-11}$	$2.5\ 10^{-11}$	$4.2\ 10^{-10}$
Re	10^{-11}	$1.0\ 10^{-09}$	$1{,}05\ 10^{-11}$	$1.7\ 10^{-11}$	$3.0\ 10^{-11}$	$5.0\ 10^{-10}$
Sr	10^{-11}	$7.9\ 10^{-10}$	$1{,}05\ 10^{-11}$	$1.7\ 10^{-11}$	$1.0\ 10^{-11}$	$1.6\ 10^{-10}$

[4] Tracer transport is calculated using a single grouped parameter to describe the retention. The parameter depends on porosity, K_d, pore diffusivity and fracture aperture. Porosity given here is back-calculated for each tracer using the values calculated in the evaluation phase for the K_d, pore diffusivity and aperture.

[5] The values given by JNC-Golder are free water diffusivities D_w since this group used a model with several types of immobile zones, there is no such thing as a unique pore diffusivity for each tracer. The order of magnitude of D_p is typically $1/100^{th}$ of the value of D_w. However, this ratio may vary.

[6] Pore diffusivity is fixed to the same value as in the tracer test evaluation. Differences in retention are assigned to the porosity.

Table A-3. Equilibrium sorption on fracture surfaces used in the numerical model predictions of the Phase C tracer tests.

K_a [m]	ENRESA-UPC/UPV	JNC-Golder	Nirex-Serco	Posiva-VTT [7]	SKB-WRE	
					MIDS	TRUE-1
Ba	No	$6.1\ 10^{-4}$	$6.0\ 10^{-4}$	$1.6 – 1.9\ 10^{-3}$	$2\ 10^{-4}$	$2\ 10^{-4}$
Br	No	0	0	$6.2\ 10^{-5}$	–	–
Ca	No	$3.0\ 10^{-5}$	$3.0\ 10^{-5}$	$5.6 – 6.8\ 10^{-4}$	$4\ 10^{-6}$	$4\ 10^{-6}$
Cs	No	$8.1\ 10^{-3}$	$1.0\ 10^{-2}$	$3.6 – 4.6\ 10^{-2}$	$8\ 10^{-3}$	$8\ 10^{-3}$
HTO	No	0	0	0	–	–
K	No	$9.7\ 10^{-3}$	$1.0\ 10^{-4}$	$6.8\ 10^{-4}$	$4\ 10^{-5}$	$4\ 10^{-5}$
Na	No	$1.3\ 10^{-5}$	$5.0\ 10^{-6}$	$1.6 – 2.2\ 10^{-4}$	$7\ 10^{-7}$	$7\ 10^{-7}$
Rb	No	$1.0\ 10^{-3}$	$4.0\ 10^{-3}$	$1.6 – 2.2\ 10^{-3}$	$5\ 10^{-4}$	$5\ 10^{-4}$
Re	No	0	0	0	–	–
Sr	No	$5.0\ 10^{-5}$	$2.0\ 10^{-5}$	$3.6\ 10^{-4}$	$8\ 10^{-6}$	$8\ 10^{-6}$

Table A-4. Equilibrium sorption in the rock matrix used in the predictions of the Phase C tracer tests.

K_d [m^3/kg]	ENRESA-UPC/UPV	JNC-Golder	Nirex-Serco	Posiva-VTT [8]	SKB-WRE	
					MIDS	TRUE-1
Ba	$2.0\ 10^{-4}$	$1.2\ 10^{-5}$	$2.0\ 10^{-4}$	–	$2.0\ 10^{-4}$	$1.0\ 10^{-3}$
Br		–	0	0	–	–
Ca	$5.2\ 10^{-6}$	$6.2\ 10^{-7}$	$5.2\ 10^{-5}$	$1.30\ 10^{-3}$	$5.2\ 10^{-6}$	$2.6\ 10^{-5}$
Cs	$6.0\ 10^{-3}$	$5.2\ 10^{-6}$	$6.2\ 10^{-7}$	$2.80\ 10^{-1}$	$6.0\ 10^{-3}$	$3.0\ 10^{-2}$
HTO		–	0	0	–	–
K		$2.0\ 10^{-4}$	$1.0\ 10^{-4}$	$5.20\ 10^{-3}$	$2.0\ 10^{-4}$	$1.0\ 10^{-3}$
Na	$1.4\ 10^{-6}$	$2.7\ 10^{-7}$	$1.4\ 10^{-6}$	$2.20\ 10^{-4}$	$1.4\ 10^{-6}$	$7.0\ 10^{-6}$
Rb	$4.0\ 10^{-4}$	$2.1\ 10^{-5}$	$4.0\ 10^{-4}$	$2.80\ 10^{-2}$	$4.0\ 10^{-4}$	$2.0\ 10^{-3}$
Re		–	0.0	0	–	–
Sr	$4.7\ 10^{-6}$	$1.0\ 10^{-6}$	$4.7\ 10^{-4}$	$6.50\ 10^{-4}$	$4.7\ 10^{-6}$	$2.3\ 10^{-5}$

[7] Calculated using the same fracture aperture as in the tracer test evaluation.

[8] K_d values are taken from the evaluation results for the fault gouge.

Appendix B

The streamtube approach

In the classical representation, which is in fracture plane 1-D, the flow dependent part is given in the form $1/(2b \cdot v)$. It is obvious that this represents the inverse of the flow rate per unit width in the fracture for the parallel plate fracture and uniform flow field. If the aperture undulates (strictly normal to the flow vector) the solution holds because the product $2b \cdot v$ is invariant due to equation of continuation.

In these simplified cases the flow dependent part can be given equally well conceptually as 2-D by $W/(2b \cdot v \cdot W) = W/q$ using any value of W (e.g. increasing W increases q, respectively, but the ratio remains constant). It can also be noted that a change in aperture does not affect the strength of matrix diffusion but only advective delay τ or t_w.

In heterogeneous fractures both flow rate (1-D or 2-D) and aperture variations occur locally. These affect consequently both the strength of matrix diffusion and advective delay. To account for the strength the varying flow rate has to be integrated over the flow and transport path (streamline). In the 1-D picture this is the "aperture reduced" velocity and in 2-D it can be depicted as a certain flow rate, which is constant, between two streamlines. These two streamlines are not necessarily parallel but depart and get closer along the transport path, i.e. the local separation between the streamlines is now $W(x)$ (x is the coordinate along the flow path). To get the strength of matrix diffusion the $W(x)$ enclosed by the two bounding streamlines need to be integrated over the transport path.

Because the total strength of matrix diffusion in a given flow path depends on integral values it is meaningful to apply the concept of (arithmetic) mean values either as $(1/2b \cdot v)_{mean}$ or W_{mean}/q with a constant q bounded by the respective streamlines.

In a streamtube concept it is thus important to keep track on the shape of the streamtube. The concept itself is based on the fact that constant q flows through the streamtube at any cross-section but the area and shape of cross-section may vary. To define streamtube the flow field has to be established.

Fractures are usually conceptualised as flat features (large width compared to aperture). In this sense it can be noted that the strength of matrix diffusion depends only on the width of the streamtube's cross-section and advective delay depends both on width and aperture (it should be remembered that q is always part of the definition of a streamtube).

Appendix C

Example cases of retention heterogeneity

It can be shown that all TRUE Block Scale models are conceptually equivalent. Since the "reality" of the TBS site is complex and heterogeneous, and the information available is limited, the key difference in the TBS modelling approaches is how the heterogeneity is accounted for. We distinguish two main types of heterogeneity:
(i) heterogeneity which affects flow and retention (e.g. aperture variability), and
(ii) heterogeneity which affects only retention ("retention heterogeneity").

Flow heterogeneity has been addressed in modelling for some time, and one can say that it is "familiar" although there are still unresolved issues as to how to deal with it under field circumstances. We believe we understand how the flow heterogeneity affects transport and retention. By contrast, impact of retention heterogeneity has been much less addressed, and at this time, we do not have a good idea as to how this heterogeneity affects transport and retention under *in situ* conditions, and even less how to effectively include its effect in modelling.

Experimental data on retention heterogeneity is limited to be useful as direct input for modelling the TBS site, however, the available evidence is conclusive that such heterogeneity exists *in situ*. We refer here to the report for the TRUE-1 site /Byegård et al, 2001/.

In the following, we shall summarise four cases with the purpose of exposing the type of retention heterogeneity which affects retention. Our basic illustration concept is one of a "streamtube", "pipe" or "channel" between the injection and detection boreholes. We emphasise that this concept is central to the JNC and Posiva approaches, whereas following trajectories (rather than streamtubes) is central for the SKB and Nirex approaches. Relevant parameters of the four system configurations are given in the figure.

The following cases (as given in the figure) reflect typical retention heterogeneity which has been observed in the field:

- **Case 1: Longitudinal retention heterogeneity.** This type of heterogeneity is evident from Figure 6-11 and 6-12 of /Byegård et al, 2001/. This case is meant to capture porosity and diffusivity variability in the direction of flow, and we exemplify it by a half domain with low matrix porosity (diffusivity) and half with relatively high porosity (diffusivity).

- **Case 2: Vertical retention heterogeneity.** This type of heterogeneity is well documented e.g. in Figure 5-5 of /Byegård et al, 2001/, i.e. the porosity varies from the fracture toward the intact rock, exhibiting a trend but also random fluctuations. In our simplified configuration example, the "rim zone" with high porosity is 5 times the aperture.

- **Case 3: Multiple retention zones.** Although there is no direct evidence, it is intuitive that there would exist "pockets" of stagnant water adjacent to the flow path, or as "islands" in the flow path. Such retention effects have been discussed in the context of TRUE-1 and also considered in TBS, although the extent of the effect is not clear at this time. In our simplified configuration, we illustrate the matrix as a "vertical" retention zone and stagnant water as a "horizontal" (or lateral) retention zone.

- **Case 4: Multiple retention zones.** This case could also be viewed as "longitudinal heterogeneity" (case 1), however, here the retention zones are active in "parallel" similar to case 3, hence reference to "multiple retention zones". In our simplified configuration, this case is essentially equivalent to case 3, but rather than stagnant water we have longitudinal sections of the matrix which exhibit different retention properties.

An interesting issue for further consideration would be to compare the results from modelling of these simple systems by different TBS groups, both in numbers (i.e. BTCs for a unit pulse input) and conceptually, for a predefined set of physical parameters. In reality, the four types of heterogeneity illustrated by Cases 1–4 occur simultaneously (superimposed) with combined statistical and deterministic features, in addition to aperture variability. This fact can have significant implications on our interpretation of observed BTCs and estimation of *in situ* retention parameters. However, the first step would be to clearly understand how these individual configuration affect retention and transport.

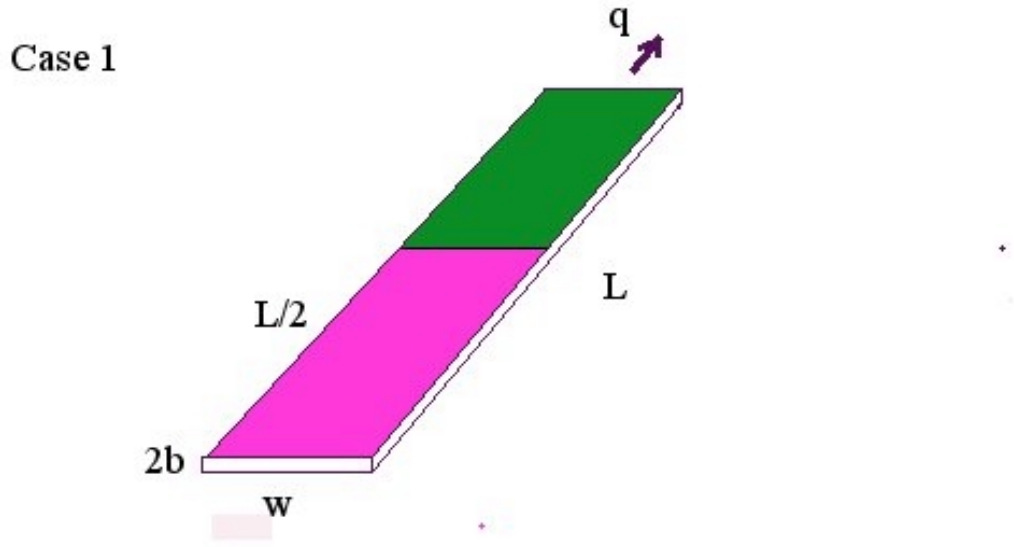

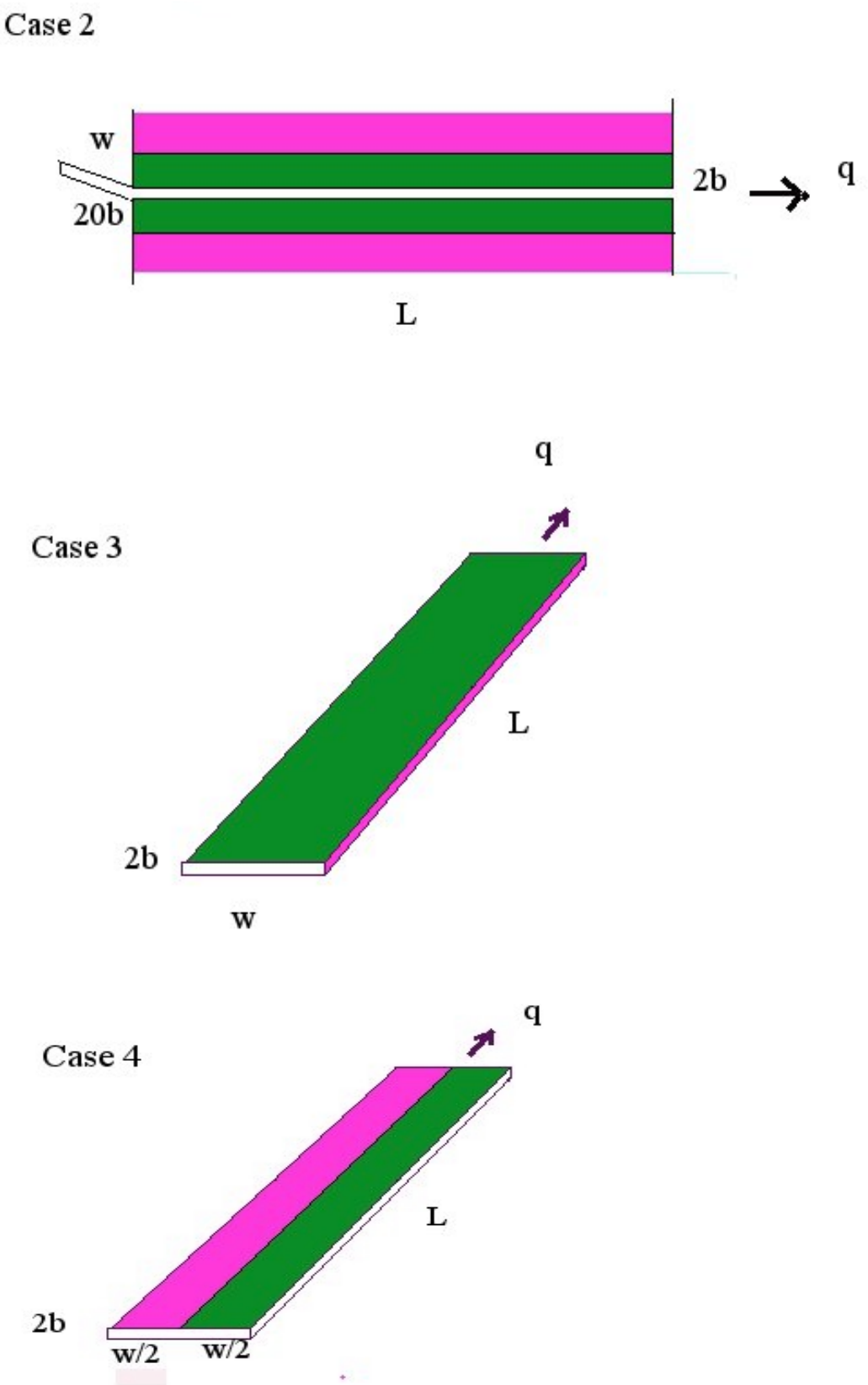

Figure B-1. *Four cases of simplified heterogeneity which affects retention and is present under field conditions. The purple region is one of high porosity/diffusivity, and green the region of low porosity/diffusivity. We assume for simplicity that the heterogeneity of the surfaces not visible in figure are symmetrical with the one visible in the figure.*

Appendix D

Evaluated transport properties related to the flow field

Table D-1. Evaluated transport properties related to the flow field: Non-sorbing tracer transit time and effective volume aperture along studied flow paths.

	ENRESA-UPC/UPV	JNC-Golder [9]	Nirex-Serco [10]	Posiva-VTT [11]	SKB-WRE
Flow path C1					
transit time, [h]	31	8.7	20.5	19	15
volume aperture, [mm]	0.3	0.5	0.86–1.79	0.62	0.5–1
Flow path C2					
transit time, [h]	306	129.2	258	126	65
volume aperture, [mm]	0.3	0.05	0.57–0.97	0.48	0.5–1
Flow path C3					
transit time, [h]	–	205.5	818	217	150
volume aperture, [mm]	0.3	0.5	13.36	0.45	0.5–1

[9] Apertures from structure transmissivities plus transport aperture scaling factor, from Phase C prediction report /Dershowitz et al, 2002b/. Flow path tested assumed to involve Structures #20, #21 (C1) , #21,23 (C2), #21 (C3), cf /Andersson et al, 2002b/.

[10] Transit times: t_{50} for conservative tracers from evaluation report. Aperture variations are from feature to feature. Same structures assumed involved as given in footnote above. Aperture scaling from Nirex-Serco evaluation report /Holton, 2002/. The presented volume aperture of the flow path tested by the C3 test represents the average transport aperture of the whole of Structure #21 based on one realisation, and may not apply to the specific flow path developed. The latter has not been quantified specifically.

[11] Transit times are calculated using mean flow velocities and path lengths, which are calculated along the structural model.

Appendix E

Porosity and diffusivity used in the evaluation models

Table E-1. Porosity, geometrical and functional relationships assigned by the modelling teams to the various immobile pore spaces in the evaluation of the TRUE Block Scale Phase C tracer tests.

	ENRESA-UPC/UPV	JNC-Golder	Nirex-Serco	Posiva-VTT			SKB-WRE
				"Rock matrix" a)	"Fault gouge" b)	"Stagn. zone"	
Porosity, %	0.3	3	0.4	0.6 [12]	3 [13]	50	1
Thickness, mm	0.1 mm	1 to 10	Max. 1 m	infinite	infinite	infinite	1–10
Depth dependence	No	No	No	no	no	no	yes (exponential)

a) values conditioned to rock matrix data.
b) values conditioned to fault gouge data.

[12] /Andersson et al, 2002a/. Table 7-1**.** mean porosity + uncertainty (~ highest porosity).

[13] /Andersson et al, 2002a/. Table 7-1**.** Fault gouge fragments (mm sized).

Table E-2. Pore diffusivities assigned to the immobile pore spaces by the modelling teams analysing the TRUE Block Scale Phase C tracer tests.

D_p [m^2/s]	ENRESA-UPC/UPV	JNC-Golder [14]	Nirex-Serco	Posiva-VTT [15]			SKB-WRE
				"Rock matrix"	"Fault gouge"	"Stagn. zone"	
Ba	$1.0\ 10^{-11}$	$2.49\ 10^{-11}$	$1.05\ 10^{-11}$	–	–	–	–
Br	$1.0\ 10^{-11}$	$6.24\ 10^{-11}$	–	$1.7\ 10^{-11}$	$1.7\ 10^{-11}$	$1.0\ 10^{-9}$	$5.20\ 10^{-10}$
Ca	$1.0\ 10^{-11}$	$2.38\ 10^{-11}$	$1.00\ 10^{-11}$	$1.7\ 10^{-11}$	$1.7\ 10^{-11}$	$1.0\ 10^{-9}$	$1.98\ 10^{-10}$
Cs	$1.0\ 10^{-11}$	$6.18\ 10^{-11}$	$2.50\ 10^{-11}$	$1.7\ 10^{-11}$	$1.7\ 10^{-11}$	$1.0\ 10^{-9}$	$5.15\ 10^{-10}$
HTO	$1.0\ 10^{-11}$	$7.20\ 10^{-11}$	$3.00\ 10^{-11}$	$1.7\ 10^{-11}$	$1.7\ 10^{-11}$	$1.0\ 10^{-9}$	$6.00\ 10^{-10}$
K	$1.0\ 10^{-11}$	$6.00\ 10^{-11}$	$1.00\ 10^{-11}$	$1.7\ 10^{-11}$	$1.7\ 10^{-11}$	$1.0\ 10^{-9}$	$5.00\ 10^{-10}$
Na	$1.0\ 10^{-11}$	$3.99\ 10^{-11}$	$1.68\ 10^{-11}$	$1.7\ 10^{-11}$	$1.7\ 10^{-11}$	$1.0\ 10^{-9}$	$3.33\ 10^{-10}$
Rb	$1.0\ 10^{-11}$	$6.09\ 10^{-11}$	$2.50\ 10^{-11}$	$1.7\ 10^{-11}$	$1.7\ 10^{-11}$	$1.0\ 10^{-9}$	$5.08\ 10^{-10}$
Re	$1.0\ 10^{-11}$	$3.00\ 10^{-11}$	–	$1.7\ 10^{-11}$	$1.7\ 10^{-11}$	$1.0\ 10^{-9}$	$2.50\ 10^{-10}$
Sr	$1.0\ 10^{-11}$	$2.37\ 10^{-11}$	$1.00\ 10^{-11}$	$1.7\ 10^{-11}$	$1.7\ 10^{-11}$	$1.0\ 10^{-9}$	–

[14] Obtained from diffusion experiments in rock cylinders of Äspo diorite (specific REF).

[15] Calculated (Dp = Dw*G) using selected molecular diffusion coefficient in free water ($1\ 10^{-9}\ m^2/s$) and fitted geometric factor G=0.017 (G have maximum allowed value of G=0.017). The geometric factor is $G=F\ \varepsilon$, where F is formation factor. In TR-98-18 it is given that $F=1.7\ 10^{-5}$ for Feature A and $\varepsilon \sim 1\ 10^{-3}$. This gives G=0.017.

Appendix F

Sorption properties used in the evaluation models

Table F-1. Equilibrium sorption (K_a) assigned to fracture surfaces in the evaluation of the TRUE Block Scale Phase C tracer tests.

K_a [m]	ENRESA-UPC/UPV [16]	JNC-Golder	Nirex-Serco [17]	Posiva-VTT [18]		SKB-WRE
				Fracture surface	Stagnant water [19]	
Ba	No	$6.08\ 10^{-4}$	$4.\ 10^{-4}$ to $3.\ 10^{-1}$	No	No	–
Br	No	0		$1.1\ 10^{-9}$	$1.1\ 10^{-9}$	–
Ca	No	$3.04\ 10^{-5}$	$4.4\ 10^{-5}$ to $2.5\ 10^{-3}$	2.5–6.7 10^{-4}	$2.5\ 10^{-4}$ to $6.7\ 10^{-4}$	$5.3–10.2\ 10^{-5}$
Cs	No	$4.03\ 10^{-3}$ (134) $8.12\ 10^{-3}$ (137)	$3.3\ 10^{-3}$ to $1.0\ 10^{-1}$	$9.3\ 10^{-3}$	$9.3\ 10^{-3}$	$2.02–3.8\ 10^{-3}$
HTO	No	0		0	0	–
K	No	$9.72\ 10^{-3}$	$2.9\ 10^{-4}$ to $6.5\ 10^{-3}$	$1.9\ 10^{-4}$	$1.9\ 10^{-4}$	$0.97–1.84\ 10^{-4}$
Na	No	$1.31\ 10^{-5}$	$3.1\ 10^{-5}$ to $1.7\ 10^{-2}$	$7.3\ 10^{-5}$ to $1.4\ 10^{-4}$	$7.3\ 10^{-5}$ to $1.4\ 10^{-4}$	$0.9–1.8\ 10^{-6}$
Rb	No	$1.01\ 10^{-3}$	$6.6\ 10^{-4}$ to $4.0\ 10^{-1}$	$1.2\ 10^{-3}$	$1.2\ 10^{-3}$	$6.7–12.8\ 10^{-4}$
Re	No	0		0	0	–
Sr	No	$5.05\ 10^{-5}$	$1.7\ 10^{-4}$ to $6.1\ 10^{-2}$	$4.9\ 10^{-4}$	$4.9\ 10^{-4}$	–

[16] Surface sorption not included in the UPC/UPV model cf Table 6-2.

[17] Fitted, assuming either hydraulic (lower values) or transport (higher values) apertures.

[18] Calculated from TRUE-1 fitted BTC retardation factors R_a using flow path apertures that were fitted for fault gouge case (apertures: C-1 0.62 mm, C2 0.48 mm, C3 0.45 mm).

[19] Assumed molecular diffusion coefficient in free water: $1{\cdot}10^{-9}$ m^2/s.

Table F-2. Sorption coefficients assigned to the immobile pore spaces in the evaluation of the TRUE Block Scale Phase C tracer tests.

K_d [m^3/kg]	ENRESA-UPC/UPV	JNC-Golder	Nirex-Serco	Posiva-VTT		SKB-WRE
				"Rock matrix" [20] a)	"Fault gouge" [21] b)	
Ba	$2.0\ 10^{-4}$	–	–	–	–	–
Br	0	0	0	0	0	0
Ca	$5.2\ 10^{-6}$	$2.1\ 10^{-4}$	$7.\ 10^{-5}$ to $2.0\ 10^{-4}$	$1.45\ 10^{-4}$	$1.3\ 10^{-3}$	$4.8\ 10^{-4}$
Cs	$6.0\ 10^{-3}$	$4.8\ 10^{-2}$	$2.\ 10^{-2}$	$1.52\ 10^{-2}$	$2.8\ 10^{-1}$	$5.8\ 10^{-2}$
HTO	0	0		0	0	0
K	–	$8.5\ 10^{-4}$	$3.\ 10^{-4}$	$4\ 10^{-4}$	$5.2\ 10^{-3}$	$5.8\ 10^{-4}$
Na	$1.4\ 10^{-6}$	$3.4\ 10^{-5}$	$1.\ 10^{-5}$ to $3.\ 10^{-5}$	$6\ 10^{-5}$	$2.2\ 10^{-4}$	$4.9\ 10^{-5}$
Rb	$4.0\ 10^{-4}$	$4.8\ 10^{-3}$	$2.\ 10^{-3}$	$2\ 10^{-3}$	$2.8\ 10^{-2}$	$5.6\ 10^{-3}$
Re	0	0		0	0	0
Sr	$4.7\ 10^{-6}$	–	$6.\ 10^{-5}$	$1.8\ 10^{-4}$	$6.5\ 10^{-5}$	–

a) values conditioned to rock matrix data
b) values conditioned to fault gouge data

[20] TR-98-18, Table 6-3. Maximum value of experiments on Äspö diorite, mylonite and altered Äspö diorite used as upper value of the K_d. Br limit (~ arbitrarily) selected to being the same as the Na limit and the K limit two times that of the Na limit.

[21] /Andersson et al, 2002a/, Table 7-4 d<125 μm maximum of the columns for KA2563A:154 m, KI0025F02:133 m, KI0023B:69.9 m, KI0025F02:66.7 m and crushed material.

ISSN 1404-0344

CM Digitaltryck AB, Bromma, 2003